

# Durham E-Theses

---

## *Investigation of the machining processes of flexible fibrous materials for applications in industrial automation.*

Saadat-Sarmadi, Mozafar

### How to cite:

---

Saadat-Sarmadi, Mozafar (1992) *Investigation of the machining processes of flexible fibrous materials for applications in industrial automation.*, Durham theses, Durham University. Available at Durham E-Theses Online: <http://etheses.dur.ac.uk/1124/>

### Use policy

---

The full-text may be used and/or reproduced, and given to third parties in any format or medium, without prior permission or charge, for personal research or study, educational, or not-for-profit purposes provided that:

- a full bibliographic reference is made to the original source
- a [link](#) is made to the metadata record in Durham E-Theses
- the full-text is not changed in any way

The full-text must not be sold in any format or medium without the formal permission of the copyright holders.

Please consult the [full Durham E-Theses policy](#) for further details.

---

Academic Support Office, Durham University, University Office, Old Elvet, Durham DH1 3HP  
e-mail: [e-theses.admin@dur.ac.uk](mailto:e-theses.admin@dur.ac.uk) Tel: +44 0191 334 6107  
<http://etheses.dur.ac.uk>



## **ABSTRACT**

### **Investigation of the Machining Processes of Flexible Fibrous Materials for Applications in Industrial Automation**

**Mozafar Saadat-Sarmadi**

PhD Thesis 1992

This thesis is concerned with the investigation of the fundamentals of machining processes of flexible fibrous materials encountered in industrial automation projects. One such project is the manufacturing of shoe uppers, which involves many processes that are strong candidates for automation. Machining of leather components by reducing thickness, in shoe manufacture, is a necessary intermediate process which is highly labour intensive. This is referred to as skiving of leather. Therefore, it is necessary to determine feasible methods to achieve automated skiving by using leather as the workpiece in the shoe upper manufacturing. To this end, two different methods of leather machining have been investigated. One involves the use of high speed machining system based on face milling technology, while the other relies on the principle of cutting by using a band knife. The former method employs a high speed router to machine leather components. This is a conventional non-continuous system which implies that the workpiece would come to a halt for the duration of machining. In the case of the latter, a linear array of independently-actuated pins are used to depress the moving workpiece against the action of a band knife. It therefore provides a continuous system. Comprehensive experimentations have been conducted to evaluate the design parameters for both methods. Furthermore, in the course of the investigation it was found that the dependency of the machining quality on the physical properties of material is significant. Therefore, experiments were also performed to evaluate the relevant material properties so that they could be related to the machining performance of leather. Relevant considerations towards the integration of automated manufacturing cells based on the two machining systems are subsequently presented.

The copyright of this thesis rests with the author.  
No quotation from it should be published without  
his prior written consent and information derived  
from it should be acknowledged.

**Investigation of the Machining Processes of Flexible Fibrous  
Materials for Applications in Industrial Automation**

**Mozafar Saadat-Sarmadi**

**A thesis submitted in fulfilment  
of the requirements for the degree of  
Doctor of Philosophy**

**School of Engineering and Computer Science  
The University of Durham**

**1992**



- 9 JUL 1993

## **DECLARATION**

The work contained in this thesis has not been submitted elsewhere for any other degree or qualification, and unless otherwise referenced it is the author's own work.

Copyright © 1992 by Mozafar Saadat-Sarmadi.

The copyright of this thesis rests with the author. No quotation from it should be published without Mozafar Saadat-Sarmadi's prior written consent, and information derived from it should be acknowledged.



## **ACKNOWLEDGEMENT**

First and foremost I would like to express my sincere gratitude to my supervisors, Dr. C. Preece and Professor J. E. L. Simmons, for their correct and efficient supervision of this work and their continued encouragement throughout the project. I would also like to thank Mr. D. Reedman, head of research at British United Shoe Machinery Ltd., for his enthusiastic support and advice during the practical work of the project.

The technical support during this work has been excellent. This is an opportunity for me to acknowledge with appreciation the technical skills of the project's mechanical engineering technician, the Late Mr. N. Dunning, for his outstanding contribution in the realisation of the various rigs and hardware in the course of this work. Thanks are also given to Mr. T. Brown for his departmental help and support, Mr. B. Blackburn for his numerous advice and cooperation in the mechanical engineering workshop, Mr. J. Greensmith for his electrical engineering assistance, Mr. P. Friend and his staff for their electronic engineering expertise, and Mr. T. Nancarrow for his computing assistance. My thanks are also due to Miss L. Graham for her superb secretarial skills and the numerous personal support she has given, and to Ms. J. Morgan for her artwork and photographic assistance.

This project was funded by the ACME (Application of Computers in Manufacturing Engineering) directorate of SERC (Science and Engineering Research Council), and was jointly collaborated with the British United Shoe Machinery Ltd. I acknowledge with thanks the support of the above organisations.

*To my parents*

## **CONTENTS**

<b>ABSTRACT</b>	<b>... i</b>
<b>TITLE PAGE</b>	<b>... ii</b>
<b>DECLARATION &amp; COPYRIGHT NOTICE</b>	<b>... iii</b>
<b>ACKNOWLEDGEMENTS</b>	<b>... iv</b>
<b>CONTENTS</b>	<b>... vi</b>
<b>LIST OF FIGURES</b>	<b>... x</b>
<b>LIST OF TABLES</b>	<b>... xvii</b>

### **CHAPTER ONE - INTRODUCTION**

1.1 A case for automation	... 1
1.2 Manufacturing of shoe uppers	... 2
1.3 Skiving of leather	... 4
1.4 Specifications for automation	... 7
1.5 Layout of the thesis	... 8

### **CHAPTER TWO - PRELIMINARY INVESTIGATION FOR AUTOMATION**

2.1 Introduction	... 9
2.2 Alternative automation concepts	... 10
2.3 Principle of machining technology	... 11
2.3.1 General system configuration	... 11
2.3.2 Face milling of leather	... 12
2.3.3 Preliminary experiments	... 14
2.4 Principle of matrix skiving	... 24

2.4.1	General system configuration	... 24
2.4.2	Linear matrix skiving	... 26
2.4.3	Preliminary experimentations	... 31
2.5	The role of the properties of material	... 39
2.6	Conclusions	... 40

## CHAPTER THREE - PROPERTIES OF MATERIALS

3.1	Introduction	... 42
3.2	Understanding leather	... 43
3.3	Method for material sampling	... 45
3.4	Selection of suitable properties	... 49
3.5	Material thickness measurement	... 51
3.5.1	Measurement technique	... 51
3.5.2	The results	... 55
3.6	Material flexibility	... 58
3.6.1	Test procedure	... 59
3.6.2	The results	... 61
3.7	Material hardness	... 65
3.7.1	Test procedure	... 65
3.7.2	The results	... 66
3.8	Material compression properties	... 68
3.8.1	Test procedure	... 69
3.8.2	The results	... 71
3.9	Material tensile strength	... 73
3.9.1	Test procedure	... 73
3.9.2	The results	... 75
3.10	Material tearing properties	... 81
3.10.1	Test procedure	... 82
3.10.2	The results	... 83

3.11	Material burst properties	... 86
3.11.1	Test procedure	... 87
3.11.2	The results	... 88
3.12	Conclusions	... 90

## **CHAPTER FOUR - HIGH SPEED MACHINING SYSTEM**

4.1	Introduction	... 92
4.2	Relevant theories in milling operation	... 93
4.3	General requirements from the experimental system	... 101
4.4	Design of the cutting tools	... 103
4.5	Design of the dynamometer	... 105
4.6	Dynamic evaluation of the dynamometer	... 109
4.7	Cutting head assembly characteristics	... 113
4.8	Operation of the combined rig	... 116
4.9	Conclusions	... 122

## **CHAPTER FIVE - MACHINING SYSTEM EXPERIMENTAL RESULTS**

5.1	Introduction	... 124
5.2	The repeatability analysis	... 125
5.3	Machine parameter results	... 130
5.4	Effects of depth of cut	... 140
5.5	Tool wear considerations	... 143
5.6	Surface finish quality and the role of materials properties	... 146
5.7	Conclusions	... 152

## **CHAPTER SIX - DYNAMIC MATRIX CUTTING SYSTEM**

6.1	Introduction	... 154
6.2	General requirements from the experimental system	... 155



6.3	Pin matrix Assembly	... 156
6.4	Method of actuation	... 159
6.5	Force measurement system	... 164
6.6	Operation of the combined rig	... 165
6.7	Experimental results	... 170
6.8	The role of properties of materials in matrix skiving	... 176
6.9	Conclusions	... 177

## CHAPTER SEVEN - INTEGRATION CONSIDERATIONS FOR AUTOMATION

7.1	Introduction	... 179
7.2	General systems considerations	... 180
7.3	Component recognition system	... 181
7.4	Component transportation system	... 184
7.5	Integration of the high speed machining system	... 186
7.5.1	Component clamping	... 186
7.5.2	The high speed machining station	... 189
7.5.3	Overall cell operation	... 193
7.6	Integration of dynamic matrix cutting system	... 195
7.6.1	The dynamic matrix skiving station	... 196
7.6.2	Overall cell operation	... 199
7.7	Conclusions	... 201

## CHAPTER EIGHT - CONCLUSIONS

8.1	Machining methods for automation	... 203
8.2	Summary	... 204
8.3	Future directions	... 208

REFERENCES	... 210
------------	---------

## **LIST OF FIGURES**

- Figure 1.1      An upper assembly of a sport shoe showing its skived edges
- Figure 1.2      Diagrammatic presentation of skiving in leather components
- Figure 1.3      A typical skiving machine (By permission, BUSM Ltd.)
- Figure 1.4      A close-up view of skiving operation (By permission, BUSM Ltd.)
- Figure 1.5      The rotating disc in skiving machine (By permission, BUSM Ltd.)
- Figure 1.6      Examples of skived components (By permission, BUSM Ltd.)
- Figure 2.1      An envisaged multi-head machining cell for automatic skiving
- Figure 2.2      Display of the cutting tools tested in leather machining system
- Figure 2.3      Performance of the cutting tools shown in fig. 2.3 compared in a subjective fashion
- Figure 2.4      A side view showing the cutting principle in matrix skiving
- Figure 2.5      Diagram showing the linear matrix assembly above the band knife
- Figure 2.6      Plan view of an envisaged linear matrix skiving cell
- Figure 2.7      Plan view of an envisaged two-dimensional matrix skiving cell
- Figure 2.8      Plan view of an envisaged cylindrical matrix skiving cell
- Figure 2.9      A side view of the envisaged cylindrical matrix skiving cell
- Figure 2.10     A typical splitting machine (By permission, BUSM Ltd.)
- Figure 2.11     The composite plate used in static matrix skiving tests
- Figure 2.12     An actual static matrix die used in the experiment

- Figure 2.13 A test sample after being skived using the static matrix method
- Figure 2.14 Surface of a test sample after the static matrix skiving test
- Figure 2.15 Graphs of surface quality results in static matrix skiving tests
- Figure 2.16 Bar and pins assembly constructed for matrix skiving experiments
- Figure 3.1 A vertical section of calf skin in diagrammatic form ( Ref. [16] )
- Figure 3.2 British Standards 3935 regional divisions of hide's surface area
- Figure 3.3 Regional divisions of hides for sampling purpose
- Figure 3.4 Thickness variation in the hide type-1
- Figure 3.5 Thickness variation in the hide type-2
- Figure 3.6 Standard deviation variation of thickness measurements, hide type-1
- Figure 3.7 Standard deviation variation of thickness measurements, hide type-2
- Figure 3.8 Essential features of the flexural rigidity measurement device
- Figure 3.9(a) Flexural rigidity variation close to backbone, hide type-1
- Figure 3.9(b) Flexural rigidity variation close to the belly, hide type-1
- Figure 3.10 Flexural rigidity variation close to the backbone, hide type-2
- Figure 3.11 Flexural rigidity variation in the hide type-1
- Figure 3.12 Flexural rigidity variation in the hide type-2
- Figure 3.13 Indentation index variation in the hide type-1
- Figure 3.14 Indentation index variation in the hide type-2
- Figure 3.15 A typical leather load-compression characteristic
- Figure 3.16 Variation of resistance to compression in the hide type-1
- Figure 3.17 Variation of resistance to compression in the hide type-2
- Figure 3.18 A typical leather load-extension characteristic



- Figure 3.19(a) Tensile strength variation close to the backbone, hide type-1
- Figure 3.19(b) Tensile strength variation in the mid-side region, hide type-1
- Figure 3.19(c) Tensile strength variation close to the belly, hide type-1
- Figure 3.20(a) Variation of elongation close to the backbone, hide type-1
- Figure 3.20(b) Variation of elongation in the mid-side region, hide type-1
- Figure 3.20(c) Variation of elongation close to the belly, hide type-1
- Figure 3.21(a) Tensile strength variation close to the backbone, hide type-2
- Figure 3.21(b) Tensile strength variation close to the belly, hide type-2
- Figure 3.22(a) Variation of elongation close to the backbone, hide type-2
- Figure 3.22(b) Variation of elongation close to the belly, hide type-2
- Figure 3.23 The form and dimensions of the tearing load test samples
- Figure 3.24 A typical leather tearing load characteristic
- Figure 3.25(a) Tearing load variation close to the backbone, hide type-1
- Figure 3.25(b) Tearing load variation in the mid-side region, hide type-1
- Figure 3.25(c) Tearing load variation close to the belly, hide type-1
- Figure 3.26(a) Tearing load variation close to the backbone, hide type-2
- Figure 3.26(b) Tearing load variation close to the belly, hide type-1
- Figure 3.27 Essential features of the 'lastometer'
- Figure 3.28 Burst load variation in the hide type-1
- Figure 3.29 Burst load variation in the hide type-2
- Figure 3.30 Graphical comparison of the mean of all properties showing hide type-2 relative to hide type-1
- Figure 4.1 A diagram showing the geometry of cutting when up-cut milling

- Figure 4.2**      Diagrammatic presentation of down-cut milling
- Figure 4.3**      Diagrammatic presentation of cutting forces in milling
- Figure 4.4**      A diagram showing chip formation during cutting
- Figure 4.5**      Periodic formation of pulses representing the cutting force
- Figure 4.6**      A diagram showing a full crescent of cut achieved by feed and normal cutting force
- Figure 4.7**      A diagrammatic presentation of the inverted dovetail tool showing the important geometric dimensions (not to scale)
- Figure 4.8**      The schematic diagram of the dynamometer assembly
- Figure 4.9**      Damped vibration shown as displacement against time
- Figure 4.10**     A schematic diagram of the cutting head assembly
- Figure 4.11**     A front view of the dynamometer and the cutting head assembly
- Figure 4.12**     A side view of the dynamometer and the cutting head assembly
- Figure 5.1**      Results of repeatability analysis for leather type-1:  $0.03 \text{ ms}^{-1}$  feed speed,  $0^\circ$  cutting tool rake angle, and 0.4 mm depth of cut
- Figure 5.2**      Results of repeatability analysis for leather type-1; 24000 rpm initial cutting speed,  $0^\circ$  cutting tool rake angle, and 0.4 mm depth of cut
- Figure 5.3**      Graphs of variations of feed cutting force in leather type-1 against cutting speed for different tool take angles, and with 0.4 mm depth of cut
- Figure 5.4**      Graphs of variations of normal cutting force in leather type-1 against cutting speed for different tool take angles, and with 0.4 mm depth of cut
- Figure 5.5**      Graphs of variations of cutting forces in leather type-2 against cutting speed for different tool rake angles,  $0.03 \text{ ms}^{-1}$  feed speed, and 0.4 mm depth of cut



- Figure 5.6      Graphs of variations of cutting forces in leather type-2 against cutting speed for different feed speeds, with 0° tool rake angle, and 0.4 mm depth of cut
- Figure 5.7      Graphs of variations of power consumption in leather type-1 against cutting speed for different tool rake angles, and with 0.4 mm depth of cut
- Figure 5.8      Graphs of variations of power consumption in leather type-2 against cutting speed for (a) different tool take angles and 0.03 ms<sup>-1</sup> feed speed, and (b) different feed speeds and 0° tool rake angle. In all cases with 0.4 mm depth of cut
- Figure 5.9      Graphs of variations of the cutting results in leather type-1 against cutting speed for different depths of cut, with fixed feed speed of 0.03 ms<sup>-1</sup>, and 0° tool rake angle
- Figure 5.10     Graphs of variations of the cutting results in leather type-1 against feed speed for different depths of cut, with initial cutting speed of 24000 rpm, and 0° tool rake angle
- Figure 5.11     Photograph of a cutting edge of the tool with 0° rake angle taken before the experiments. Magnification factor = 100
- Figure 5.12     Photograph of the same cutting edge as in fig. 5.11 taken after the experiments. Magnification factor = 100
- Figure 5.13     A subjective comparison of the surface finish quality of leather type-1 samples shown graphically for different tool rake angles against cutting speed, with 0.4 mm depth of cut
- Figure 5.14     Presentation of the leather sample positions in their original hides, shown graphically in the same way as the surface finish results in fig. 5.13
- Figure 5.15     Photograph of a typical test sample with very good machined surface quality
- Figure 5.16     Photograph of a typical test sample with poor machined surface quality

- Figure 6.1 Design of a pressure bar to house matrix pins (all dimensions in mm, sketch not to scale)
- Figure 6.2 Schematic diagram of a matrix pin and the associating nut (Drawing not to scale)
- Figure 6.3 Discrete skiving impressions on leather samples by a linear array of pins, when all pins are simultaneously depressed
- Figure 6.4 Pin skiving impressions on a leather sample when pins are sequentially depressed
- Figure 6.5 A schematic diagram showing the complete plunger actuation assembly
- Figure 6.6 Diagram showing contact surfaces of a pin and the cam
- Figure 6.7 Design of the load cell used in matrix skiving tests (not to scale)
- Figure 6.8 A close-up view of the matrix skiving rig in operation
- Figure 6.9 A view showing the complete matrix skiving rig
- Figure 6.10 Diagram showing method of measurement of matrix skiving surface quality results
- Figure 6.11 Graphs of skiving quality variation against pin spacing
- Figure 6.12 Graphs of skiving quality variation against pin diameter
- Figure 6.13 Graphs of skiving quality variation against feed speed
- Figure 6.14 Graphs of skiving force variation against pin diameter
- Figure 6.15 Graphs of skiving force variation against pin spacing
- Figure 6.16 Graphs of skiving force variation against feed speed
- Figure 7.1 Diagram showing the vision system and the conveyor belts
- Figure 7.2 Integration of the vision system with a process operation station
- Figure 7.3 Sectional view of a vacuum cup with circular inlet
- Figure 7.4 Example of a distributed vacuum system

- Figure 7.5**      **An illustration of a machining station with a stationary component**
- Figure 7.6**      **Illustration of the features of a vacuum belt**
- Figure 7.7**      **An illustration of a moving gantry type machining station**
- Figure 7.8**      **A front view of the constructed bank of solenoid-lever-pin assembly**
- Figure 7.9**      **A side view of the constructed bank of solenoid-lever-pin assembly**
- Figure 7.10**     **Integration of the feed conveyor belt with the matrix skiving station**
- Figure 7.11**     **A view of the dynamic matrix skiving rig complete with the bank of computer-controlled activated pins and a built-in feed conveyor belt**



## **LIST OF TABLES**

<b>Table 2.1</b>	<b>Names and tip materials of the cutting tools shown in fig. 2.2</b>
<b>Table 3.1</b>	<b>Thickness measurement results for the hide type-1 using a micrometer</b>
<b>Table 3.2</b>	<b>Thickness measurement results for the hide type-2 using a micrometer</b>
<b>Table 3.3</b>	<b>Thickness measurement results for the hide type-1 using a vernier calliper</b>
<b>Table 3.4</b>	<b>Thickness measurement results for the hide type-2 using a vernier calliper</b>
<b>Table 4.1</b>	<b>Measured no-load characteristics of the router motor</b>
<b>Table 5.1</b>	<b>Overall mean values for cutting forces</b>
<b>Table 7.1</b>	<b>Time evaluation of a typical component visit to the machining cell</b>
<b>Table 7.2</b>	<b>Time evaluation of a component visit to the matrix skiving cell</b>

# **CHAPTER ONE**

## **INTRODUCTION**

### **1.1 A case for automation**

Flexible materials are used as the workpieces in many manufacturing processes in the apparel and footwear industries. In these industries the workpiece is either manufactured to pre-determined specifications or is produced as a natural material. The products of the textile industry are examples of the former, while those of the leather manufacturing industry are examples of the latter. Another example of the use of flexible material as the workpiece is in the automotive industry where car seat covers are manufactured. Handling and processing of flexible materials has traditionally been achieved with a high involvement of skilled human operators in conjunction with mechanised machinery. The inexorable move towards automated production in the recent years has made many such labour intensive manufacturing industries candidates for automation [1].

Traditional methods have long been established to perform the required manufacturing operations on the flexible materials. These often rely heavily on the skills of the human operator whose experience and the 'feel' of the workpiece greatly contribute to the satisfactory execution of the operations. The introduction of automation is however synonymous with the transfer of skills from the operator to the intelligent machinery. An area where this is most applicable is the manipulation of the workpiece for a particular operation. To this end, flexible materials pose several areas of difficulties since the conventional techniques do not easily lend themselves to straightforward solutions. It therefore follows that new techniques will have to be developed to perform the desired automated manufacturing operations on flexible materials. The characteristics of these techniques are such that the relevant parameters relating to the workpiece and the particular operation are fully evaluated in an engineering sense by a computer-controlled machine system.



An example of a manufacturing operation on flexible material is the material removal process. Though this application is largely limited to the shaping of the surface of the material by reducing its thickness, its use is made in many industries. However, the most widespread use of flexible material machining is in the footwear industry where thickness reduction of the shoe upper material is often required prior to the joining process of various components. Leather however remains the most widely used material for shoe uppers for both comfort and fashion reasons. It is a fibrous, natural material and comes in irregular shapes and sizes whose quality and characteristics are varied within a hide as well as between hides. The application of automation of machining of leather, as a flexible fibrous material, therefore requires the implementation of novel manufacturing methods so that both its flexible and fibrous characteristics can be catered for. The aim of this project is to investigate the fundamental principles of the material removal processes of flexible fibrous materials for applications in industrial automation. In this work, the automation of shoe upper manufacturing with leather as the workpiece material is considered throughout.

In the following sections the various shoe upper manufacturing processes are introduced. Then, leather machining technology of today is described. Later, specifications for a new machining system are given. A description of the layout of the thesis is given at the end of this chapter.

## **1.2 Manufacturing of shoe uppers**

Shoe uppers are the 3-D part of shoe that is attached above the sole. Upper material is cut from the flat sheets of either synthetic materials or leather. The individual upper components are initially cut from the original hides (in the case of leather) by a skilled operator. Then, stitchmarking and lining marking on the components take place. These operations are performed to assist the stitching operators at a later stage. After marking the shoe components a process of material thinning along the edges or lines is performed in the areas where stitching with another component will take place. This is to ensure that the combined component retains a uniform thickness throughout. This process is called *skiving*. Later, component folding and stitching take place [2]. Fig. 1.1 shows a completed upper assembly of a sports shoe clearly showing its skived edges. The concentration of this work is focused in the application of automation in the skiving process.





*Figure 1.1 An upper assembly of a sports shoe showing its skived edges.*



The work-in-progress in the above processes consist of batches of components requiring similar operations. Often these batches are unbundled/bundled several times for each process. The transportation to the correct processing station, as well as the wasted time in unbundling/bundling the components result in considerable logistics problems and a large volume of work-in-progress. Furthermore, the problem associated with the retooling of the machines for each component design is a major drawback in the present system. It is for these reasons that the manufacturing of shoe uppers is a strong candidate for flexible automation.

### 1.3 Skiving of leather

Leather machining, or skiving, is a process where the excess material from the fibrous side of a leather component is removed. This is often achieved in the form of a chamfer along the edges of the components that are to be stitched together. If no skiving takes place, the thickness of the overlap area consists of the combined thicknesses of the individual components. Thus, non-uniform thickness throughout the combined component results. However, this problem is eliminated when skiving takes place prior to stitching. Fig. 1.2 gives a sketch of two skived components before stitching.

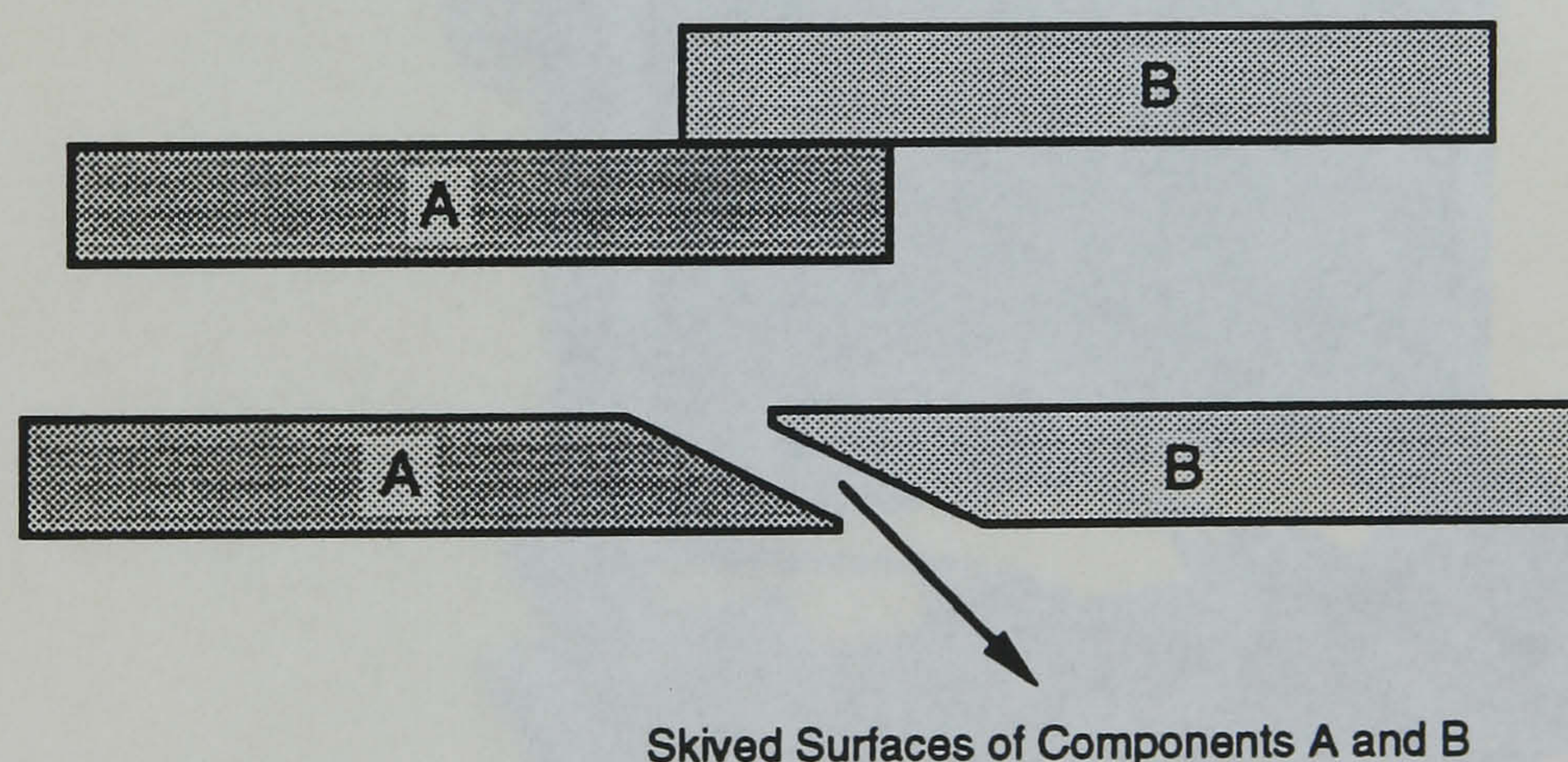
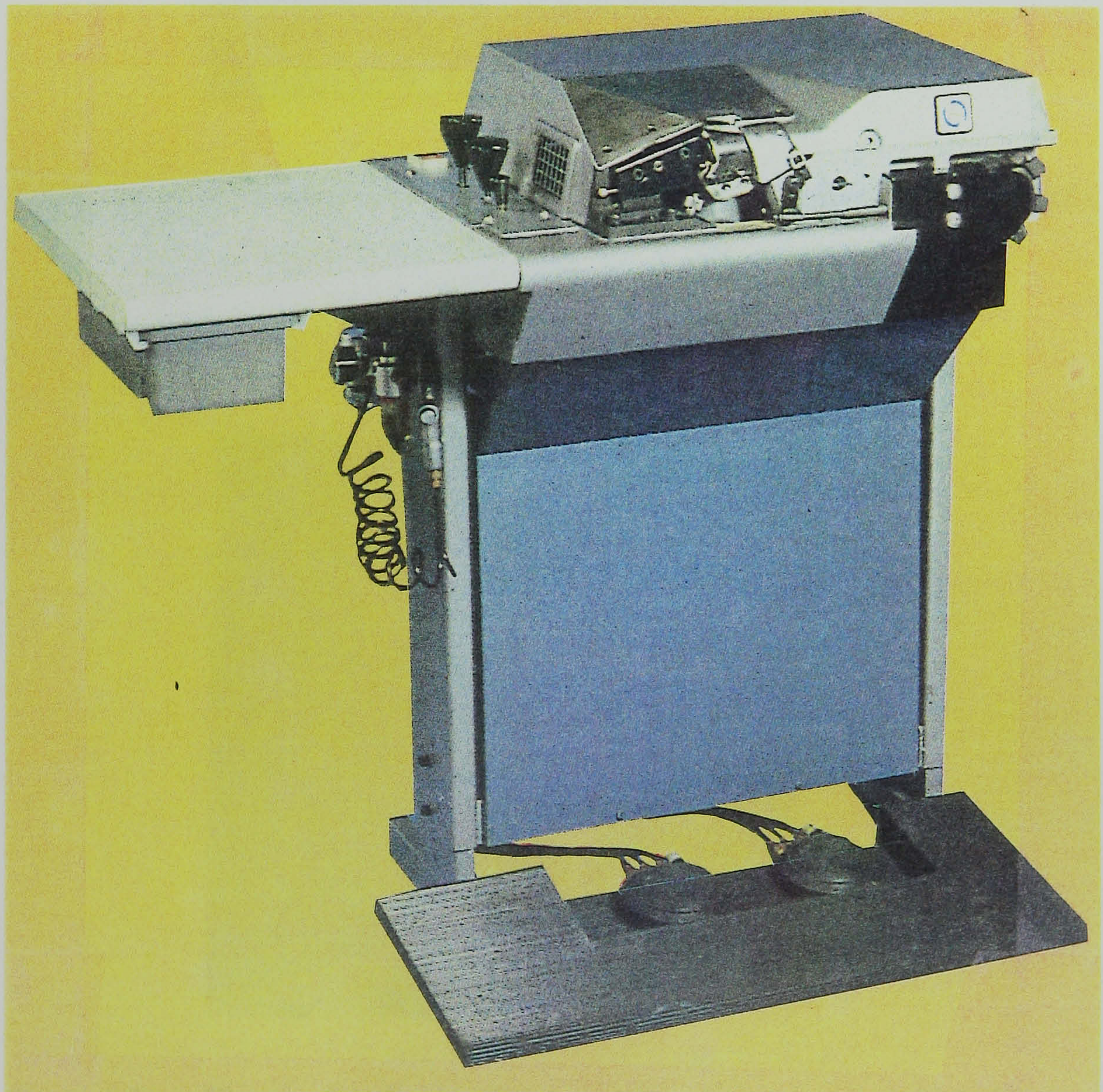


Figure 1.2 Diagrammatic presentation of skiving in leather components.



The operation of skiving is achieved when the human operator offers the shoe components to a skiving machine. This machine employs a rotating disc which is continuously sharpened at its perimeter. By correctly manipulating the component through a feed mechanism, and against the sharp edge of the disc, the required material removal takes place. A typical lifetime of the skiving disc is approximately 3 to 4 weeks. Typically, in a small to medium sized factory, there are 8 to 10 skiving machines in operation, each operating between 4 to 8 hours each day. The length of the time that an operator takes to achieve skiving on a component depends on the size of the component and the number of skived edges it requires. A small component can take the operator under 4 seconds to complete skiving, while a large component can take the operator over 9 seconds [3].

Figs. 1.3, 1.4, and 1.5 show the features of a typical skiving machine, and fig. 1.6 show some examples of skived parts.



*Figure 1.3 A typical skiving machine (By permission, BUSM Ltd.).*





*Figure 1.4 A close-up view of skiving operation (By permission, BUSM Ltd.).*

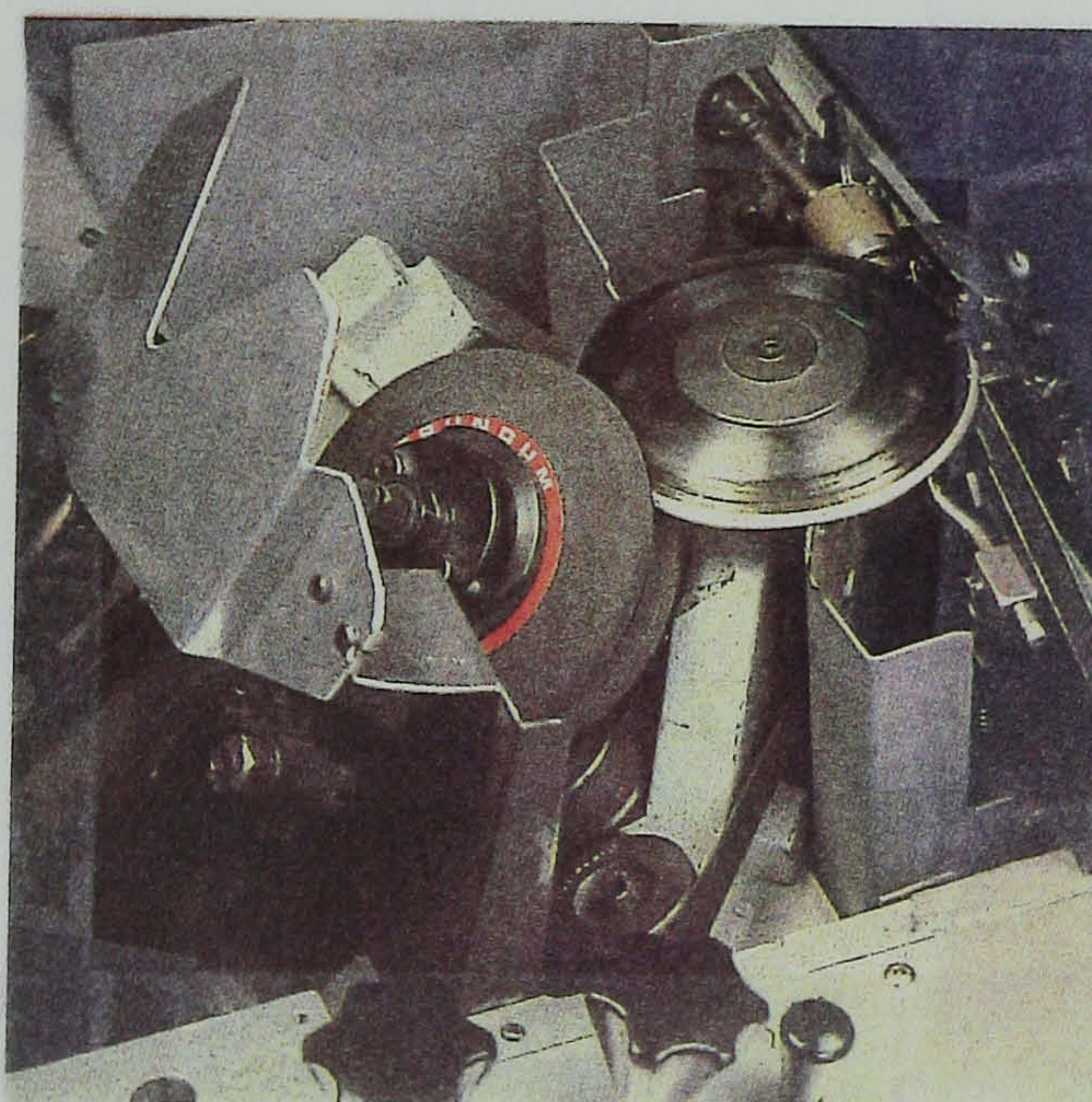


*Figure 1.5 The rotating disc in skiving machine (By permission, BUSM Ltd.).*





*Figure 1.6 Examples of skived components (By permission, BUSM Ltd.).*

#### **1.4 Specifications for automation**

The research into the automation of the skiving process in the manufacture of shoe uppers was required to be carried out with certain specifications. These specifications were to ensure two sets of conditions; (a) to ensure that the developed automated skiving machine maintains the standards of the present day technology in terms of quality and production rate, and (b) to ensure that the developed automated skiving machine is compatible with other automated process machinery in the shoe upper manufacture.

In order for automated the skiving process to be compatible with other automated processes, a production rate of 5 to 10 seconds per component is required. This figure is based on the specifications of an already developed automated stitchmarking machine [4]. The automated skiving machine must also be able to accept most common leather components types and sizes. For this



reason a maximum component length of 0.5 m (to cater for a boot length) is assumed.

### **1.5 Layout of the thesis**

The main body of the thesis is divided into four main areas of work. The first area of the work, in Chapter Two, covers a preliminary investigation to identify and examine two different methods for leather machining, namely High Speed Machining of leather and Matrix Skiving. The second area of the work is presented in Chapter Three where the physical properties of leather are examined so that their likely effects on its machining properties can be determined. The third area of the work deals with the evaluation of the machining properties of the two established methods of leather machining by way of theoretical and experimental determination. Chapter Four deals with the theoretical and experimental description of a rig that was specifically built to measure important parameters in the High Speed Machining system. The results of these experiments are subsequently produced in Chapter Five. The method of experimentation and the results of the tests of the Matrix Skiving system are presented in Chapter Six. The fourth area of this work is given in Chapter Seven where some of the important integration considerations for systems automation are discussed.

## **CHAPTER TWO**

### **PRELIMINARY INVESTIGATION FOR AUTOMATION**

#### **2.1 Introduction**

In this chapter initial investigations are carried out to examine the feasibility of the possible techniques that can be implemented for the automation of the skiving process in the manufacture of shoe uppers. In these investigations, where new methods for the operation of dedicated devices are examined, work was directed towards the feasibility demonstration of two alternative automation principles. The characteristics of the desired technique will become more apparent where, at a later stage of the investigation, more detailed design characteristics develop. This is particularly true when there is no overwhelmingly preferred method available at the initial stages of the investigation. However, the techniques that are considered are initially thought to possess the potential to satisfy the specifications that are laid down in Chapter One so that the industrial justifications are met. The aim of this chapter is therefore to introduce those principles that show signs of realistic capability for implementation, and are within the scope of this work. The initial examination of these methods is given in this chapter where the important and critical design parameters are identified. A more thorough and systematic investigation aimed at the evaluation and optimisation of these parameters is then presented, separately for each principle, in the later chapters.

In the following sections conceptual configurations based on two inherently different techniques are presented with the aim of arriving at the most suitable designs worthy of further investigation. Initially, the techniques are introduced. Then, introductory description of these principles, together with their possible design configurations and the associated critical parameters are discussed. Upon identification of these designs, preliminary experimental investigations are subsequently carried out, in later sections, to ensure that the results they produce are potentially in line with the principal aim of this work. Finally, the role of the



properties of materials in the skiving methods that are considered is briefly introduced.

## 2.2 Alternative automation concepts

Two distinctly different material removal principles of a fundamentally mechanical nature are considered. The first principle involves the application of machining operation in skiving, and the second principle relies on the action of a knife to achieve skiving. The operational techniques in these methods contain different features that play a critical role in the shape of the final system; ie. the actual principle by which the material is cut and removed from the workpiece.

The machining operation, in the form of milling, in a skiving system involves a material removal process whereby the profile of the machined surface is the resultant of a combined rotary and linear motion of a cutter such that the outline of the body of revolution generated by the cutter determines the geometry of the machined profile [5]. In such a system, leather as the workpiece is initially clamped on a work surface, while a cutter, rotating about its own axis and mounted on a moving head assembly capable of traversing in three dimensions, produces the required skived pattern on the leather. Alternatively, the operation that employs a knife to achieve skiving involves passing the leather component by means of a feed roller over a rotating band knife such that the whole area of the leather is exposed to the knife, but not engaged with it. Any local engagement of the leather with the knife results in removal of material from that part of leather. Correct synchronisation of this engagement with its speed of travel over the band knife produces a desired skived pattern on the leather. This technique is termed *dynamic matrix skiving* since it involves the application of localised knife engagement with the leather component. The method is principally similar to the case of the present matrix skiving machine which uses a two dimensional matrix plate to bring the leather in contact with the knife.

Sections 2.3 and 2.4 discuss these concepts in more details, both in terms of systems general configuration and specific design proposals, and attempt to extend their applications to the automation of skiving process in the manufacture of shoe uppers by conducting initial experimental investigations.

## **2.3 Principle of machining technology**

In this section the method of operation of the machining technology as applied to the automation of skiving of leather is introduced. First, general and introductory notes on this principle are presented, and then, a more specific system configuration and its more critical design areas are discussed in more details. Later in this section, the description and the results of preliminary experimental investigations are produced.

### **2.3.1 General system configuration**

The technology of machining operations has traditionally progressed in the area of metal cutting [6]. This includes the milling operation with numerous work published on both the application and its machining science where emphasis is placed on the optimisation and efficiency of metal removal in manufacturing engineering environments [7][8][9][10][11][12]. Some work has also been done in the machining of plastics [13]. However, there is no relevant published work in the application of milling technology on leather as the workpiece and, if they exist, like many other industrial processes of leather, are invariably treated as confidential material confined to the private libraries either in specialised research establishments or commercial sectors. The main reason for this restricted public access is related to the few, but specialised, applications of leather in certain industries such as shoemaking and car manufacture where market competition necessitates commercial sensitivity. Nevertheless, the techniques employed in the traditional application of milling are well documented and many areas of its design and technology could be applied to new applications. Milling of leather is therefore considered to be an alternative method for the skiving process in the manufacture of shoe uppers worthy of investigation. Furthermore, the advances in the development of modern machine tools such as computer numerical control systems can help the automation of skiving process by milling technology. However, successful implementation of this technology in the skiving process requires major investigation so that its critical design parameters are suitably optimised.

Several cutting configurations using different types of milling machine systems and cutters are available, but the most suitable realisation for the skiving process is the concept of a vertical-axis face-milling system. Emphasis on the face milling system is due to the nature of its operation where cutting is accurately



achieved on flat surfaces [9], thus making it suitable for sheet workpiece components such as leather. The main components in a typical configuration of a face milling system comprise of a horizontal platform upon which the workpiece is firmly clamped, a vertical spindle capable of rotation about its axis, and a cutting tool mounted on the spindle. Typically the platform assembly can be traversed in two axes in the horizontal plane and the spindle can be moved in the vertical plane, but other configurations are encountered where 3 to 6 axes are provided by a combination of platform and spindle motions. The spindle is normally rotated by an electric motor capable of delivering sufficient power to overcome all resistive forces encountered during the cutting operation.

It is clear that such a material removal technique using conventional equipment would require a halt in the flow of the workpiece components during which machining takes place. It therefore offers a non-continuous flow, discrete part manufacturing system.

### **2.3.2 Face milling of leather**

Leather is not only a fibrous material variable in type and characteristics from skin to skin, but also an abrasive material, and thus the design of the cutting tool becomes highly critical for two main reasons. Firstly, its shape and the degree of its cutting edge sharpness must be capable of producing acceptable surface finishes regardless of the leather type. Secondly, since in the milling operation the unwanted material takes the form of small particle chip elements that are produced by the action of the toothed cutter where certain amount of rubbing is present, the inherent problem of tool wear cannot be ignored. The cutting tool material must therefore have a reasonable lifetime so that its use is economically justified. Cutting speed (rotational speed of the cutting tool) and feed speed (linear speed of travel of the cutting tool relative to the workpiece) are other design variables that must be optimised for a given tool geometry to give acceptable machining quality.

The implementation of the milling operation on leather as a possible technique for the automation of skiving process in the manufacture of shoe uppers therefore requires extensive preliminary investigation in order to evaluate and optimise several important design parameters as mentioned above. Also, in order to qualify as a serious proposition, there must be clear indications that an automated skiving machine employing this technique provides speeds of operation comparable to those of the today's technology, or better, as discussed in Chapter

One. Furthermore, the problems associated with the satisfactory clamping of leather material on the milling platform need to be addressed. Nevertheless, milling is a well established machining operation, and as such, many of its general machine design problems relating to machine stability and operation control have been solved. It is therefore the specific design parameters as mentioned earlier, rather than the general configuration of the system, that require further investigation.

The main features of an integrated machine system will include an optical recognition system to identify the shoe upper components, conveyor belts to transport the components, and the skiving machine to include the milling head assembly. When the conveyor belts deliver a shoe component to the milling platform, the component then becomes stationary and the flow of the parts on the conveyor belt to and from the skiving station is disrupted. An automated skiving system that employs milling technology is, therefore, not a continuous flow manufacturing system. This is a major disadvantage of the system and must be compensated for by increasing the speeds of operation involved so that the time interval between subsequent parts entry to the process cell, as well as the total skiving time, are minimised. The latter is achieved by maximising the feed speeds in the cutting operation, while the former can be achieved by introducing a multi-head system, whereby at any given time several parts are being skived as diagrammatically shown in fig. 2.1. The management of the tasks allocated to each cutting head can, say, either allow a complete skiving per component per section, or, allow a shared system such that the complete skiving task per component is performed by different cutters, one after the other, from the component delivery belt to the component departure belt. The advantage of the task sharing system is that it optimises the use of the cutting heads and facilitates faster flow of the parts through the skiving cell. The disadvantage of the system is, however, the introduction of a complex management control system requiring efficient and fast distribution of tasks between the cutting heads, as well as the increased machinery costs per cell.



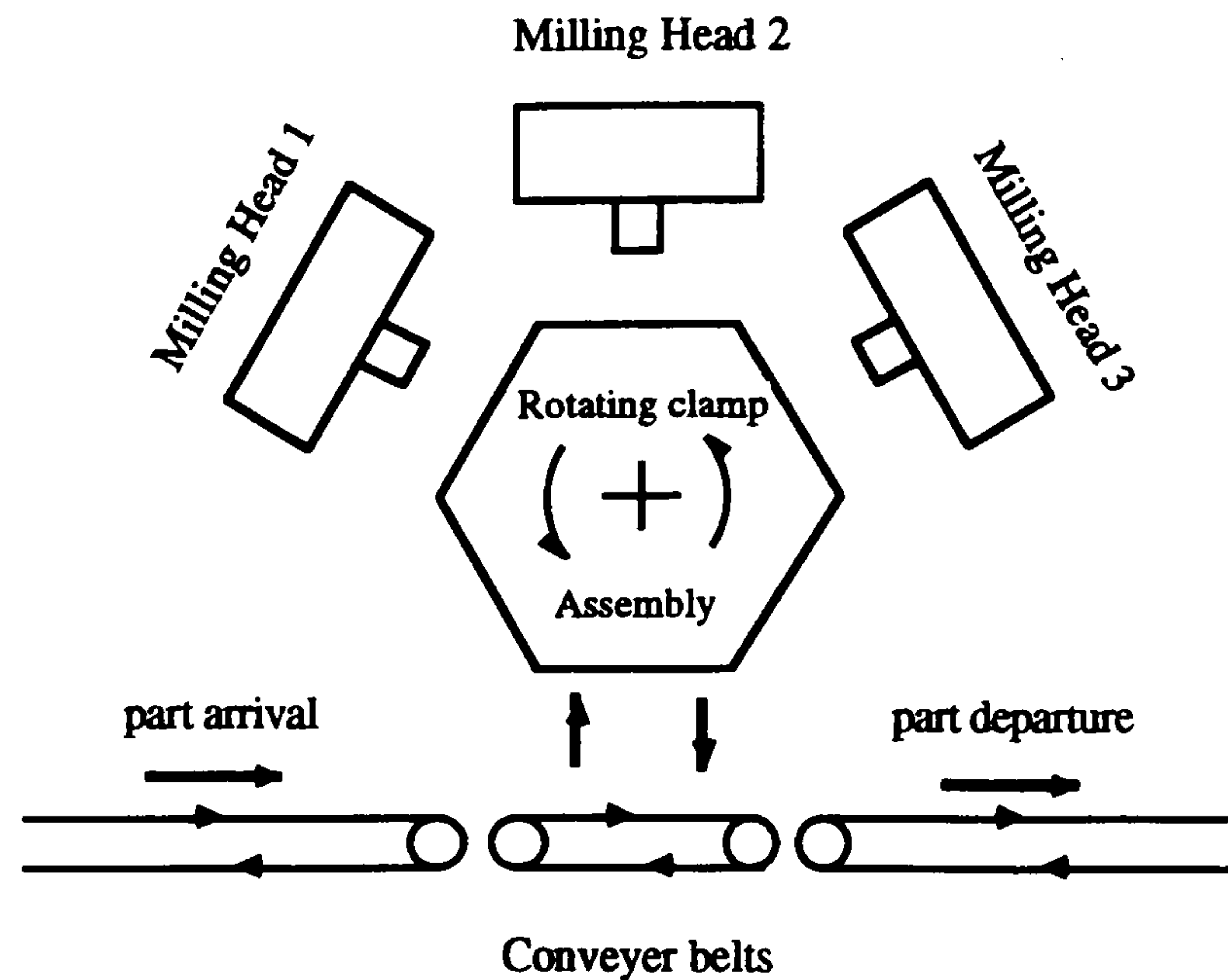


*Figure 2.1 An envisaged multi-head machining cell for automatic skiving.*

### **2.3.3 Preliminary experiments**

The preliminary experiments of the face milling operation involved the evaluation of several basic and fundamental parameters including the optimal geometric shape and type of the cutting tool, its tip material, the level of the dependency of the results on the leather type, and the method of cooling of the cutting tool required from the associated heat generation during cutting. Upon satisfactory completion of this initial stage of the experimentation, further experiments were then carried out to determine the range of magnitude of feed and cutting speeds involved. The preliminary evaluation of these parameters in this chapter are later used to help the design of a more extensive set of experiments so that their optimisation in terms of the quality of the surface finish of the machined materials, the transmitted cutting forces from the cutting tool to the workpiece, as well as the system power consumption are achieved. In general, high surface finish quality and low cutting forces and power consumption are to be desired. The information regarding the last two criteria is related to the efficiency of the system through which phenomena such as tool wear may be monitored.

Devising an efficient and automatic method of clamping of leather is of paramount importance for the practical implementation of such a system which relies heavily on clamping. Indeed, the evaluation of the likely range of cutting forces as mentioned above gives the required theoretical minimum clamping forces. Nonetheless, it is equally important to concentrate, initially, on the viability of the cutting mechanism of the system thus evaluating the cutting-related parameters before giving due attention to the clamping difficulties. Hence, to proceed with the work, leather samples were clamped on the milling bed by using strips of double sided adhesive tapes for experimentation purposes only. The associated bonding force provided by these tapes was sufficient to overcome any cutting force exerted by the cutting tools on the leather samples. Though use of these tapes are made throughout this work, proposals are made, in the final chapter, for a computer-controlled automatic method of quick clamping and releasing of leather and similar workpiece materials.

Milling of leather was performed using different types of standard milling cutters and rotary burrs with a standard vertical-axis milling machine. With feed speed of  $250 \text{ mm min}^{-1}$  ( $4.2 \times 10^{-3} \text{ ms}^{-1}$ ) and top cutting speed of 3000 rpm most of the samples showed poor results exhibiting material tear and totally unacceptable surface finish. In all cases the depth of cut was kept at 1 mm. Since the abrasiveness and fibrous nature of leather material as the workpiece resembled that of wood, its machining therefore required much higher cutting speeds. An electric domestic wood router of 450 W power rating was used to continue with the experiments. The router, mounted vertically on a manually operated 3-axis platform assembly, was capable of achieving no-load spindle speed range of up to 26000 rpm. The use of a portable router and the platform assembly, though quite inflexible, provided the first dedicated skiving research rig employing milling technology. The basic machining design areas mentioned earlier in this section are subsequently dealt with under separate headings as follows:

#### **i. Cutting-tool shape**

Several different cutting tools were tried and tested at the onset of the investigation each with different tip geometry. Fig. 2.2 displays the tools used at the initial stage of the investigation in the order in which they were tested, while table 2.1 gives their descriptions and tip materials. Against this figure, fig. 2.3 gives a subjective comparison of these tools in terms of their skiving quality



performance on an arbitrary scale where visual and tactile inspection of the surface finish of the machined surfaces of the test pieces are the basis of the results. Amongst the host of the cutting tools displayed in fig. 2.2 some tools are of identical geometrical shapes but with different cutting tip material. The effect of the tool material on skiving quality is discussed later in this section.

The quality performance figure shows a general steady improvement in skiving up to tool no. 8, ie. the spiral slot drill. The conical slot drill and the two cylindrical burrs (ie. tool numbers 1, 2, and 3) performed very poorly due to the insufficient sharpness at their cutting edges. However, the end mill cutter (tool no. 5) improved the results. Then the dovetail tools were tested, and were found to produce even better results. At this stage the shape geometry of the tools have been drastically changed. The reason for this improvement is thought to be the increase in the tool diameter and increase in their sharpness. The increase in the tool diameter produces higher periphery speeds of tool edge relative to the workpiece, and this seemed to improve cutting quality. However, at this stage of the experiments it was realised that tool shape played an important role in the surface quality results. Nevertheless, the results were so far very poor and below the level of acceptability.

Further trials of the tools with chamfered heads (tools no. 9 and 10) did not improve the surface quality. Due to their geometric shapes, these tools fundamentally offered single point cutting at their centre. Further trials seemed to slightly improve the results, but not to any significant measure. Indeed tool no. 13, the standard dovetail cutter, sharply decreased the skiving quality. When the standard inverted dovetail cutter, shown as tool no. 14, was tested, a dramatic improvement in the results was observed, where the skiving quality improved to a level far better than the acceptable level. The continuing concentration of the research for the geometric design of the tool shape was thus directed towards the optimisation of the inverted dovetail cutting tools. Further variation of this design with different tool angles and tip materials were tried and tested between the tool numbers 15 and 23. The critical tool shape parameters that were identified as a results of these tests, including the effect of centre cutting and the importance of rake and clearance angles, are discussed in depth in Chapter Four.



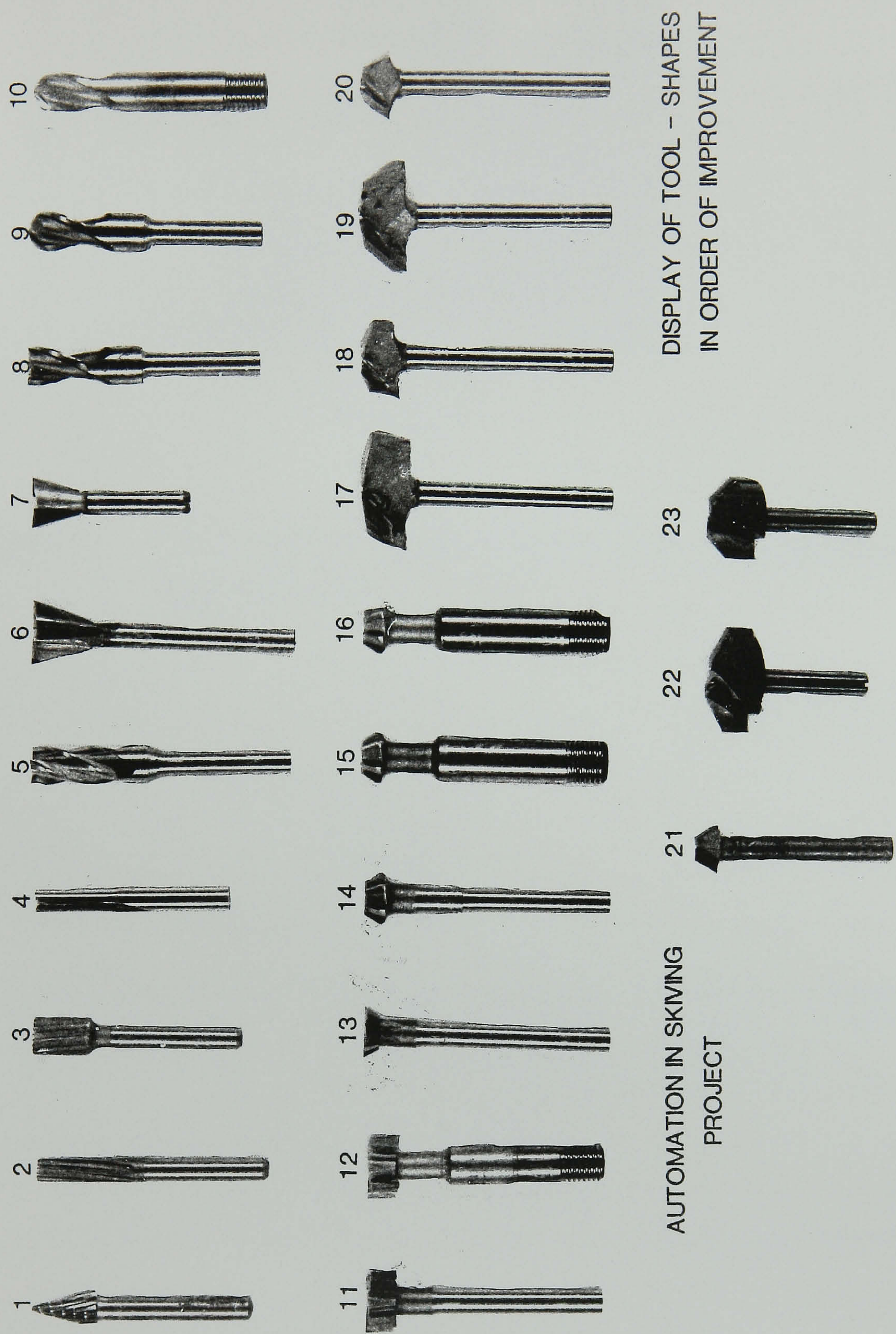


Figure 2.2 Display of the cutting tools tested in leather machining system.



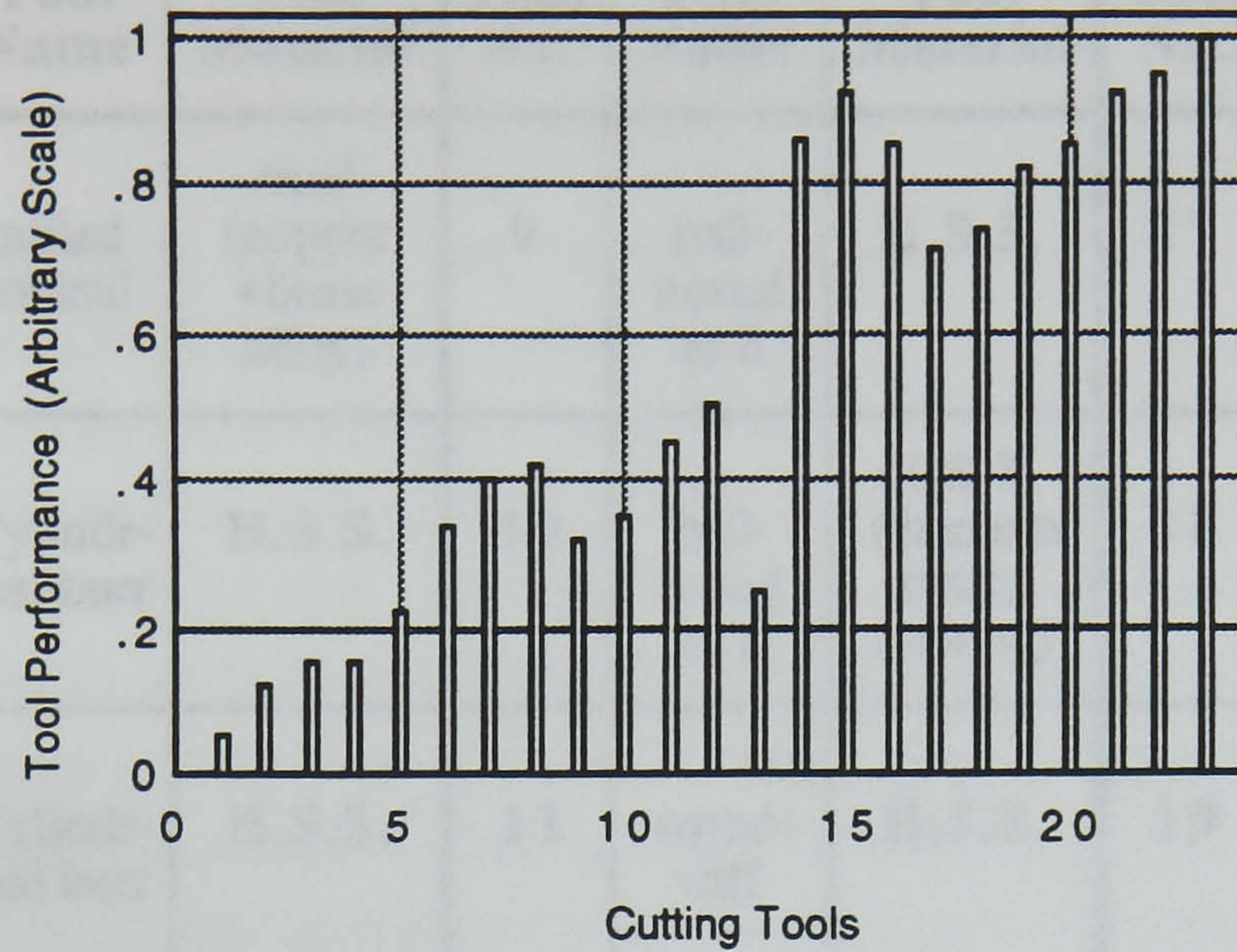


Figure 2.3 Performance of the cutting tools shown in fig. 2.3 compared in a subjective fashion.



Tool No.	Tool Name	Tool Material	Tool No.	Tool Name	Tool Material	Tool No.	Tool Name	Tool Material
1	milled conical	steel (copper +brass alloy)	9	ball-nosed as 8	H.S.S.	17	design-ed inverted dovetail	cemented tungsten carbide
2	Cylindrical burr	H.S.S.	10	ball-nosed as 8	H.S.S. (titanium nitrite coating)	18	design-ed inverted dovetail	cemented tungsten carbide
3	Cylindrical burr	H.S.S.	11	wood-ruff	H.S.S.	19	design-ed inverted dovetail	cemented tungsten carbide
4	straight edge router	H.S.S.	12	wood-ruff	H.S.S. (titanium nitrite coating)	20	design-ed inverted dovetail	cemented tungsten carbide
5	end mill	H.S.S.	13	dovetail router	H.S.S.	21	design-ed inverted dovetail	cemented tungsten carbide
6	dovetail router	H.S.S.	14	inverted dovetail router	H.S.S.	22	bevel trimmer	tungsten carbide
7	dovetail router	cemented tungsten carbide	15	inverted dovetail router	H.S.S. (carbide impregnated)	23	combination trimmer	tungsten carbide
8	spiral slot drill	H.S.S.	16	inverted dovetail router	H.S.S. (titanium nitrite coating)	-----		

*Table 2.1 Names and tip materials of the cutting tools shown in fig. 2.2.*

*Note: (H.S.S. = High Speed Steel)*

## **ii. Cutting-tool material**

An important criterion for the selection of a suitable cutting tool in an automation exercise where high amount of per hour cutting under normal conditions is expected, is the ability of the tool material to yield a reasonable operation time without excessive wear. On the other hand, leather is a very abrasive material and tends to wear out the tools made from soft tip materials such as high speed steel. The experiments with tools shown in fig. 2.2 also included tests where different tip materials are used as indicated in table 2.1. Initially, the standard tools were chosen from high speed steel materials. In the best case, where the inverted dovetail tool (tool no. 14) was employed, although near perfect surface finish quality was achieved with a new tool, after a couple of short test runs, the same tool gave poorer surface finish to an extent that any further cutting resulted in the generation of excessive heat and the subsequent burning of the test piece. This was due to the fact that much more rubbing than cutting took place.

To this end, several approaches to harden the tool tips were adopted including the impregnation of the tips with carbide and their coating with titanium nitride. Both of these methods tended to improve slightly the tool lifetime. However, when tungsten carbide tips were cemented on the tools their lifetime sharply improved to an extent that no significant deterioration of their machining quality due to lack of tool sharpness throughout this work was noticed. Detailed examination of tool wear during the course of the extensive and systematic leather machining experimentation is presented in Chapters Five. Tungsten carbide tools were therefore employed throughout this work. Accordingly, cutting tool no. 23 was used in the experiments that are discussed later in this section.

## **iii. Cooling**

The heat due to friction generated during cutting as the result of rubbing between the cutter tips and the leather samples was such that there was a tendency to burn the leather material in the process of material removal. As a consequence, several approaches were considered:

- a. The samples were sprayed with cold water just before cutting. No improvement was observed.



- b. The samples were immersed in cold water for 24 hours prior to cutting. Although the samples were soaked with water, again, the generated heat due to cutting tended to burn the leather material.
- c. Liquid nitrogen was sprayed over the samples just before cutting. The sub-zero temperature of the leather responded slightly better to the generated heat. However, the use of liquid nitrogen for cooling was abandoned due to its unknown future effects on the samples.
- d. A jet of high pressure damp air was directed at the tip of the cutter during cutting. The results were subsequently improved considerably such that the cutter tip together with the machined surface of the leather samples were kept at room temperature. No material burning was thus resulted.

Achievement of the satisfactory milling of leather, insofar as eliminating the heating problem by using an air jet coolant, resulted in using this method of cooling throughout the experiments.

#### **iv. Feed and cutting speeds**

Earlier in this section it was mentioned that satisfactory face milling of leather requires high cutting speeds. It is therefore important to evaluate the range of the cutting speeds so that effective skiving is achieved. It is generally desired to produce an acceptable surface finish with a minimum cutting speed. This is so because cheaper and more compact spindle drives can be employed. Also, since the production rate of an automated skiving system is directly related to the system's feed speed it is the consistent aim of this work to achieve the highest possible feed speeds within the physical limits of the experiments.

The experimental rig now consisted of a clamped router mounted on a bridge assembly such that it could be manually traversed along the horizontal span of a bridge platform through recirculating linear ball bearings thus giving the router a horizontal degree of freedom. The second degree of freedom was achieved by providing the router clamp assembly with a manual precision vertical adjustment in order to achieve the desired depth of cut. The entire cutting head assembly was placed directly above a horizontal flat platform on which leather samples were firmly clamped. The platform was mounted on an assembly which was allowed small, and low-friction perturbation in the direction of the cut. In the process of machining, the exerted cutting forces caused restricted deflection of the platform



whose magnitude was directly related to that of the component of the resultant cutting force in the direction of the cut. This made the platform assembly a simple dynamometer capable of measurement of quasi-static cutting forces. More detailed description of the dynamometer together with the initial cutting force results are presented later in this section.

At this stage of the initial investigation, and given the simplistic design of the rig, only approximate guide-lines of the effects of the feed and cutting speeds on the surface finish quality could be sought. The linear feed was therefore achieved by manually traversing the router along the length of the test pieces in two speeds of  $0.01 \text{ ms}^{-1}$  and  $0.1 \text{ ms}^{-1}$ . The rotational cutting speeds were achieved through an electronic variable speed switch provided in conjunction with the router thus enabling it to deliver no-load rotational speed range of up to 26000 rpm. A practical difficulty associated with the cutting speed was that, under load conditions, the torque developed at the head of the spindle caused a reduction in its rotational speed to such an extent that torques beyond a certain magnitude dropped the speed to zero. This problem was solved by in-process monitoring of the true cutting speeds while employing a higher powered router in the extensive experiments discussed in Chapter Four. For the purposes of the requirements of this chapter however, a subjective comparison of cutting speeds was carried out by using the initial no-load speeds in the analysis.

The test pieces were cut from various regions of similar hides and were randomly mixed to reduce the effects of variable physical properties within the hides. The tungsten carbide tipped combination trimmer cutting tool (no. 23 in fig. 2.2) was used. By changing one variable at a time and using initial cutting speeds of 18000, 21000, 24000, and 26000 rpm, and feed speeds of  $0.01$  and  $0.1 \text{ ms}^{-1}$ , tests were then carried out to observe the effects of their variation on the surface finish quality. Each test was replicated four times and the mean values of the results were calculated.

Based on the visual inspection of the machined test pieces, three subjective surface finish quality categories of “good”, “acceptable”, and “failure” were given. These results showed that for all of the cutting speeds considered good skiving quality was achieved at  $0.01 \text{ ms}^{-1}$  feed speed. The quality results at  $0.1 \text{ ms}^{-1}$  feed speed were good at cutting speeds around 26000, but tended to deteriorate at lower cutting speeds. While only acceptable results were produced at intermediate cutting speeds of 24000 to 21000 rpm, the tests carried out at cutting speed of 18000 rpm resulted in failure. These tests therefore showed that the patterns



governing the machining conditions of leather are such that the quality of the surface finish of the machined leather improves with the increase of the cutting speed and the decrease of the feed speed.

#### **v . The cutting forces**

The dynamometer briefly described above acted as a cutting force measurement instrument. The rectangular milling platform was allowed to traverse freely along two parallel shafts, one at each side, through journal air bearings fixed at its corners. The function of air bearings was to minimise the frictional forces opposing the platform movement. At each side of the platform, and in the line of its traverse, a spring balance of 10 N maximum scale was positioned in such a way that under no-load conditions the platform was stationary in equilibrium. During milling, the amount of deflection of the platform along the shafts of its air bearings was directly proportional to the magnitude of the transmitted cutting force in that direction, which in turn was directly indicated by the spring balances.

The resultant cutting force is normally measured in two components, one in the direction of the cut, and the other in the normal direction to that of the cut. (Detailed theoretical analysis of the cutting forces are produced in Chapter Four). Using the test conditions and the testing rig described earlier, maximum reading obtained on the balances for each test was recorded to give the component of the cutting force in the direction of the cut. When the cutting head assembly was rotated through 90° with the dynamometer at its original position, similar tests gave rise to the readings of the cutting forces normal to the direction of the cut.

The cutting force measurement results showed a general trend of their increase when higher feed speeds were employed. Except for the lower cutting speeds of 18000 and 21000 rpm where the cutting force components in the direction of the cut actually decreased with the increase of the feed speed, the other cutting force results gave just under 60% increase from 0.01 ms<sup>-1</sup> to 0.1 ms<sup>-1</sup> feed speeds. So far as the cutting speeds are concerned, for each feed speed, mixed bands of cutting force results were obtained. However, the band with the maximum difference between its upper and lower limits occurred in the case of 0.01 ms<sup>-1</sup> feed speed giving around 65% differential in results. This value is considerably lower for the 0.1 ms<sup>-1</sup> feed speed. The cutting force magnitudes measured in both parallel and normal directions to that of the cut fell in a similar range of values.



The method of force measurement in these preliminary tests produced significant sources of error that can greatly influence the results. Nevertheless, since the object of these experiments was to observe the likely trends of the results and to determine the quantified range in which they fall, the conclusions reached so far in this section help to develop further and more accurate investigation of the machining method fully presented in Chapter Four.

Initial observation of the results of the experiments in this section also indicates that the physical properties of different leather test pieces vary greatly according to their original type of hide, or the location of the hide from which they are sampled. These variations are thought to influence the results. For example, the quality of the surface finish produced from samples cut from the hide's backbone area is, in general, better than those cut from the hide's belly area. Section 2.5 introduces the importance of the properties of materials in this work.

The primary conclusion of the experiments so far is therefore that good quality skiving is feasible by milling of leather though requiring more research to examine its possibility of achieving it at higher feed speeds.

## **2.4 Principle of matrix skiving**

The principle of matrix skiving can be realised in many different configurations. Section 2.4.1 attempts to sketch the general characteristics of a matrix skiving system giving its main design areas while section 2.4.2 discusses the most suitable arrangement chosen from a host of alternative designs giving its crucial design parameters. Later in the following sections the preliminary experimental investigation based on matrix skiving, together with the results, are presented.

### **2.4.1 General system configuration**

The concept of matrix skiving was introduced in section 2.2. Unlike the milling system, here the material is removed from the main body of the workpiece by the action of a rotating band knife. The unwanted leather material in this system of skiving takes the form of leather 'peels' that are sliced away from the workpiece. The band knife is mounted over two parallel axes pulleys whose effective perimeters lie on the same vertical plane. A supporting horizontal platform is positioned over the band knife assembly. An incorporated electric motor produces the rotation of the band knife. A feed roller is positioned in



parallel with the line of action of the band knife, and in a very close proximity to it. The feed roller is responsible for the delivery of the leather components over the band knife, and is driven by another electric motor whose speed determines the speed of the skiving operation. The leather component is clamped between the feed roller and a supporting roller while it is in motion. This is a continuous flow discrete part manufacturing system where the workpiece component is not subjected to a halt during the process.

In the system that is explained above it is assumed that the feed roller delivers the workpiece over the band knife without engaging it with the knife, such that no cutting takes place. In order to achieve a desirable removal of the unwanted material from the leather component, there has to be a positive action in a way of depressing the desired locations of the component onto the knife, just as the component is being passed over it. This depression consequently brings the desired part of the component in contact with the knife, and hence matrix skiving takes place. Fig. 2.4 shows the main features of such a system of automated skiving in a schematic form.

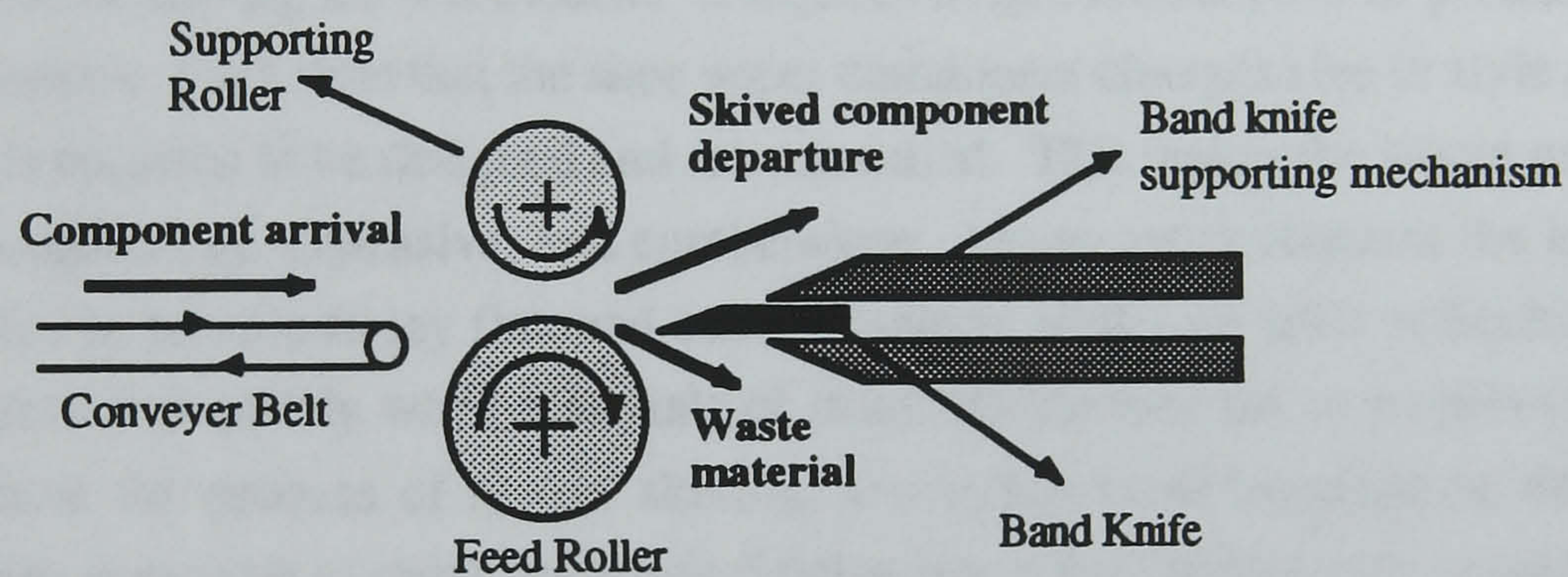


**Figure 2.4** A side view showing the cutting principle in matrix skiving

It is evident that, for a given skiving pattern, the speed of the feed roller determines the period of time that a particular section of the component is depressed. The precise synchronisation of the feed speed of the component with the time and duration of its engagement with the knife is therefore crucial.



Furthermore, it is conceivable that at any given instant it is very likely that more than one section of the component is to be skived. Provisions must therefore be made to facilitate instantaneous and simultaneous depression of the component as it is being passed over the knife, and at any necessary location along the effective part of the line of the knife.

There is already a form of man-operated mechanised matrix skiving machine available today [14]. The existing technology however has a very limited practical use and only a few shoemaking factories employ these machines for a small percentage of their skiving work. Though the present matrix skiving machines work on the same principle as described above, they allow no provision for the automation of the skiving process. In these machines, the local depression of the leather component for its subsequent engagement with the band knife is achieved by using a pre-formed three dimensional plate that is placed over the top surface of the components such that the component is forced to take the exact 3-D shape of the plate. When the leather component together with the plate are passed over the knife, and assuming there is no slip between them, those areas of the leather component falling sufficiently downwards will be engaged with the knife, and hence matrix skiving takes place. It is therefore clear that the matrix plate must have been initially so formed that the troughs it produces on the leather component match exactly the desired skiving pattern to be achieved. The drawbacks of such a method for skiving are self evident. It requires a rigid matrix plate to produce just one pattern. Each time that the shoe upper component changes size or style a new plate is required to be designed and manufactured. This makes the whole process time-consuming, expensive, and cumbersome. Moreover, it requires the leather material to be able to lay flat, and cannot perform well with rolls or buckles. It also performs poorly when materials of small thicknesses are to be skived. To automate the process of matrix skiving, provisions must be made so that the machine is capable of quick automatic adjustments when dealing with new skiving patterns. A system of self-forming mechanisms imitating the three dimensional effects of a an envisaged matrix plate is therefore desired.

#### **2.4.2 Linear matrix skiving**

In section 2.4.1 it was established that an automated matrix skiving system would require a mechanism with capabilities of quick automatic adjustments when dealing with new skiving patterns.



This calls for a system of actuators, that are independently controlled, and that can be programmed to depress the leather component, in the correct timings through their connecting pin mechanism. It is easily seen that each local engagement of the leather component with the knife, while the component is travelling over the knife, produces a groove on the leather whose width and depth to a large extent depend upon, respectively, the width of the actuator's pin and the force it exerts on the component.

The process of actuation can be achieved using several methods including the use of electric solenoids. For the reasons of system demonstration, readily bought solenoids offer simple laboratory installation and experiments. The position control of the solenoids may be achieved simply and cheaply through the use of microprocessor control systems. In general, it is envisaged that a bank of solenoids would operate reliably, quietly, and could be designed to occupy small space. They are also quite inexpensive.

Three main system configurations to achieve automatic matrix skiving can be envisaged giving different assembly arrangements for the required bank of solenoids. These are namely, linear, planar, and cylindrical matrix skiving systems. In each method however, the mechanism of the material removal remains unchanged. For the reasons of design simplicity and cost, the system of linear matrix skiving is chosen for further investigation. This configuration employs a single linear array of solenoid-actuated pins fixed and positioned over the band knife as shown in figs. 2.5 and 2.6. This is the most simple arrangement using the smallest number of solenoids and occupying the smallest amount of space. The design problems associated with this arrangement are relatively few, but it requires more complicated actuation control to produce a desired skived pattern on the leather component. The reason for this is because the occurrence and the duration of each stroke of each solenoid must be so accurately controlled that correct synchronisation with the speed of the feed roller takes place.



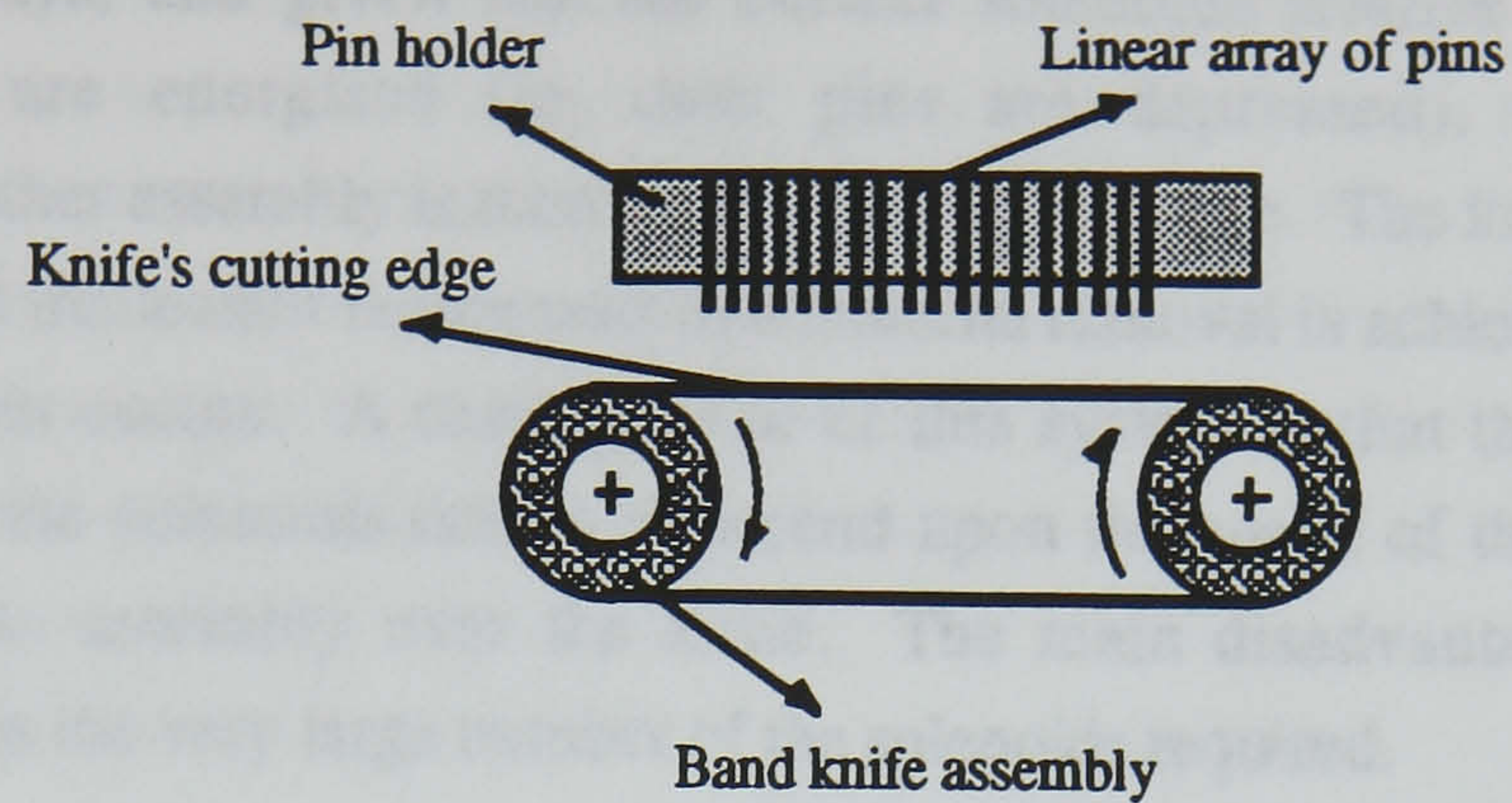


Figure 2.5 Diagram showing the linear matrix assembly above the band knife.

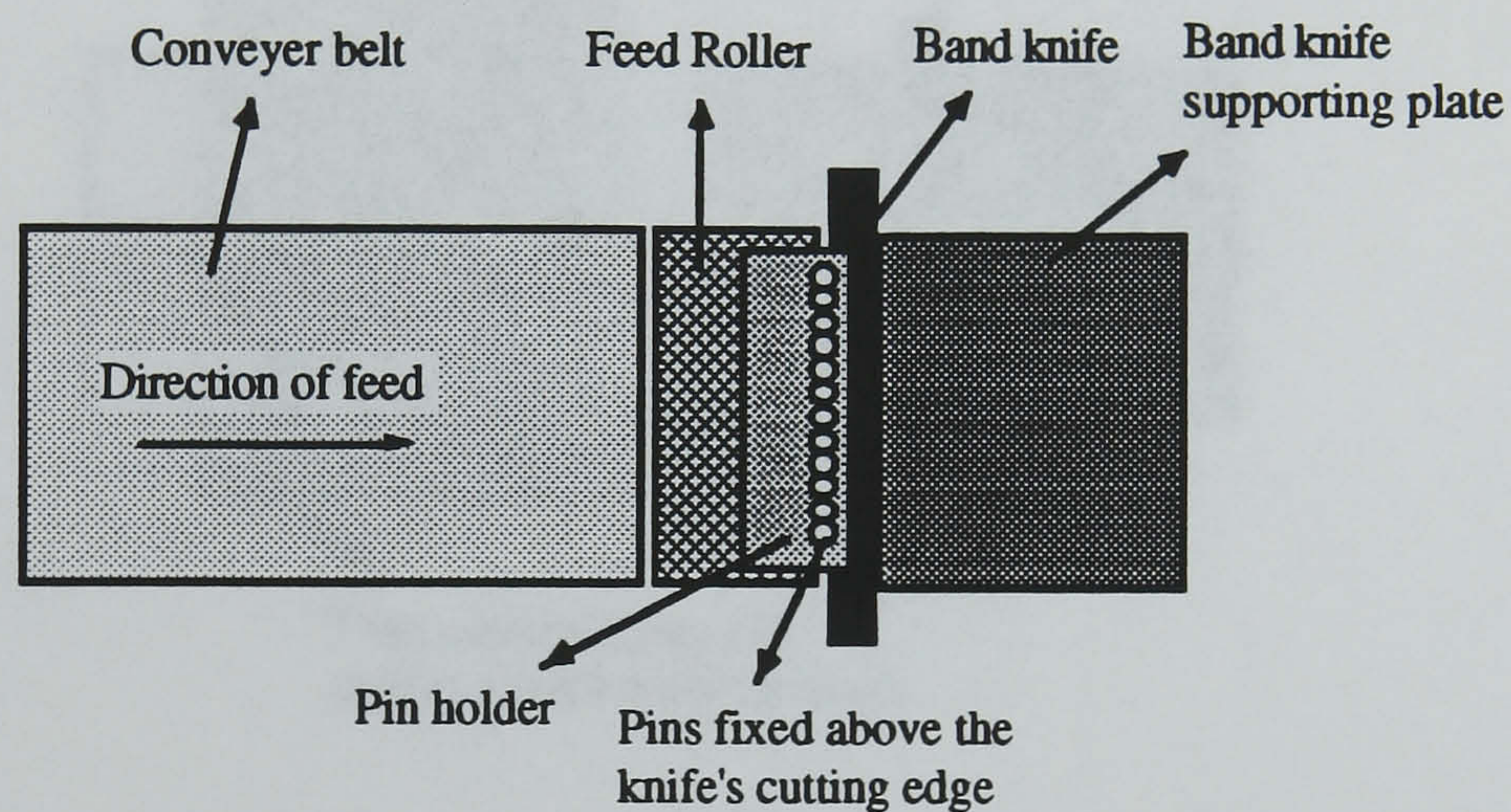
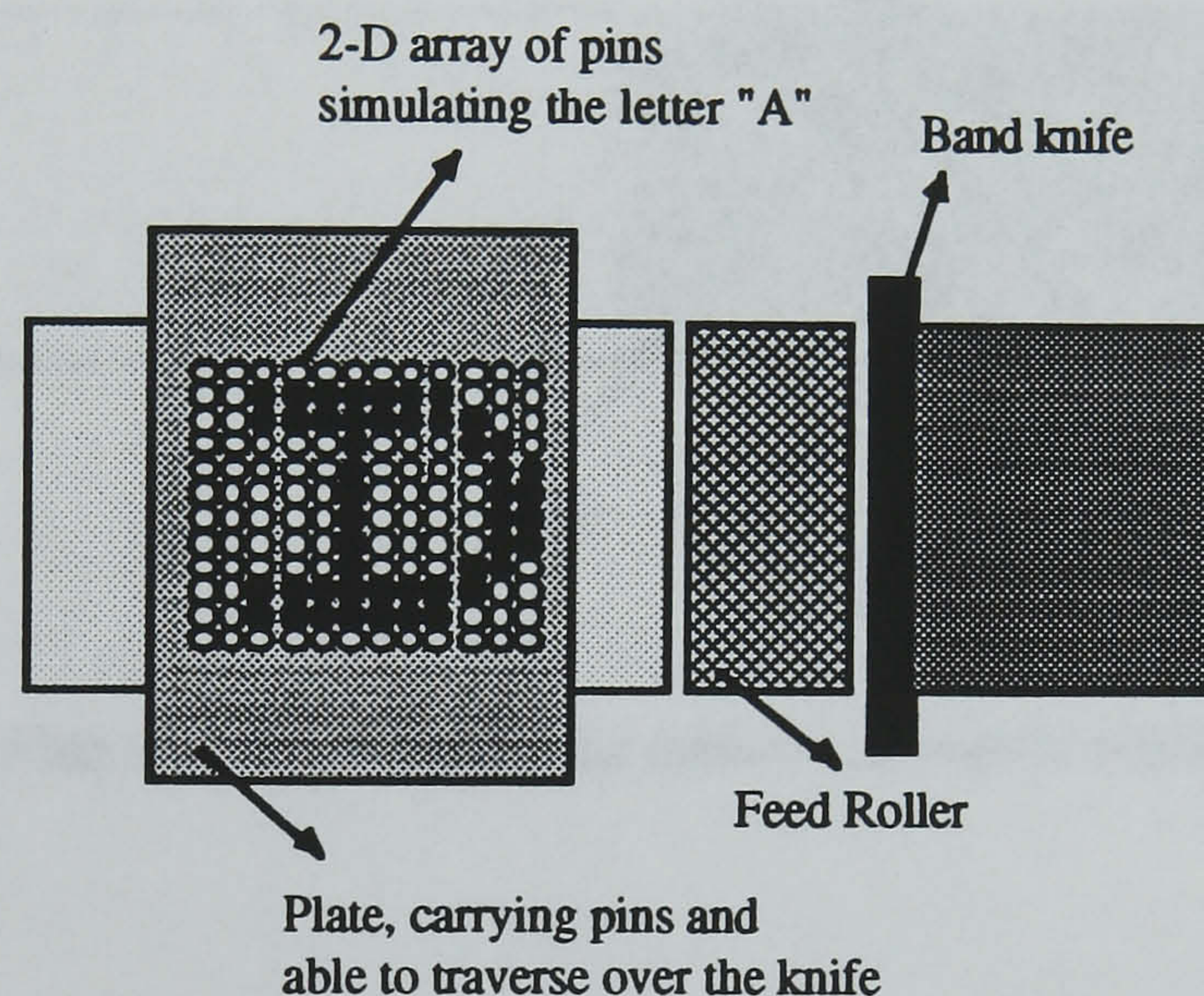


Figure 2.6 Plan view of an envisaged linear matrix skiving cell.

The planar or two-dimensional matrix skiving configuration employs a two-dimensional array of solenoids that is capable of traversing over the band-knife in a similar fashion to the matrix plate employed in the present day matrix skiving machine described in section 2.4.1. In such a system, the shape of the desired 2-D skiving pattern is mapped on the solenoid arrays prior to cutting. That is to say, the arrangement of the energised solenoids matches the desired skiving pattern, as shown in fig. 2.7. When the leather component is fixed under the



solenoid arrays, and given that the correct solenoids relative to the leather component are energised (ie. their pins are depressed), the combined solenoids/leather assembly is then traversed over the knife. The knife is therefore engaged with the leather component and material removal is achieved wherever a pin depression occurs. A characteristic of this system is that the speed of the actuation of the solenoids does not depend upon the speed of the travel of the solenoids/pins assembly over the knife. The main disadvantage of the 2-D arrangement is the very large number of the solenoids required.



*Figure 2.7 Plan view of an envisaged two-dimensional matrix skiving cell.*

And finally, the cylindrical matrix skiving configuration is an arrangement that gives a cylindrical bank of solenoids. Here, a cylinder is envisaged whose surface houses packed arrays of solenoids with stroke directions away from the axis of the cylinder. The whole assembly is positioned in such a way that the axis of the cylinder lies in parallel to, and above the band knife. The cylinder is allowed rotation about its axis. Having mapped the desired skiving pattern on the solenoids in a similar fashion to the case of the 2-D arrangement, and having set the speed of the rotation of the cylinder equal to that of the feed roller, skiving then



takes place as the leather component is traversed over the knife and under the cylinder as shown in figs. 2.8 and 2.9. Conceptually this is a more preferred arrangement to the 2-D configuration since it offers a faster, and a more continuous parts flow system. There are, nevertheless, two main disadvantages associated with this method. Firstly, it requires a large number of solenoids to cover the surface of the cylinder, and secondly, the design of such a physical assembly becomes complex.

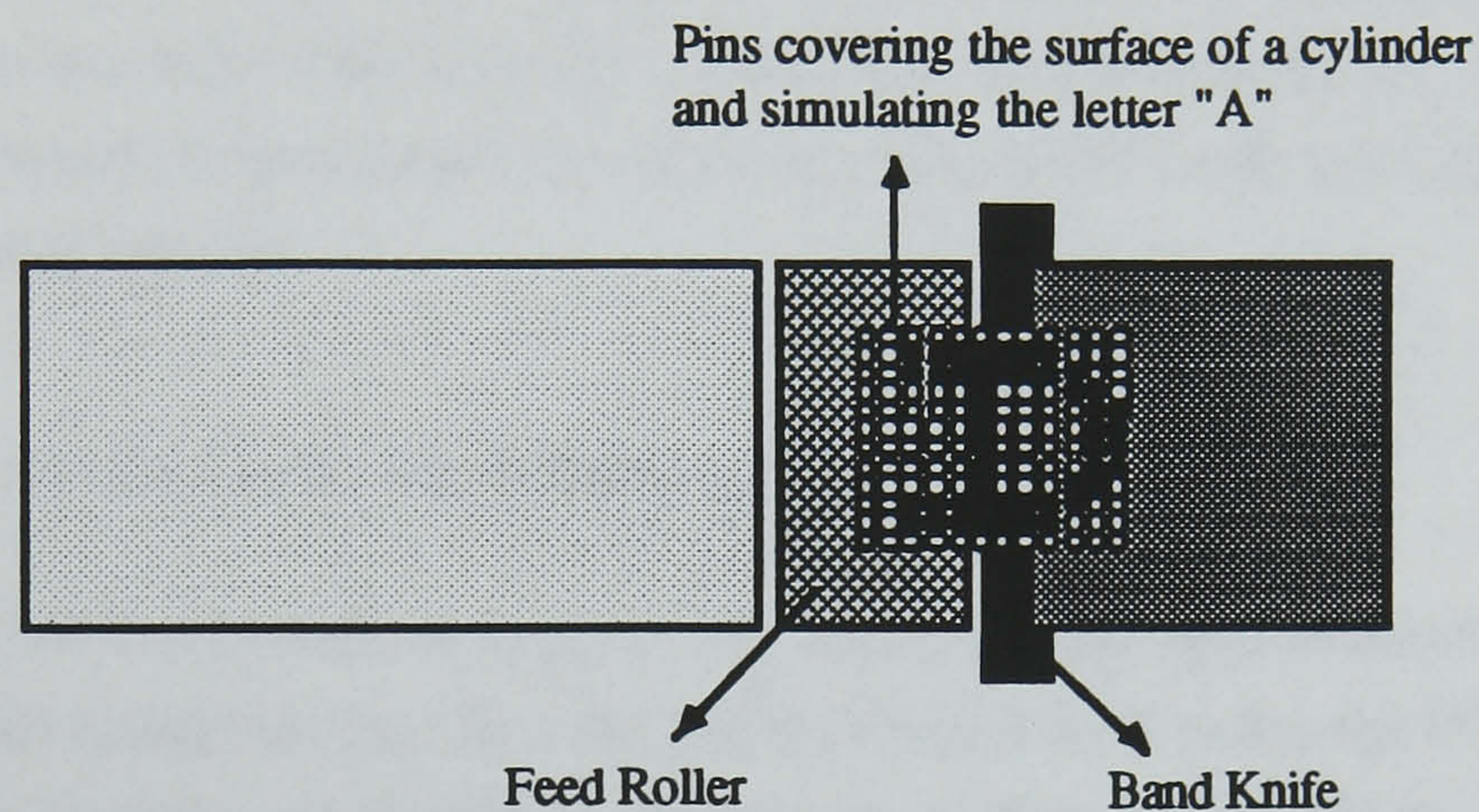


*Figure 2.8 Plan view of an envisaged cylindrical matrix skiving cell.*

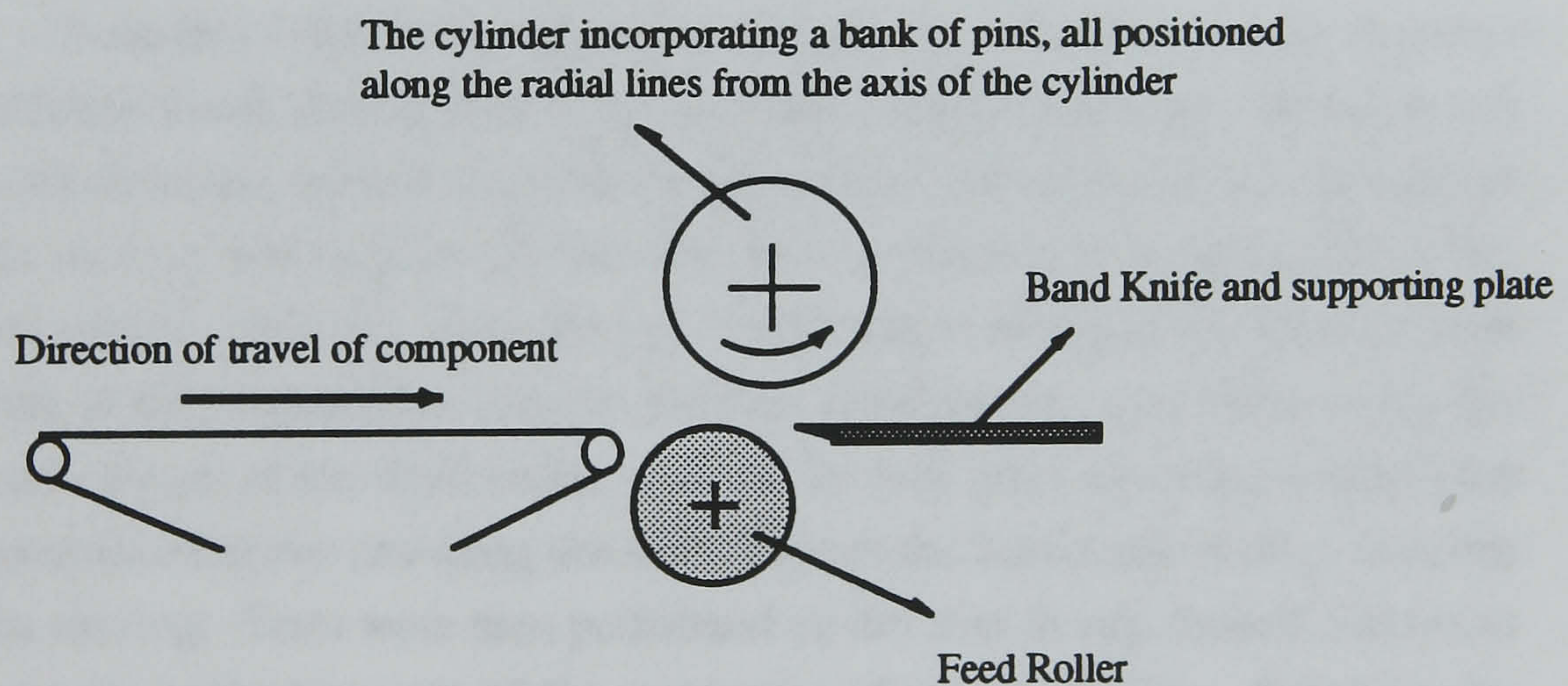


*Figure 2.9 A side view of the envisaged cylindrical matrix skiving cell.*



Since the desired skiving patterns can take almost any shape at random with skived lines of varying widths, it is evident that a high resolution matrix skiving system becomes a more attractive proposal in that a more accurate definition of a surface finish is achieved. There are however two principal reasons that such a high resolution system cannot be readily achieved. Firstly, the number of the solenoid actuators together with their associated independent control switches will dramatically increase, and as such tend to increase the cost of the system beyond the economical limits. Secondly, for a given span of effective knife length, the theoretical width of each actuator will decrease in such a way that a practical implementation becomes almost unrealistic. Nevertheless, acceptable skiving resolution must be achieved. Thus, the physical size of the actuators and their spacing are the two major critical design parameters in the investigation of the matrix skiving system.

#### **2.4.3 Preliminary experimentations**

One of the operations in the manufacture of shoe uppers involves splitting of the leather component so that the desired thickness is achieved [15]. This can also ensure that the component is of uniform thickness throughout. Splitting is carried out by using a mechanised hand-operated dedicated machinery known as the “splitting machine”. This machine uses a rotating band knife and a feed roller similar to those described in section 2.4.1. Since the actual cutting action of the knife on the leather components is successfully achieved by the splitting machine, its use is made to perform matrix skiving experiments by making changes and adaptations to it where necessary.

In section 2.4.2 it was argued that the size and the spacing of the actuators in the linear matrix skiving method are the major design parameters. Research was thus concentrated towards a sound understanding of the mechanics involved in matrix skiving, and in particular the effects of its resolution on the quality of the skived leather surfaces. The test rig, employing a splitting machine, did not provide drive mechanisms used to produce simultaneous actuations along the effective length of the band knife. Instead, a linear array of spring-loaded pins was positioned above and along the sharp edge of the band knife so as to simulate matrix skiving. Tests were then performed on the pins in any desired fashion to observe the critical aspects of the mechanics of matrix skiving. Based on the results of the preliminary experiments in this section, the descriptions of a more extensive experimentations in matrix skiving is presented in Chapter Six.



A more detailed description of the splitting machine together with the description and the results of the initial tests are presented below:

#### **i. The splitting machine**

The essential characteristics of the splitting machine include a band knife rotating at high speed, a feed roller, and a straight-edged clamping bar. The basic design of this machine is very much similar to the matrix skiving system described in section 2.4.1, except that the straight-edged clamping bar, instead of the supporting roller, is permanently positioned horizontally above the feed roller. The bar material is hard steel and the roller is of steel whose surface is knurled to increase its gripping power. When a leather component is fed to the machine by the operator, the feed roller begins to transport the component forward and towards the band knife in such a way that it remains continually clamped between the feed roller and the clamping bar. Therefore, the pressure area of the clamping takes the form of a straight line just before the sharp edge of the rotating band knife, and in parallel to it. A purpose of clamping is that it ensures that all sections of the leather component acquire an identical and uniform speed as it continues to be engaged with the knife, and is free of any buckling. It further acts to restrict the travel of the component only in the direction of the feed. The amount of splitting through the thickness of the component is determined by the amount of gap allowed between the feed roller and the clamping bar. This gap is manually adjustable through a mechanism on which the clamping bar is mounted.

The feed roller and the band knife are both driven by the same three-phase electric motor. The power transmission to the feed roller is achieved by means of a gear and a pulley system. There is a provision of sharpening the knife edge, while it is rotating, by a mechanism of two rotating grinding wheels. Fig. 2.10 shows a typical splitting machine that is used in practice.



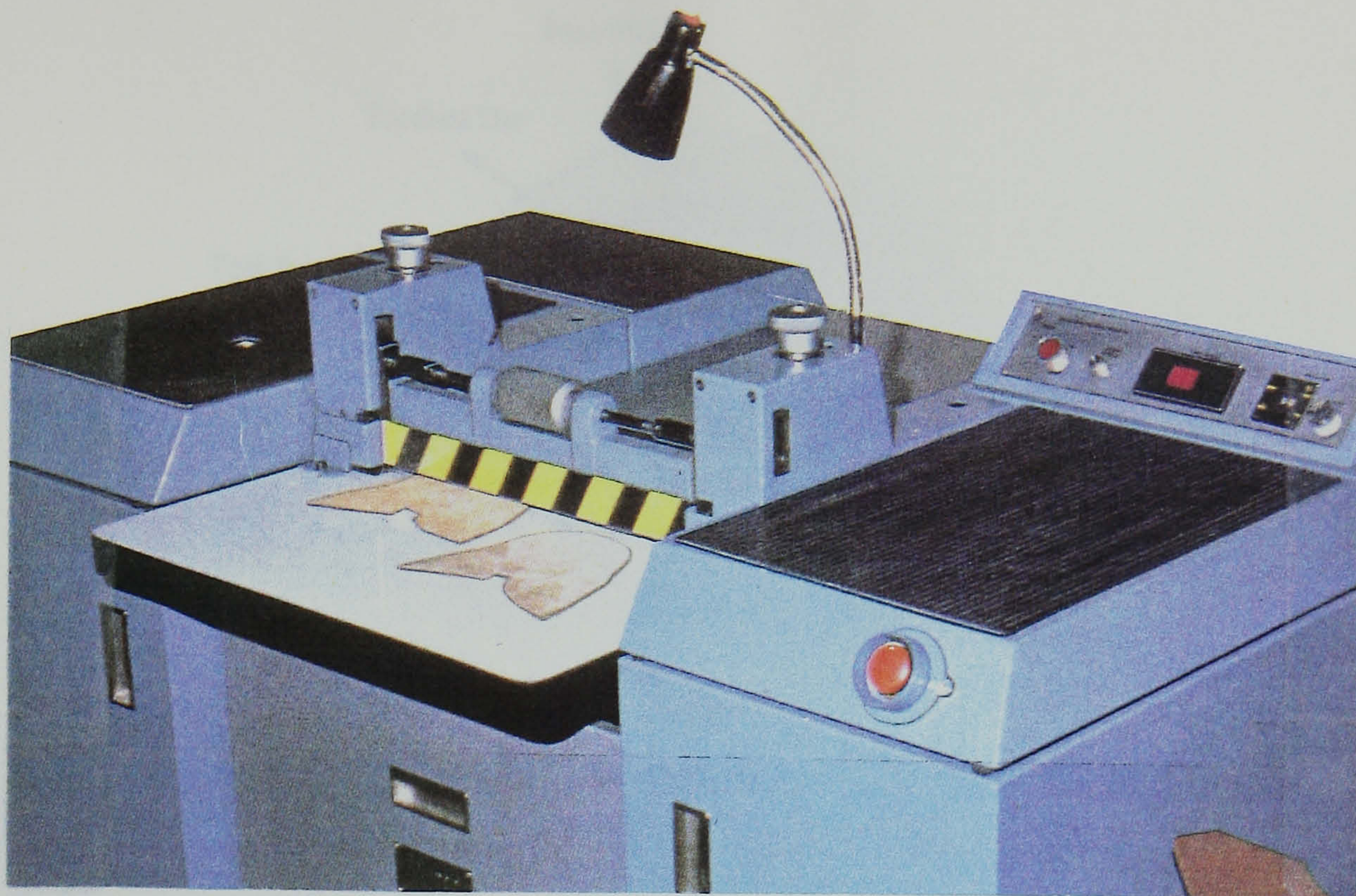


*Figure 2.10 A typical splitting machine (By permission, BUSM Ltd.).*

## **ii. Static matrix tests**

Simple matrix skiving experiments were carried out to primarily observe the performance of the existing splitting machine when used as a matrix skiving test rig. In these experiments semi-circular and toothed dies were cut from thick and stiff leather materials such that the peak to peak distances of the triangular teeth were fixed for each die. Each of these dies were then firmly stuck on a very stiff circular leather base plate of larger diameter. As a result, an elevated stepped triangular waveform was produced on the surface of the resulting composite plate. Circular leather test pieces of smaller diameter were then prepared. When a test piece was firmly attached on a composite plate so that it covers the teeth of the underlying die, a step on its surface was resulted, hence making the test piece partially elevated. Fig. 2.11 shows a diagrammatic illustration of a test piece on a composite plate, while figs. 2.12 and 2.13 show an actual static matrix die and a skived sample respectively.



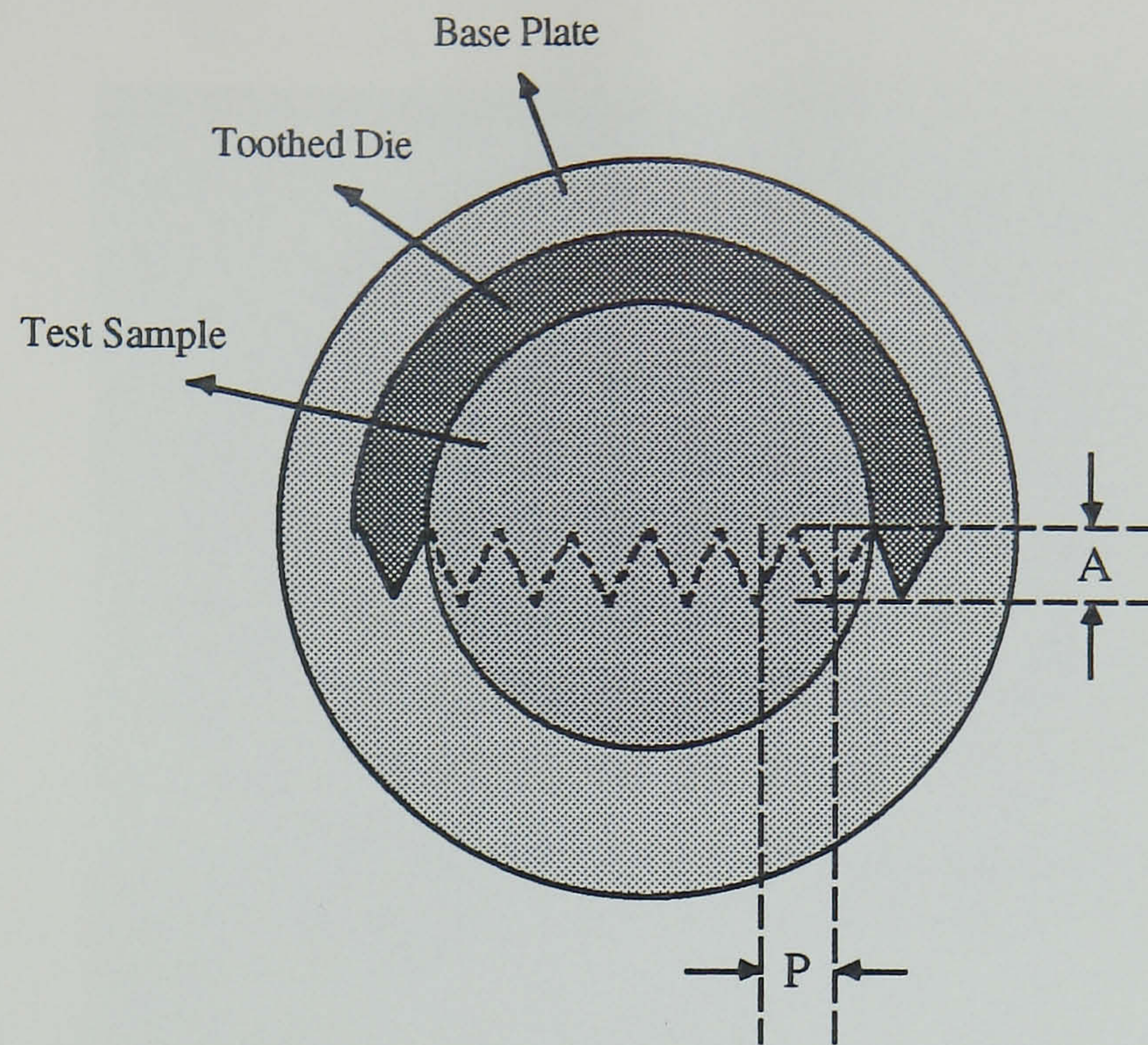


Figure 2.11 The composite plate used in static matrix skiving tests.

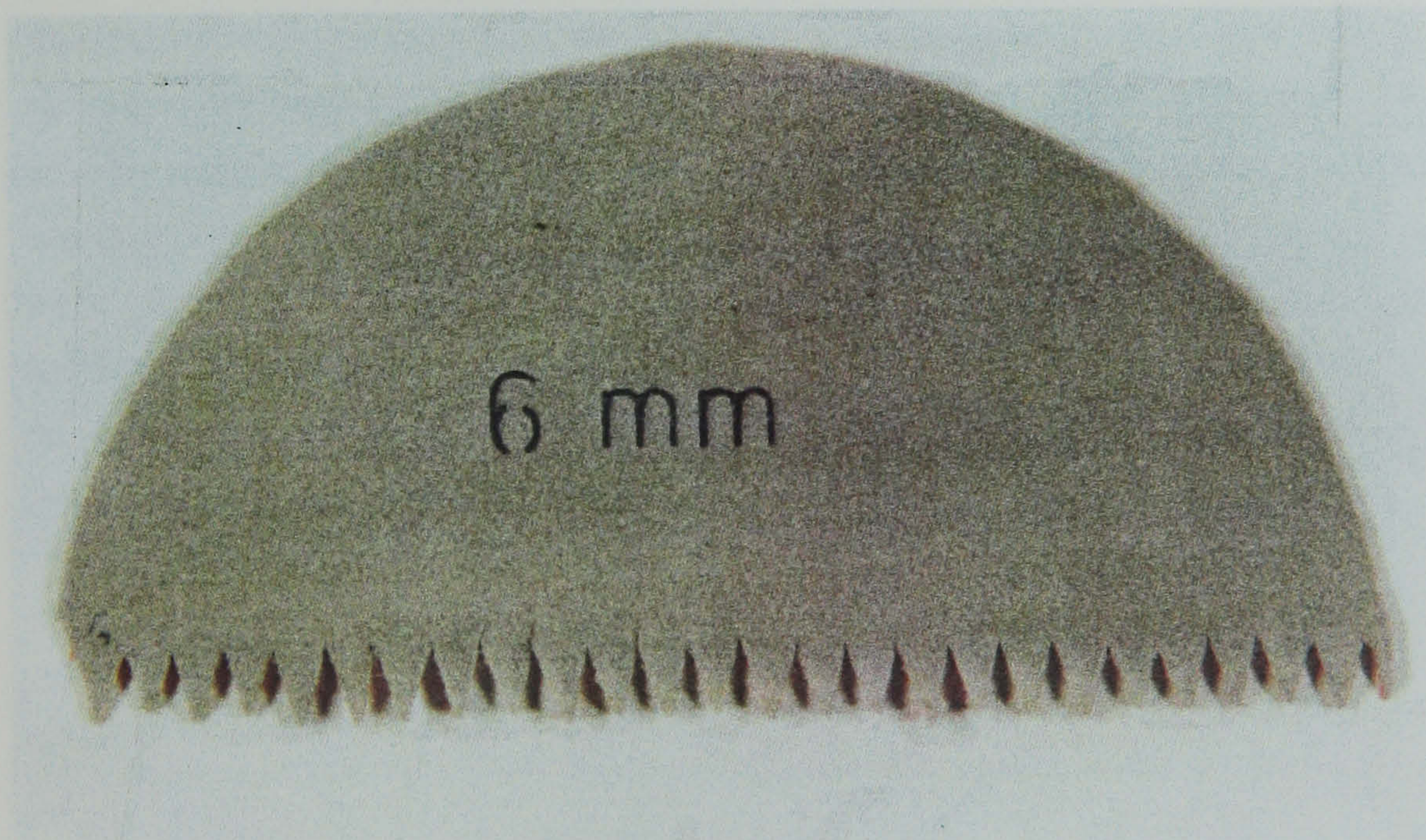


Figure 2.12 An actual static matrix die used in the experiment.





*Figure 2.13 A test sample after being skived using the static matrix method.*

The gap between the feed roller and the clamping bar in the splitting machine was so adjusted that only the elevated section of the leather test piece was allowed to be engaged with the band knife. The complete assembly was then fed into the splitting machine. Splitting of the elevated section of the leather test piece was then achieved on which imitations of the stepped teeth of the underlying die were produced. On separation of the test piece from the composite base plate matrix skiving had been achieved where the shape of the border region between the skived and the unskived sections was of triangular wave pattern of the same frequency as its original matrix. This is clearly depicted in fig. 2.14.



Skived section

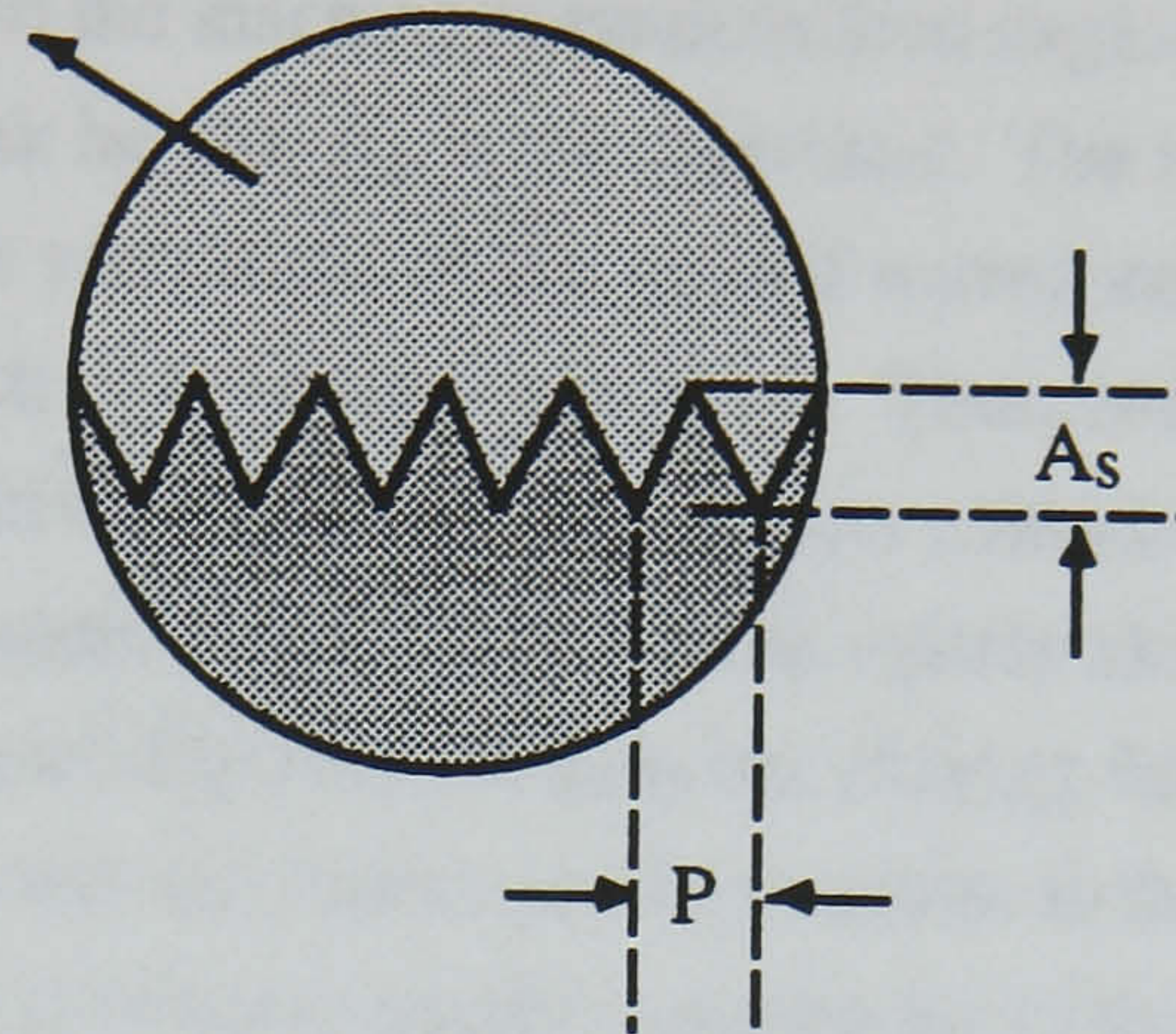


*Figure 2.14 Surface of a test sample after the static matrix skiving test.*

The object of this exercise was therefore to determine, as a first guide, the effects of matrix resolution on the quality of the skived surface. Also, since the concept of matrix skiving involves, to a certain extent, bending of material in the process of cutting, leathers of different flexibility were used in the tests to compare their skived qualities. This is particularly crucial when the effects of different matrix resolutions are sought.

Referring to fig. 2.11, the peak to peak distance between the teeth is marked by the variable  $P$ .  $P$  therefore is the pitch used in the matrix. Also, the amplitude of the triangular waveform, different for each die, is denoted by  $A$ . In order to quantify the performance of the skiving quality, the amplitudes of the waveforms produced on the skived samples,  $A_s$ , as shown in fig. 2.14, were directly measured from the test pieces. In a matrix skiving system the aim is to produce waveforms with as small amplitudes as possible (the desired case is a waveform of zero amplitude, hence a straight line), using the minimum number of matrix elements (thus reducing costs). The magnitude of  $A_s$  is therefore a measure for the skiving quality of a matrix system. The value of  $P$ , however, remains unchanged in the resulting skived surface.

The tests were then carried out with three different dies of 4 mm, 6 mm, and 8 mm peak to peak spacings on leather samples cut from three different hides of high, average, and low flexibilities. The selection of the hides according to their bending flexibility was, however, a subjective exercise and was performed



through hand examination only. All tests were repeated 10 times, where at each time the samples were fed to the machine at random feed angles. The mean values of the resulting peak to peak height,  $A_s$ , were measured. The results showed that, for all leather samples, the amplitude of the skived waveform pattern increased with an increase in the pitch of the matrix elements. Thus, increase in the matrix spacing deteriorated the skiving quality. The results also clearly indicated that leather flexibility had an appreciable effect on the matrix skiving quality. The leather samples of lower flexibility resulted in better skiving finishes than those of higher flexibility. It means that the former is less sensitive to the matrix resolution in skiving than the latter by producing smaller amplitudes of the skived waveform. The graphical presentations of the results are shown in fig. 2.15.

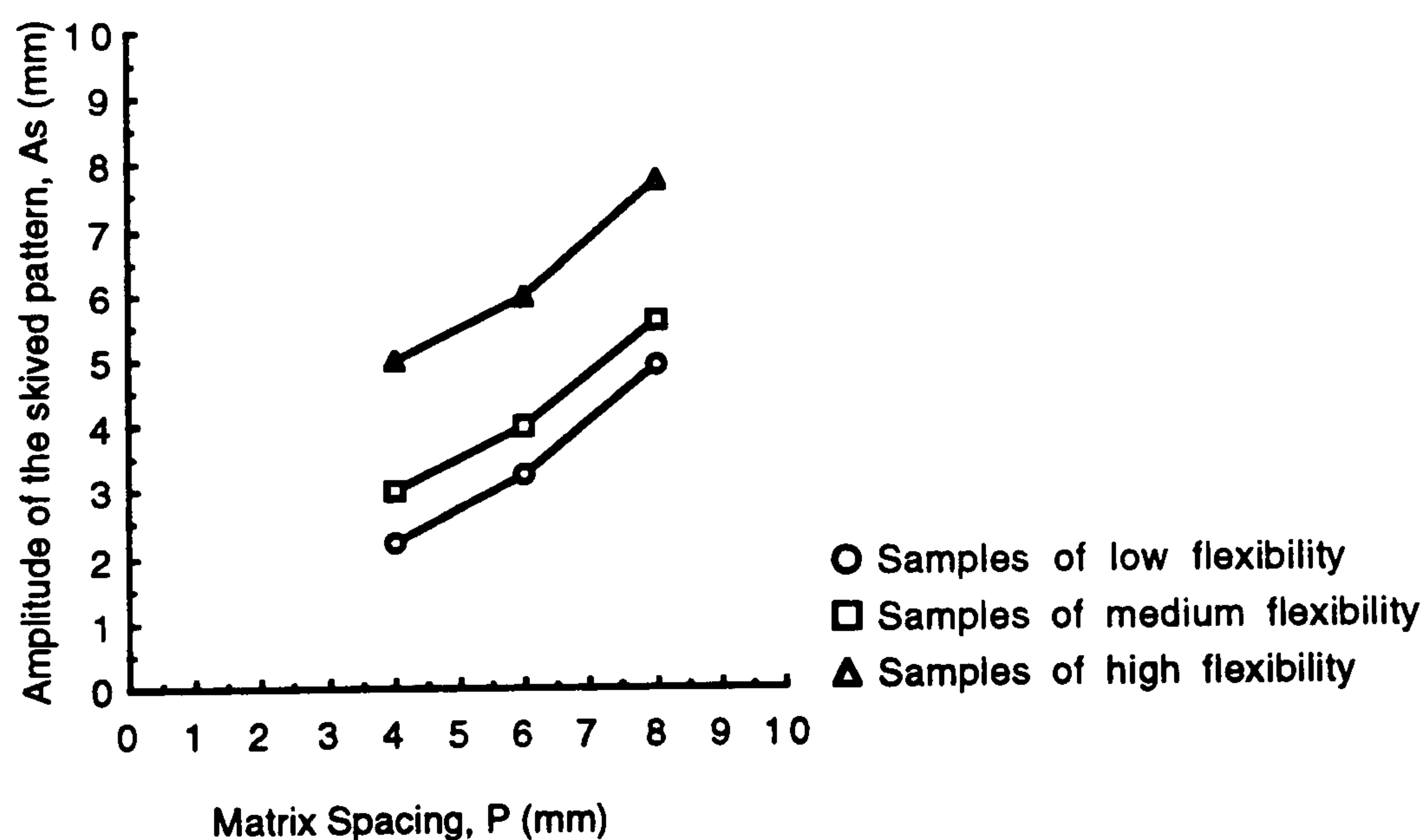


*Figure 2.15 Graphs of surface quality results in static matrix skiving tests.*

### iii. Design for a dynamic matrix system

The results of the above static experiments show that the basis of a splitting machine can be used to perform skiving, and that the quality of the end result



depends to a large extent on the matrix resolution and the properties of leather material. In the next stage of the preliminary experimentation it was desired to build a matrix system that is capable of independent activation of each constituent matrix element so that more comprehensive investigation becomes possible. To this end, the clamping bar of the splitting machine was replaced with a specially constructed hard steel matrix bar. The new bar incorporated a linear equidistant array of small and equal-sized holes through which identical spring-loaded pins were positioned. Each pin assembly was normally held in its most upward position, trapped between the associated compression spring and the stop provided in its hole, such that no further upward travel was possible. The pins could, however, be pushed down to their maximum reach against the action of their springs. Once released, the springs forced the pins to return to their normal positions again. The pins were manufactured from silver steel material. Fig. 2.16 shows a constructed matrix assembly giving pin diameter of 3 mm and edge to edge spacing of 2 mm.

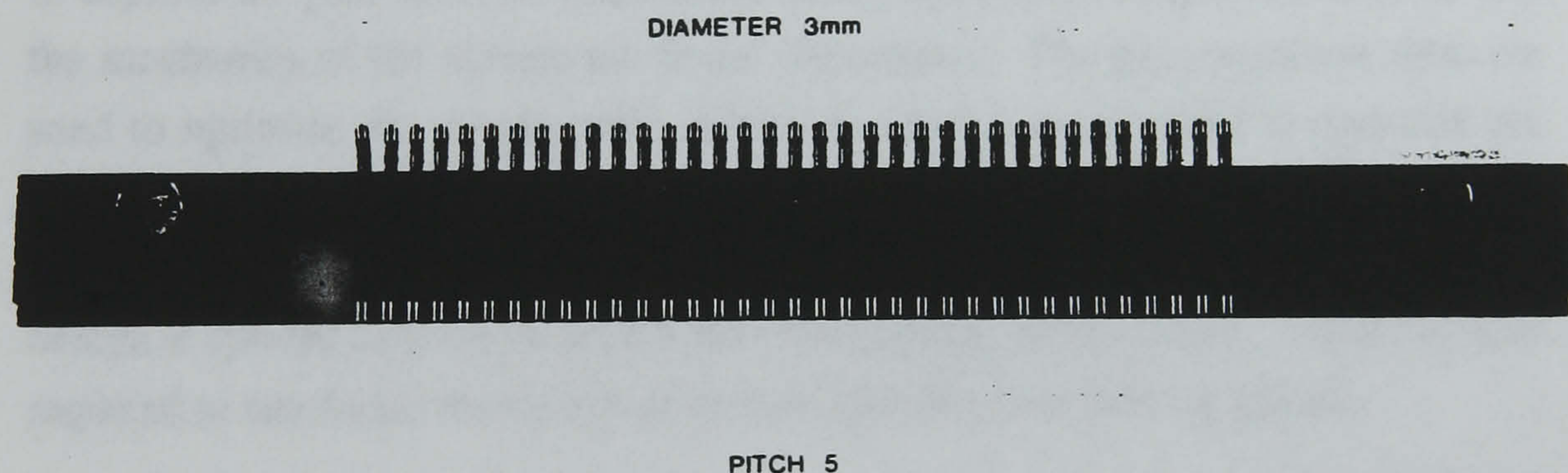


*Figure 2.16 Bar and pins assembly constructed for matrix skiving experiments.*

The bar itself was designed to continue to clamp the leather component by exerting pressure on the component as it is being transported by the feed roller. The line of application of this pressure was directly in line with the top centre line



of the roller, whereas the line of application of the pins was further along the direction of motion of the leather, and just before the knife edge.

With the complete pressure bar and pins assembly mounted on the splitting machine, the gap between the pressure bar and the feed roller was adjusted so that a leather component was passed through the system without being engaged with the knife. In other words, the component was passed by the roller beneath the array of pins and over the knife. If, however, during the passage of the leather component, a pin was actuated by being depressed sufficiently down so that it brought in contact the travelling leather with the knife, a groove was produced on the leather. When all of the pins are capable of such independent actuation, and assuming correct synchronisation between their actuation timing and the speed of the roller, a desired pattern may be cut on the leather component, and hence matrix skiving takes place. Initial tests showed promising signs insofar as the machine ability for matrix skiving is concerned.

In a system of pins explained above it is now possible to determine the effects of matrix resolution on skiving quality more systematically. In this case the variables become the effective pin diameter and pin spacing. Comprehensive tests are therefore required to be carried out to determine the effects of different pin diameters and spacings, as well as different leather types, on the skiving quality as described earlier in the static matrix experiments. Furthermore, the force required to depress the pins must be determined under different cutting conditions so that the mechanics of the system are better understood. The pin resolution tests are used to optimise the matrix array, while the force tests are used to optimise the actuation mechanisms such as solenoids. Since the speed of the skiving process is directly determined by the speed of the feed roller, it is critically important to design a system capable of high feed roller speeds of operation. Tests are also required to determine the effects of various speeds on the skiving quality.

The description of the rig together with the design of more detailed and systematic experimentations are presented in Chapter Six.

## **2.5 The role of the properties of material**

Leather is a natural material and is manufactured from different animal skins. It therefore carries within itself an inherent degree of variability in terms of physical properties. Some leathers are much lighter than others, while some are more fibrous than others whose fibre networks may or may not be densely



packed. Besides, The appreciable regional variabilities of physical properties within the same hide add even more to the degree of variabilities between different leather samples. Consequently, given the same cutting conditions, it is unreasonable to expect identical machining results from leather samples of different hides, or indeed, from different regions within a hide. The initial experimental investigations of this chapter prove just that.

In the machining experiments, when samples of densely packed fibres taken from the backbone region were machined, better surface finish was resulted than those taken from the belly region. In the case of matrix skiving, it was found that leather samples of lower flexibility gave rise to better surface finish than those of higher flexibility. These results showed a great amount of dependency on the material being skived. It is therefore appropriate to carry out extensive tests on the material's physical properties so that their correlations can be made to the skiving results. Optimisation of the skiving parameters, for both methods considered, are therefore made in order to minimise the material dependency of the results.

The subject of properties of material in relation to skiving is fully presented in Chapter Three.

## **2.6 Conclusions**

In this chapter preliminary investigations are carried out to examine two inherently different methods for the automatic skiving of leather in the manufacture of shoe uppers. The first method involves the application of high speed face milling of leather where fundamental machine design parameters were identified and discussed. The results showed that inverted dovetail cutting tools of tungsten carbide tip material, when used in conjunction with high cutting speeds and relatively low feed speeds give good surface finish quality. Leather burning was avoided by directing a jet of damped air at the cutting tool tip. This is traditionally a non-continuous manufacturing flow process whereby an interruption is made in the flow of the workpiece while cutting takes place.

In the second method, a linear array of independently actuated pins, placed over a rotating band knife, was envisaged to bring in contact the moving leather component with the band knife. A feed roller was employed to traverse the leather. A leather splitting machine was used to carry out static matrix tests where different resolutions are considered. The results showed that better skiving quality can be achieved when a higher resolution matrix array is used. In a design of



matrix assembly employing an array of identical pins, where dynamic tests can be carried out, the critical machine parameters would include pin diameter and edge to edge spacing, as well as the speed of the roller. Matrix skiving is a continuous flow manufacturing process since skiving takes place while the workpiece is moving.

In both cases it was found that the physical properties of material influence the quality results. Chapter Three, therefore, discusses the relevant issues of the properties of material. Chapter Four presents the complete description of the investigation in the machining method with the analysis of the results given in Chapter Five. The details of the investigation in matrix skiving is fully presented in Chapter Six.



## **CHAPTER THREE**

### **PROPERTIES OF MATERIALS**

#### **3.1 Introduction**

It has been established in Chapter Two that the properties of materials play an important role in determining their machining performance. It follows that in order to arrive at a set of optimum operating conditions a sound understanding of these properties is required. This requirement is particularly critical when dealing with materials exhibiting great variability in their shape and form even when they are considered to be of the same type or origin. It means that these materials are not necessarily exactly repeatable in terms of their, say, physical characteristics. The phenomenon that is described above is often observed in natural materials.

In the manufacture of shoe uppers, leather as a natural material is by far the most preferred material as mentioned in the earlier chapters. Preliminary investigation, as described in chapter two, shows that the performance of leather skiving is dependent on the material properties of leather. It is therefore the intention of this chapter to investigate thoroughly the role that leather, as an upper material, plays when it is subjected to the skiving process. This is done by closely examining the hides, and choosing suitable properties by which a quantitative approach can be adopted to define, describe, and compare leathers from various sources and with various characteristics. The information obtained as a result of this subjective analysis will be used later, in Chapters Five and Six, to correlate material properties to the machining results of the two skiving methods considered, namely high speed machining and dynamic matrix cutting. The importance of this correlation in any automated skiving system is vital. Leathers of similar properties may be grouped together to form qualitative classes of materials. Machine cutting parameters are then optimised according to these classes so that effects of materials properties on skiving quality are accounted for and minimised.



The sections that follow explain the methods used to treat different hides in order to produce appropriate testing samples so that suitable property tests could be carried out on them. For each property, the test method and measurement together with an analysis of the results are separately given. Finally, a comparative study of the results is presented. However, in order to understand better the nature of the work-material a brief background introduction to leather is given first.

### **3.2 Understanding leather**

Leather is made by subjecting the proteins of animal skin to a process known as tanning, whereby the skin becomes more durable and capable of being used for a wide range of purposes such as shoe making. Some of the new synthetic materials have replaced leather for certain specialised uses but as yet no other flexible sheet material has been made which has so many inbuilt and desirable characteristics as leather.

In general, preparation of leather consists of three main processes namely, pre-tanning, tanning, and finishing, within which many variations are possible. Different aspects of the physical, chemical, and biological nature of the material need to be studied if leather characteristics are to be understood. For example the structure and chemical behaviour of such complex materials as proteins, carbohydrates, vegetable tanning, and basic chromium salts have to be fully understood.

Three main layers in skin have been identified as follows [16]:

Epidermis	the outermost layer,
Dermis	the immediate underlying tissue,
Hyperdermis	the tissue between dermis and skin muscle.

Only dermis layer is used in making leather; before tanning, the epidermal structures are loosened chemically and then removed to a large extent in the unhairing operation; much of the tissue below the dermis is likewise removed during the operation of fleshing.



Thus, the dermis layer is used for leather manufacture. It has layers of densely packed, fibrous and relatively stable regions of skin, consisting of a papillary layer and a fibre network layer. Fig. 3.1 shows a vertical section of calf skin in a diagrammatic form showing papillary and fibre network layers.

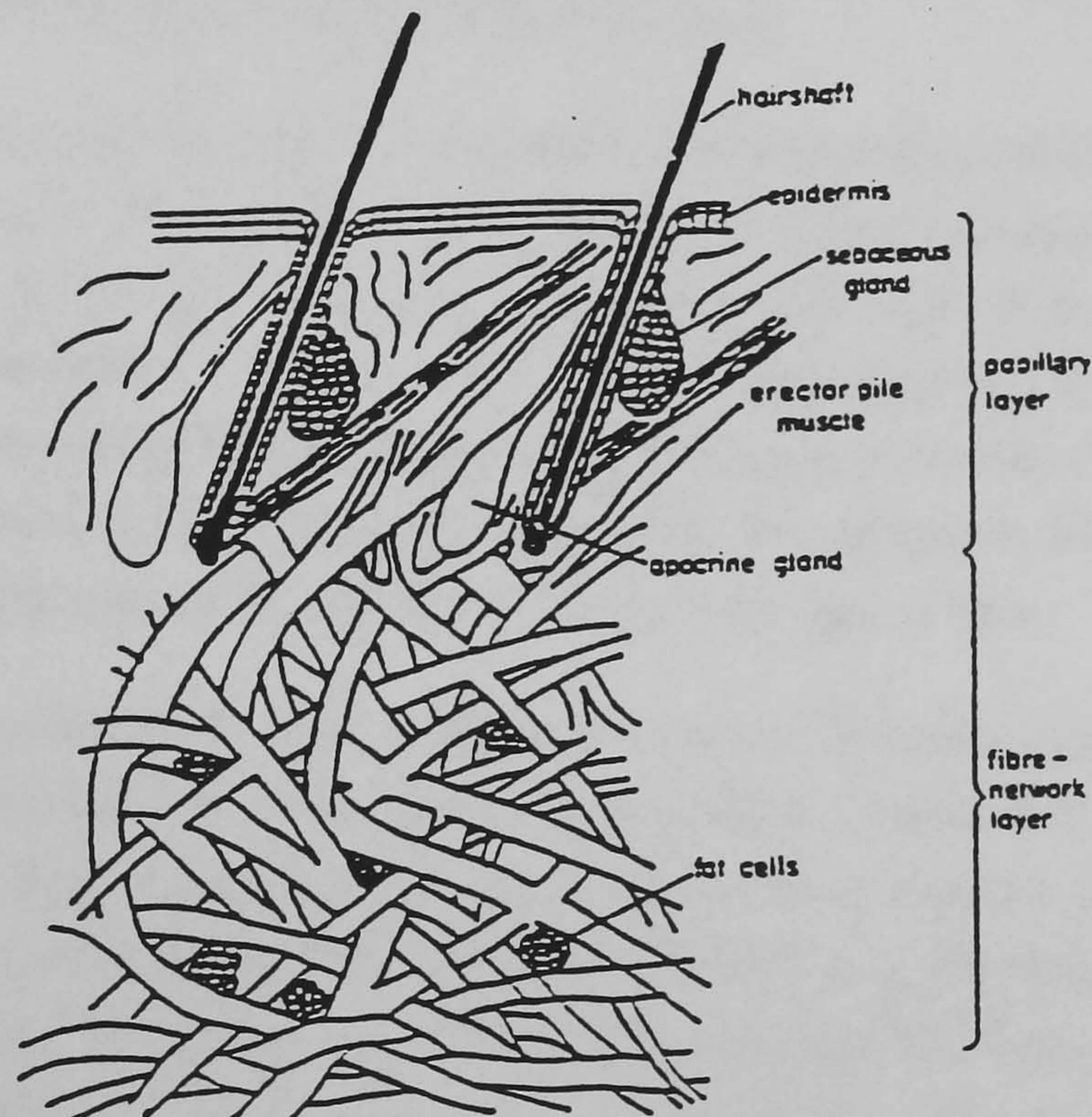


*Figure 3.1 A vertical section of calf skin in diagrammatic form ( Ref. [16] ).*

The surface of the papillary layer exposed after unhairing is known as the grain pattern. Grain pattern is one of the characteristics of leather. Poor quality leathers are sometimes overprinted with grain pattern which is considered more decorative and which may serve to hide grain defects. Although grain layers do not contribute to the firmness of leather their tightness and integrity is a good indication to the quality of the original skin and the processing it has undergone in being converted into leather.



The papillary layer is the upper region of dermis. Its surface is papillate due to hair shafts sweat glands. However the major part of leather is the lower and main region of dermis, the fibre network layer. It consists almost entirely of connective tissue fibres, the main component being the collagen fibres which are organised in long wavy bundles which in width vary from 1 to 20  $\mu$ . These interpenetrate to form a complex fibre network on which many of the characteristic qualities of leather depend. Collagen fibres are mostly cylindrical in form and appear of great length. These are important factors in determining physical properties of the dermis and the leather produced from it.

The waviness of the collagen fibres varies with the location on the skin and with the type of skin. In most skins, the fibre weave appears to run almost at random. In heavy cattle hides fibres appear to be arranged at random in directions parallel and perpendicular to the backbone as well as perpendicular to the grain surface. The random weave of the collagen fibres in hides and skins develops a physical structure that is highly porous. The porosity depends upon the tightness of the weave and this again is the function of location and type of skin.

A study conducted by Stromberg and Swerdlow [17] used a porosimeter and the electron microscope. When the complex fibrous structure of leather is examined with a light microscope the fibres appeared as bundles of smaller components known as primitive fibres. These fibres then viewed with an electron microscope are found to be made up of fibrils which contain the filaments. The filaments are smallest fibre-like structures so far resolved by the electron microscope.

The most important factor influencing the physical properties of leather is the original fibre structure in the hide. The effects of the fibre structure may be altered by the tannage, the application of filling materials, and by mechanical action. In the case of shoe uppers, leather is typically prepared from thinner skin, either calf or split cow hides. It is usually tanned with chrome, which does not fill the pores, and finished by the application of greases to maintain high flexibility.

### **3.3 Method for material sampling**

Hides are natural materials and as such exhibit random variations in their size, shape, and quality. These variations exist even in hides traditionally and qualitatively thought to be identical. It is easily argued that no two hides are scientifically identical since there are no two animal skins that are scientifically



identical. The application of engineering methods in using hides as the work material thus requires quantification of descriptions and classification of similar hides, or sections of hides, that exhibit similar engineering properties. The analysis however remains largely subjective. Fig. 3.2 shows the general shape of a hide drawn in a planar fashion and in its entirety. It is assumed that a split is made along the length of the belly of the hide. British Standard 3935 [18] specifies the regional divisions of the hide as shown. These divisions are primarily drawn up in terms of material uniformity, strength, and flexibility. The hide is divided into three main areas namely Butt, Belly, and Shoulder.

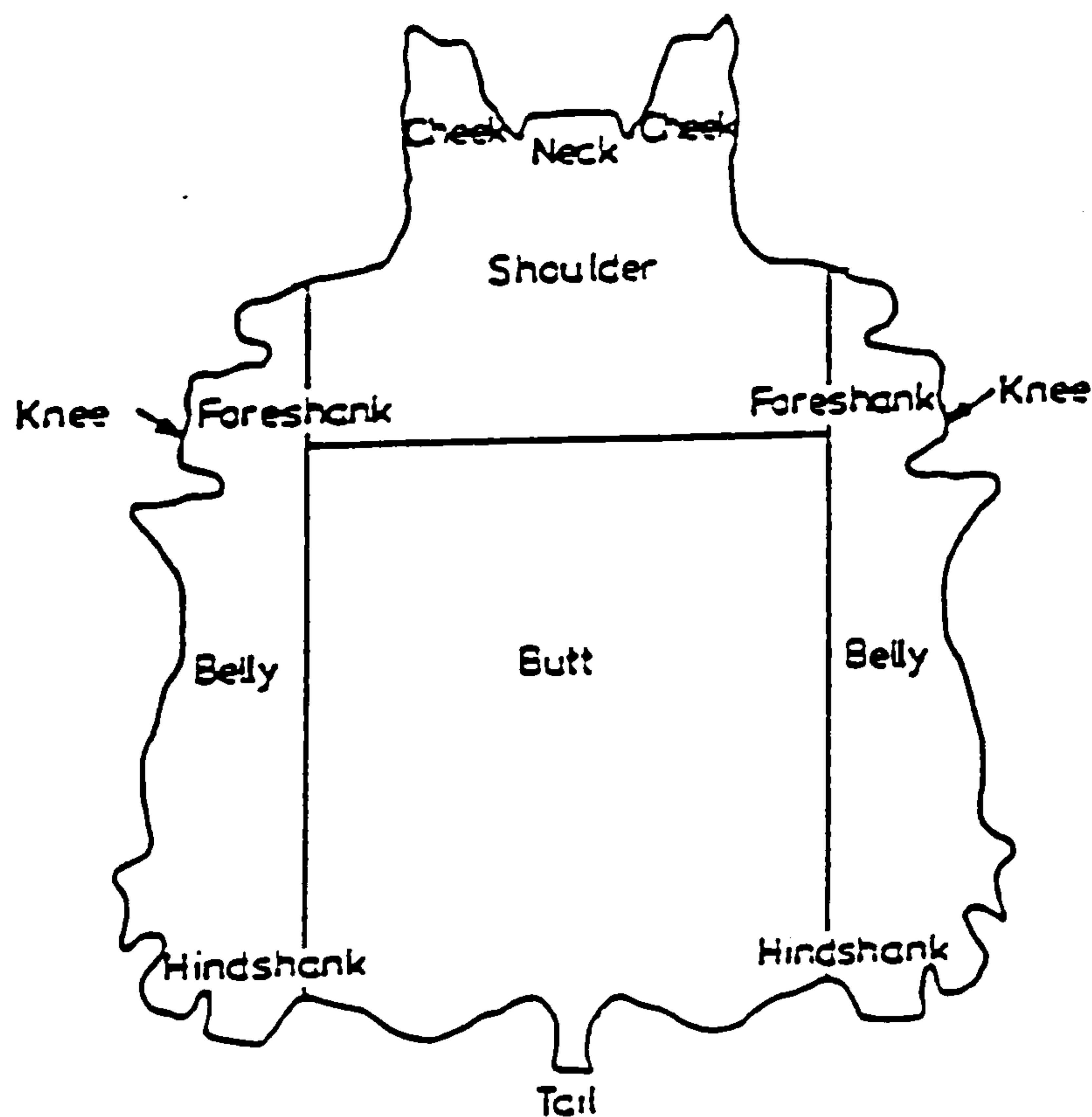


*Figure 3.2 British Standards 3935 regional divisions of hide's surface area.*

It is widely believed that physical properties show systematic patterns of variability over the surface of a leather hide in that the structural arrangement of the fibres is more firm in the shoulder and butt area than in the belly area. In this respect, though a hide may show great heterogeneity in properties, the heterogeneity is systematic and predictable. For sampling purposes however, a hide may be considered to consist of two symmetrical pieces or Sides obtained by splitting the hide along the backbone. Hodus and Stubbings [19] showed also that locations situated symmetrically with respect to the backbone have similar properties.



It is important that much care is exercised in choosing the location of samples for testing of properties. It is equally important to choose correctly from a wide range of hides typically used in shoe upper manufacture for the reasons of economy and variabilities in the hides. Mandel and Mann [20] examined statistically some physical properties of leather and concluded that in order to obtain the maximum information from a given amount of testing, a location must be selected that shows the greatest degree of correlation, for the property in question, with the average value for the entire hide. In different studies, Randall *et al* [21] and Kanagy *et al* [22] subdivided a side into 21 locations and produced their results obtained from 15 sides. They emphasised the importance of selecting an appropriate sampling location for physical tests, since many of these tests exhibit considerable variation over the leather side. Their objective however, was a general study of the properties of leather with no specific application in mind. In the case of automatic skiving as an objective for studying leather properties, the entire hide area, as far as possible, must be tested. This is because non-defective areas from the entire hide surface are normally used in shoe uppers.

Taking advantage of the symmetry and regional classification in the hide as mentioned earlier, test pieces were taken from entire areas of the sample hides, and their original relative positions recorded, with the backbone as the reference. That is, each test piece is identified by two coordinate locations both across and along the backbone. The location across the backbone is the relative distance from the backbone expressed as a percentage of the total width of the side. The location along the backbone is simply expressed as upper, central, and lower sections of the hide. Fig. 3.3 shows such an arrangement of test pieces.



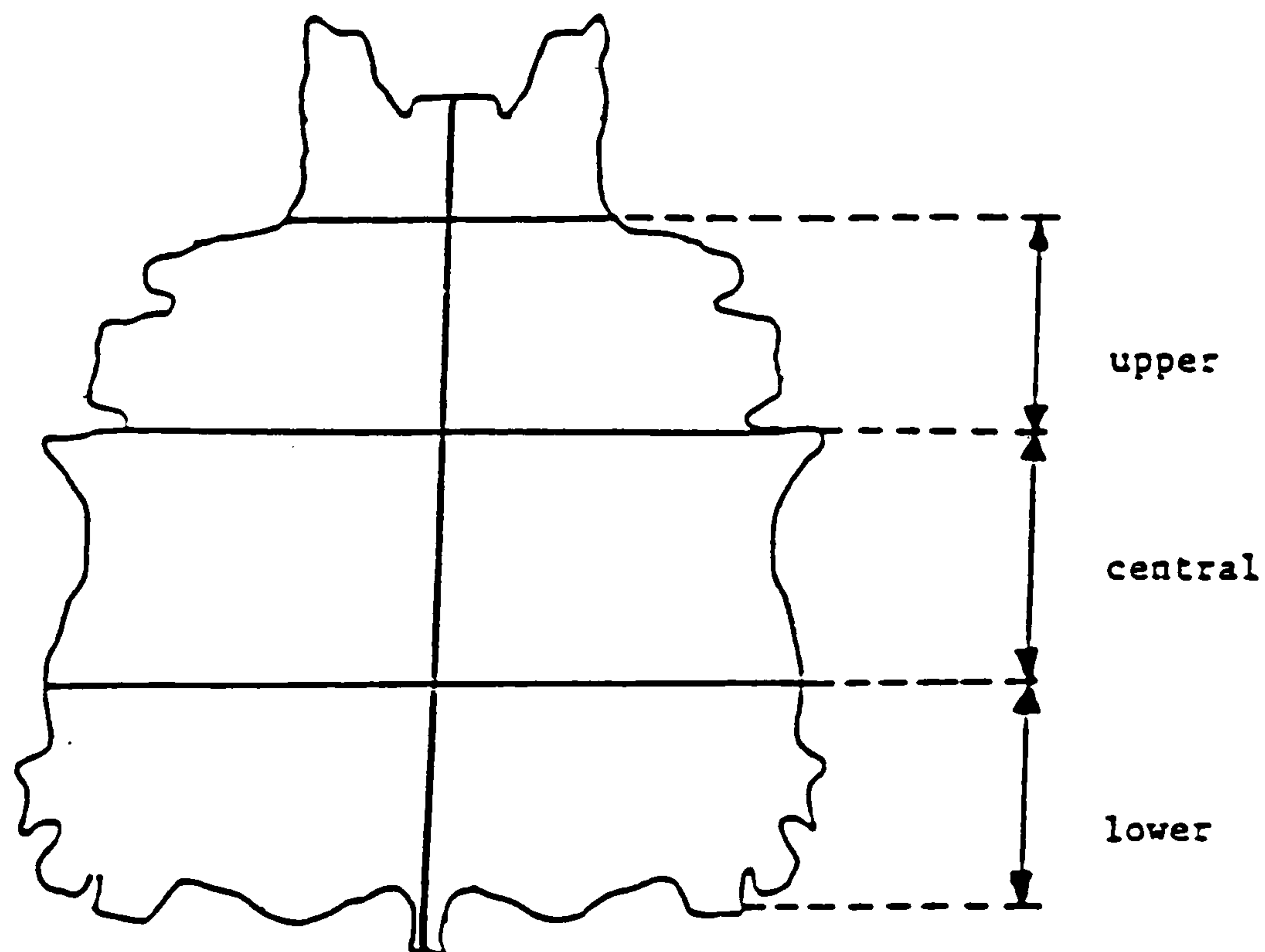


*Figure 3.3 Regional divisions of hides for sampling purposes.*

Hides are discrete entities, and as such come in varying thickness and physical characteristics, (and tanning composition). It is therefore inevitable that these parameters affect their physical properties. In order to accommodate such variations two typical but distinct types of hides were chosen to represent approximately the upper and lower extremes. As a starting point, these extremes were taken in terms of material thickness and hence flexibility; see section 3.6. The thicker leather was of sheep skin, larger in surface area, and vegetable tanned while the thinner leather had a smaller surface area, originates from calf skin with full chrome tannage. For simplicity the two types of hides are hereafter referred to as type-1 and type-2 respectively. Ultimately the properties of the two types of hides are to be correlated to the machining properties of the skiving systems in consideration, and for that reason the same types of leather are to be used in skiving tests. It is therefore imperative that hides are selected with great care and with a minimum deviation from the standard materials. The terms 'leather type' and 'hide type' are used synonymously throughout.



### **3.4 Selection of suitable properties**

In chapter two a conclusion is reached with a recommendation to investigate two different systems for the automation of shoe upper skiving. Both systems however, exploit the application of predominantly ‘mechanical’ material removal techniques. The workpiece is subjected to the action of cutting forces being exerted by a rotary cutting tool in the case of high speed machining system, and a band knife in the case of dynamic matrix system. It is therefore more appropriate to concentrate on the ‘mechanical’ properties of leather. Furthermore, since the objective for their evaluation is a subsequent correlation with the materials’ machining properties, it is important to select appropriate mechanical properties that are more suitable to the task.

Leather is available as a shoe upper material in various sizes and thicknesses. Variability in the form of its surface irregularity and fluffiness makes it almost impossible for any precision dimensional measurement such as thickness. However, an ability to perform consistent and systematic thickness measurement is important.

Leather is also a flexible material, and as such flexibility is an important factor responsible for the many variations that exist in different hides, or even different regions within a hide. Inspection shows that although thin leather is more flexible than thick leather, flexibility is also a function of location in the hide. Its variation therefore is of importance in the determination of the optimum automated skiving parameters.

Much research is conducted to evaluate the tensile properties of leather [23][24][25][26]. The majority of this work has been nevertheless with the objective to determine the effects of chemical compositions in leather, whereby different tanning processes are studied and compared. In the techniques used for the automation of skiving, leather is treated as a workpiece being subjected to an engineering process involving the applications of cutting and other types of forces such as those associated with workpiece feeding and gripping. As such, the tensile properties of leather are important data in determining its strength under load. Correlation between tensile strength and cutting properties is used to predict the optimum cutting conditions in skiving.

Similarly, leather compressibility and leather hardness tests provide a body of relevant information in a cutting process. For example, in the case of high



speed machining, the operation of face milling involves a degree of compressing the fibre network of leather immediately prior to cutting. Another example is that, from initial investigation of matrix skiving, it appears that softer leather results in better cutting quality. In general, these properties are principally related to the resistance to material deformation. Their correlation to the cutting properties therefore seems appropriate.

Section 3.2 showed that the major part of leather is the fibre network layer, consisting of fibres organised in long wavy bundles that form the basis for the strength of leather. Tensile strength is one such measure, as mentioned above. There are also other measures for the strength evaluation. Leather tearing load is often quoted to describe material's separation force from a split. Another measure is that of burst load. Leather burst is achieved by gradually forcing a small ball through the fibrous side of leather sample until a rupture takes place. The required force to rupture is called the burst load. It is a measure of strength through stretch to final break, and unlike tensile test is omni-directional. That is to say, stretch is applied in all directions on the sampling point on leather.

There are other mechanical property tests carried out on leather to examine the effects of various external conditions such as humidity and temperature [23]. Nevertheless, only those properties that are suspected to have primary effects on the skiving process are considered for further investigation. They are:

- i. thickness
- ii. flexibility
- iii. hardness
- iv. compression
- v. tensile strength
- vi. tearing load
- vii. burst load

In all cases tests were carried out on both hide types 1 and 2. Hide type-1 (the thicker leather) was approximately twice the width and 1.5 times the length of hide type-2. In order to maintain identical test methods for both types of leather, it became clear that the number of test pieces that were extracted from hide type-2, and hence the number of property test results, would be less than those of hide type-1. Relevant British standards 3144 [27] were used throughout as guide-lines for the test methods with the results expressed accordingly. The properties were



evaluated for each hide type regardless of their thickness variations. A section on thickness measurement is however introduced at the beginning so that correlation of the results may be made with reference to thickness. The sections that follow present, for each property, a brief introduction, the test procedure, and the results. The results are then summarised and compared in section 3.12.

### **3.5 Material thickness measurement**

Thickness is an important dimensional property of leather, and its variation affects the results of other properties. The problems associated with leather thickness measurement are mainly related to the irregularities that exist in the fibrous characteristic of the hide surface in terms of the degree of tightness (and hence fluffiness) of its constituting fibre mesh. As a general guide, the backbone region in a hide is the tightest, with the tightness decreasing in the direction of the belly [16]. The reverse is true for the degree of fluffiness. The method of thickness measurement of such a material is therefore critical. Only average values can be meaningful. Measurement procedure must remain consistent and systematic at all times. Thickness is a property that is measured frequently as an intermediate parameter to evaluate other mechanical properties, often in different laboratories. It is therefore desirable that the method used in its measurement be relatively easy, fast, and employs portable instruments.

#### **3.5.1 Measurement technique**

In accordance with the regional divisions in the hide described in section 3.3, a square sample of 50 x 50 mm were cut from each region of the two types of leather. There were 9 samples from the hide type-1 and 6 samples from the hide type-2.

A practical method for thickness measurement of sheet material is to use two flat and parallel plates, one fixed, and the other moving. The material is placed on the fixed plate which is positioned horizontally. The moving plate is then gradually lowered until its surface reaches the corresponding surface of the material. The distance between the two plates is therefore taken as the thickness of the material. Normally a pre-determined pressure is applied by the moving plate on the material to standardise the practice. When considering flexible fibrous materials as the workpiece, factors such as the amount of this pressure, and the surface area of the plates, are critical.



A standard metric micrometer was used to examine the variation of thickness across leathers type-1 and type-2. For each specimen a total of 8 readings were taken. The experiments were performed by the same experimenter and in identical fashion. Mean and standard deviation values per specimen were thus calculated. The values of mean thickness of each specimen are subsequently used as the average regional thicknesses of the hides while the standard deviation values are used to demonstrate the scatter in the results. Table 3.1 shows the results of thickness measurement readings relating to leather type-1 and table 3.2 shows the same results relating to leather type-2. These results are discussed in section 3.5.2.



Sample Number	Thickness measurement replications (mm)								Mean (mm)	S.D.
	1st	2nd	3rd	4th	5th	6th	7th	8th		
1	1.54	1.40	1.38	1.55	1.54	1.53	1.43	1.40	1.48	.0749
2	1.42	1.38	1.39	1.41	1.37	1.45	1.41	1.38	1.40	.0264
3	1.43	1.38	1.35	1.37	1.38	1.46	1.39	1.39	1.40	.0350
4	1.26	1.26	1.31	1.26	1.23	1.28	1.34	1.25	1.28	.0354
5	1.33	1.33	1.30	1.33	1.34	1.30	1.33	1.35	1.33	.0177
6	1.20	1.13	1.26	1.36	1.33	1.17	1.20	1.35	1.25	.0882
7	1.17	1.28	1.08	.93	1.16	1.24	1.10	.93	1.11	.1297
8	1.40	1.41	1.30	1.29	1.32	1.28	1.37	1.32	1.34	.0504
9	1.42	1.56	1.55	1.38	1.50	1.41	1.50	1.48	1.48	.0659

*Table 3.1 Thickness measurement results for the hide type-1 using a micrometer.*

Sample Number	Thickness measurement replications (mm)								Mean (mm)	S.D.
	1st	2nd	3rd	4th	5th	6th	7th	8th		
1	.59	.62	.61	.60	.59	.60	.60	.57	.60	.0149
2	.58	.58	.60	.60	.58	.57	.57	.59	.58	.0119
3	.62	.67	.71	.64	.58	.58	.55	.56	.61	.0570
4	.62	.56	.55	.57	.55	.53	.58	.59	.57	.0280
5	.60	.60	.59	.61	.63	.62	.58	.58	.60	.0181
6	.56	.51	.53	.53	.58	.58	.61	.60	.56	.0362

*Table 3.2 Thickness measurement results for the hide type-2 using a micrometer.*



Sample Number	Thickness measurement replications (mm)								Mean (mm)	S.D.
	1st	2nd	3rd	4th	5th	6th	7th	8th		
1	1.58	1.56	1.48	1.50	1.56	1.46	1.45	1.60	1.52	.0582
2	1.42	1.45	1.50	1.46	1.44	1.40	1.41	1.49	1.45	.0362
3	1.41	1.46	1.50	1.43	1.46	1.48	1.42	1.40	1.45	.0355
4	1.28	1.30	1.30	1.36	1.34	1.30	1.26	1.33	1.31	.0327
5	1.40	1.41	1.42	1.38	1.37	1.40	1.37	1.36	1.39	.0217
6	1.31	1.17	1.25	1.36	1.26	1.17	1.25	1.39	1.27	.0802
7	1.27	1.35	1.26	1.16	1.31	1.24	1.04	1.27	1.24	.0968
8	1.35	1.32	1.50	1.37	1.38	1.26	1.44	1.28	1.36	.0798
9	1.49	1.42	1.59	1.58	1.42	1.49	1.60	1.61	1.53	.0798

*Table 3.3 Thickness measurement results for the hide type-1 using a vernier calliper.*

Sample Number	Thickness measurement replications (mm)								Mean (mm)	S.D.
	1st	2nd	3rd	4th	5th	6th	7th	8th		
1	.62	.61	.61	.60	.60	.61	.59	.62	.61	.0104
2	.60	.58	.61	.59	.60	.57	.57	.58	.59	.0149
3	.61	.64	.69	.62	.64	.58	.56	.59	.62	.0410
4	.66	.60	.56	.56	.56	.54	.57	.64	.59	.0431
5	.60	.59	.59	.63	.64	.65	.64	.57	.61	.0298
6	.58	.50	.52	.57	.60	.59	.60	.57	.57	.0370

*Table 3.4 Thickness measurement results for the hide type-2 using a vernier calliper.*



It is necessary to confirm the validity of these results by another technique. For this reason a battery-operated digital metric vernier calliper was used to measure the same specimen thicknesses. In the same way as before, a total of 8 readings were taken from each specimen with mean and standard deviation of thicknesses calculated. The vernier test results relating to hide type-1 and type-2 are shown in Table 3.3 and Table 3.4 respectively. Comparison of these results with those obtained by the micrometer suggests that both techniques are in very close agreement in the way they predict the regional thickness variations of both leather types in the test. However, the regional mean values obtained by the micrometer are consistently lower than those obtained by the vernier. This phenomenon is present in the measurements of both types of leather.

The presence of scatter in the results are due to a variety of factors including the non-homogeneous nature of the material, as explained earlier in this chapter. Thickness measurement of a material like leather is also sensitive to the particular method of measurement, and to the experimenter in the case of the use of hand-held measuring devices. To minimise these effects, use of a metric micrometer with an anvil diameter of 6.8 mm, by the same experimenter, was therefore made throughout.

### **3.5.2 The results**

The results shown in Table 3.1 and Table 3.2 of section 3.5.1 are the basis of the analysis here. The regional thickness in the hide type-1 varies from 1.11 mm to 1.48 mm giving 0.37 mm change between the thickest and thinnest sections (greatest thickness change). The regional thickness in the hide type-2 however, varies from 0.51 mm and 0.61 mm giving 0.1 mm change between the thickest and thinnest sections. Considering that the total mean thicknesses for the hides type-1 and type-2 are 1.33 mm and 0.58 mm respectively, then the respective ratios of their greatest thickness change to mean thickness, expressed as percentages are 28% and 17%. It means that the average thickness in the hide type-1 is subject to a total of 28% fluctuation around the mean, and that of the hide type-2 is subject to a total of 17% fluctuation. Thickness of the hide type-2 is thus more uniform and less variable than type-1. Figs. 3.4 and 3.5 show these variations for the hides type-1 and type-2 respectively.



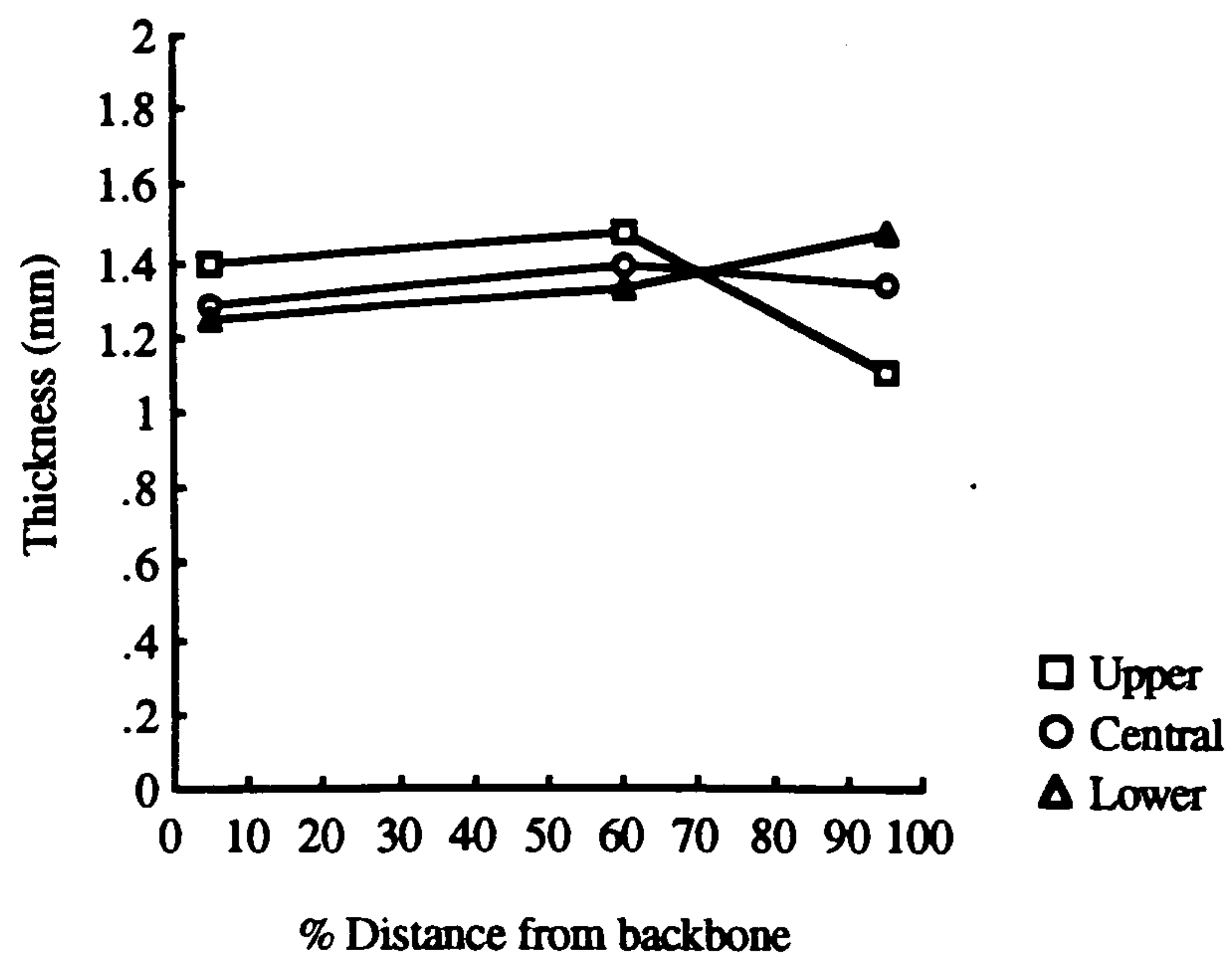


Figure 3.4 Thickness variation in the hide type-1.

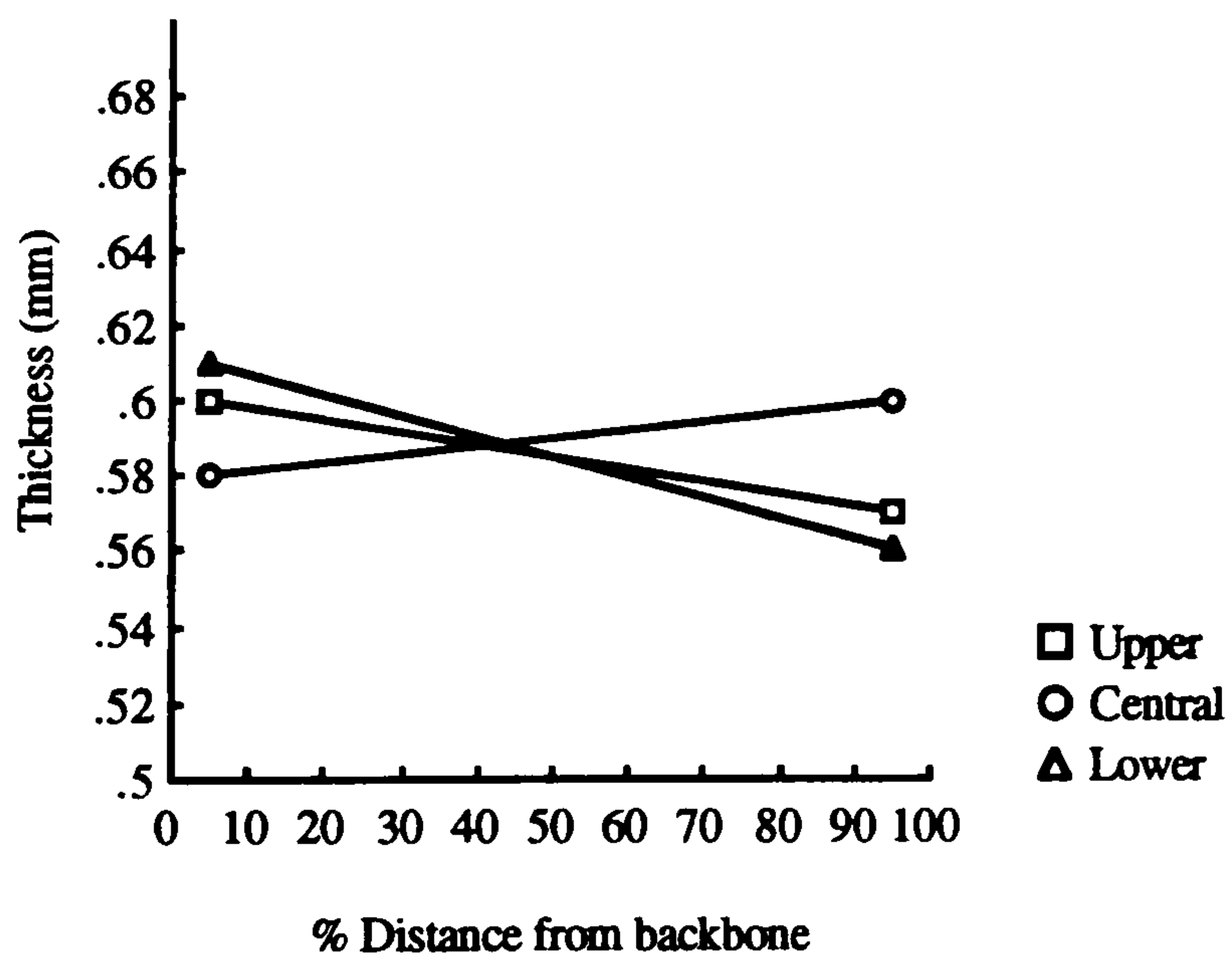
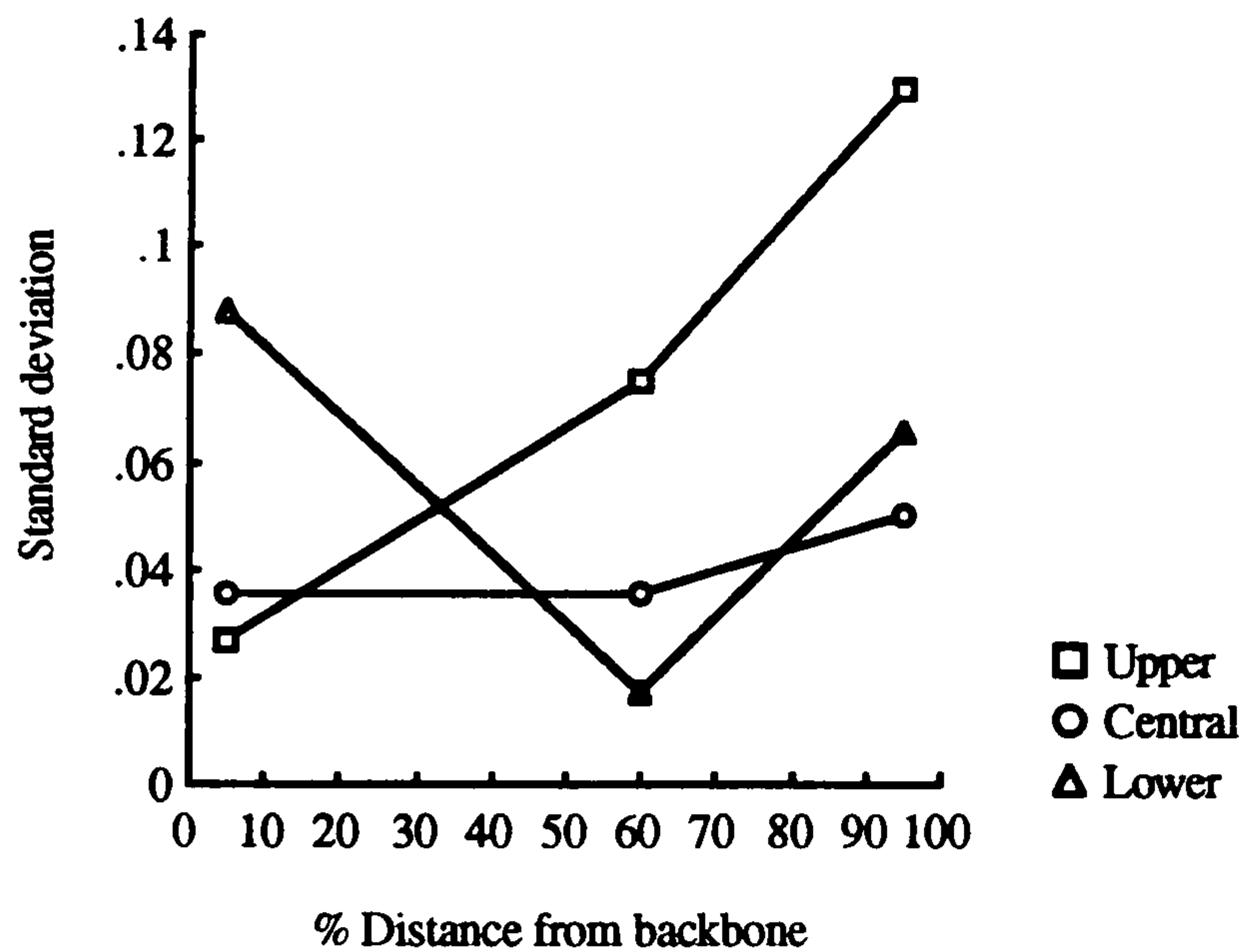


Figure 3.5 Thickness variation in the hide type-2.



Lower sections of the hides exhibit relatively higher degree of thickness variability. This is more clearly shown by the values of regional standard deviation. Plotted in a similar fashion as thickness values, regional standard deviations relating to both hide types are shown in fig. 3.6 and fig. 3.7. In the upper and central sections of hides the standard deviations in both hide types are low close to the backbone and increase towards the belly area. Therefore, thickness is more uniform in the backbone area and this uniformity drops as the distance from the backbone increases.



*Figure 3.6 Standard deviation variation of thickness measurements, hide type-1.*



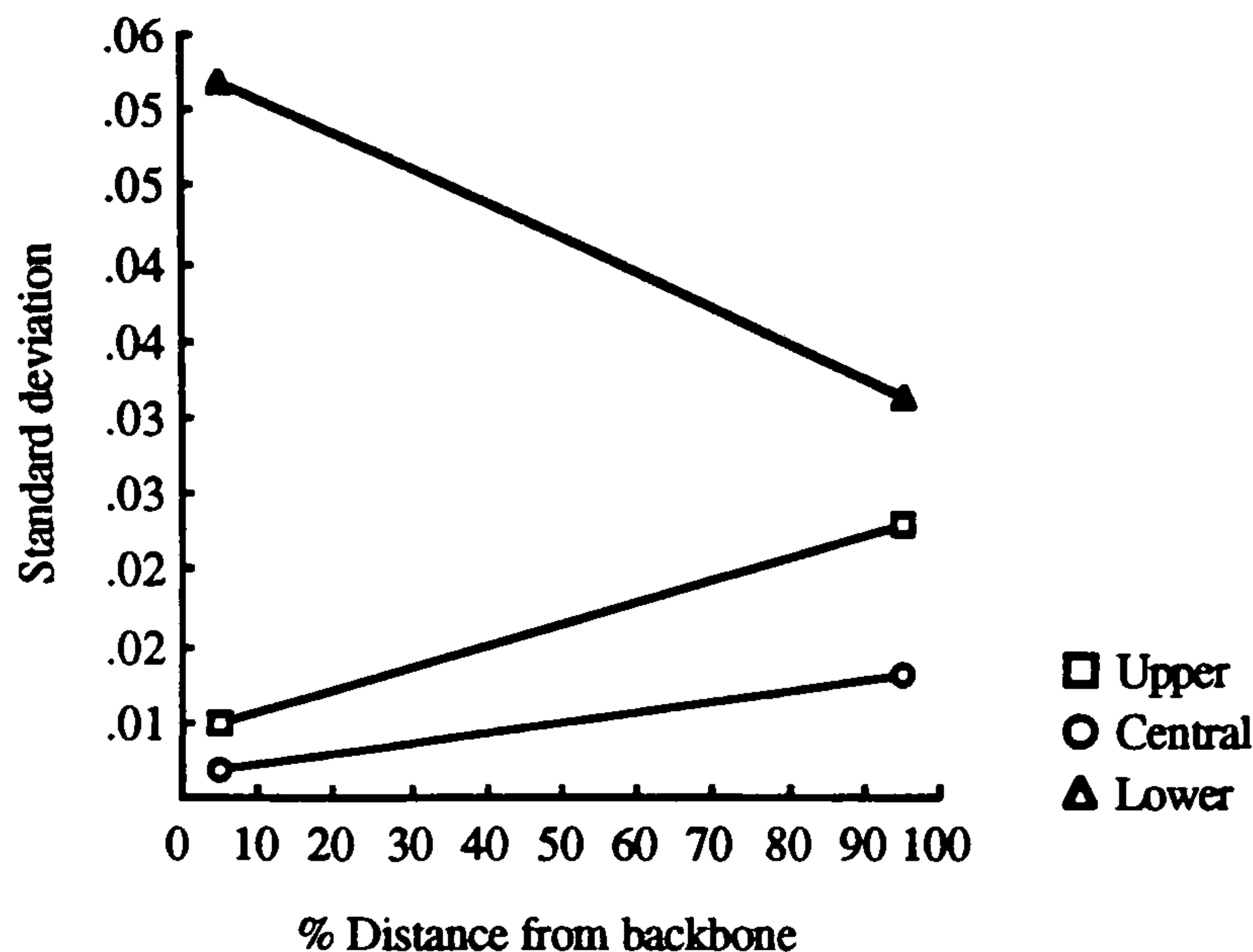


*Figure 3.7 Standard deviation variation of thickness measurements, hide type-2.*

### 3.6 Material flexibility properties

Leather is a flexible material. The degree of its flexibility differs from hide to hide, and even from region to region within the same hide. It is therefore an important property of leather that may affect its skiving performance. Also, due to a high degree of mechanical handling processes involved in the design of the automated skiving techniques considered in this work such as component feeding and gripping, the flexibility factor must be accounted for.

High flexibility and stiffness are often used as terms to describe flexibility, and are on opposite ends of a scale which measures ease of bending. Generally if a low load is required to bend a piece of leather it is more flexible than if a high load is required. The degree of porosity affects leather flexibility in that a leather which is more flexible is usually very porous, but one that is less flexible usually is a filled leather. Empty pores permit the fibres to assume new positions when leather is bent. On the other hand, if the pores are filled, the fibres are unable to move to new positions and the leather is considered to be less flexible because a large load is required to move the fibres to new positions. Thickness is also another factor affecting leather flexibility. In leathers of identical fibre structure and tanning composition the thinner one is more flexible than the thicker one.



In order to be able to assess its degree of variation in shoe uppers for correlation with skiving properties, flexibility must first be quantified. A method to evaluate flexibility is to determine the flexural rigidity of the material. Flexural rigidity is defined as the ratio of small change in bending moment per unit width of the material to the corresponding small change in curvature, and is measured in gramme meter (g.m). This quantity is a measure of the resistance of the material to bending by external forces. Flexibility is therefore inversely related to flexural rigidity. Relevant British Standards 3356 [28] are used for the determination of flexibility. A subjective study of leather flexibility was performed by comparing values of flexural rigidity of various regions of the two hide types. The method for evaluating material flexural rigidity is given in section 3.6.1.

#### **3.6.1 Test procedure**

Samples were taken from the two hide types, and from hide regions mentioned in section 3.3. These samples were rectangular strips of 25 mm by 200 mm. In order to account for the possible directionality of leather flexibility in a hide, the strips were cut in the directions making angles of 0°, 30°, 45°, 60°, and 90° to the backbone in the case of hide type-1, and 0°, 45°, and 90° to the backbone in the case of hide type-2.

The strip of leather was supported on a horizontal platform in a direction perpendicular to one edge of the platform. The strip was traversed in the direction of its length so that an increasing part overhangs and bends down under its own weight. When the tip of the specimen had reached a plane passing through the edge of the platform and inclined at an angle of 41.5° below the horizontal, the overhanging length was measured. Fig. 3.8 shows the essential features of the testing instrument used.



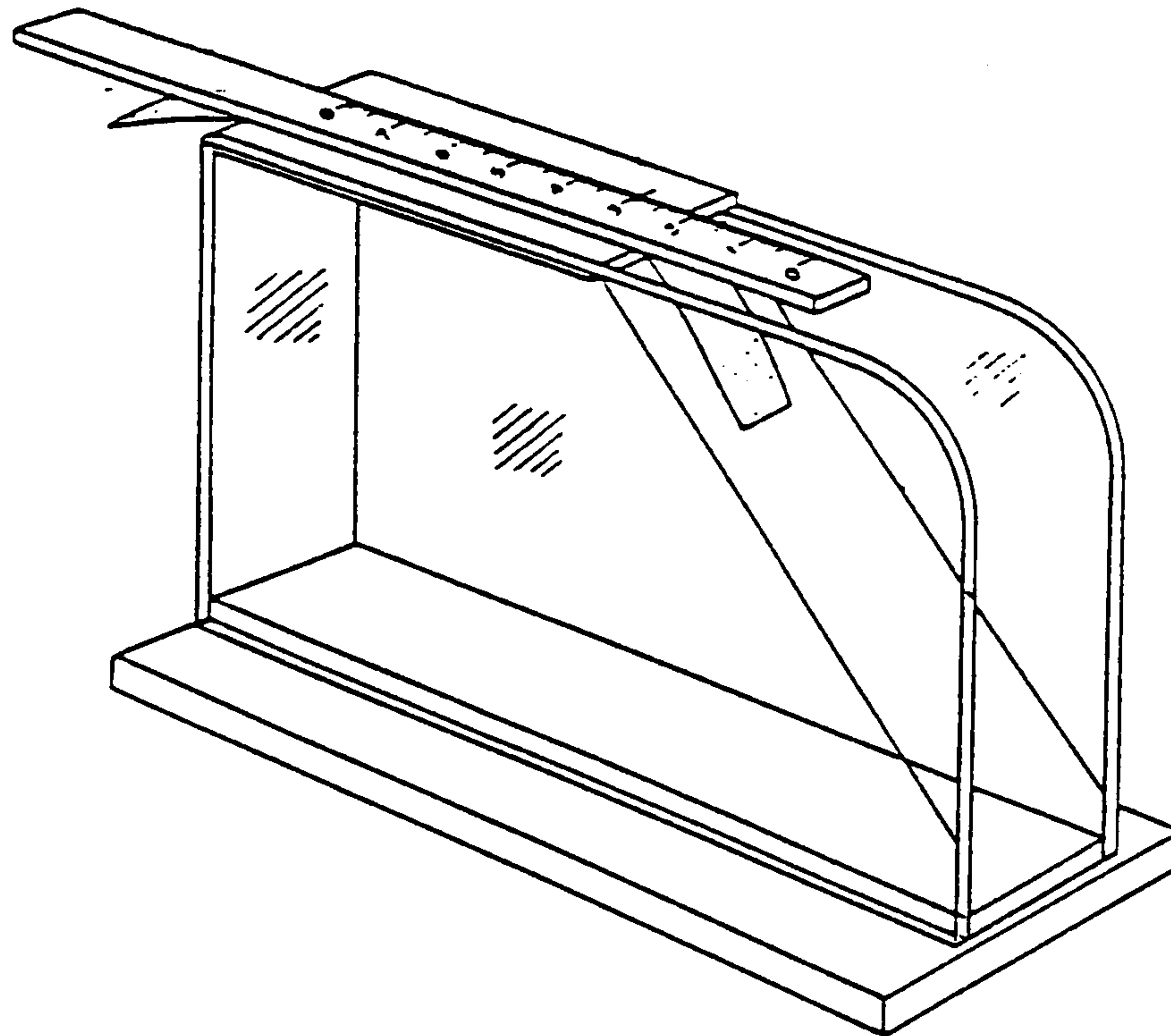


*Figure 3.8 Essential features of the flexural rigidity measurement device.*

Based on the work carried out by Peirce [29], flexural rigidity is then obtained as follows:

$$G = M \cdot L^3 \quad (3.1)$$

Where:  $G$  = material flexural rigidity in g.m

$M$  = material mass per unit area in g.m<sup>-2</sup>

$L$  = 1/2 overhanging length in m (= Bending Length )



Each strip of leather was tested with each end separately as the test leading edge, and with the grain side both facing up and down<sup>†</sup>. Each test was repeated twice and an average value produced. The mean of the four separate test results was then quoted as the mean flexural rigidity of the strip. Values of flexural rigidity of samples were evaluated with reference to their positions in the hide, and their angles relative to the backbone direction of the hide. Two lateral positions in the hide for both hide types were considered. In the case of hide type-2, samples close to belly were obtained in the direction of backbone only. This is due to the long strip samples used relative to the dimensions of the hide.

### **3.6.2 The results**

Generally hide type-1 is much less flexible than type-2. Flexural rigidity ranges from 0.07 to 0.66 g.m in the former while the range is from 0.02 to 0.05 g.m in the latter. Moreover, the overall mean flexural rigidity of the hide type-1 is 0.21 g.m, and the corresponding value for the hide type-2 is 0.03 g.m. Therefore variations in material flexibility of the hide type-1 are significantly larger than those of type-2, with an overall mean value of about 8 times that of the hide type-2. In hide type-1 the flexural rigidity of all sections close to the backbone do not vary significantly with respect to the change of the angle from the backbone direction and stays in a band limited by 0.10 and 0.28 g.m. This band widens for the sections close to the belly whereby its upper and lower values are 0.07 and 0.66 g.m respectively. This high variability is particularly noted in the lower sections of the hide where the material tends to be the least flexible, with the flexibility decreasing with the increasing angle from the direction of the backbone. Flexibility in other sections of the hide close to the belly, however, increases as the angle from the backbone direction increases. In the case of the hide type-2, the general tendency is that flexibility decreases with the increase of the angle from the backbone direction, with the central sections of the hide being the most flexible. Unlike the hide type-1, in this hide the upper sections are the areas of least flexible. Figs. 3.9(a) and 3.9(b) show the flexibility results in terms of flexural

---

<sup>†</sup> It was noticed that tests with leather grain side facing up produced smaller values of flexural rigidity than tests with grain side facing down by approximately 14%.



rigidity of all the tests for hide type-1, while fig. 3.10 shows the results in the same way for hide type-2.

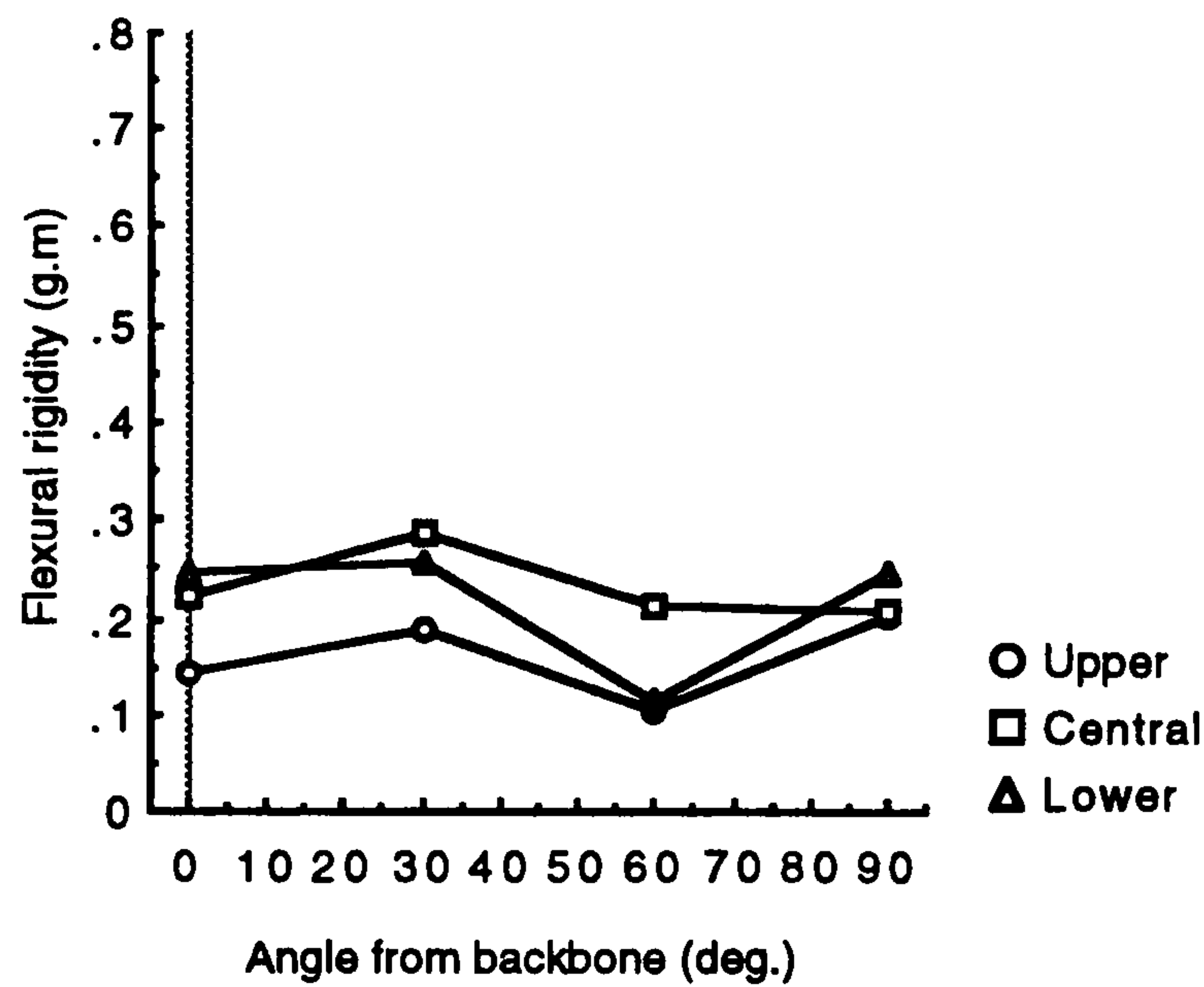


Figure 3.9(a) Flexural rigidity variation close to backbone, hide type-1.

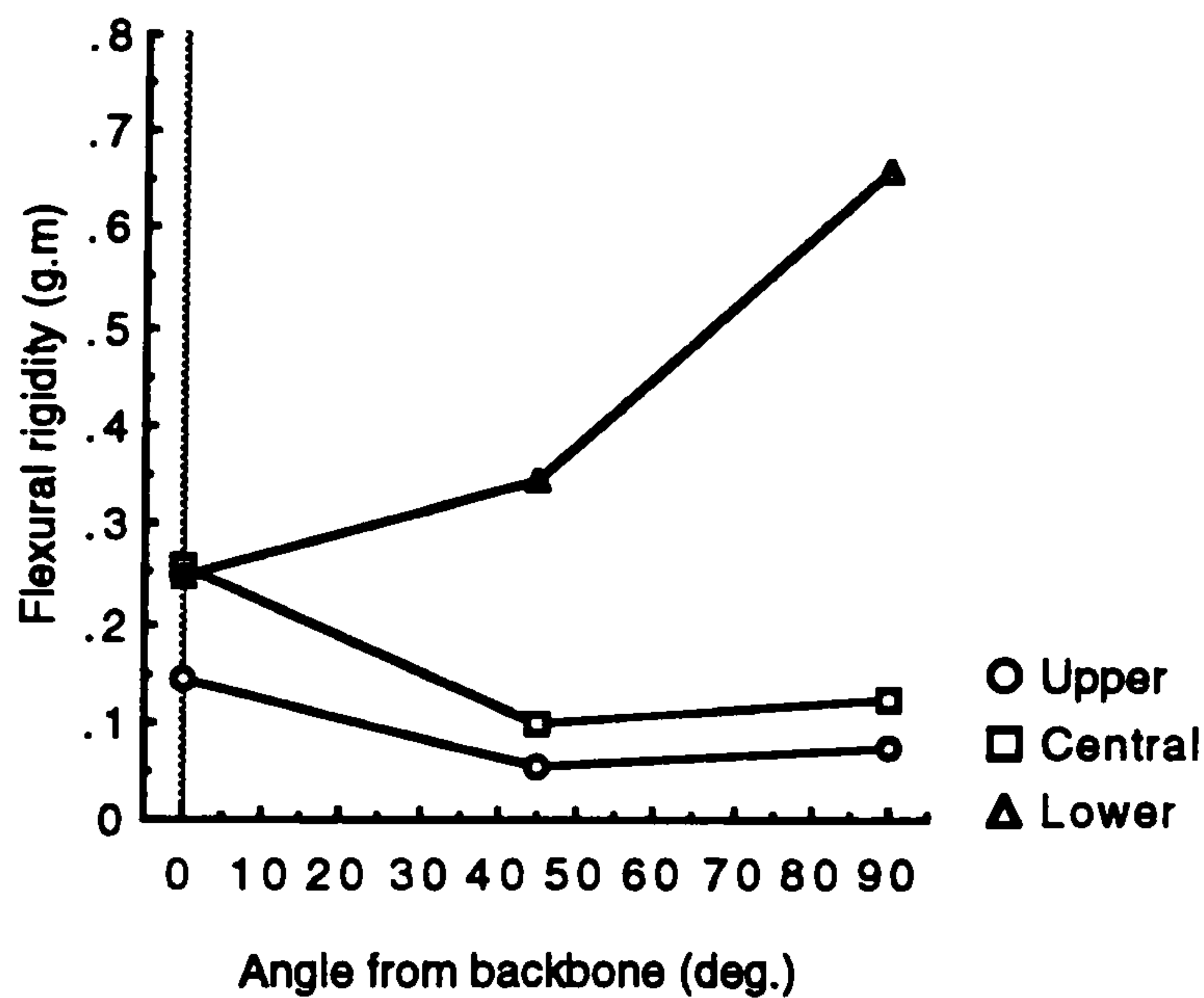
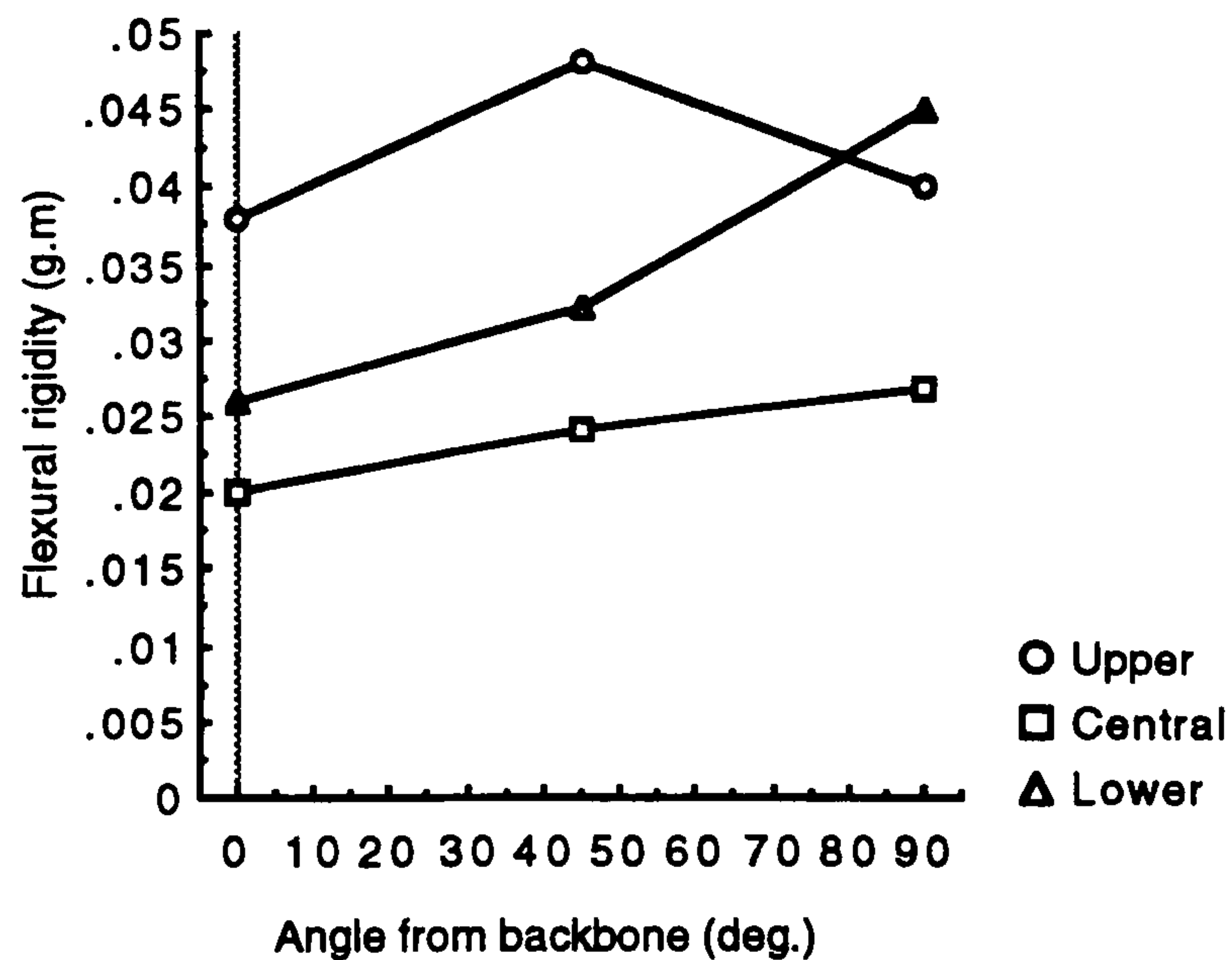


Figure 3.9(b) Flexural rigidity variation close to the belly, hide type-1.





*Figure 3.10 Flexural rigidity variation close to the backbone, hide type-2.*

To obtain a more general pattern of flexibility variation in both hides, mean value of flexural rigidity of all the tests carried out in each hide regional area is evaluated. The results, shown in fig. 3.11 and fig. 3.12, therefore give the mean regional flexibility variation within the hides. In most sections of both hide types flexural rigidity decreases in the direction from the backbone to the belly. This implies that around the belly area the material is more flexible than it is around backbone area.



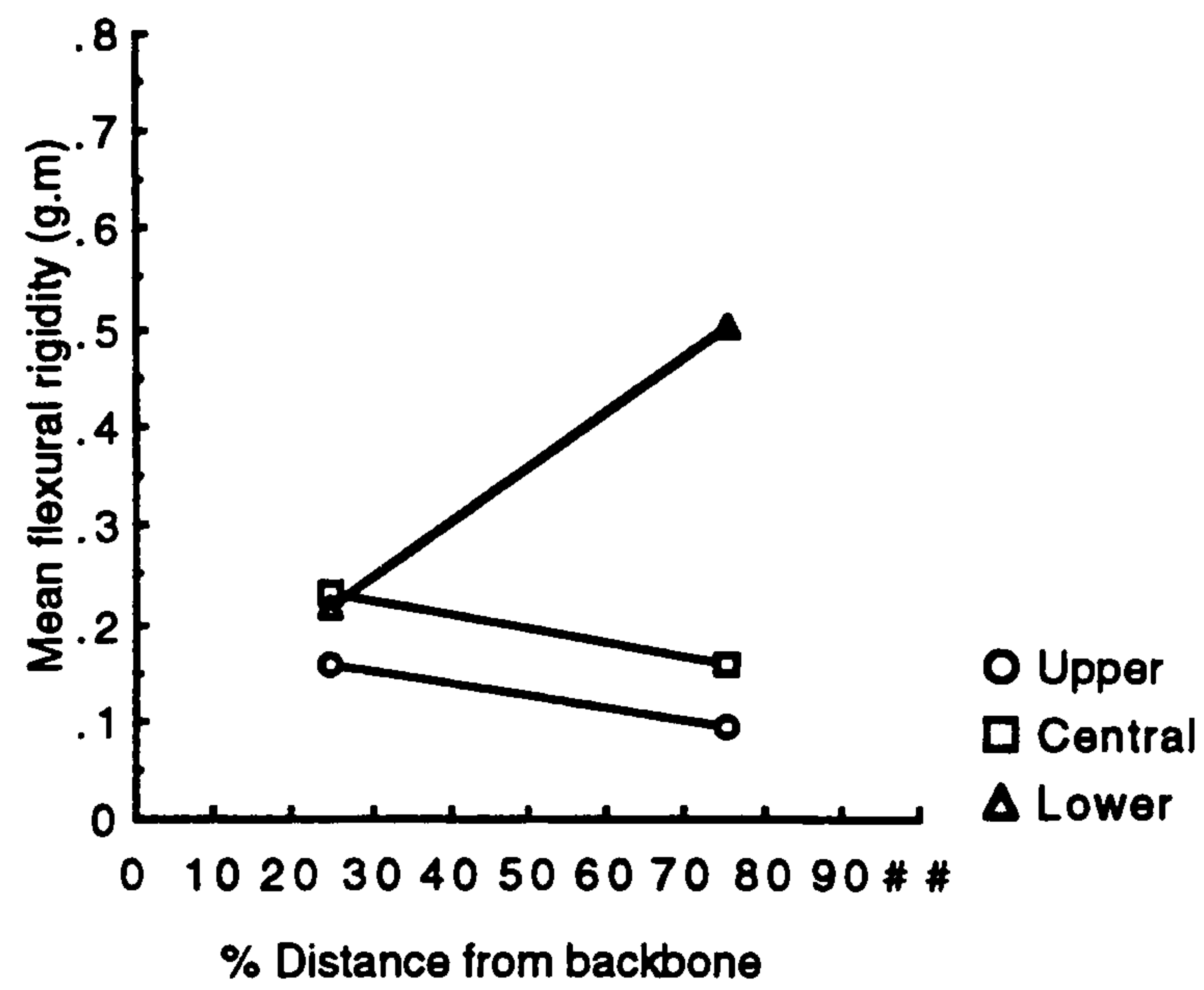


Figure 3.11 Flexural rigidity variation in the hide type-1.

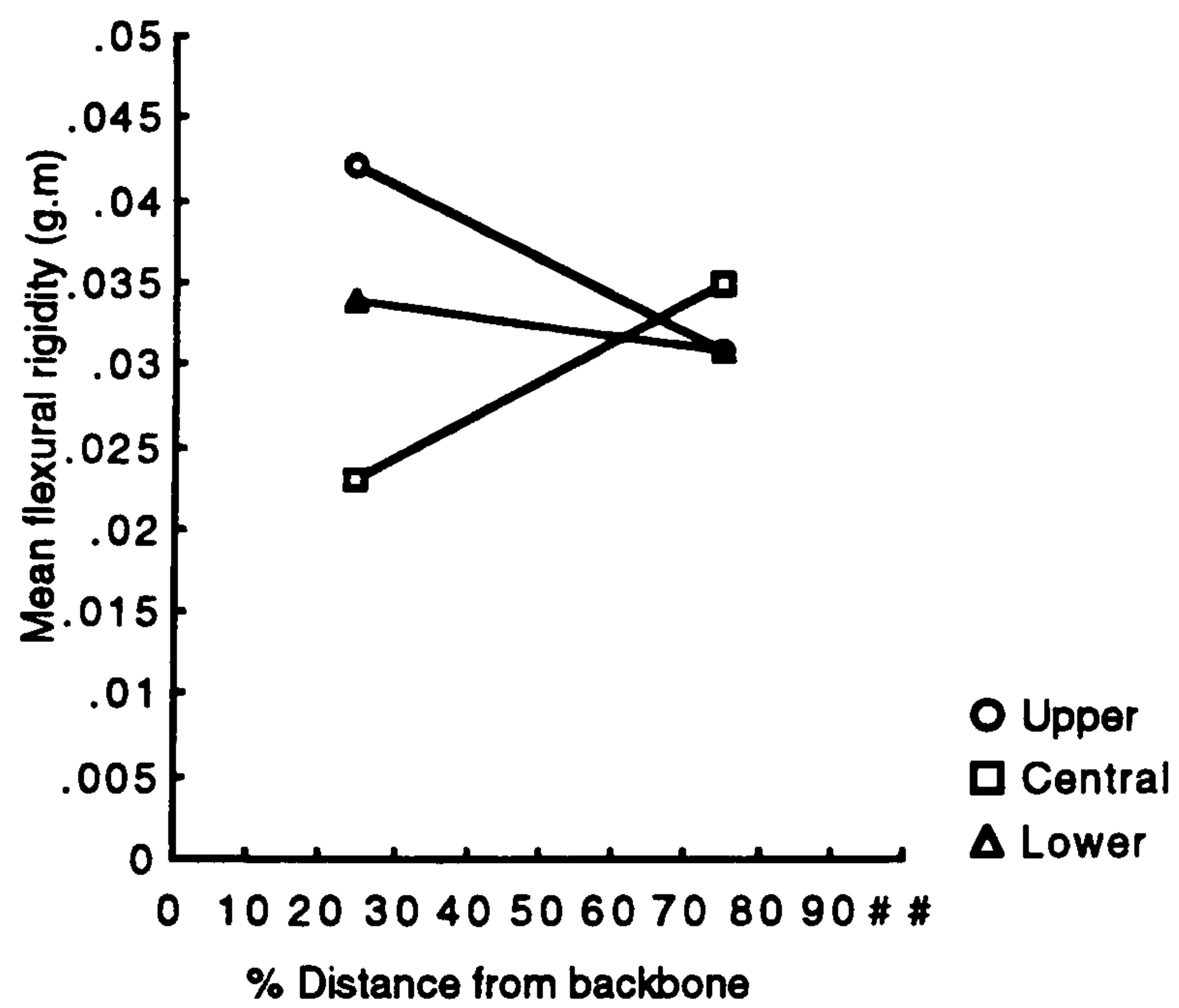


Figure 3.12 Flexural rigidity variation in the hide type-2.



### **3.7 Material hardness properties**

The skiving operations considered in this work are principally involved with the material removal by penetration under pressure. In the process of such operations, apart from machining, other types of material deformation such as indentation or abrasion may take place. A measure of the material's resistance to such deformations is therefore a useful tool in optimising the skiving parameters. This measure is referred to as material's hardness. Furthermore, preliminary tests on leather matrix skiving show that softer leathers produce better results. These tests are originally carried out on leathers of various characteristics with their degree of softness (or hardness) determined purely by human-hand tactile examinations. There are however unavoidable uncertainties relating to the presence of the influence of other properties, such as compressibility, in the final judgement of such examinations. It is therefore appropriate to evaluate systematically the hardness properties of the two standard leather types so that their effects on the cutting properties of leather may be more definitely determined.

An established method for evaluating material's hardness is to evaluate its resistance to indentation. British Standards 3144 [27] specify a method for measurement of indentation index for leather. Indentation index is obtained by measuring the amount of penetration of a small diameter ball under a specified load on a leather flesh surface. The mean value of five such measurements is quoted as material's indentation index. Since hardness is the resistance to deformation by pressure then the harder is the material the lower is its indentation index.

#### **3.7.1 Test procedure**

Square samples of 50 x 50 mm were cut from the two types of leather taken from the regional divisions in the hide described in section 3.3. A total of 9 samples from the hide type-1 and 6 samples from the hide type-2 were used. The size of each sample provided ample surface area to conduct indentation tests at five different locations.

An Hounsfield H25K universal tension-compression testing machine was used for leather hardness tests. The essential features of this machine included a fixed flat steel platform acting as an anvil, a cylindrical steel rod axially attached to a vertical moving axis with a controllable speed of travel, and an incorporated load cell measuring the axial load exerted on the rod. The sample was placed on the



anvil with its flesh side facing up. A steel ball of 3.2 mm diameter was placed on the sample and directly below the flat surface of the rod. The rod was gently lowered to make contact with the ball so that it exerted a load of  $0.1472 \pm 0.0049$  N ( $15 \pm 0.5$  g force) on the ball. This position of the rod was noted as its initial position. It was subsequently lowered gently to its final position so that it exerted a further load of 1 kg force on the ball. The distance travelled by the rod from its initial position to its final position was measured. The value of leather indentation index was calculated by taking the mean of 5 such measurements at different locations within the sample.

### **3.7.2 The results**

In general, indentation index of the hide type-2 is approximately just less than half of that of the type-1 suggesting that the former is just over twice as hard as the latter. Also, in both leather types the indentation index variations in the upper, central, and lower sections of hides follow one another closely. Hardness therefore does not vary greatly along the length of hides. Graphs of fig. 3.13 and fig. 3.14 show the results of hardness tests on the hides type-1 and the type-2 respectively. Hardness variation along the width of the hides follow different patterns in both leathers. In the case of the hide type-1 the values of indentation index increase from the backbone area towards half way through the width of the side before levelling off again in the belly area. This means that the backbone area is harder than the belly area with their respective indentation index values as 0.31 mm and 0.37 mm. In the case of the hide type-2 however, the belly area is harder than the backbone area with the corresponding indentation index values as 0.14 mm and 0.17 mm. It is also noted that the range between upper and lower values of the indentation index across the hide type-1 is about twice that of the corresponding values across the hide type-2.



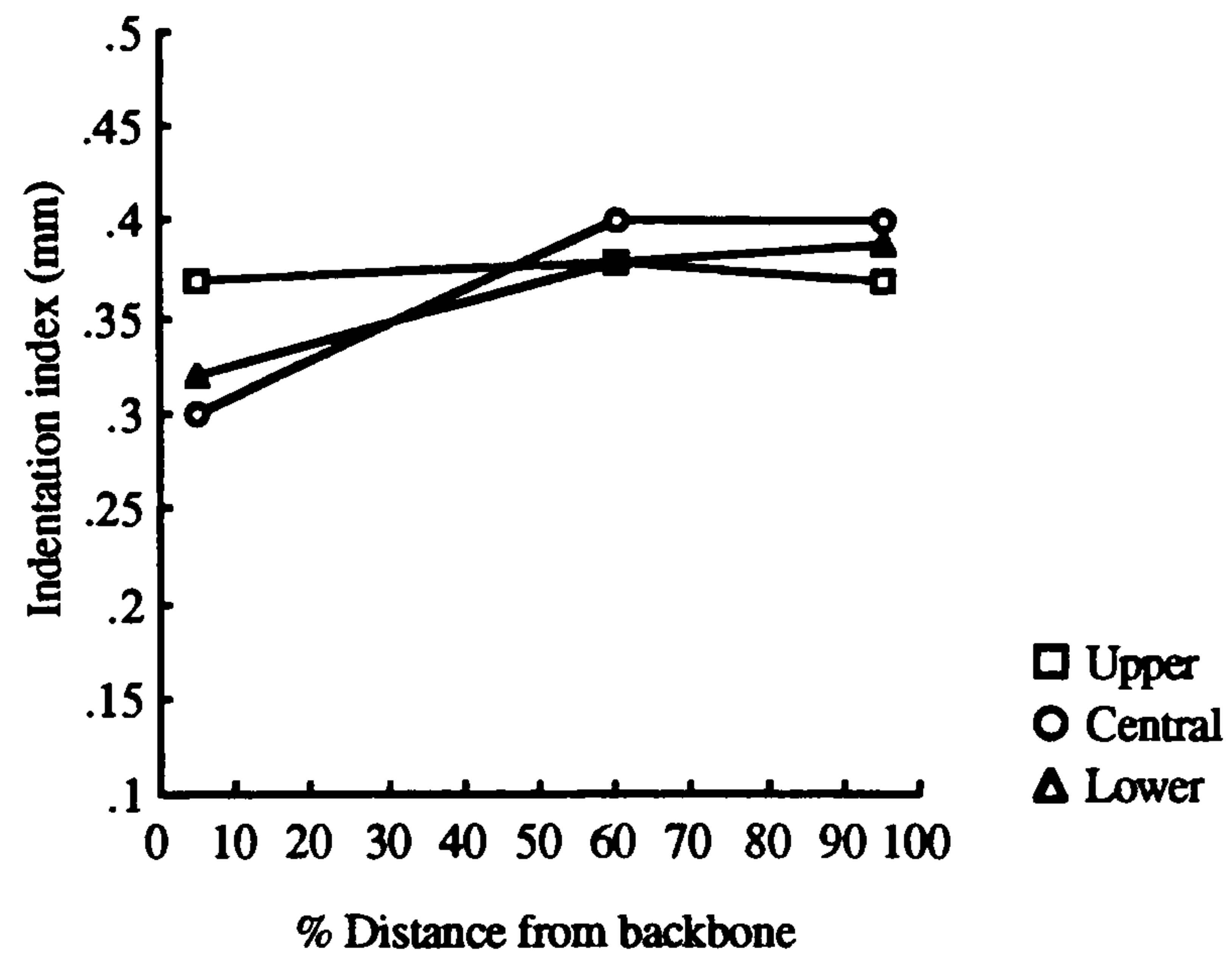


Figure 3.13 Indentation index variation in the hide type-1.

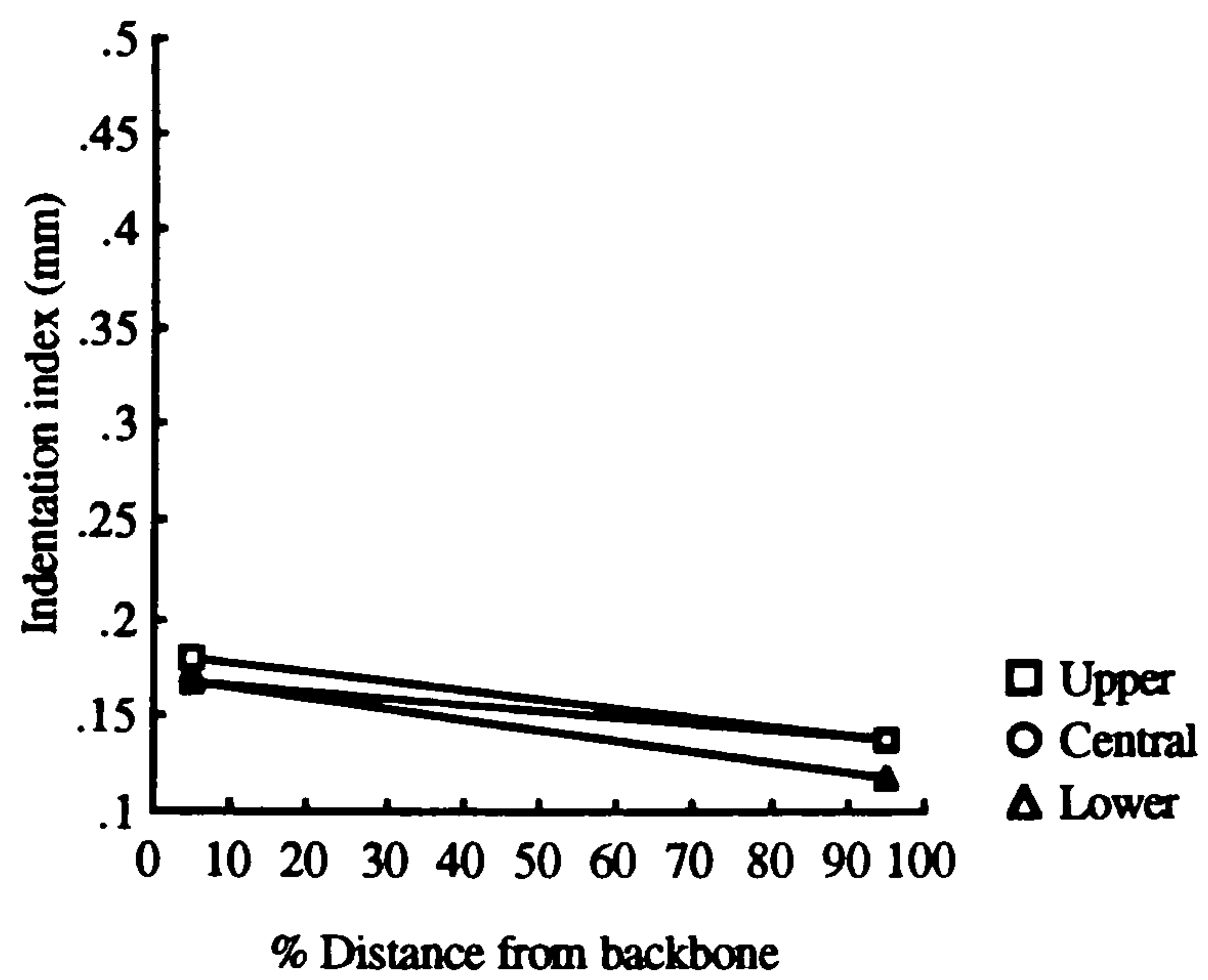


Figure 3.14 Indentation index variation in the hide type-2.



It is further thought that the leather material's apparent density is related to its hardness properties in that the denser the material the harder it is. Apparent density of leather is evaluated when the volume is calculated without allowance for the different-sized pores present in leather. The ratio of the mass to the volume is therefore known as apparent density. On evaluation of overall apparent density of the hides type-1 and type-2 it is found that the former has an apparent density of  $0.598 \text{ gcm}^{-3}$  while the latter has an apparent density of  $0.806 \text{ gcm}^{-3}$ . The difference in density in the two leather types is reflected in the materials' fluffiness of their flesh side. The values of indentation index further confirm the higher degree of fluffiness of the hide type-1 over the hide type-2.

### **3.8 Material compression properties**

The differences between the degree of compressibility of leather materials are not easily detectable through tactile inspection alone. Nevertheless this is a property that could influence the skiving conditions in many ways. In the case of high speed machining the cutting tool tips are caused to subject the leather fibres to a certain degree of compression just prior to cutting. This results in a better surface finish quality by avoiding free cutting of the material. Thus, for a fixed cutting tool position relative to the workpiece the degree of compressibility of different leathers could, on its own, influence the resulting surface finish. So far as matrix skiving is concerned the leather material is subjected to the cutting action of the rotating band knife. In a similar analogy to the case of the high speed cutting tool mentioned above, a higher degree of material resistance to compression at the time of the action of the band knife results in a better surface finish.

In both methods of material removal it is therefore expected that, for a given depth of cut, materials with higher resistance to compression yield better surface finish quality. The effect of material compressibility on the cutting surface finish may however be insignificant in the presence of other dominant factors in the skiving process. The tests in this section provide the information regarding the degree of variation of resistance to compression of various regions of the two hide types. This information may then be compared with those of skiving tests to establish their significance and any possible correlation.



### 3.8.1 Test procedure

Samples of 50 x 50 mm were cut from the two types of leather taken from the regional divisions in the hide described in section 3.3. A total of 9 samples from the hide type-1 and 6 samples from the hide type-2 were used. The size of each sample provided ample surface area to conduct compression tests at four different locations.

The tension-compression testing machine, as described in section 3.7.1, was used to determine the resistance to compression of the samples. The vertical rod attached to the moving axis of the machine had a flat circular lower base of 10 mm diameter. After measuring its thickness, the leather sample was placed on a horizontal platform, with its flesh side facing up, such that the location to be tested was placed directly under the rod. The rod was gently lowered to make contact with the sample such that it exerts a load of  $0.2453 \pm 0.049$  N ( $25 \pm 5$  gm force) on the sample. This position of the rod was noted as its initial position. The rod was lowered again to its final position so that it exerted a further load of 250 N on the sample. Using the automatic data acquisition system incorporated with the machine a graphical record of the load in N against compression in mm was obtained. Fig. 3.15 shows a typical load-compression graph. This procedure was repeated 4 times for each sample. From each graph the value of compression corresponding to 25 N load was recorded and a mean value for each hide region was obtained.



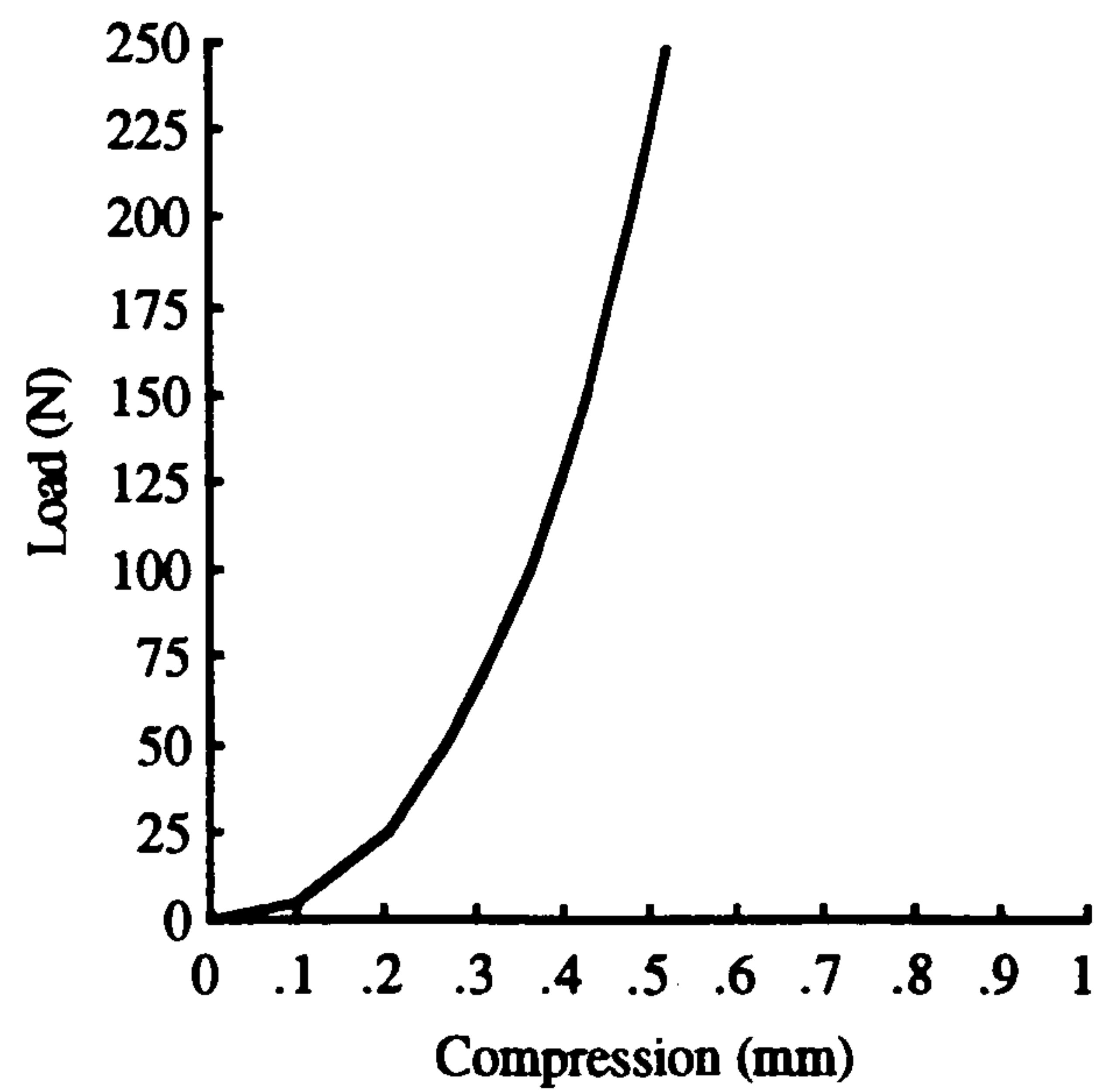


*Figure 3.15 A typical leather load-compression characteristic.*

The value of resistance to compression,  $R$ , is defined as [27]:

$$R = \frac{\text{increase of load per unit area}}{\text{decrease in thickness per unit thickness}}$$

$$\therefore R = \frac{F/A}{\Delta d/d_0} \quad (3.2)$$

where:  $R$  = resistance to compression in  $\text{Ncm}^{-2}$

$F$  = applied load in  $\text{N}$  [ = 25 N ]

$A$  = area under compression in  $\text{cm}^2$  [ =  $\pi/4$  at 10 mm diameter ]

$\Delta d$  = mean decrease in thickness due to compression

$d_0$  = mean original thickness under no compression



The value of  $F$  was chosen at 25 N since it falls within the realistic range of the kind of forces involved in the skiving processes considered. Values of resistance to compression for each region was thus calculated for the two leather types.

### 3.8.2 The results

On evaluation of the materials' compressibility for both hide types, it is found that the results do not vary greatly in both cases, with the hide type-2 slightly more compressible than the hide type-1. Values of resistance to compression across the hide type-1 lies in a range bound by 222 and 362  $\text{Ncm}^{-2}$  while the corresponding values for the hide type-2 are 235 and 308  $\text{Ncm}^{-2}$ . The total mean value of the resistance to compression for the entire regions of the hide type-1 is 281  $\text{Ncm}^{-2}$  with a standard deviation of 44.7. The corresponding values of mean and standard deviation for the hide type-2 are however 262  $\text{Ncm}^{-2}$  and 27.2 respectively. This suggests that although the mean values are quite close to each other there is more variability of the compressibility in the hide type-1. In this hide type, the backbone areas are noted for their highest resistance to compression, and in particular the upper section where the resistance to compression reaches a value of 362  $\text{Ncm}^{-2}$ .

The differences between the pattern of change of this property within each hide type are noteworthy. Whereas in the hide type-1, and close to the backbone, the lower section is the most compressible and the the upper section is the least compressible areas, the case is the reverse for the hide type-2. The central regions in both hide types do not vary widely in the backbone and belly areas. Fig. 3.16 and fig. 3.17 show the variations of material resistance to compression in the two hide types.



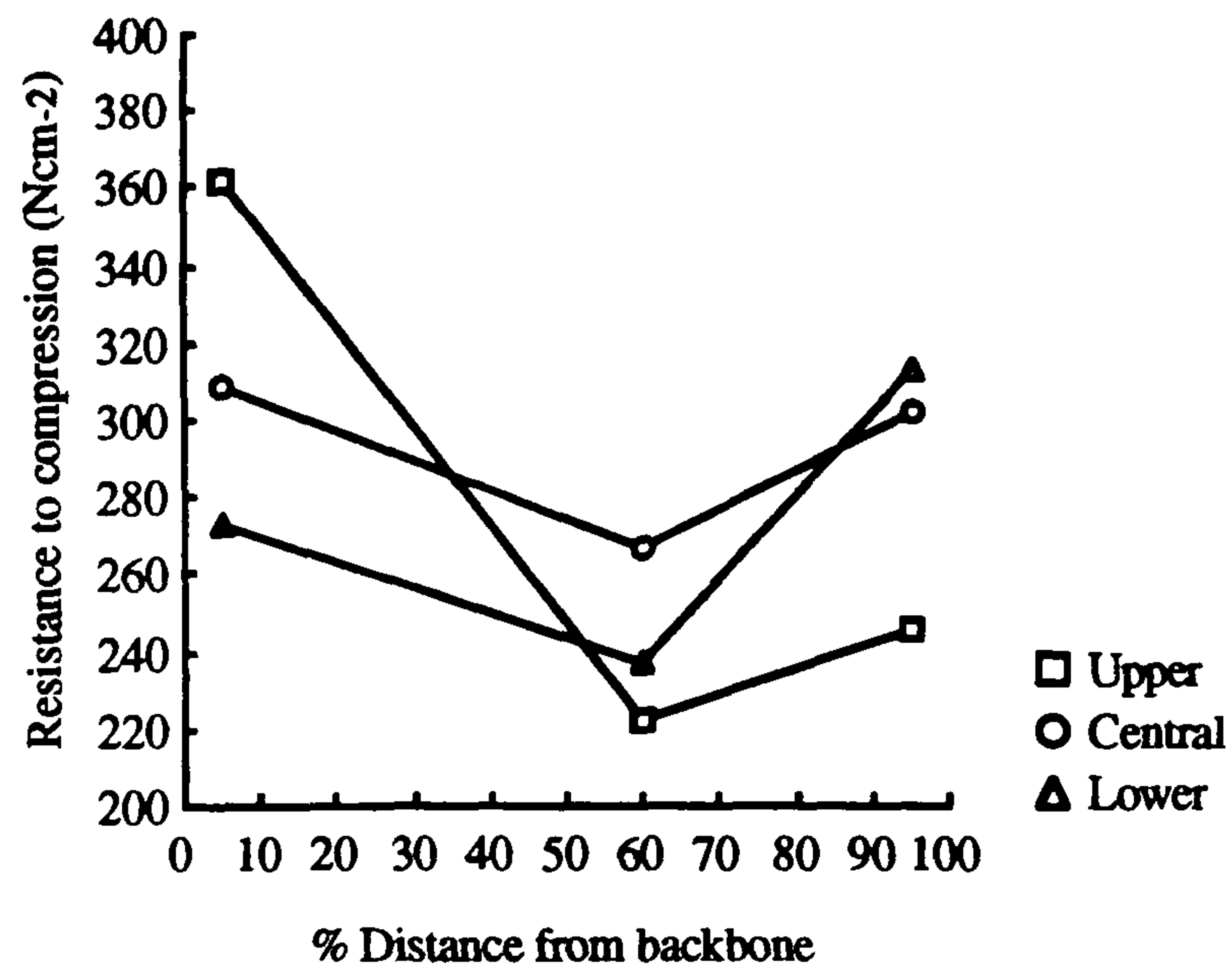


Figure 3.16 Variation of resistance to compression in the hide type-1.

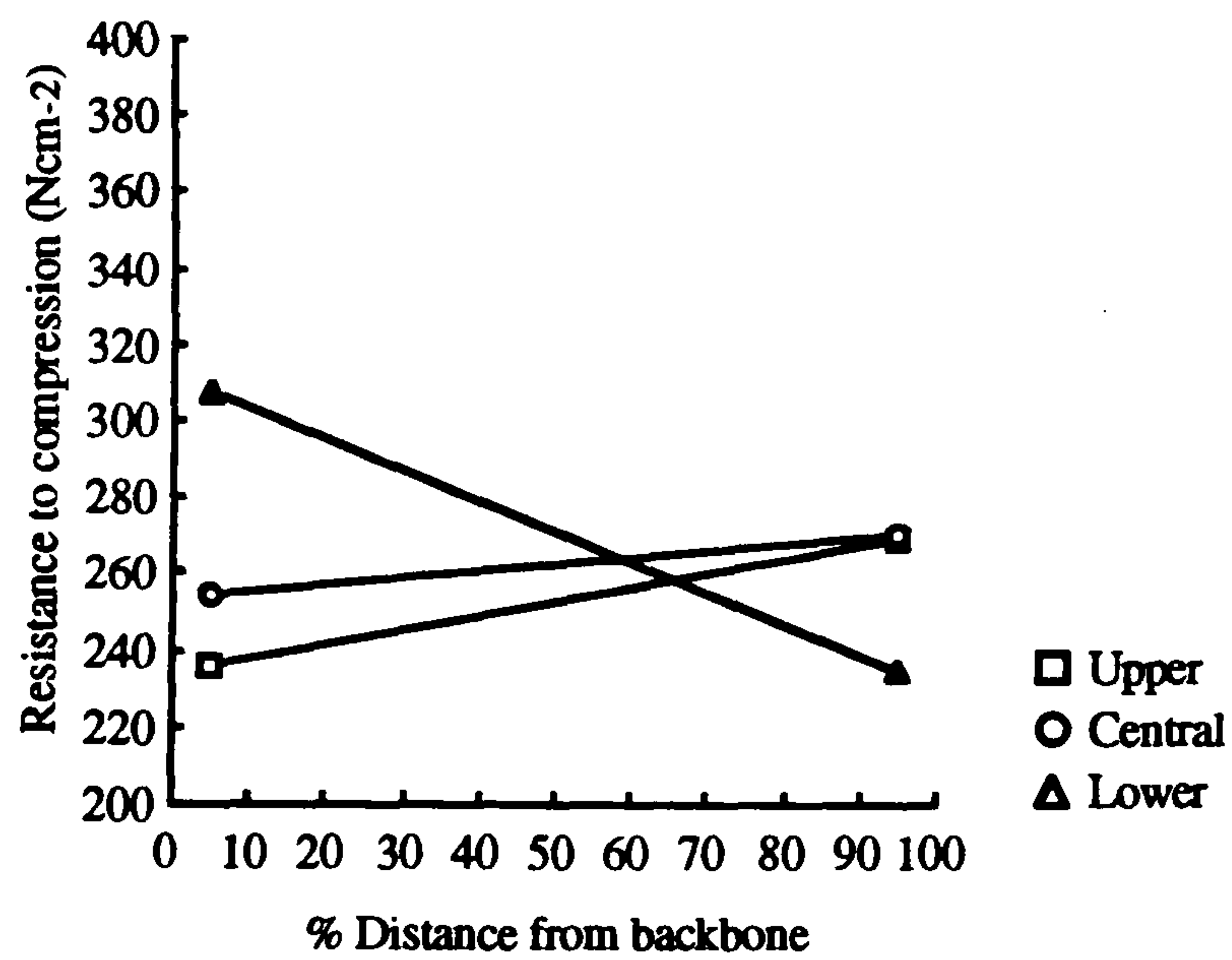


Figure 3.17 Variation of resistance to compression in the hide type-2.



### **3.9 Material tensile strength properties**

For any component that is subjected to the action of various mechanical forces resulted from engineering applications such as material removal and static/dynamic clamping, as in skiving, the determination of its strength properties gives vital information. The tensile strength is one such property. Much of the existing work in the examination of tensile strength of leather, as referred to in section 3.4, concentrate on an objective study of leather with its variation in terms of, say, chemical composition and source of origin. The work in this section, however, employs similar strategies for specimen preparation and testing method but concentrates on a subjective study where possible correlations with the skiving parameters may be made. Use of British Standards 3144 [27] for the determination of leather tensile strength was made to evaluate its pattern of variation across the two standard hide types, and the results are given in  $\text{Ncm}^{-2}$ . For each value of tensile strength the corresponding value of percentage elongation was also calculated.

#### **3.9.1 Test procedure**

Test specimens were taken from the two hide types, and from hide regions mentioned in section 3.3. The effective length and width of the specimens were 33 mm and 6.5 mm respectively. In order to account for the possible directionality of tensile strength in a hide, the specimens were cut in the directions making angles of  $0^\circ$ ,  $30^\circ$ ,  $45^\circ$ ,  $60^\circ$ , and  $90^\circ$  to the backbone in the case of hide type-1, and  $0^\circ$ ,  $45^\circ$ , and  $90^\circ$  to the backbone in the case of hide type-2.

An Instron model 1000 tension-compression testing machine with an incorporated chart recorder was used. Mean thickness of each specimen was evaluated prior to its tensile testing up to the point of rupture. The load-extension graph for each test was recorded for each test in real time. From this graph the tensile strength, in  $\text{Ncm}^{-2}$ , together with the percentage elongation of the material for each specimen was calculated. A typical load-extension graph for leather is shown in fig. 3.18. Referring to this graph, the material shows a region of linear deformation between the points A and B. This confirms a significant amount of elastic characteristic of leather. However, further extension beyond point B, and up to the point of rupture at C, is noted by a region of non-linearity. Point B therefore represents the load at apparent departure from the linear deformation region, while point C represents the load at rupture.



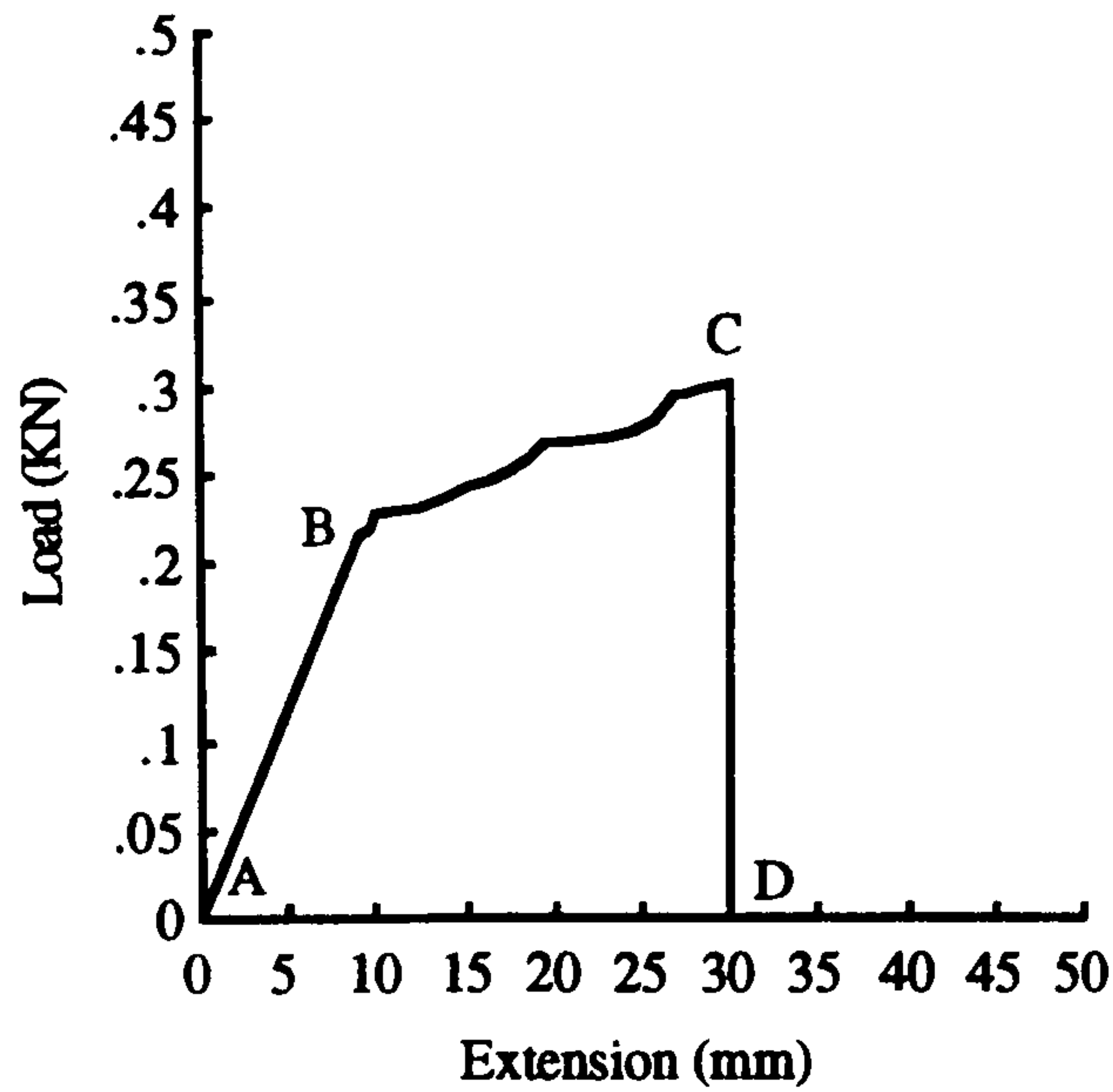


*Figure 3.18 A typical leather load-extension characteristic.*

The values of tensile strength,  $S$ , and percentage elongation,  $e$ , are obtained as follows:

$$S = \left[ \frac{F}{A} \right] \quad (3.3)$$

where:  $S$  = tensile strength in  $\text{Ncm}^{-2}$

$F$  = Load at rupture in  $\text{N}$

$A$  = cross sectional area of specimen (ie. width x thickness) in  $\text{cm}^2$

and also;

$$e = \left[ \frac{\delta l}{l_0} \times 100 \right] \quad (3.4)$$

where:  $e$  = percentage elongation

$\delta l$  = extension of the specimen up to the rupture

$l_0$  = original length of the specimen



### 3.9.2 The results

Tensile strength of leather is the greatest around the backbone area and is the weakest around the belly area. This phenomenon is more clearly observed in the case of the hide type-1 where the differences between the backbone and the belly areas in terms of material fluffiness and compactness are distinct. The tensile strength of this type of leather reaches as high a value as  $4.0 \text{ KNcm}^{-2}$  in the backbone area while it falls to  $2 \text{ KNcm}^{-2}$  in the belly area. In the case of the hide type-2 the variation of tensile strength remains relatively small with upper and lower limits of  $4.2$  and  $3.3 \text{ KNcm}^{-2}$  respectively. In both hide types however, in the regions further away from the backbone, and close to the belly, the central sections of the hides are less stronger than either the upper or the lower sections. The material in these regions of the hide is characteristically noted for its floppiness where the original skin had been subjected to large amounts of stretch. Indeed the percentage elongation relating to samples tested from these areas are typically higher than areas close to the backbone.

In general, the variation of tensile strength is approximately and reversely matched with that of percentage elongation (stretch). That is to say, increases in tensile strength are in conjunction with decreases in elongation. It is also noted that, in order to reach the point of rupture, the hide type-2 experiences a comparatively higher percentage elongation than the hide type-1. For example, whereas the hide type-1 at areas near the backbone has a percentage elongation reaching 95%, the hide type-2 in the same region has a percentage elongation reaching 120%. The directionality of the tensile strength tests do not seem to have general and significant correlations with the tensile strength values.

Figs. 3.19(a), 3.19(b), and 3.19(c) show the regional variations of tensile strength at distances 5%, 60%, and 95% of the hide's width from the backbone for the hide type-1, while figs. 3.20(a), 3.20(b), and 3.20(c) show the corresponding variations of percentage elongation. Similarly, figs. 3.21(a) and 3.21(b) show the variations of tensile strength at distances 5% and 95% of the hide's width from the backbone for hide type-2, while figs. 3.22(a) and 3.22(b) show the corresponding variations of percentage elongation.



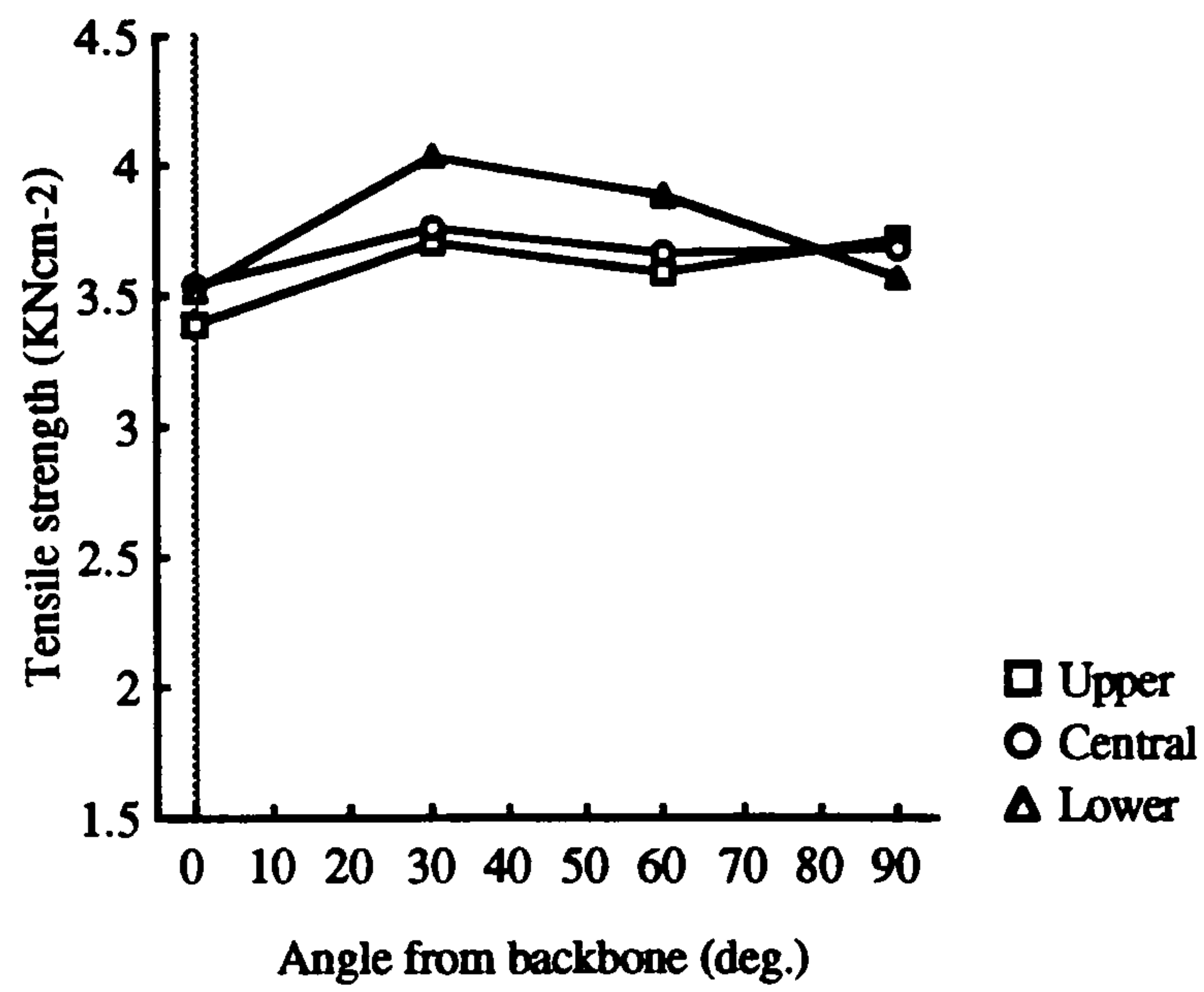


Figure 3.19(a) Tensile strength variation close to the backbone, hide type-1.

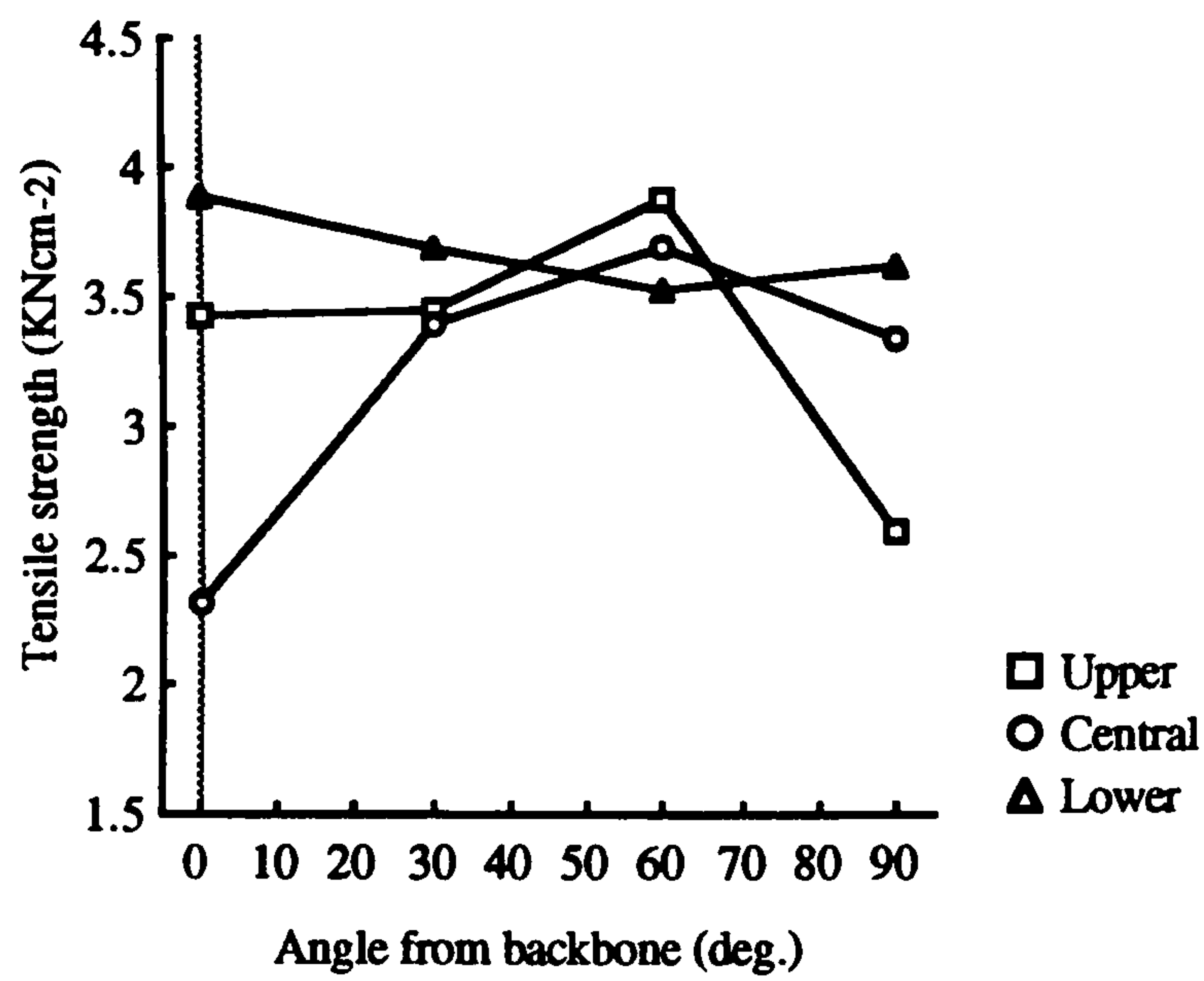


Figure 3.19(b) Tensile strength variation in the mid-side region, hide type-1.



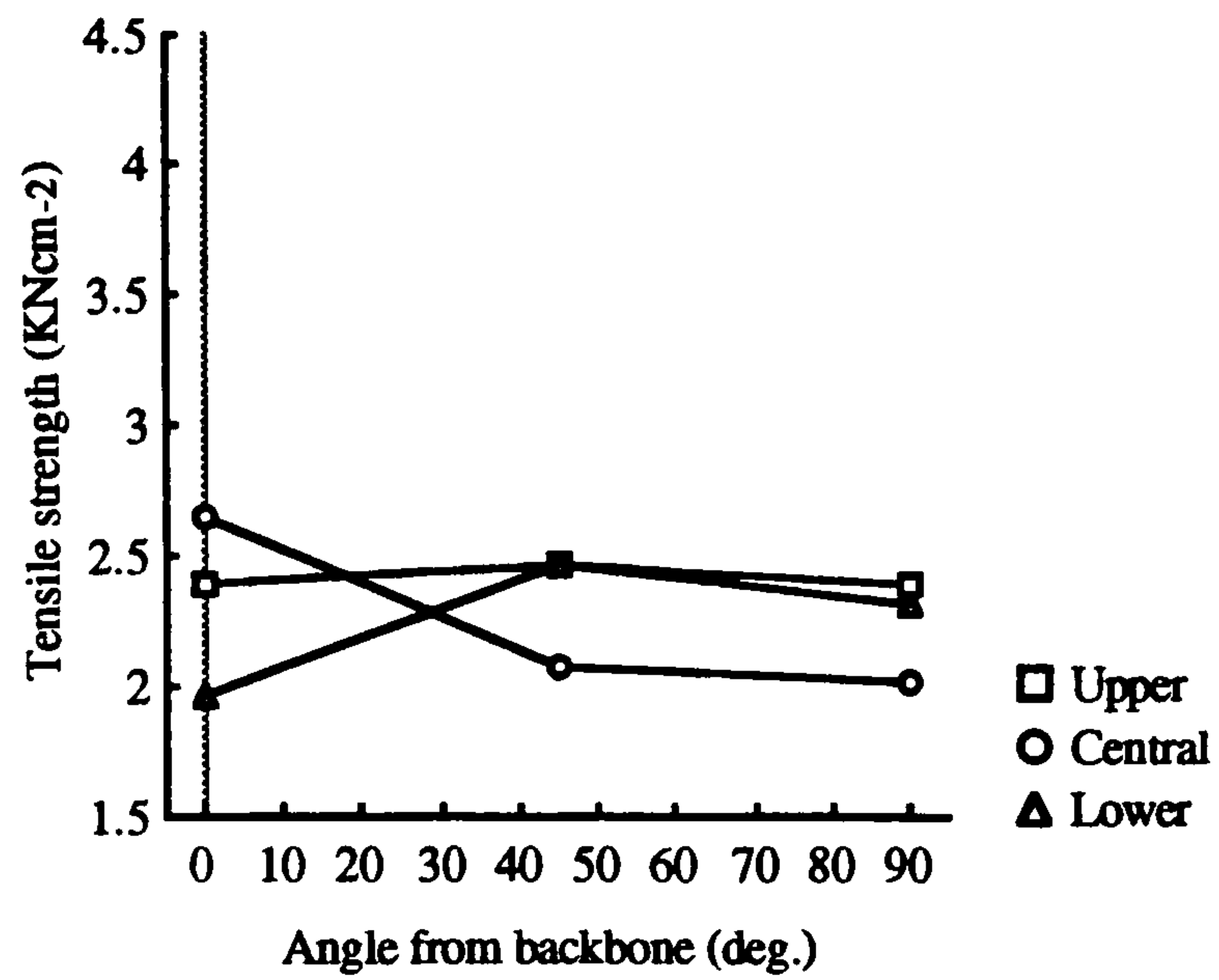


Figure 3.19(c) Tensile strength variation close to the belly, hide type-1.

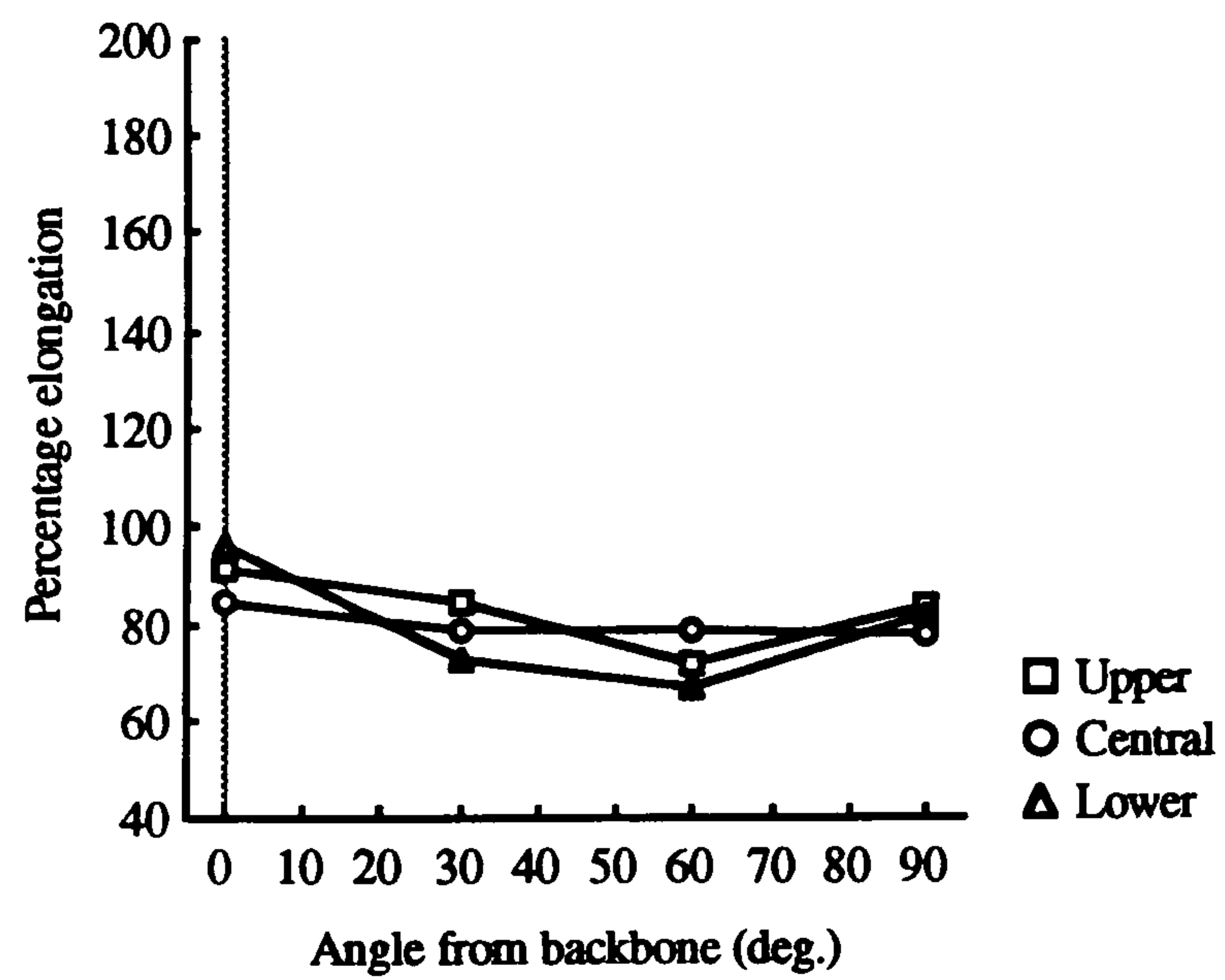


Figure 3.20(a) Variation of elongation close to the backbone, hide type-1.



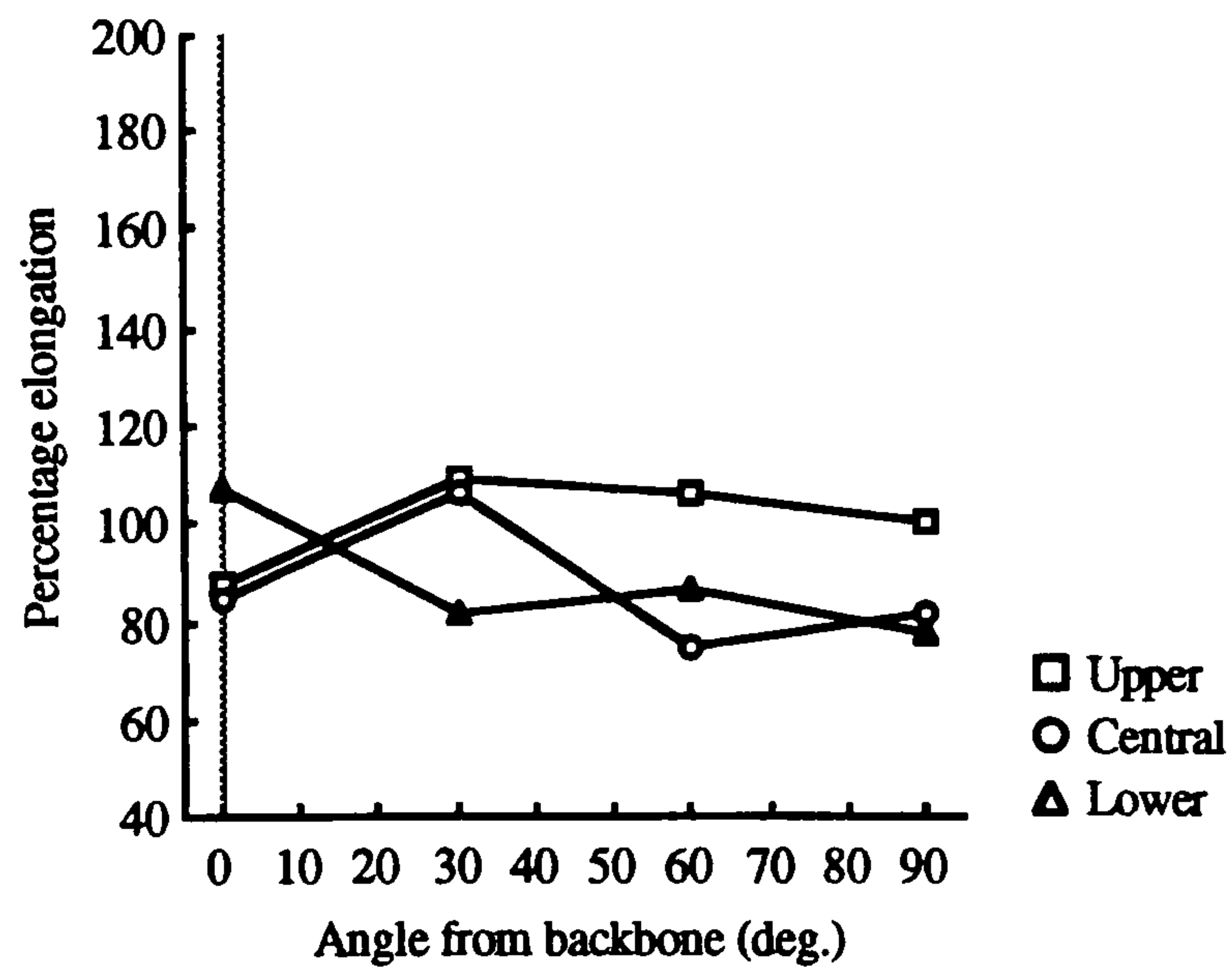


Figure 3.20(b) Variation of elongation in the mid-side region, hide type-1.

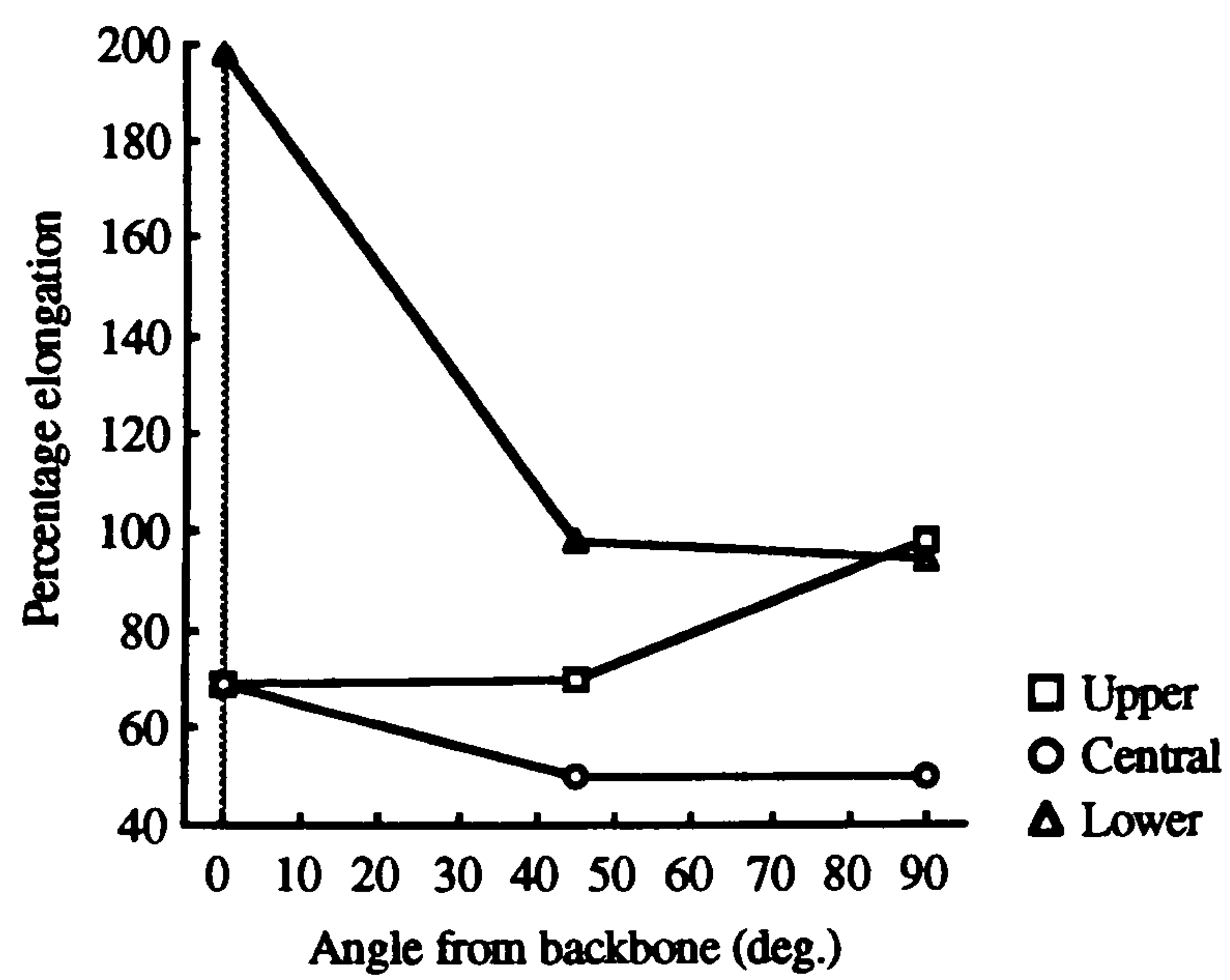


Figure 3.20(c) Variation of elongation close to the belly, hide type-1.



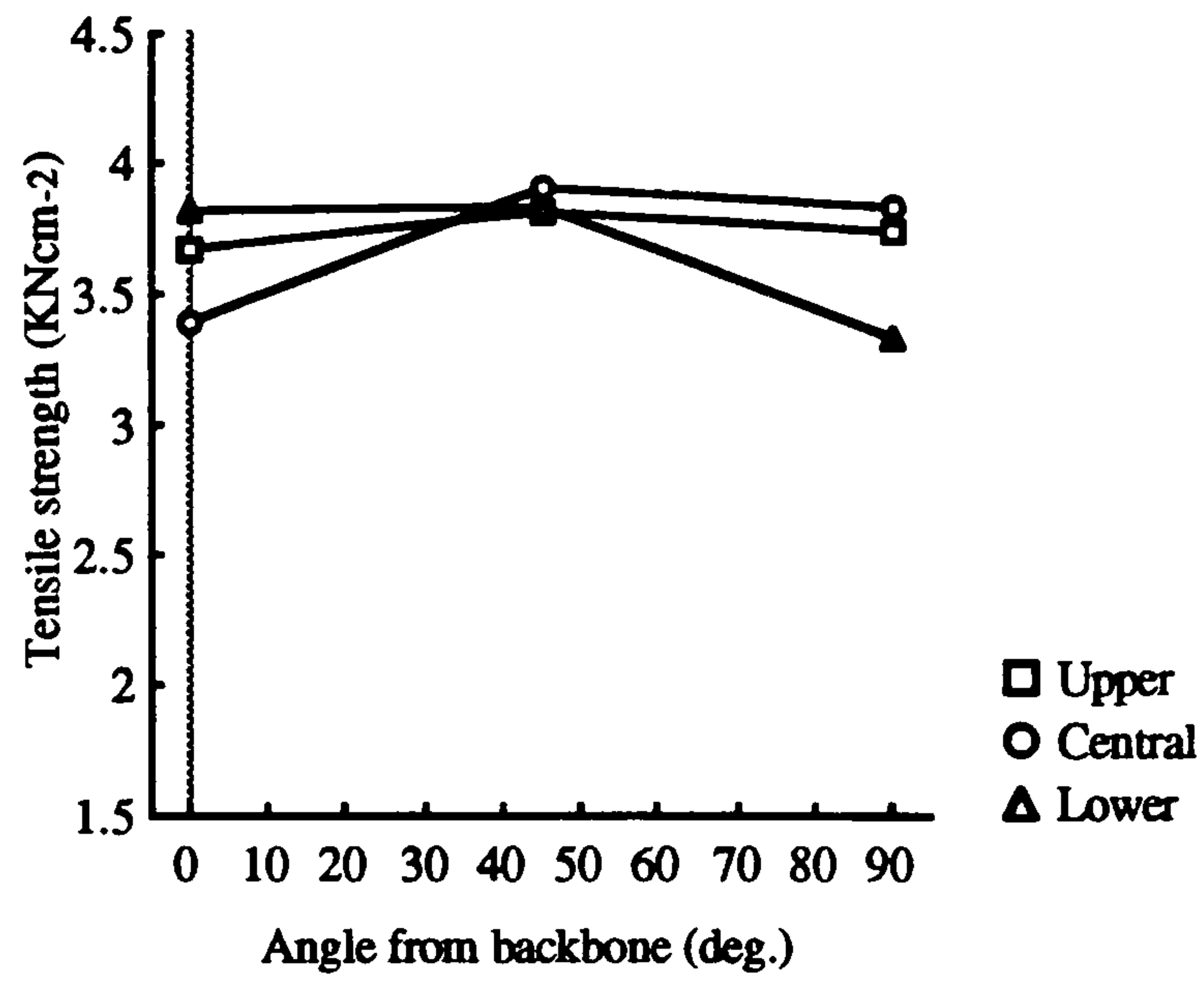


Figure 3.21(a) Tensile strength variation close to the backbone, hide type-2.

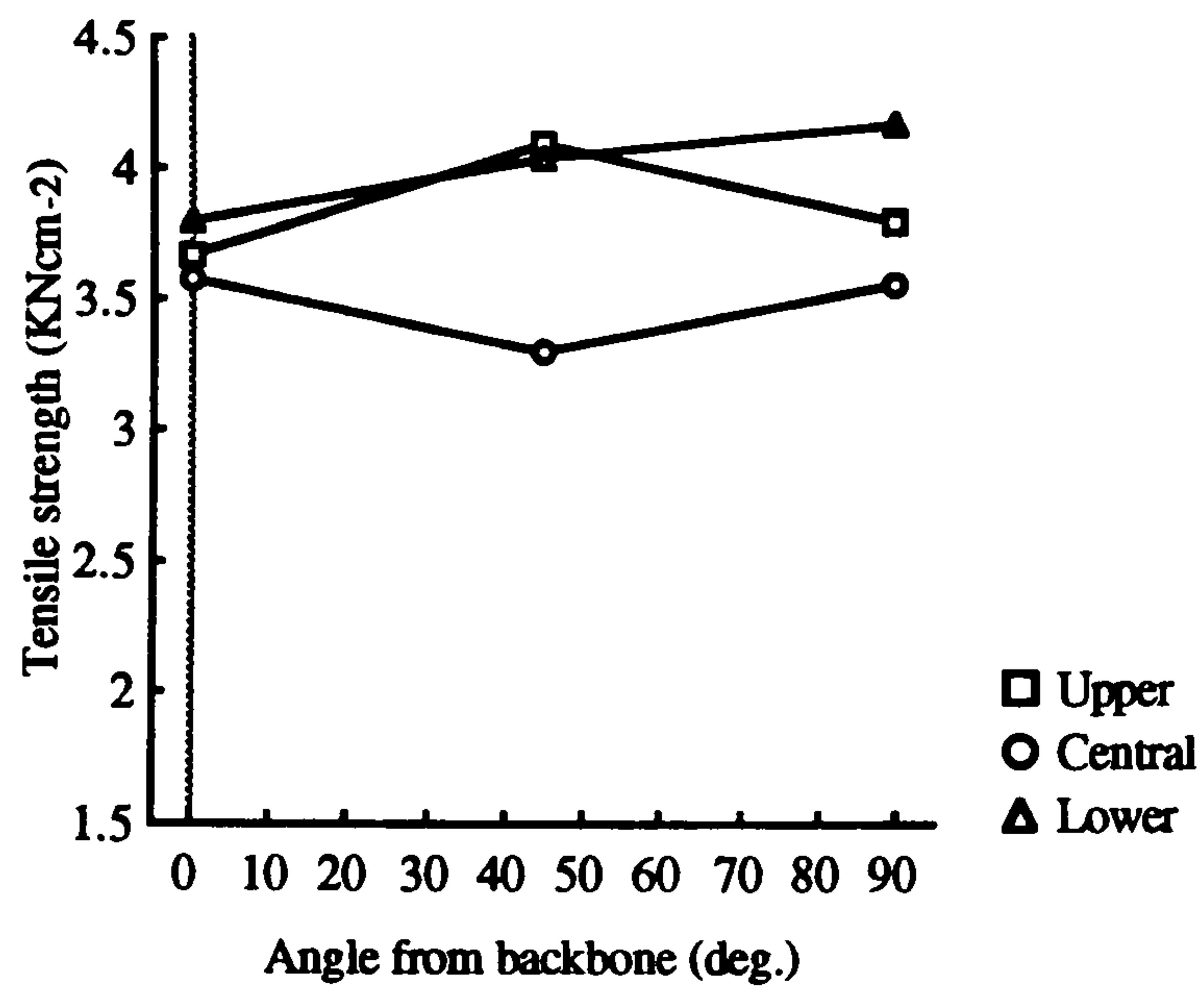


Figure 3.21(b) Tensile strength variation close to the belly, hide type-2.



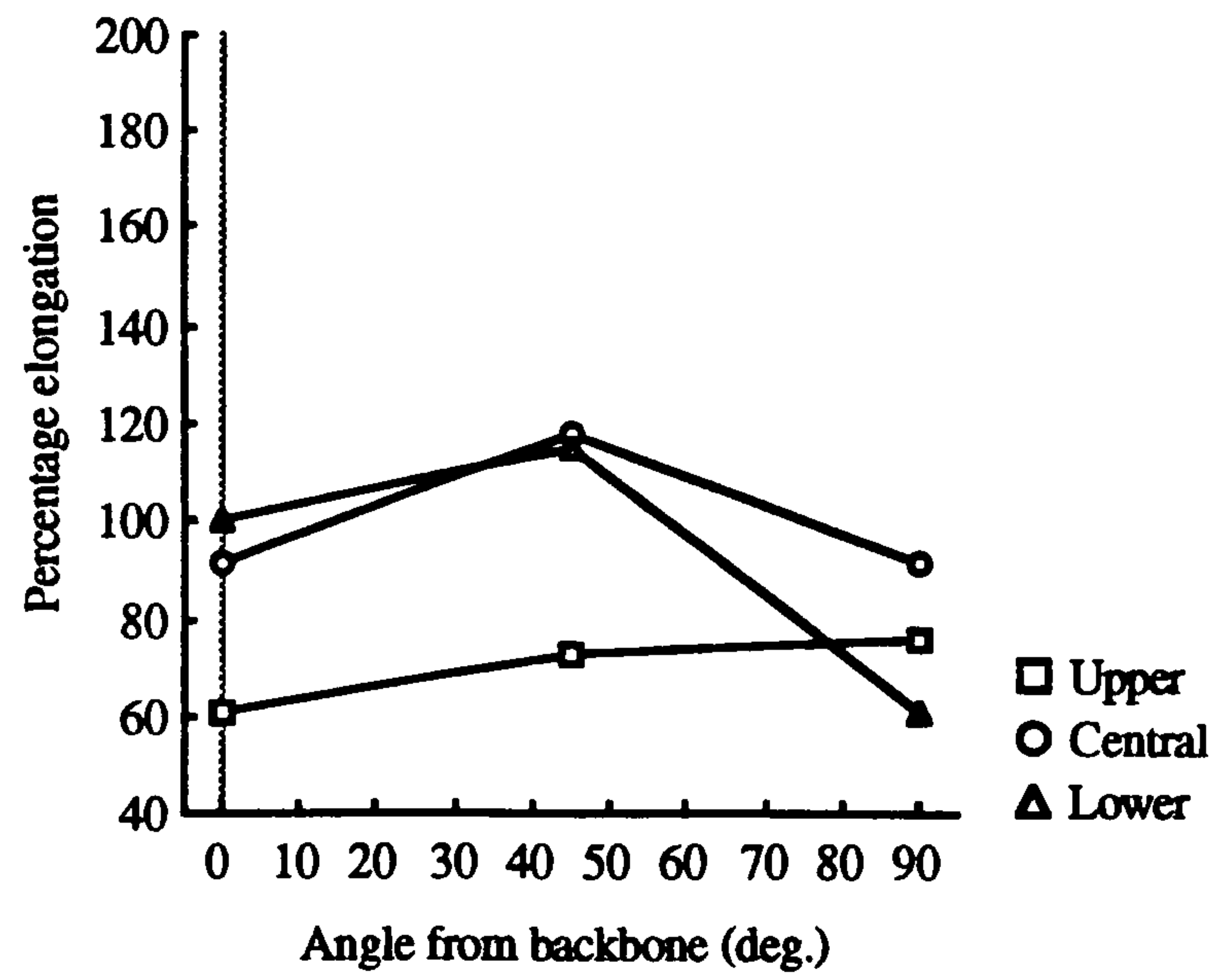


Figure 3.22(a) Variation of elongation close to the backbone, hide type-2.

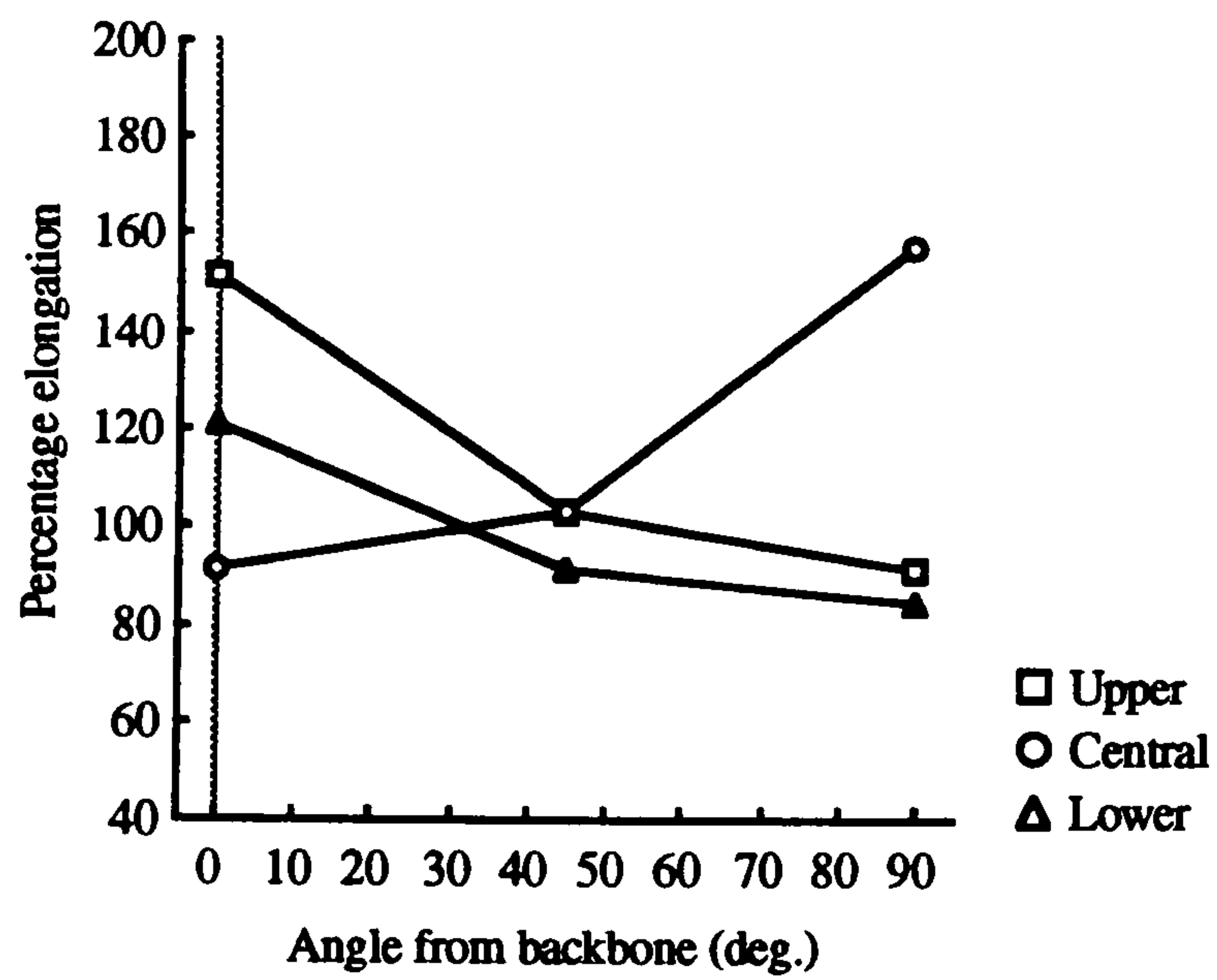


Figure 3.22(b) Variation of elongation close to the belly, hide type-2.



It is mentioned in section 3.9.1 that the leather load-extension curve includes a region of apparent departure from its linear part. On evaluation of the maximum linear stress it was found that this quantity exhibits generally less fluctuation than tensile strength. However, in the hide type-1 the average maximum linear stress (at  $2.4 \text{ KNcm}^{-2}$ ) is 35% lower than tensile strength, whereas no appreciable change is noted between the same quantities in the hide type-2. This implies that the deformation behaviour in the hide type-2 is very nearly linear followed by a short region of non-linearity.

### **3.10 Material tearing properties**

Elements of leather fibre network, consisting of fibres organised in long wavy bundles, are subjected to a tearing process when skiving takes place in the forms considered in this work. The ease with which material, in the form of chip, is removed from leather is therefore related to the fibre strength of its fibre network. Section 3.9 considers the effects of tensile strength on skiving. This property is used to describe the required force (and hence stress) in producing a rupture in leather as a result of material stretch. A test that describes the required force in producing a rupture with little or no stretching, simply involves tearing of the material. The advantage of the tearing test is that it involves no measures other than pure tearing. Determination of material's tearing properties may therefore be correlated to its skiving properties for any possible correlation.

To measure the tearing force the test specimen was split initially by a small amount at one side so that two tongues at either sides of the split were produced. Further separation of the tongues from each other resulted in increase of the length of the split, and tearing takes place. The force required to perform the tearing test was quoted as the material's tearing load. This method measures the tearing load relating to a single tear. Alternatively, double tearing test may be conducted by simultaneously propagating two initial splits, one at each side of a cut out section within the test piece. The magnitude of the force quoted for the double tearing test is twice that of the single tearing test. In this section the procedure and the results of the double tearing test in accordance with British Standards 3144 [27] are given. For all tests the tearing load was measured in N.



### 3.10.1 Test procedure

Test samples were obtained from the two hide types, and from hide regions mentioned in section 3.3. In order to account for the possible directionality of the tearing load, test pieces were cut in the directions making angles of  $0^\circ$ ,  $30^\circ$ ,  $45^\circ$ ,  $60^\circ$ , and  $90^\circ$  to the backbone in the case of the hide type-1, and  $0^\circ$ ,  $45^\circ$ , and  $90^\circ$  to the backbone in the case of the hide type-2.

Fig. 3.23 shows the form and dimensions of a test sample. The profile of the cut out section in the middle of the sample consists of two curved 'V'-shaped sides opposite each other at A and B. When the sides CD and EF were simultaneously pulled in the opposite directions, and in the plane of the test piece, simultaneous tearing took place both at A and at B, and along the line AB. An Instron tension-compression testing machine with an incorporated chart recorder was used to produce the separation of the sides CD and EF. Fig. 3.24 shows a typical tearing load graph during a test. After an initial resistance to the applied load the material began to experience rupture in the form of tearing. The load required to maintain the tearing process remained principally constant but was subjected to small fluctuations due to the non-homogeneity of the material in terms of the random distribution of its fibre network bundles. The tearing load is thus a measure of the force needed in breaking these bundles.

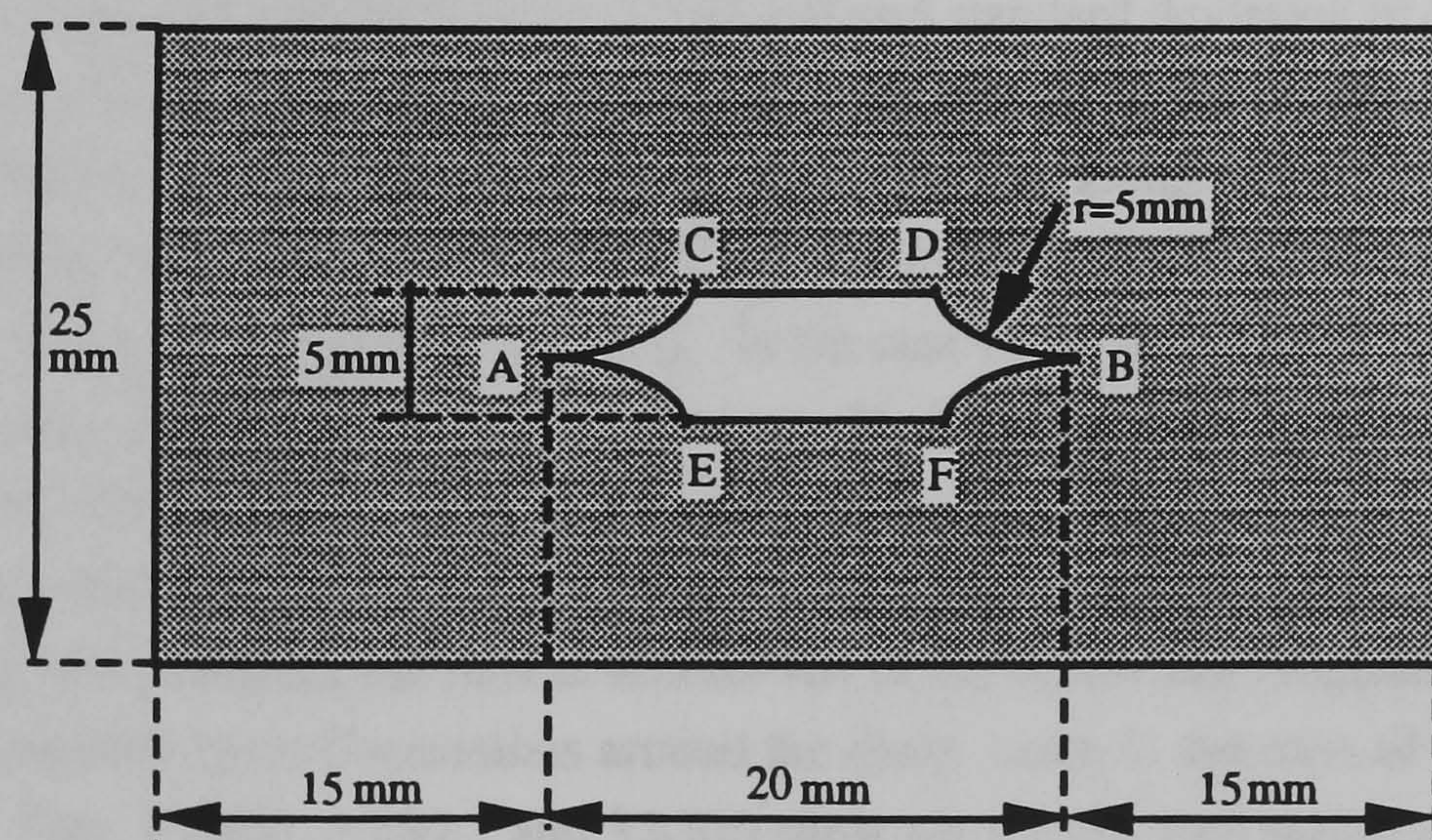
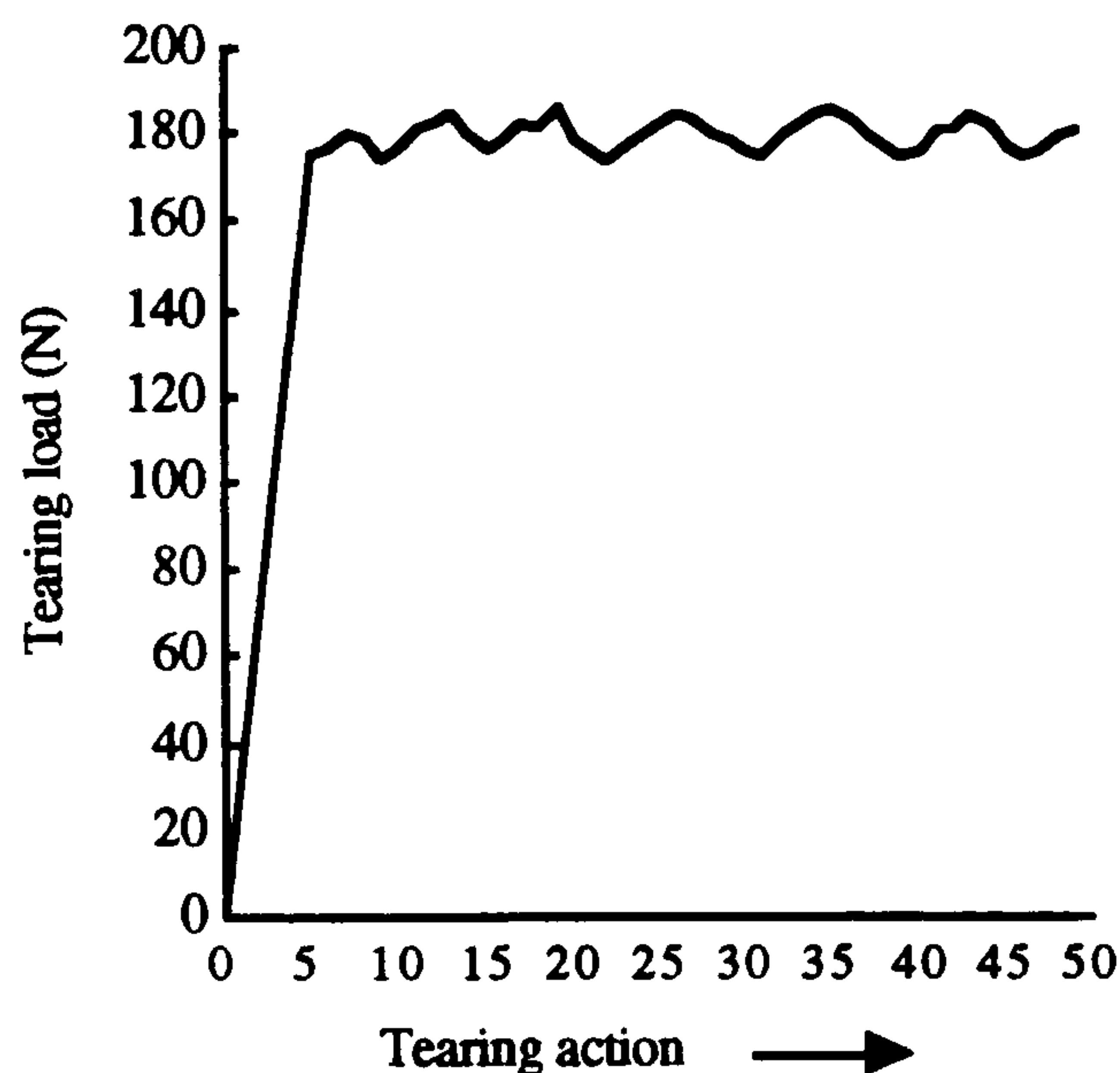


Figure 3.23 The form and dimensions of the tearing load test samples.





*Figure 3.24 A typical leather tearing load characteristic.*

### 3.10.2 The results

Tearing load in the hide type-1 has a small variation with a mean value of 164.5 N and standard deviation of 8.2 while it has a more fluctuating variation in the hide type-2 with a mean value of 163.1 N and standard deviation of 26.2. In both cases the effect of the direction of tear with respect to the backbone seems insignificant. So far as the location of the samples along the length of the backbone is concerned the values of tearing load in hide type-1 remain unaffected and the results are close to one another. In the case of the hide type-2 the central hide sections exhibit higher resistance to tear with the tearing load reaching as high a value as 196 N close to the backbone. The same value drops to around 120 N in the upper and lower hide sections. It may therefore be noted that leather tearing load remains generally uniform at around 164 N across the hide regions in both hide types with more fluctuations around the mean value in the case of the hide type-2. Figs. 3.25(a), 3.25(b), and 3.25(c) show the tearing load variation for the hide type-1, and figs. 3.26(a) and 3.26(b) show the same variation for the hide type-2. In all cases the tearing load is plotted against the direction of tear with



respect to the backbone direction, with separate plots for the original sample locations across the width of the hides.

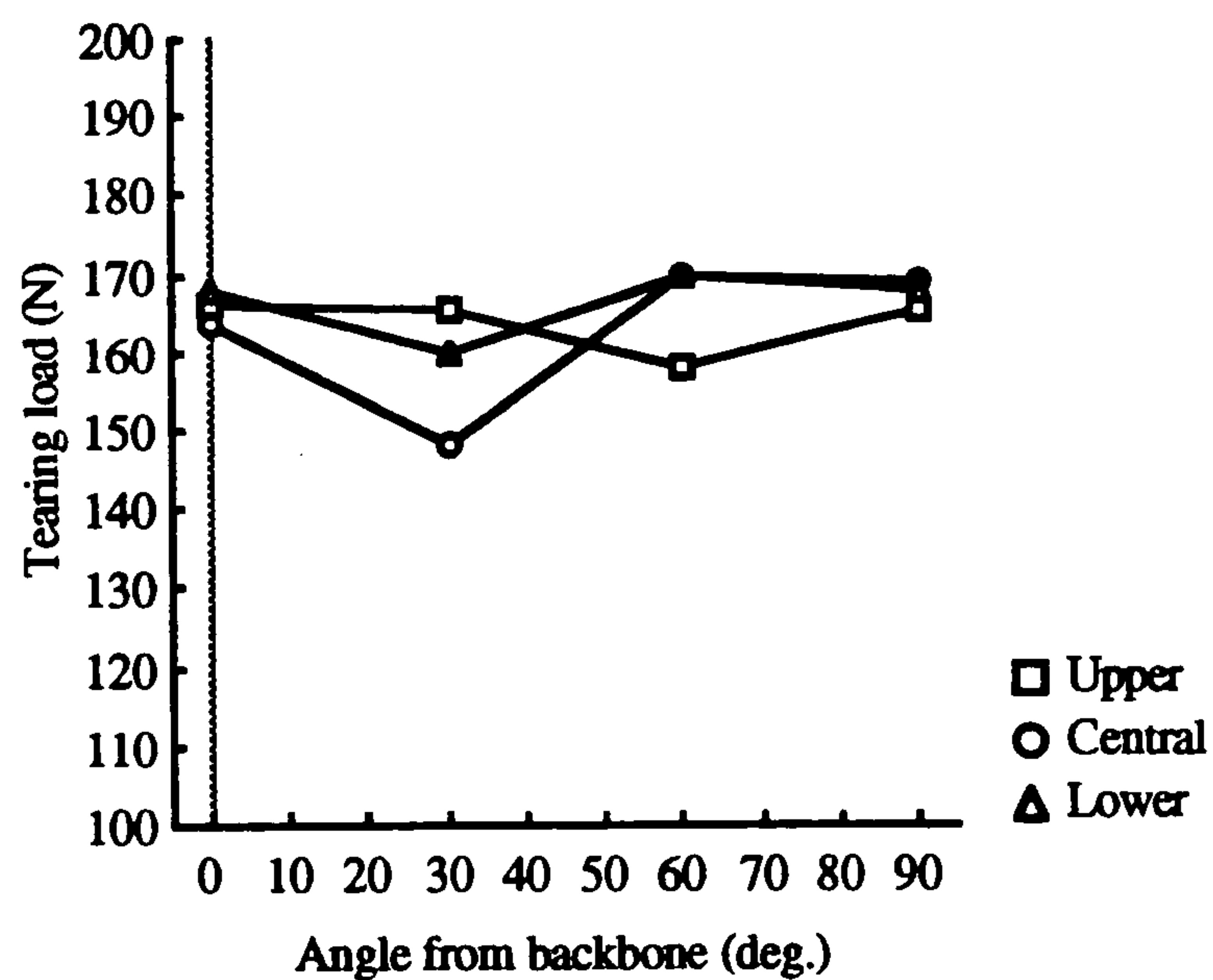


Figure 3.25(a) Tearing load variation close to the backbone, hide type-1.

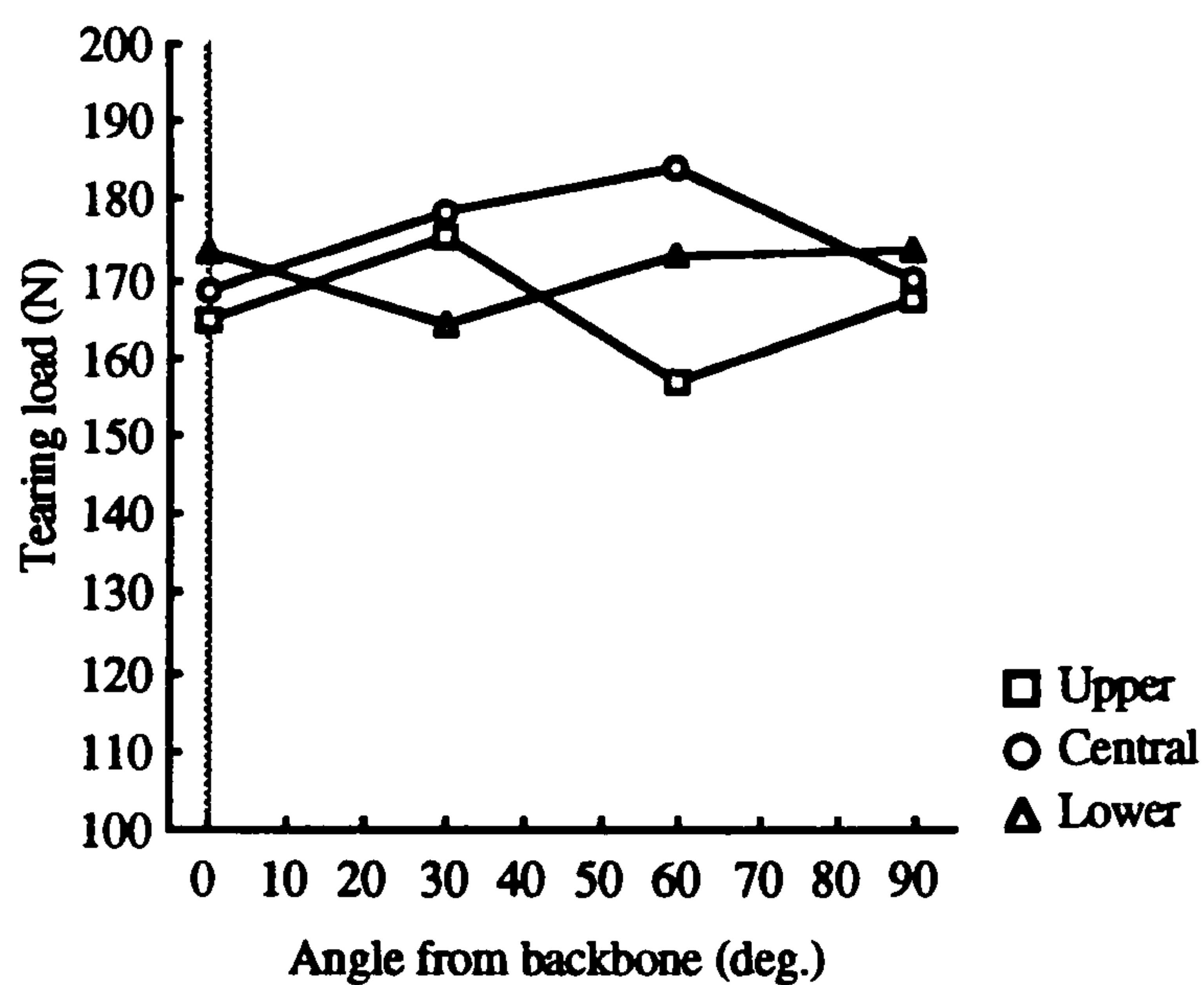


Figure 3.25(b) Tearing load variation in the mid-side region, hide type-1.



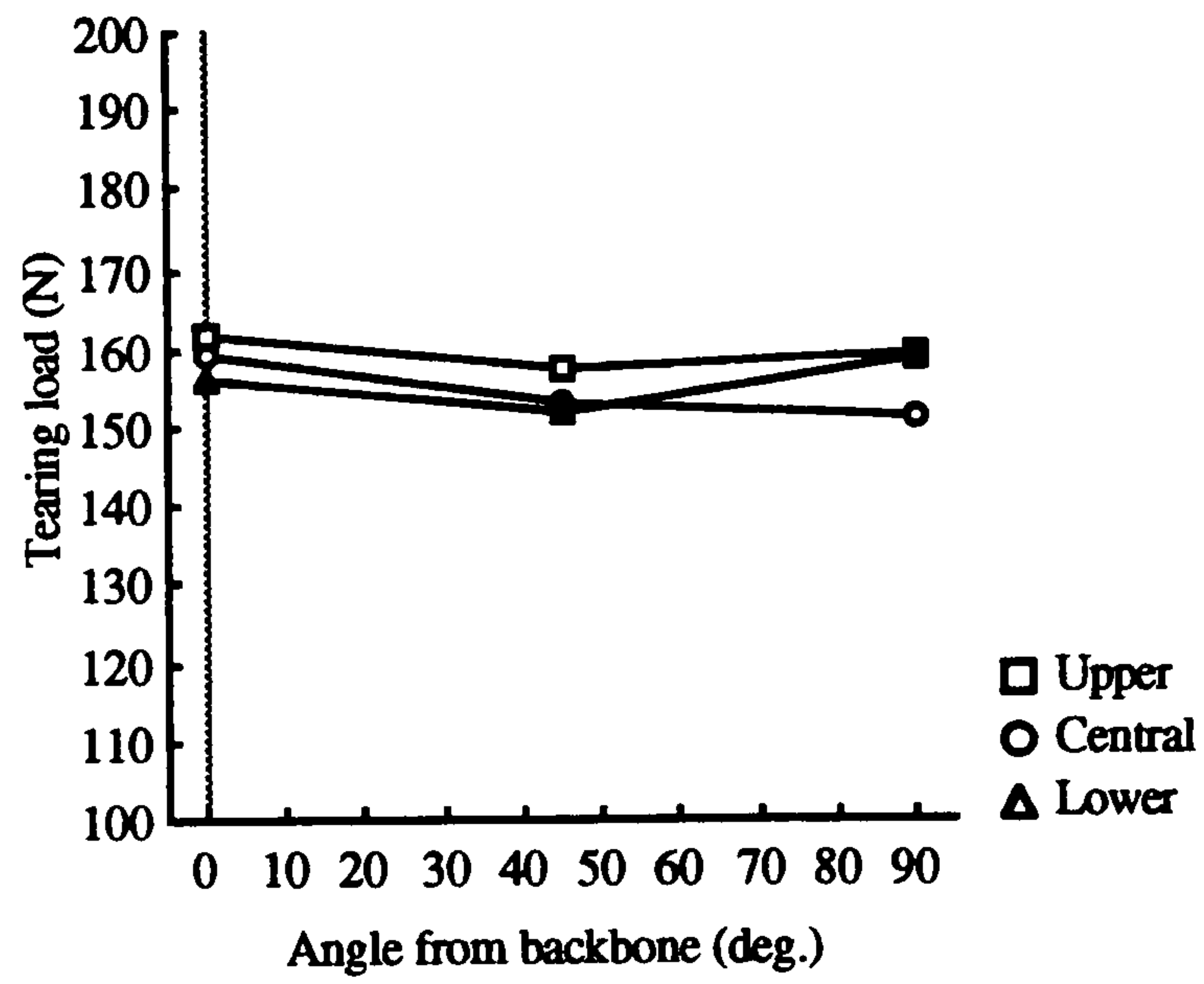


Figure 3.25(c) *Tearing load variation close to the belly, hide type-1.*

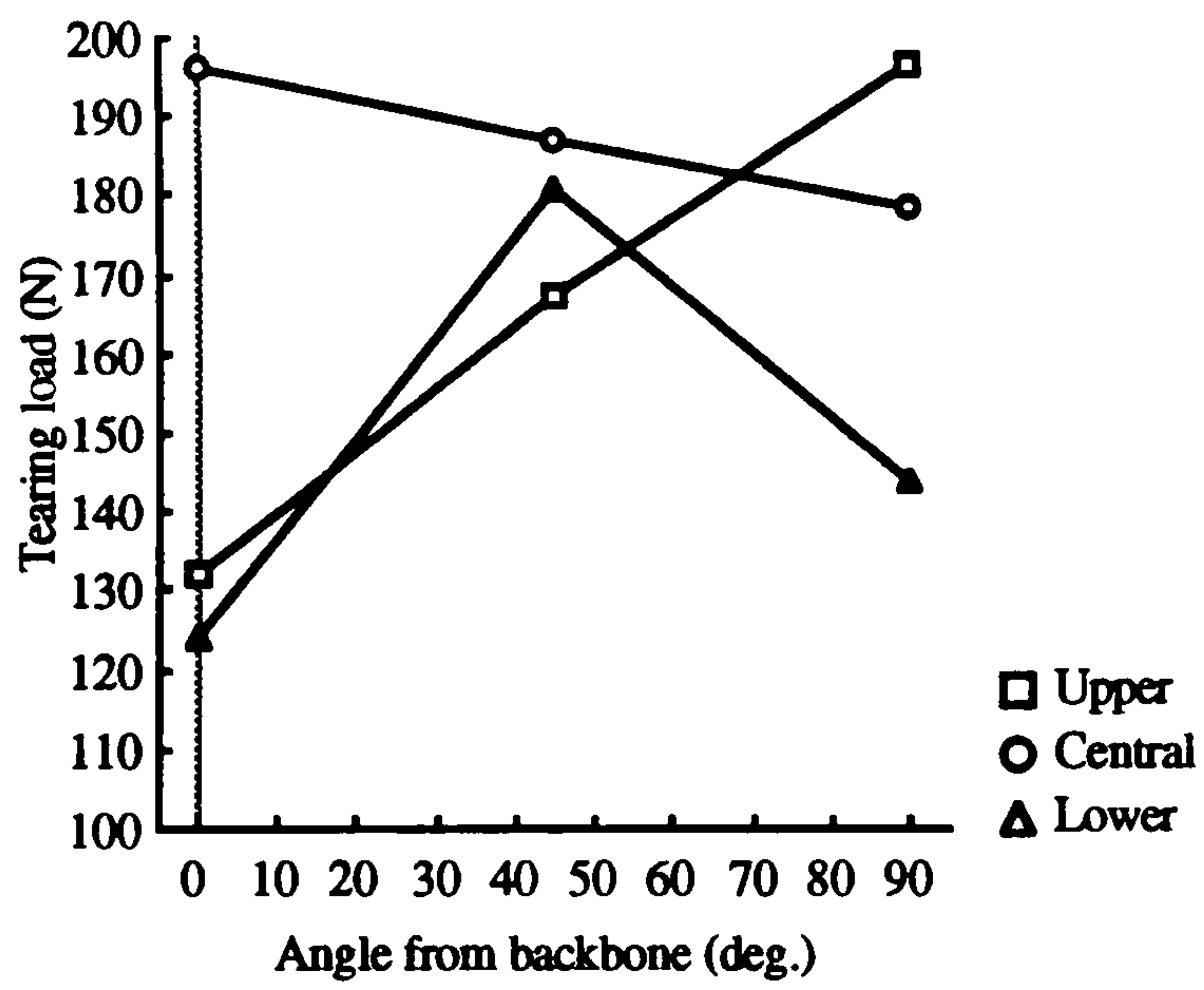
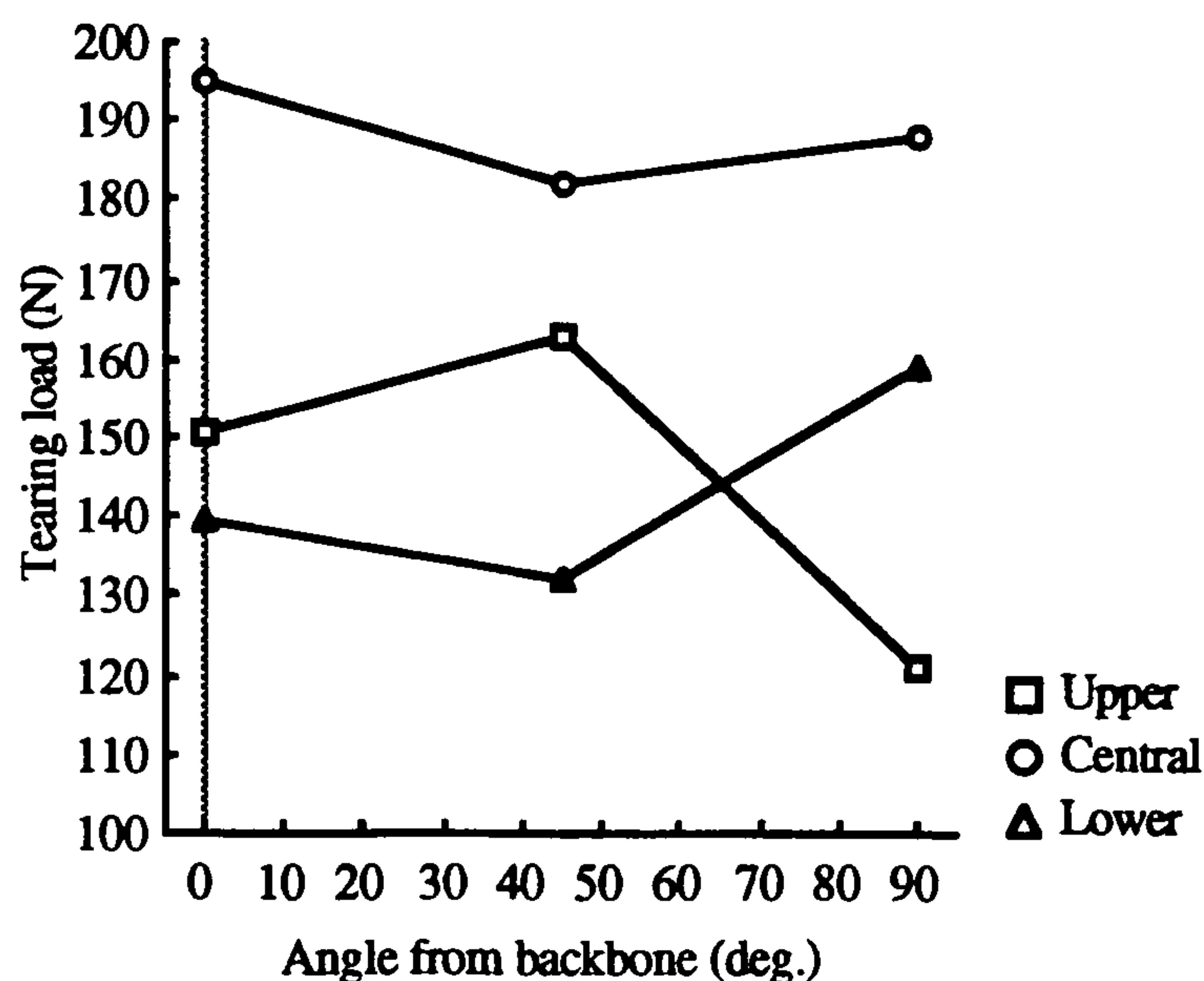


Figure 3.26(a) *Tearing load variation close to the backbone, hide type-2.*





*Figure 3.26(b) Tearing load variation close to the belly, hide type-2.*

### 3.11 Material burst properties

Leather is a stretchable material with a variable degree of stretchability (and hence strength) at different locations within the hide, and at different directions with respect to the backbone. In section 3.9.2 it was indicated that the directionality of the test does not seem to affect the general tensile strength result (and hence percentage elongation or stretchability results). The tensile tests however show strength and stretch variabilities at pre-selected directions in the hides. Nevertheless, since the material is subjected to stresses at random directions under the action of various skiving forces it is helpful to determine the regional strength of the material at a direction where it is a minimum. This calls for a testing method that applies an omni-directional strain onto the material and determines the load to rupture at its weakest direction. The application of this strain is achieved by thrusting a small spherical steel ball through the centre of the flesh side of a circular leather specimen whose perimeter is clamped throughout. The device used for this test is called 'lastometer' and is widely used in the leather and fabric industry for various strain and strength measurements. Use of the lastometer in this work was confined to the measurement of the minimum load that



was required to break the material. The break was invariably sudden and was in the form of a material burst. Accordingly, the load to break was called the burst load and was measured in N. Evaluation of the burst load on the leather was achieved in accordance with the relevant British Standards 3144 [27].

#### **3.11.1 Test procedure**

Circular samples of 44.5 mm diameter were cut from the two types of leather taken from the regional divisions in the hide described in section 3.3. A total of 9 samples from the hide type-1 and 6 samples from the hide type-2 were used.

A full description of the lastometer is given in the instruction manual prepared by Satra [30]. Fig. 3.27 shows the main features of the device. It consists of a circular clamp and a rod that is capable of traversing at right angle to the plane of the clamp. The longitudinal axis of the rod, which is carrying a fixed steel ball of 6.25 mm  $\varnothing$  at its leading end, passes through the centre of the circle of the clamp. Use of a load cell was made to measure the axial load applied on the rod. The amount of this load was shown by an associated load gauge. When a leather specimen was positioned on the device and is secured by the clamp the rod was driven towards the leather until the ball just touched the centre of the leather. Further thrust of the ball by distension on the leather caused stretch, in all directions, at the centre of the specimen. At a sufficiently high distension the leather reached its maximum stretch over the ball, and burst. The burst load was read from the load gauge.



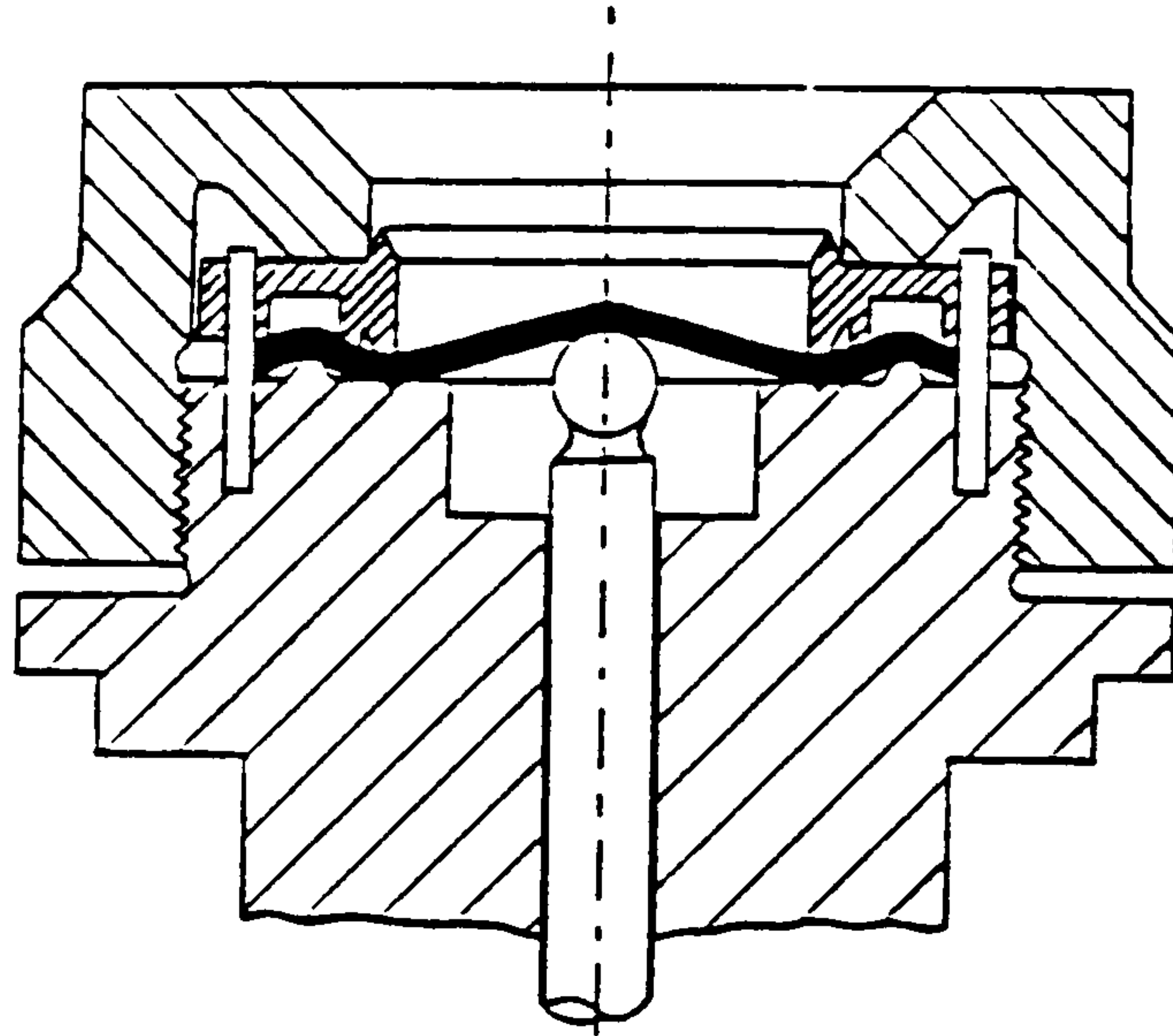


*Figure 3.27 Essential features of the 'lastometer'.*

### **3.11.2 The results**

The burst load variation along the width of the hide is similar in both hide types. In the upper and central sections the burst load decreases as the distance from the backbone increases, and in the lower hide sections this trend is the reverse. Also, the upper sections consistently require higher burst load than the central sections. The values of the burst load measured in the hide type-1 are somewhat higher than those measured in the hide type-2. At the backbone area in the hide type-1 the burst load is a maximum at 520 N dropping to a minimum of 160 N at the belly area. The corresponding values in the hide type-2 are 350 N and 130 N respectively.

The results suggest that, except for the lower sections, in both hide types the resistance to an applied load, and along its weakest direction, is lower in the belly area than in the backbone area. Figs. 3.28 and 3.29 show these results graphically for the hides type-1 and type-2 respectively.



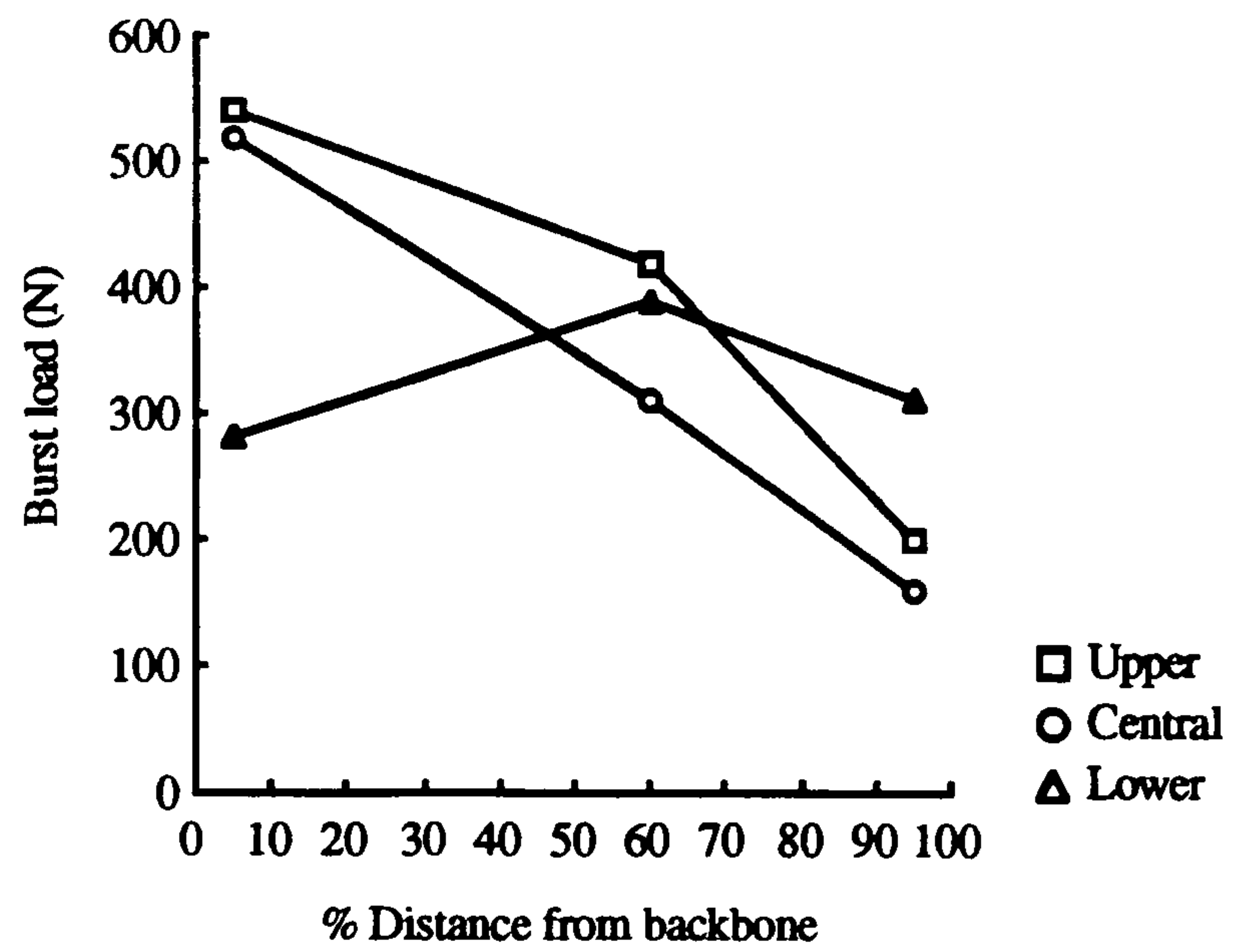


Figure 3.28 Burst load variation in the hide type-1.

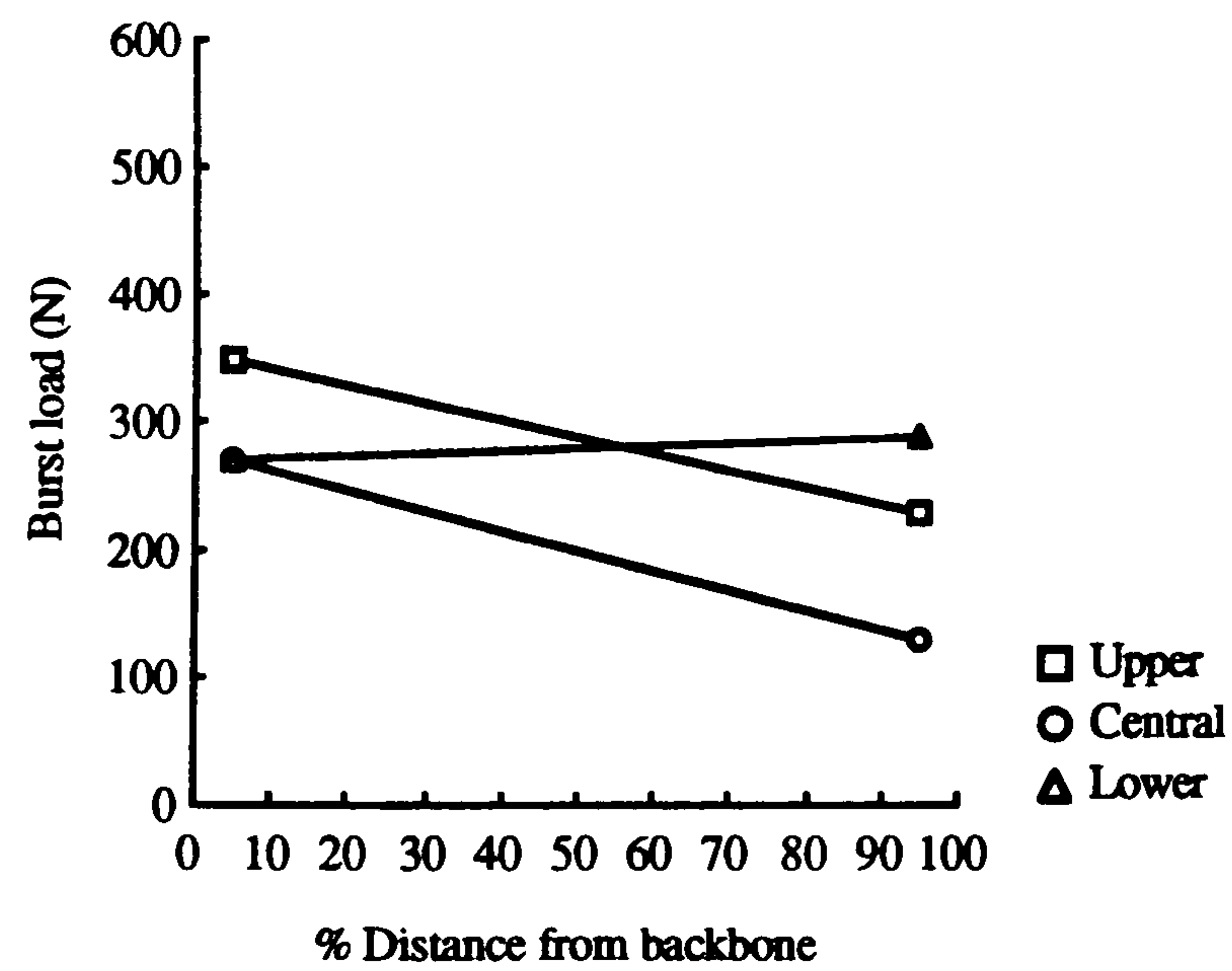


Figure 3.29 Burst load variation in the hide type-2.



### 3.12 Conclusions

Following an initial introduction to the structure of leather material, in this chapter various relevant properties of two types of leather are investigated. The selection of the properties to be investigated, and the material sampling methods are first presented. The properties that were evaluated included material thickness, flexibility, hardness, compression, tensile strength, tearing load, and burst load. For each property an explanation of its relevance to the aim of this work together with the test and measurement method and the results are given.

It is established that the thickness of the hide type-1 is on average over twice that of the hide type-2. It is further established that the former is on average 8 times less flexible than the latter. The examination of material hardness in both hide types suggests that the leather material of the hide type-2 is just over twice as hard as that of type-1. This relationship is more clearly seen from the material's density viewpoint. The mean apparent density of the hide type-1 is approximately 25% lower than that of the hide type-2. This lower density suggests higher material fluffiness, and hence lower material hardness. The mean value of tensile strength of the hide type-1 is about 16% lower than that of type-2. The difference is however the result of the greater regional variability of tensile strength in the former whereby at areas close to the belly the material is of appreciably lower tensile strength.

So far as material compressibility is concerned the two hide types have close mean resistance to compression with the hide type-2 being slightly more compressible than the hide type-1. Similarly, their mean tearing loads are very close to each other despite the higher scatter of the results in the hide type-2. The mean burst load in the case of the hide type-1 is about 26% higher than that of type-2.

Table 3.5 shows the tabulation of the mean values and the corresponding standard deviations for all the property test results. In a different representation, these results are also shown graphically in fig. 3.30 where the percentage difference in the mean values of all the properties for the two hide types are shown.



	Tensile stress Ncm <sup>-2</sup> [S.D.]	Tearing load N [S.D.]	Resist. to comp. Ncm <sup>-2</sup> [S.D.]	Burst load N [S.D.]	Thickness mm [S.D.]	Indent. index mm [S.D.]	Flexural rigidity g.m [S.D.]
Hide type-1	320 [65.4]	164.5 [8.22]	281 [44.7]	347.8 [131.4]	1.34 [.1178]	.37 [.0349]	.21 [.1311]
Hide type-2	374 [24.4]	163.1 [26.20]	262 [27.2]	256.7 [73.4]	.59 [.0197]	.15 [.0231]	.03 [.0087]

Table 3.5 Mean and standard deviation values of all properties.

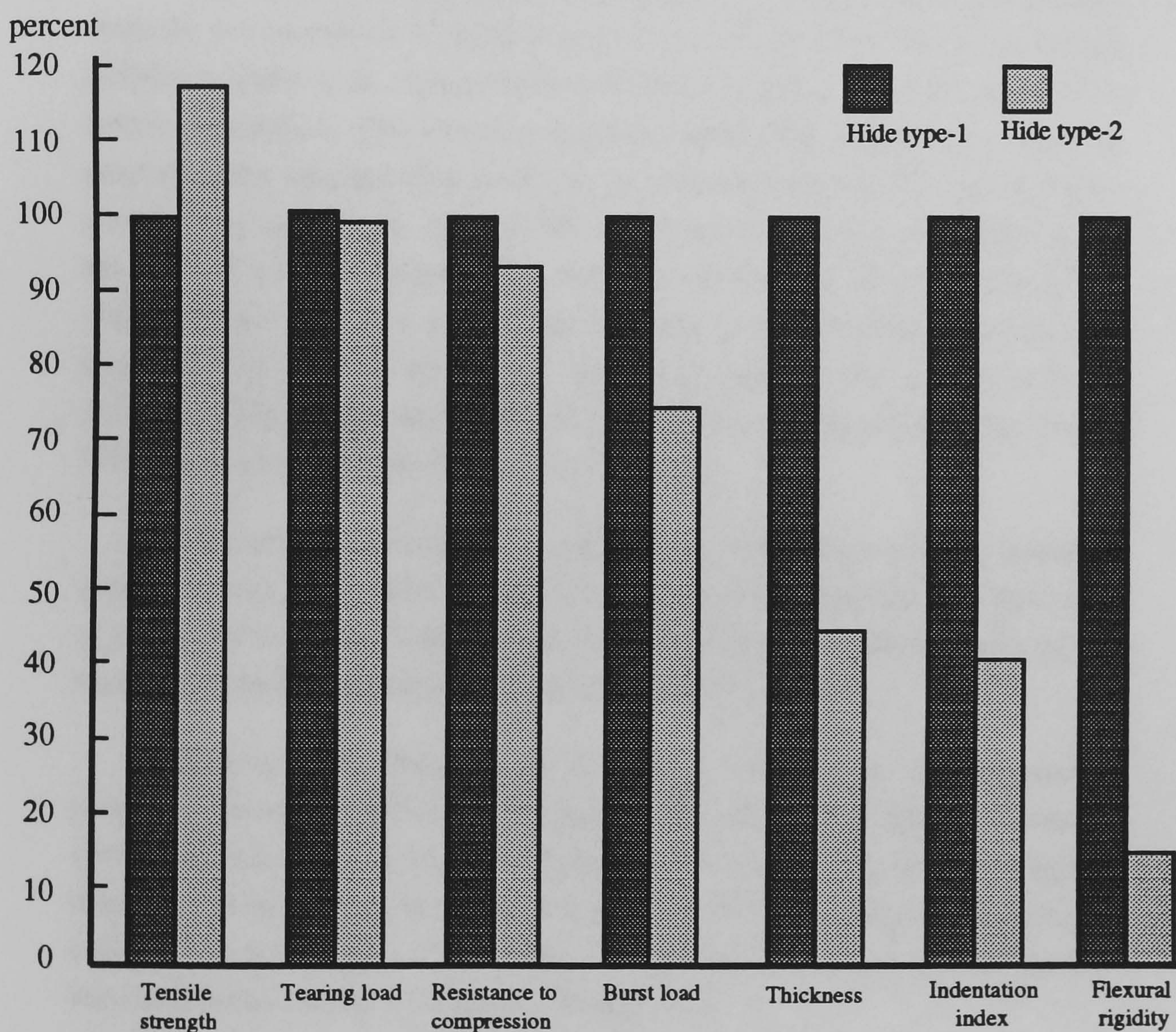


Figure 3.30 Graphical comparison of the mean of all properties showing hide type-2 relative to hide type-1.



## **CHAPTER FOUR**

### **HIGH SPEED MACHINING SYSTEM**

#### **4.1 Introduction**

One of the material removal principles that is considered earlier in this work for the automation of skiving process involves the application of a milling technique, where high cutting speeds are used to achieve machined surfaces on leather components. This method is initially introduced in Chapter Two where its general system configuration as well as its more specific skiving-related design parameters are discussed. Also, preliminary experimentations were conducted to test the viability of the method under different cutting conditions so as to be able to determine the operational range of the important parameters such as cutting tool shape and tip material, feed speed, and cutting speed. The results of these preliminary experiments suggest that leather machining is a candidate for skiving automation worthy of more extensive investigation.

The contents of this chapter is therefore devoted to the machining operation of leather components where details of a dedicated research rig are described. Use of a personal computer is made to monitor and capture the output results of the experiments such as cutting forces and the power consumption.

The sections that follow begin with an introduction to the relevant theories of milling science. Then the general requirements from the proposed experimental system are outlined. The design and operation of different elements of a dedicated experimental rig are then presented. Finally, the combined operation of the rig is explained. A full account of the analysis of the results of the experiments that are described in this chapter will appear in Chapter Five.



## 4.2 Relevant theories in milling operation

The section on theories of milling operation that is presented here provides some of the more important aspects of the milling science that are thought to be of relevance to this work [31][32]. Some of the materials are referred to and used later in the thesis while some others are solely presented for the purpose of background interest to the work.

Milling is a process of removing the excess material from the workpiece in the form of small individual chips. These chips are produced by the intermittent engagement with the workpiece of the teeth (or cutting edges) of the cutting tool. The intermittent engagement is produced by feeding the rotating cutting tool into the field dominated by the workpiece. The finished surface, therefore, consists of a series of elemental surfaces generated by the individual cutting edges of the cutter.

Owing both to the limited period of engagement of each tooth and the results of the combination of translatory and rotary motions of the milling cutter, the direction of motion of cutting edge of the tool is continuously changing with respect to the workpiece. The path thus produced by a tool cutting edge on the workpiece is geometrically described by the path of a point taken along a radial line, originated at the centre of a circle, while the circle rolls on a straight line. The resulting curve is termed a *trochoid*. Fig. 4.1 illustrates this cutting condition.

In fig. 4.1 the cutter axis is imagined to lie at the centre of a circle of radius  $r$  which rolls without slip along the straight line ST. A point Q on the cutter periphery, at radius  $R$  from the axis of the circle, will trace out the path of the cutting edge relative to the workpiece. The curve described by Q is therefore trochoidal. The machined surface lies between the trochoid AB, traced by the cutting edge, and the trochoid AC cut by the previous tooth. In the example shown in fig. 4.1 the direction of the motion of the cutter is opposite to that of the feed. This is called *up-cut milling* since the waste material is cut from A to B. If the direction of the feed is now reversed the waste material will be cut from B to A and *down-cut milling* will take place as shown in fig. 4.2. Whereas the trochoid thickness in the case of up-cut milling increases from zero to a maximum  $t_{\max}$ , for down-cut milling  $t_{\max}$  occurs almost at the start of the cut.







In the particular case of face milling however the machined surface is that left by the face of the cutter where the shape of the cut material consists of up-cut milling and down-cut milling as laid within the crescent bounded by the trochoids. In this case full cutting takes place. This will be more fully explained later in this section.

In analysing the trochoidal tooth path generated in milling, it is sufficient to assume a point on the cutting edge of the tool located at the maximum distance from the geometric centre of the cutter. However, in actual milling a tooth has definite dimensions, and its geometric shape must conform with definite requirements, among which are the following:

- (a) The contact between cutter and workpiece must be established on the cutting edge of the teeth, and at no time should interference develop between the body of the tooth and the workpiece.
- (b) Due to the requirement (a) above, the flank of a tooth should be located on a plane deviating from the tangent to the periphery of the cutter, by an angle  $\alpha$ , known as *clearance angle*.
- (c) To improve cutting action, the face of the tooth is formed by a plane which deviates from a radial plane by an angle  $\gamma$ , known as *rake angle*.

The clearance angle is provided for the specific purpose of preventing an interference between the flank of the tooth and the surface of the workpiece. In metal cutting it also has an important function of limiting the area of the flank exposed to the action of the built-up edge particles escaping in the cutting process. The built-up edge occurs due to cold forming of the chip material and the cutting edge of the cutter; its relevance is however questionable in the case of leather milling. Also, This angle must be made sufficiently large so that rubbing on any portion of the tooth path is prevented.

The rake angle has been shown to have a determining influence on the pressure and temperature of the cutting edge of the advancing tooth, as well as on the power required in the process of material removal [32]. It is also shown that the rake angle influences the type of chip produced though in the case of leather milling this is of small significance since the waste material is invariably in the form of small dust-type particles as previously mentioned.



The force system in this method of cutting is shown in fig. 4.3. This figure shows those components of the force exerted by the work on a cutting tooth, which act in a plane perpendicular to the cutter axis. The *tangential force*,  $F_t$ , determines the torque on the cutter, and the *radial force*,  $F_r$ , may be regarded as the rubbing force between the workpiece and the tooth.

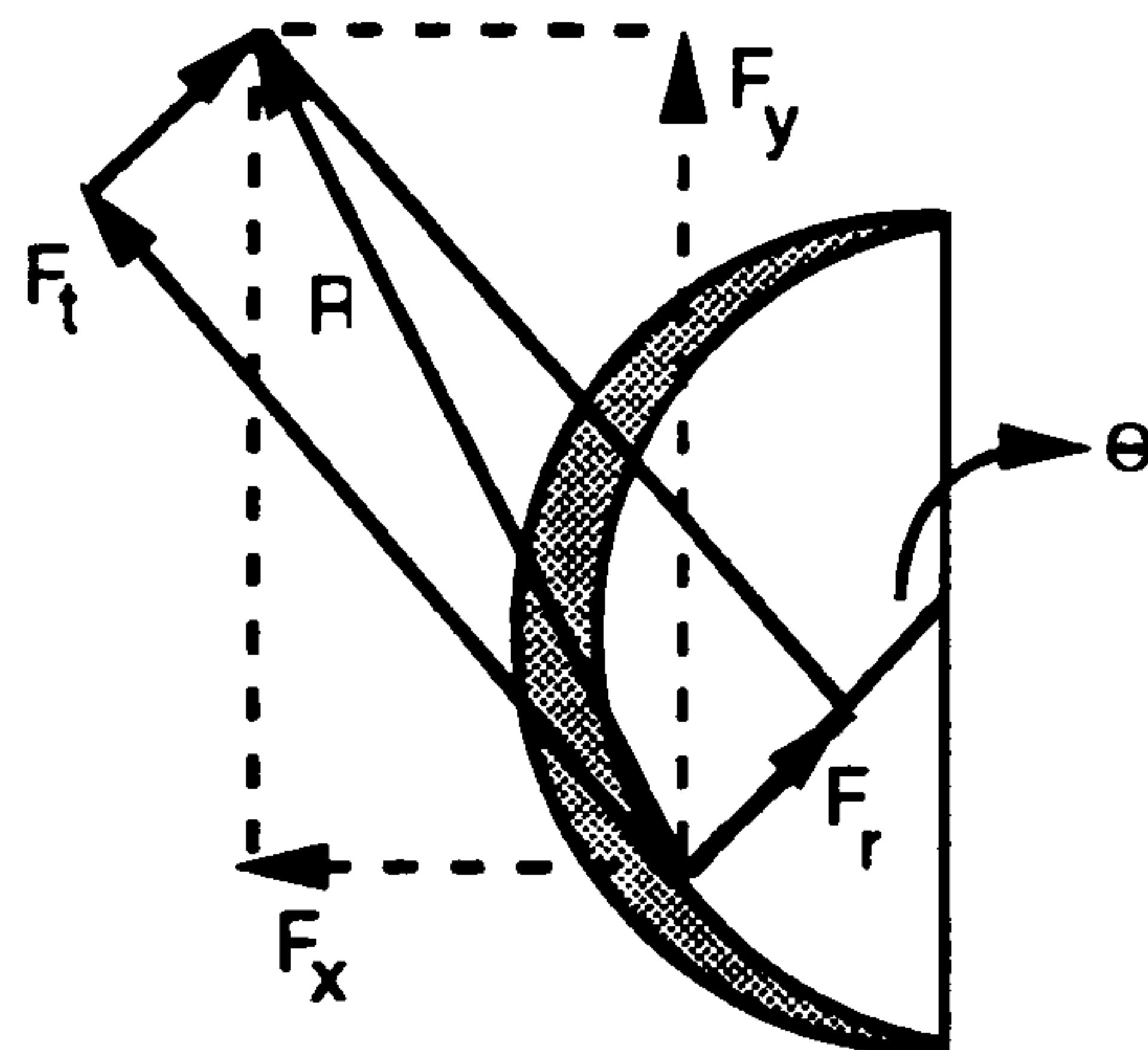


Figure 4.3 Diagrammatic presentation of cutting forces in milling.

In fig. 4.3 the vector summation of the tangential and radial forces  $F_r$  and  $F_t$  give rise to the resultant force  $R$  which is the active force acting on the tool edge in the plane containing  $F_t$  and  $F_r$ . This force can also be resolved to give the magnitude of the reactions of the cutter into parallel and normal components to the direction of the feed [33]. These two components of the resultant force are denoted by  $F_x$  and  $F_y$  respectively. For a single tooth cutter the following transfer matrix therefore relates these force components to the tangential and radial forces:

$$\begin{bmatrix} F_y \\ F_x \end{bmatrix} = \begin{bmatrix} -\cos\theta & \sin\theta \\ -\sin\theta & -\cos\theta \end{bmatrix} \cdot \begin{bmatrix} F_r \\ F_t \end{bmatrix} \quad (4.1)$$

Extensive work has been done to mathematically determine the value of the cutting forces as functions of other cutting parameters. Thusty and MacNeil [34]



assume a rather simple formula for the tangential cutting force on a part of one tooth as follows:

$$F_t = K \cdot b \cdot h \quad (4.2)$$

where  $K$  = a constant

$b$  = width of chip

$h$  = instantaneous chip thickness

Therefore the magnitude of the tangential force depends on chip width and thickness, and the value of  $K$ . The product of chip thickness and the width of chip gives rise to an area that is being cut when the cutter is rotated at some angle  $\theta$ , as shown in fig. 4.4, while the value of  $K$  is a measure of the resistance to cutting offered by the workpiece material and is referred to as *specific cutting pressure*. Its value is dependent on the material of the workpiece, tool geometry, and the average chip thickness.

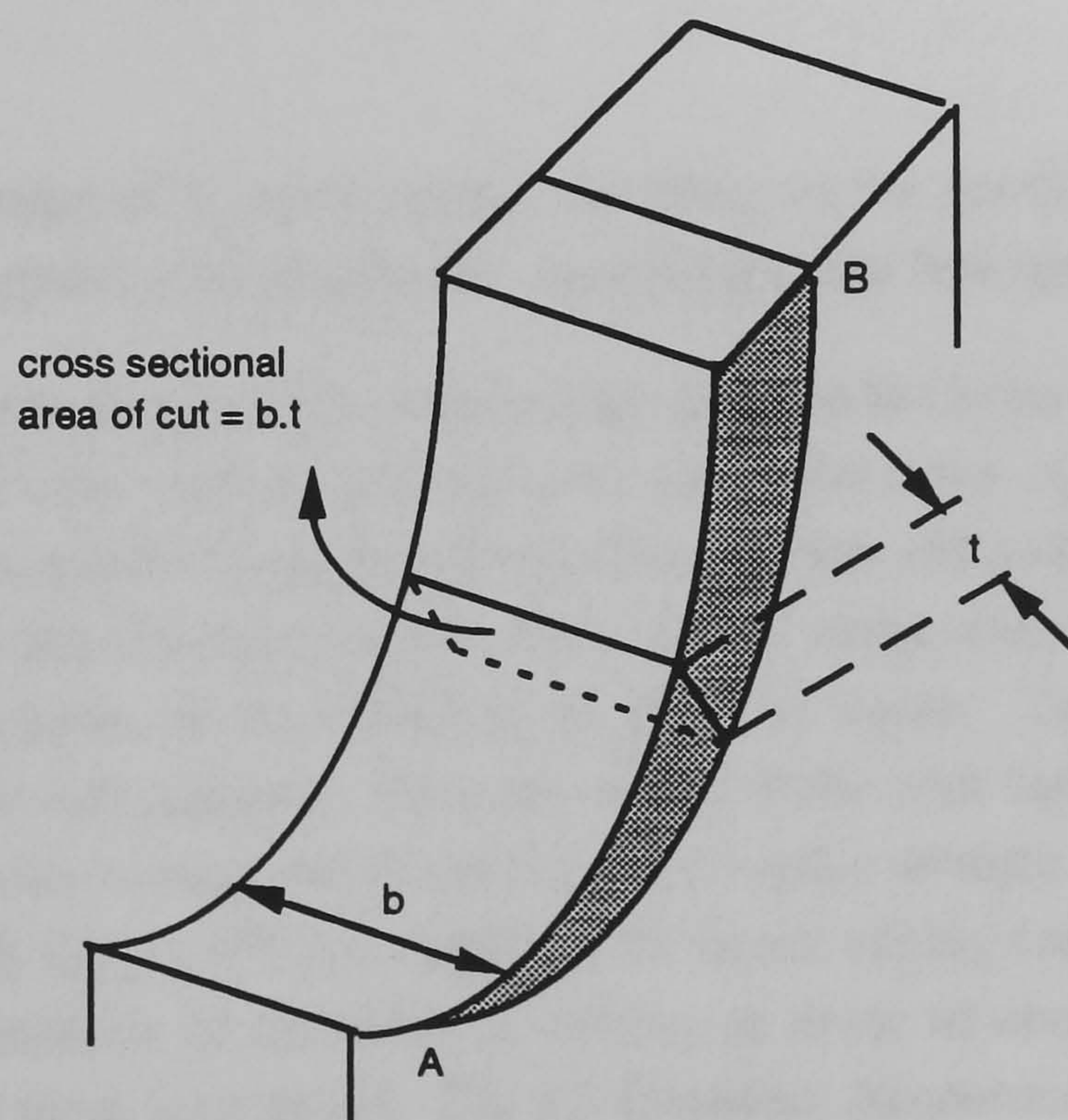


Figure 4.4 A diagram showing chip formation during cutting.



Also, Koenigsberger and Sabberwal [35] showed that for the particular case of face milling the value of the tangential force at any instant can be given by the following formula:

$$F_t = K \cdot a \cdot s \cdot \sin\theta \quad (4.3)$$

where  $K$  = specific cutting pressure

$a$  = depth of cut

$s$  = feed rate per tooth of the cutter

$\theta$  = angle of rotation of the cutter

An extensive investigation of this formula has been attempted by Kronenberg [32]. However, the following relationship between the tangential and radial forces is often quoted:

$$F_r = \eta \cdot F_t \quad (4.4)$$

where  $\eta$  = radial to tangential force ratio.

The value of  $\eta$  varies greatly according to the conditions of cutting including sharpness of the cutting tool, cutting angle, and feed speed [36].

The main characteristic of the milling operation lies in the regular sequence of individual cuts, corresponding to each successive tooth engagement. The cutting edges periodically enter and exit the workpiece, and according to this the cutting force alters in the form of series of pulses whose frequency is therefore directly dependent on the rotational speed of the cutter. These pulses may sometimes be well separated, but in the case of multi-tooth cutters where many cutting edges are working simultaneously, they overlap strongly. Much work has been done by Gyax [33] who assumed the above cutting force model in the theoretical analysis of dynamics of milling in order to obtain fundamental properties of these force pulses. Fig. 4.5 illustrates, diagrammatically, a typical waveform produced as a result of milling cutting force excitation on time base.



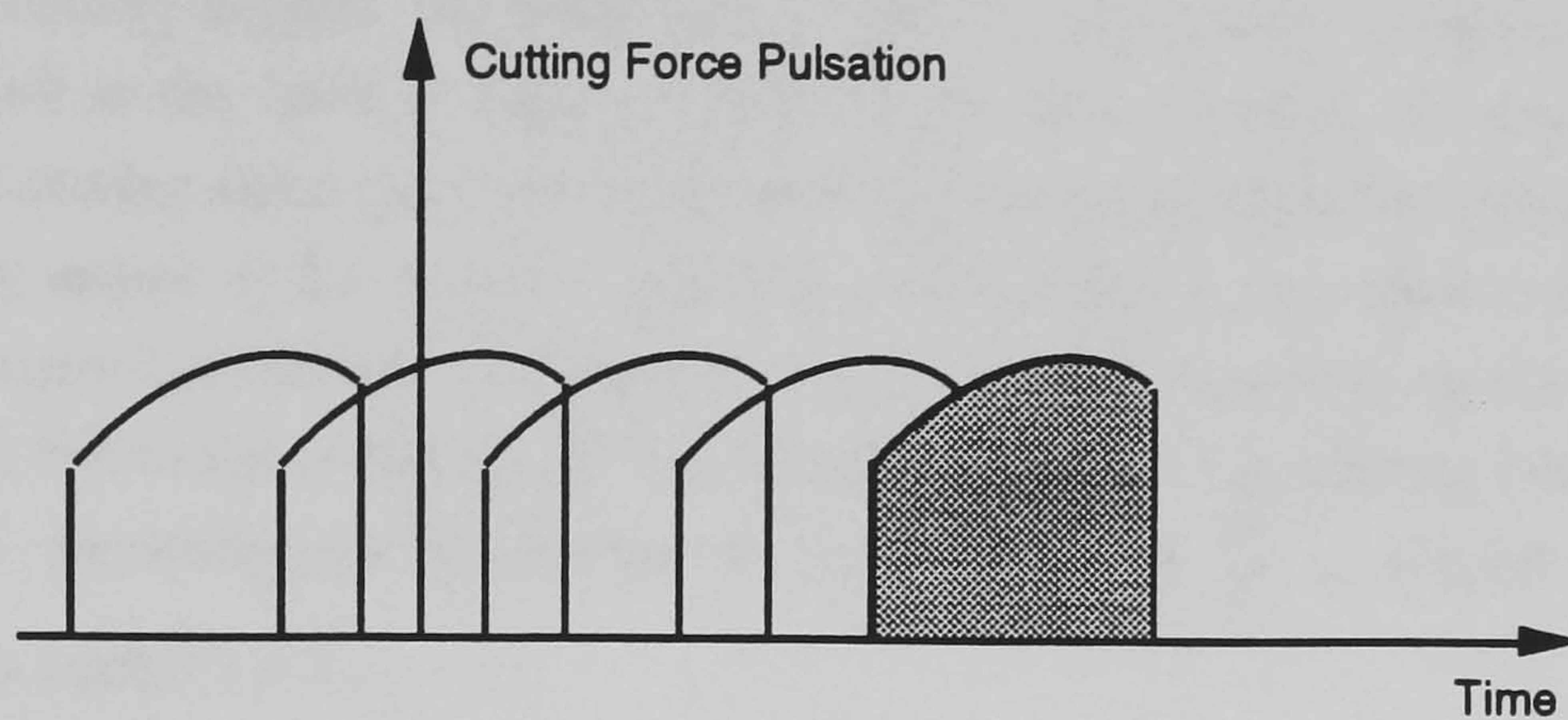


*Figure 4.5 Periodic formation of pulses representing the cutting force.*

In practice it is difficult to measure the cutting forces directly since they rapidly oscillate during the cutting as explained above. For this reason suitable dynamometers are employed to record the fluctuations on a time base. It is common to employ dynamometers that are capable of measuring forces in three dimensions. This is due to the presence of an axial force in a milling cutting system. The axial force is in the direction of the spindle of the cutter and is normal to the plane of the tangential and radial forces. It is also easier to measure the planar cutting forces in the direction of feed,  $X$ , and normal to feed,  $Y$ , instead and later relate the results, if desired, to the actual tangential and radial forces through the transfer matrix given earlier. It is however possible to interpret the measured results directly as obtained in the form of  $F_x$  and  $F_y$ , hereafter referred to as *feed* and *normal* cutting forces respectively.

Both normal and feed components of the resultant cutting force contribute to the removal of the trochoidal segment from the leather at each revolution of the cutting tool. Referring to fig. 4.6, point A represents the beginning of the cut. At this point the values of both feed and normal cutting forces begin to increase. When the cutter begins to exert pressure on the workpiece material, it spends an initial period of time building up sufficient pressure on the material so that cutting can take place. From the moment of this cutter/material engagement, until actual cutting takes place, rubbing force is the only force present in the system. This force is a radial force, and is directed towards the centre of the cutter. At this instance, the radial force is also in the



direction of the normal cutting force. Therefore, at the very beginning of the cutter engagement, the normal cutting force increases as a result of rubbing. Once the actual cutting begins, the force responsible for the material removal will be measured in the form of the feed and normal cutting forces. At point B, the normal cutting force reaches a maximum for it is responsible for cutting of the thickest section of the trochoid. Between points C and A, the cutter is travelling over a machined surface. In soft and springy workpiece materials, certain amount of back rub can also contribute towards of the increase of rubbing force in the system. Depending on the geometry of cut, the ratio of  $\frac{F_x}{F_y}$  is related to  $\eta$ , as given in equation 4.4.

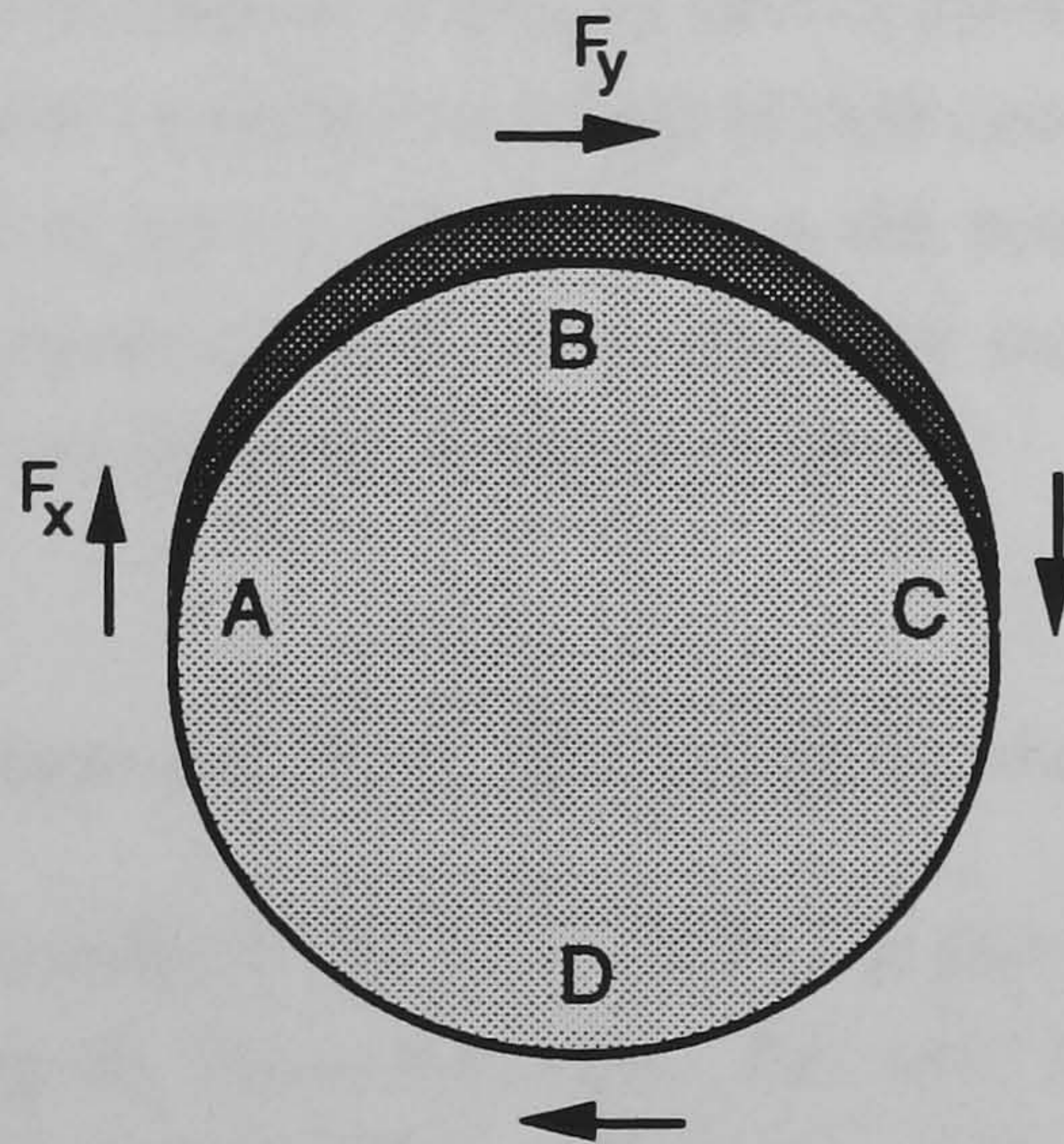


**Figure 4.6** *A diagram showing a full crescent of cut achieved by feed and normal cutting force.*

Another important characteristic of a milling condition is the evaluation of its power consumption during cutting. The power required to remove a unit volume of the material per unit time can be regarded as a measure of the material's resistance to cutting, as well as a measure of the effectiveness of the cutting condition. It can be shown that power is related to specific cutting pressure,  $K$ , and thus to tangential cutting force,  $F_t$ , by the following relationships [31]:



$$P = K \cdot \omega \quad (4.5)$$

and,

$$P = \frac{F_t \cdot \omega}{a \cdot s} \quad (4.6)$$

where  $P$  = power

$\omega$  = material removal rate

$a$  = depth of cut

$s$  = feed rate per tooth of the cutter

In practice, measurements of milling cutting power consumption are taken by monitoring the power consumption of the electric motor attached to the cutter spindle. If the value of power supplied when the machine is running idle is subtracted from the power reading taken under the cutting load, a reasonable estimate of the power consumed in cutting is obtained.

### 4.3 General requirements from the experimental system

The theoretical analysis that are presented in section 4.2 have been chiefly developed for the purpose of metal cutting. However, the principles of milling should remain unchanged though the nature of the workpiece material may differ. For example, in the case of milling of leather the chips produced are in the form of fine particles cut from the fibre network layer of the hide. Also, as established in Chapter Two, the rotational cutting speeds involved in leather milling are much higher than those involved in the milling of metals. Based on the milling analysis of section 4.2 an experimental rig was designed and built so that important and fundamental characteristics of leather milling conditions could be evaluated. The rig was designed so that during a set of systematic experiments the critical variables can be accurately controlled and changed in the desired range while true values of the output results are observed and recorded. However, since this work is concerned with the automation of skiving process, the rig was designed so that only important cutting conditions and parameters in milling of leather are considered.





In Chapter Two it was explained that the object of this exercise is to identify those cutting conditions that are most efficient, produce acceptable surface finishes on hides of different physical properties, and are achieved with maximum possible feed speeds. In the preliminary tests that were carried out in that chapter it was found that both the feed speed and the rotational speed of the cutter affect the end results. However all the tests were carried out with tools of zero rake angle. It is the object of this chapter to observe more closely the effects of these variables on the desired results. These results indicate the efficiency of the cutting conditions. To this end, the feed and normal cutting forces and the power consumed during cutting are used. The results of the cutting forces are also to be used as the minimum clamping forces in designing the automatic clamp assembly required by the envisaged automated skiving machine. The two cutting forces, the power consumption, together with the quality of the machined surface finish constitute the four output results, whilst, the linear feed and the rotational cutting speeds of the cutter, the rake angle of the cutting face of the cutting tool, the depth of cut, and the hide-types of varying physical properties are the five principal input variables.

For the practical purposes of this work, maximum values of the forces and power obtained in any cutting condition are of interest. This is particularly of importance in the case of cutting forces since the results can also become the basis for estimating the planar clamping force that would be required when designing an automatic leather clamping mechanism. The experimental set-up is therefore designed so that only maximum values reached are of interest without due regard to any intermediate recorded values.

The cutting tool is to be rotated by an electric motor capable of producing high and variable rotational speeds that can be accurately monitored under varying load conditions. The cutter assembly is linearly traversed by another electric motor so as to produce a feed of known speed. Leather components are to be mounted on a suitable dynamometer, and under cutting conditions, the output results of the cutting forces and a measure of the power consumption are automatically monitored and recorded. The data captured during cutting is automatically stored in computer data files for further processing.

For the reasons of safety, as well as noise and dust pollution during the tests, the complete rig was enclosed by perspex panels where an air extractor was channelled to the system to remove the unwanted leather dust produced during the cutting process.



The design of the experimental rig to evaluate the cutting conditions of leather milling is given in the following sections. Sections 4.4 to 4.7 are concerned with the physical design and construction of the cutting tool, the dynamometer, and the cutting assembly respectively, while section 4.8 deals with the combined operation of the rig together with monitoring and recording of the results.

#### **4.4 Design of the cutting tools**

The initial investigation in designing the cutting tool shape and its tip material has been described in section 2.3.3, and as a result, the inverted dovetail shape with tungsten carbide cutting tips were found to be the most effective combination when skiving leather workpieces. In this section more detailed geometric design of the tool is given.

In the theoretical analysis of cutting explained in section 4.2 the importance of rake and clearance angles in cutting was clearly pointed out. It is also clear that the role of the rake angle is more crucial than that of the clearance angle. This is because the rake face (hence the rake angle) of the cutting tool is directly connected with the cutting mechanism and therefore directly and instantaneously influences the cutting conditions. Changes in its value can therefore critically affect the results. The role of the clearance angle in the cutting mechanism is however largely confined to providing ample relief for the waste material and preventing excessive rubbing below the cutting edge. So far as the clearance angle is concerned, it is common practice to keep this angle between  $3^\circ$  to  $5^\circ$  for practical purposes. A cutter diameter of 10 mm was used.

Fig. 4.7 shows the schematic diagram of an inverted dovetail cutting tool containing two cutting teeth.



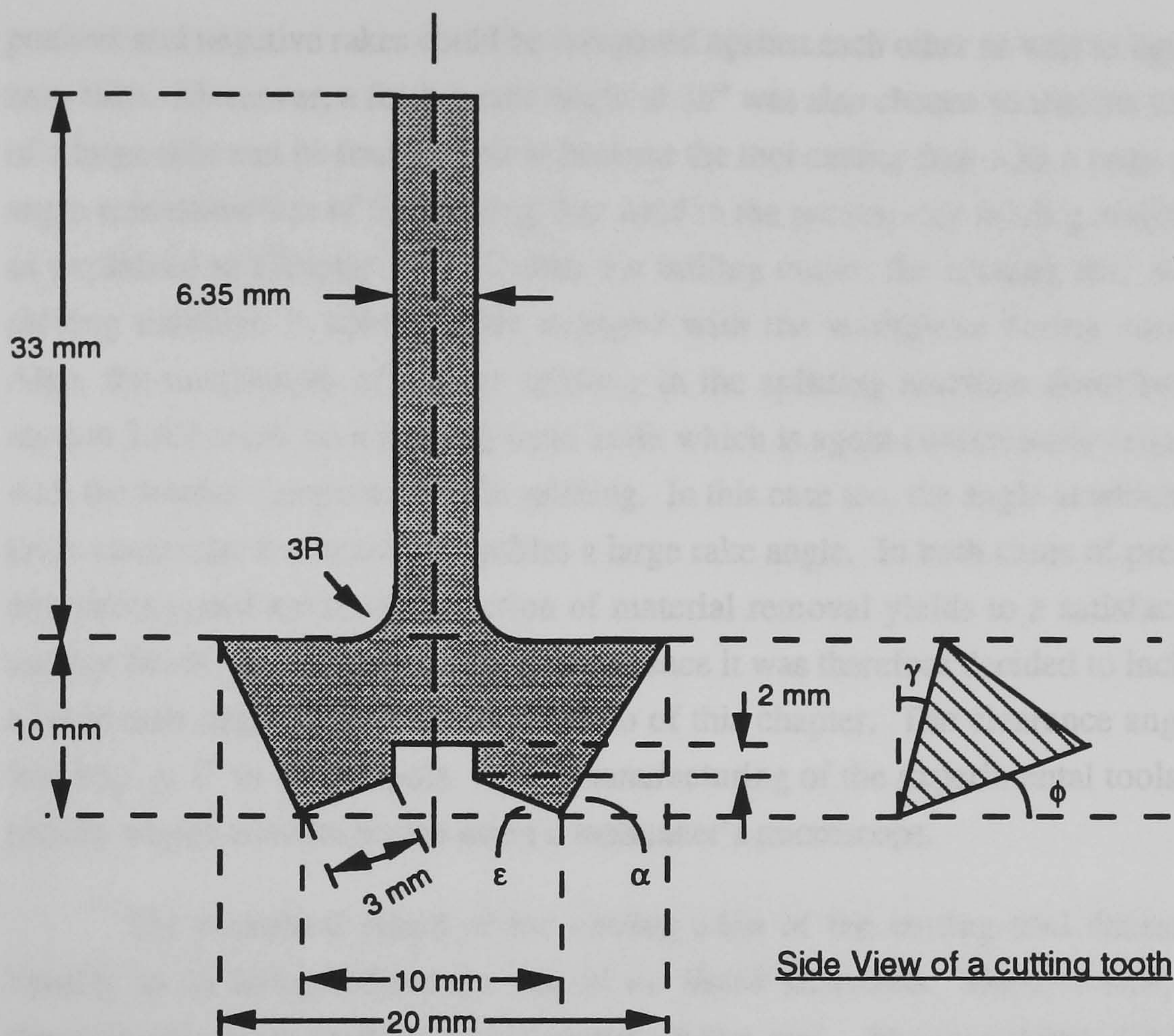


**Figure 4.7** A diagrammatic presentation of the inverted dovetail tool showing the important geometric dimensions (not to scale).

The angles in the above figures are termed as follows:

$\gamma$  = rake angle

$\epsilon$  = clearance angle

$\phi$  = clearance angle

$\alpha$  = side angle

To avoid a large number of non-crucial experimental variables it was decided to design and make tools of various rake angles but keep all other angles fixed. Three different rake angles of  $0^\circ$ ,  $19^\circ$ , and  $-17^\circ$  were chosen so that both



positive and negative rakes could be compared against each other as well as against zero rake. Moreover, a further rake angle of  $35^\circ$  was also chosen so that the effect of a large rake can be found. This is because the tool cutting face with a large rake angle resembles that of the rotating disc used in the present day skiving machines as explained in Chapter One. Unlike the milling cutter, the rotating disc in the skiving machine is continuously engaged with the workpiece during cutting. Also, the mechanism of leather splitting in the splitting machine described in section 2.4.3 relies on a rotating band knife which is again continuously engaged with the leather component while splitting. In this case too, the angle at which the knife enters the workpiece resembles a large rake angle. In both cases of present day skiving and splitting the action of material removal yields to a satisfactory surface finish. On the grounds of this evidence it was therefore decided to include a large rake angle in the experimentation of this chapter. The clearance angle  $\epsilon$  was kept at  $3^\circ$  in all the tools. Upon manufacturing of the experimental tools the precise angles were inspected using a toolmaker's microscope.

The rotational speed of the cutting edge of the cutting tool decreases linearly as its distance from the axis of the shank decreases. There is therefore theoretically no movement at the centre of the tool. At areas where there is considerable reduction in cutting speed, effectively more rubbing than cutting takes place. This can lead to heat generation and results in burning the material as well as rapid tool wear. This phenomenon was clearly identified in the initial investigation described in section 2.3.3. Thus another characteristic of the tool is that there is no provision for centre cutting by providing an empty space or a hole at the centre of the tool and along its axis of rotation. Tools of two cutting teeth were used in this work for the reasons of simplicity in design and cost.

#### **4.5 Design of the dynamometer**

A quasi-static dynamometer was designed and built for the measurement of cutting forces involved in the face milling experimentation of leather components. Force measurements in the dynamometer is based on the static calibration of linear displacements of a horizontal flat platform (or plate) in two perpendicular directions, as diagrammatically shown in fig. 4.8. The platform was allowed free traverse in the two directions with the aid of thrust and journal air lubricated bearings. To restrict the movements of the platform it was initially kept at rest and in equilibrium by eight compression springs, two in each side of each one of the two directions. Any displacement occurring by the platform was monitored and



measured with the aid of a displacement transducer, again, positioned along each one of the two perpendicular directions.

A mild steel plate of 400 mm × 200 mm × 8 mm was mounted on a single linear journal bearing, along one edge and two thrust (or pad) bearings along its other parallel edge. The plate was therefore supported on three points.

The journal bearing was restricted to traverse along the axis of a seamless mild steel tube of 2" outside diameter. The thrust bearings are circular brass pads of 2.5" diameter and rest on the plate surface of a supporting bar. The journal bearing's maximum loading is 550 N and has a calculated stiffness value of 86.7 MNm<sup>-1</sup> while for the same maximum loading the thrust bearing has 62.4 MNm<sup>-1</sup> stiffness. The role of the journal bearing was to restrict the traverse of the platform along one direction only (ie. along the line of the axis of the journal bearing shaft ), while the role of the thrust bearings was simply to provide unrestricted lubricated support for the plate. This arrangement therefore ensured that not only the plate can traverse along one linear direction, but also free play was allowed so that no seizure by the journal bearings may occur<sup>†</sup>.

Compressive springs of each 2609.5 Nm<sup>-1</sup> stiffness were trapped between fixed frames at both sides of the plate so that the plate is held at equilibrium. A linear variable differential transformer (lvdt) was placed between the plate and the fixed frame at one side of the plate such that its incorporated spring was in parallel with the corresponding supporting springs of the plate. The lvdt acts as a displacement transducer and comprises a central coil energised from a d.c. power source and two overwound secondary coils [37]. A near linear output relationship results when its spring-loaded internal magnetic core moves. The stiffness of the spring in the displacement transducer was 109.87 Nm<sup>-1</sup>.

The mechanism that is described above can only measure forces in one direction. In order to be able to also measure cutting forces in the perpendicular direction, the fixed frames of the above complete assembly was similarly mounted on another set of assembly through a journal bearing and two thrust bearings. The mounting was such that the axes of the shafts of the two journal bearings were perpendicular to each other. In exactly similar fashion as described for the plate,

---

<sup>†</sup> If the journal bearings are used along both sides of the platform in parallel, then any slight misalignment of their axes might cause seizure of the bearings.



the complete assembly was kept in equilibrium by compressive springs. Another lvdt was also similarly positioned between the frames of the plate assembly and another set of fixed frames of the overall assembly. The dimensions and specifications of all journal bearings, thrust bearings, springs, and transducers are identical. Fig. 4.8 shows the schematic diagram for the overall assembly.

The mechanism that is shown in fig. 4.8 is the force dynamometer giving independent force measurements by providing facilities for recording the displacement of its platform in two perpendicular directions. The method for the calibration of the dynamometer is presented in section 4.8.



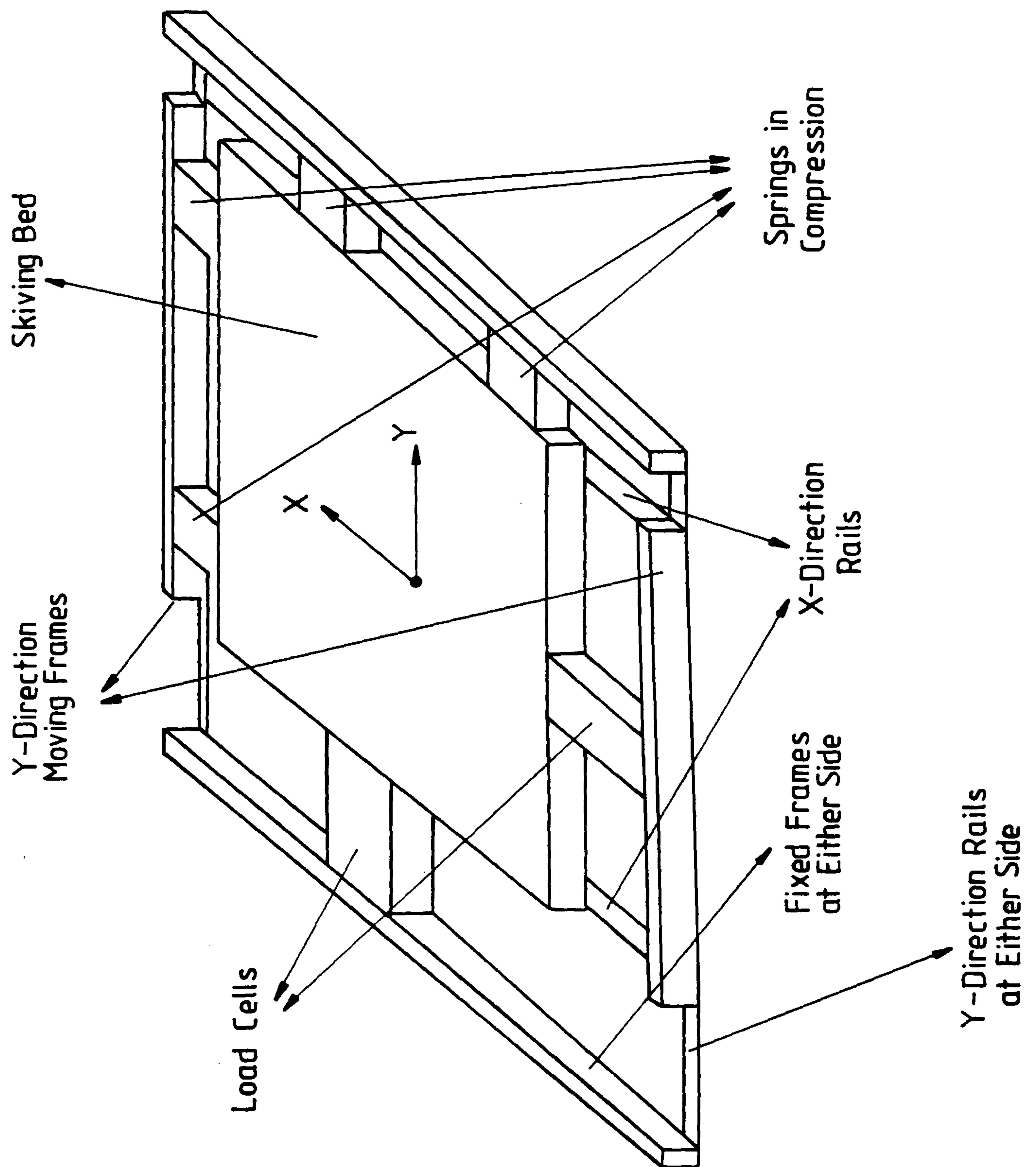


Figure 4.8 The schematic diagram of the dynamometer assembly.



#### 4.6 Dynamic evaluation of the dynamometer

The dynamometer that is described above must be able to give reasonable estimates of the cutting forces achieved in milling of leather components. The accuracy and the precision of the dynamometer depends not only upon the principle by which it measures forces, but also on the stiffness and natural frequency of its measuring axes. In order to be able to describe its characteristics fully, an analytical account of the dynamic behaviour of the dynamometer is presented in this section.

If no cutting takes place then the plate of the dynamometer stays in equilibrium and at rest. When this plate is perturbed in the direction of one of its moving axes, then the combination of the actions of the corresponding compressive springs and the inertia of the moving parts will subject the plate to a damped vibration. The profile of this vibration is shown in fig. 4.9.

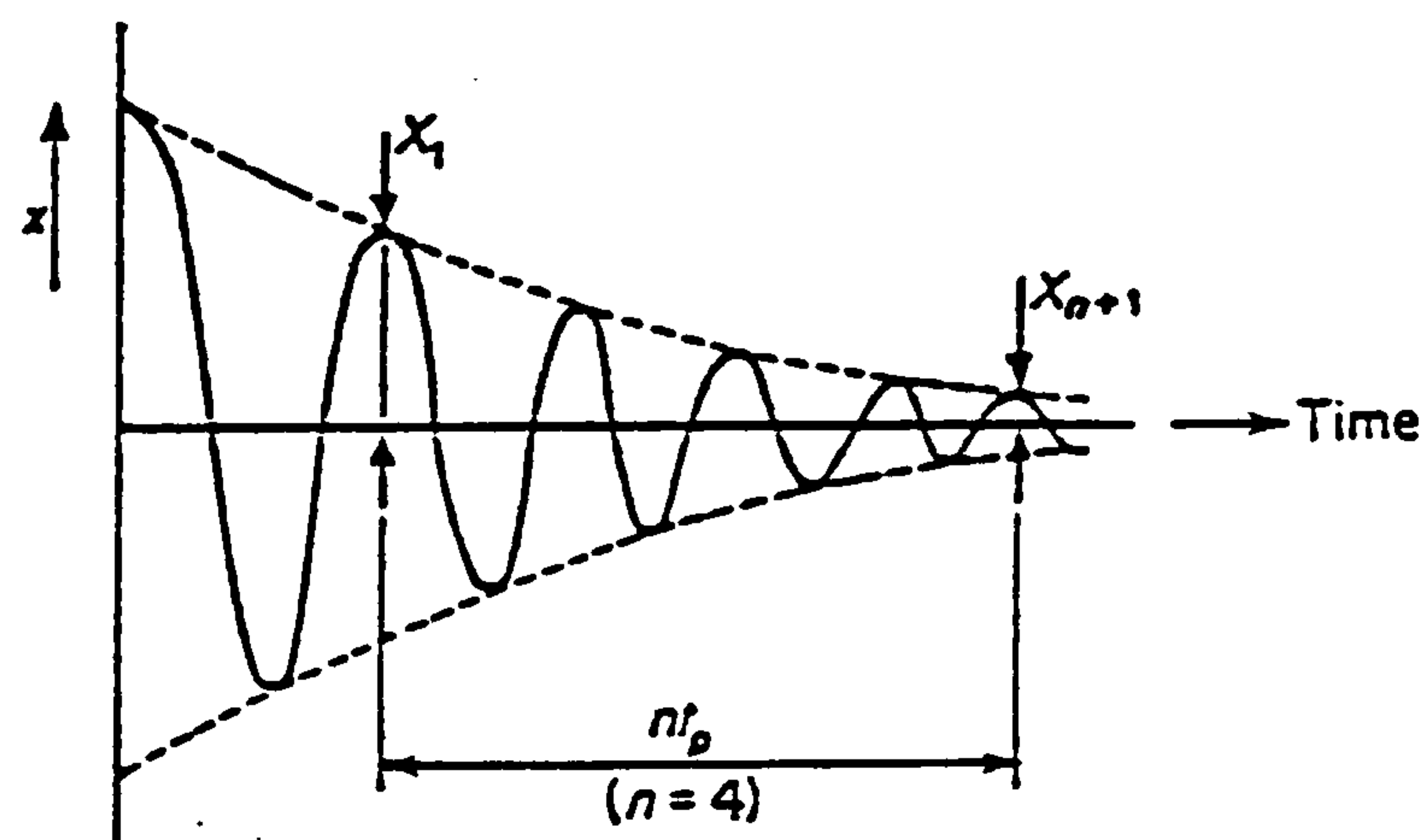


Figure 4.9 Damped vibration shown as displacement against time.

where  $x$  = displacement

$t$  = time

$t_p$  = period of damped vibration

$n$  = no. of revolutions



The equation of motion of the system is thus a second order damped system given by [38][39]:

$$mx'' + cx' + kx = 0 \quad (4.7)$$

where  $x$  = displacement

$x'$  = velocity

$x''$  = acceleration

$m$  = mass

$c$  = damping constant

$k$  = stiffness (spring constant)

The above equation may also be written in the following way:

$$mx'' + 2\zeta m\omega_n x' + m\omega_n^2 x = 0 \quad (4.8)$$

where  $\omega_n$  = undamped natural frequency of the system

$\zeta$  = damping ratio

Thus:

$$c = 2\zeta m \omega_n \quad (4.9)$$

and.

$$\omega_n = \sqrt{\frac{k}{m}} \quad (4.10)$$



By measuring the value of  $t_p$  and obtaining the ratio of the successive peaks on the corresponding displacement response waveforms in the feed and normal directions of the dynamometer, as shown in the example of fig. 4.9, the damping ratios in both directions are found by the following formula:

$$\zeta = \frac{1}{\omega_n \cdot n \cdot t_p} \ln \frac{x_1}{x_{n+1}} \quad (4.11)$$

Using the measured characteristics of the dynamometer:

$$m_{(\text{feed})} = 16.7 \text{ kg} \quad \text{and} \quad k_{(\text{feed})} = 10547 \text{ Nm}^{-1}$$

$$\text{therefore:} \quad \omega_{n(\text{feed})} = 25.13 \text{ rad.sec}^{-1} \quad \text{and} \quad \zeta_{(\text{feed})} = 0.026$$

and,

$$m_{(\text{normal})} = 7.27 \text{ kg} \quad \text{and} \quad k_{(\text{normal})} = 10547 \text{ Nm}^{-1}$$

$$\text{therefore:} \quad \omega_{n(\text{normal})} = 38.09 \text{ rad.sec}^{-1} \quad \text{and} \quad \zeta_{(\text{normal})} = 0.017$$

The general equation of motion described above is related to the dynamic behaviour of the dynamometer in the absence of any external force such as cutting force. However, when milling takes place, the resulting cutting forces will suddenly cause the plate of the dynamometer displace in both feed and normal directions. Suitable forcing functions can be therefore regarded as suddenly applied forces of magnitude  $F_{(\text{feed})}$  and  $F_{(\text{normal})}$  in the feed and normal directions respectively. The equations of motions in the feed and normal directions of the dynamometer are then obtained as follows:



$$16.70 x''_{(feed)} + 21.82 x'_{(feed)} + 10547 x_{(feed)} = F_{(feed)} \quad (4.12)$$

$$7.27 x''_{(normal)} + 9.42 x'_{(normal)} + 10547 x_{(normal)} = F_{(normal)} \quad (4.13)$$

The solution of these equations are comprised of the summation of the transient or complementary function represented by the left hand sides of the equations, and the particular integral contributed by the external forcing functions. In the steady-state conditions where the transient vibration has died away, a static system results such that the displacement is proportional to the applied force by the ratio of  $(m \cdot \omega_n^2)$ . In milling, this corresponds to the situation where maximum cutting force has been reached. The complete solution in a general form is given as follows:

$$x = A e^{-\zeta \omega_n t} \cdot \cos \left[ \omega_n \sqrt{1-\zeta^2} t + \Phi \right] + \frac{F}{m \cdot \omega_n^2} \quad (4.14)$$

where A and  $\Phi$  are arbitrary constants depending on the starting conditions, and t is time. If at the start of cutting the dynamometer's plate starts from rest then it can be shown that, when t is large, the above expression reduces to:

$$x = \frac{F}{m \cdot \omega_n^2} \quad (4.15)$$

and,

$$x = \frac{F}{K} \quad (4.16)$$

Equation 4.16 shows that the cutting force is simply related to the dynamometer's spring stiffness.



#### **4.7 Cutting head assembly characteristics**

The cutting head assembly consisted of a variable speed industrial router, capable of producing a no-load speed of 24000 rpm, mounted on a manually-operated precision vertical bed assembly of 0.1 mm displacement resolution. The vertical position of the router can therefore be accurately adjusted so that correct depths of cut during cutting can be achieved. The speed of the router was adjusted by changing the voltage supply to its motor using a step-down transformer. When running idle, therefore, the voltage supply to the router motor increased with the increase of its speed. For a no-load fixed speed however, the corresponding voltage supply remained fixed at all times.

The above assembly is further mounted on two horizontal and parallel rails so that the router was able to traverse along the rails on wheel bearings. The traverse of the router is provided by a lead screw of 25 mm lead that was rotated by a 4-phase, 200-step stepping motor. The operation of the stepper motor was achieved by operating the electronic switches on its control panel where its speed and direction of rotation could be adjusted. Limit switches were used to stop the motor traversing the cutting head assembly beyond its required span of operation. Fig. 4.10 shows the cutting head assembly in a schematic form. Achieving 400 steps per revolution, the stepper motor produced a minimum available feed speed of  $2.5 \times 10^{-3} \text{ ms}^{-1}$ , and a maximum available feed speed of  $625 \times 10^{-3} \text{ ms}^{-1}$ .

The mechanism that is described above provided facilities capable of milling of leather surfaces along a straight line of action where cutting speeds and feed speeds were controlled by adjusting the speed of the router and the speed of the stepping motor respectively. Further facilities included the accurate adjustment of the depth of cut prior to cutting by the precision vertical bed assembly, as well as provision for mounting of cutting tools of different tip characteristics. Although only linear path cutting was required to obtain the necessary information in the milling experiments, facilities were provided to manually displace, and lock in position, the cutting head in the normal direction to the direction of the traverse of the router. This therefore enabled the cutter to cover an area of the workpiece where several adjacent experiments could take place on the same workpiece without having to replace the test pieces after each experiment. This was achieved by mounting the complete assembly that is described above on another two horizontal and parallel rails similar to those in the motor lead screw direction, but in normal direction to them.



Earlier in this section it was mentioned that the router was capable of rotational speeds of up to 24000 rpm. This corresponded to no-load running of the router. However, under load conditions it was likely that the developed torque at the spindle of the router causes its actual speed to drop by a certain amount. It would therefore be desired to monitor the actual speed of the cutter during cutting so that true cutting speeds could be recorded. To this end, an electronic optical tachometer was positioned on the cutting head assembly such that by continuously monitoring the rotation of the router spindle it could independently record its actual speed.



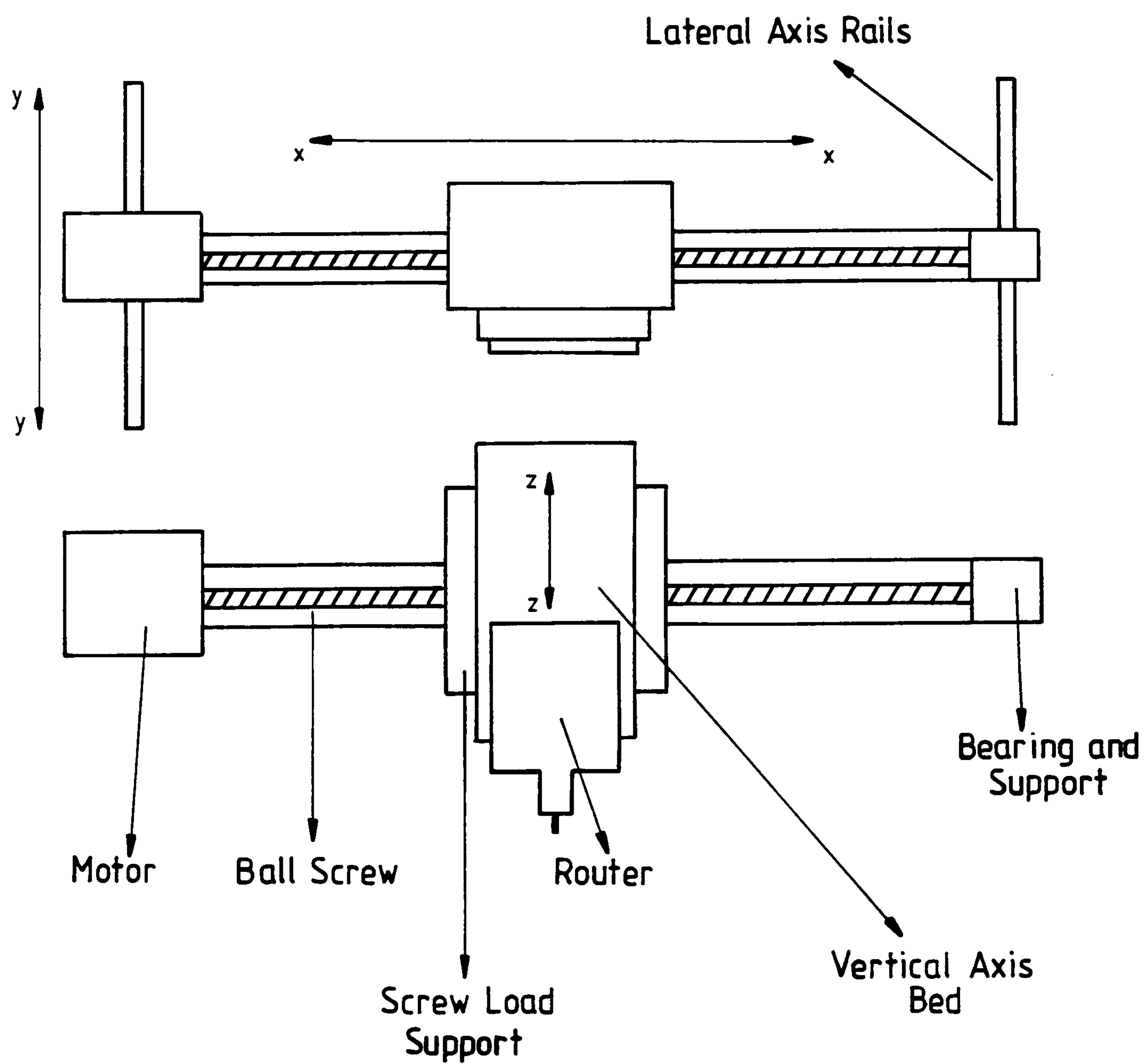


Figure 4.10 A schematic diagram of the cutting head assembly.



#### **4.8 Operation of the combined rig**

The complete leather milling experimental rig consisted of the combination of three main elements including the dynamometer, the cutting head assembly, and a data acquisition system so that the output of the various sensory devices could be recorded and analysed. In their physical forms as described in previous sections, the cutting head assembly was placed over the dynamometer such that the cutting tool of the router was placed over and above the plate of the dynamometer. Therefore, the axis of the cutting head lead screw was parallel to one of the two measuring axes of the dynamometer. The cutter was able to access the surface of the dynamometer plate where leather samples were to be clamped. The adjustment of the depth of cut was made by the precision vertical bed assembly which housed the router. The combined rig was placed in an enclosed perspex housing providing easy access to the rig for cutting tool and test sample replacements while avoiding noise and dust to pollute the environment as a result of router cutting of leather. A vacuum suction was provided to extract the leather particles in the form of dust from the perspex housing. Figs. 4.11 and 4.12 show the combined dynamometer and the cutting head assembly from different angles.



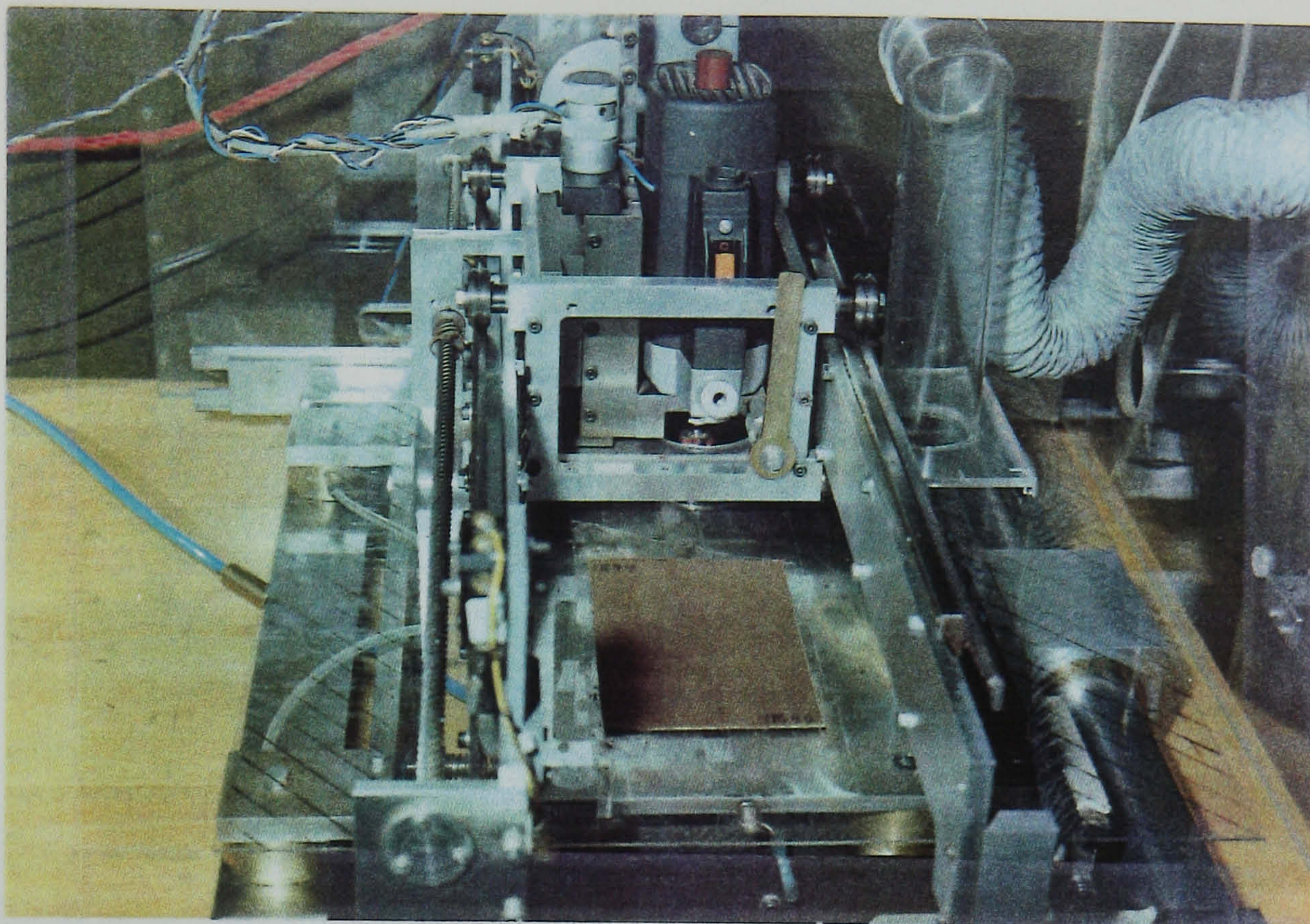


*Figure 4.11 A front view of the dynamometer and the cutting head assembly.*

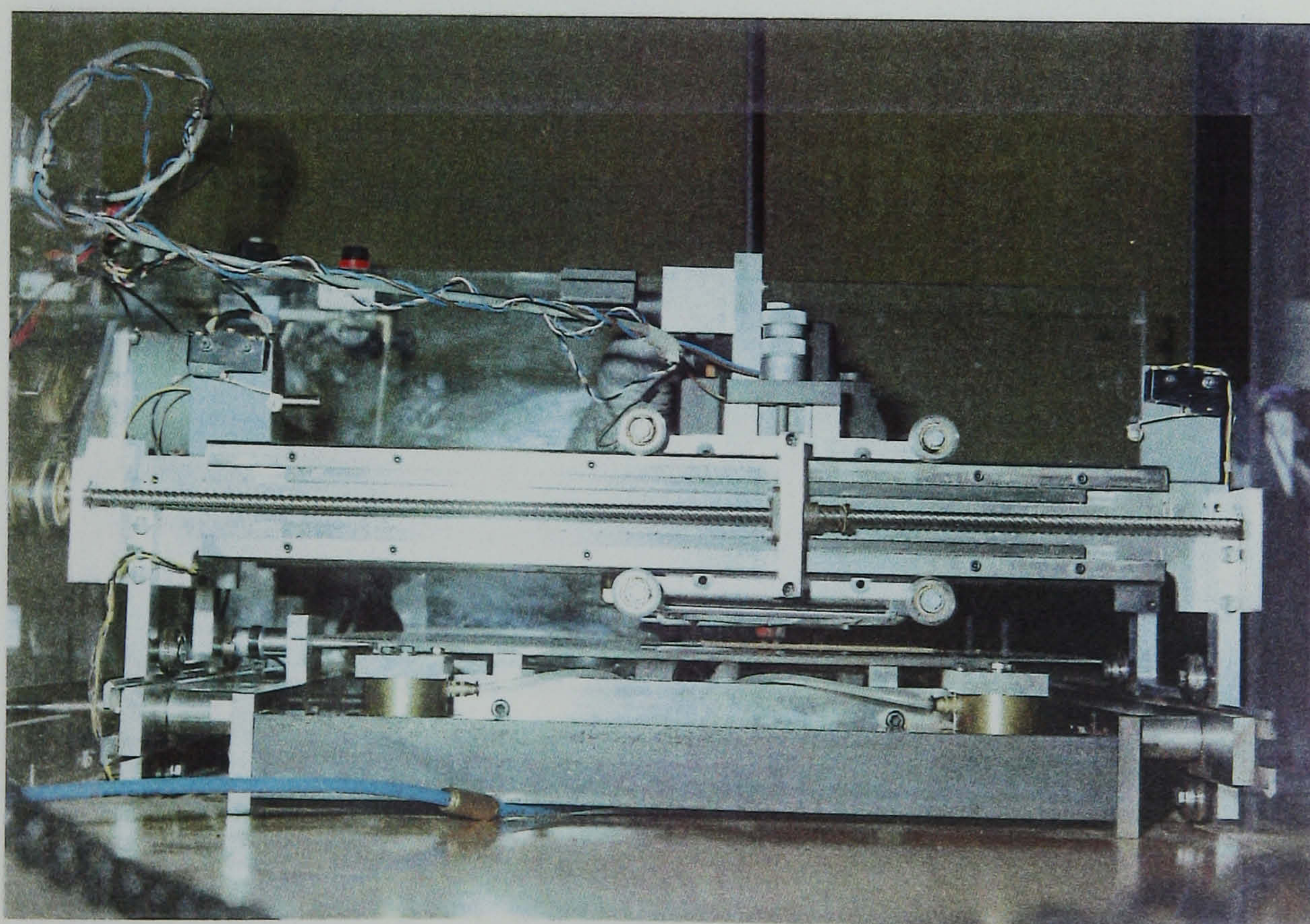


*Figure 4.12 A side view of the dynamometer and the cutting head assembly.*



When pressurised air was supplied to the air bearings of the dynamometer, the dynamometer plate assumes an equilibrium position trapped between its constraining springs. Upon energisation of the two displacement transducers fitted along its feed and normal directions, static calibrations were performed to relate the analogue output signals of the transducers to the displacement, and thus the applied force, in those directions of the dynamometer plate. This was achieved by applying known forces to the plate, in the form of hanging weights, in the feed and normal directions and recording the output signal from the corresponding transducers.

In the previous sections it was mentioned that one of the output results of the milling experimental rig was the measurement of the power consumption when cutting. In Section 4.2 it was explained that a reasonable estimate of this power consumption can be obtained by subtracting the value of the power supplied to the router when it is running under no load, from the power reading taken under load condition. Theoretically, power is calculated by the product of the rms values of current, voltage, and a factor called *power factor*. The value of the power factor is equal to the cosine of the angle that the active component of current vector makes with the voltage vector in the phasor diagram relating to the characteristics of the router motor [40]. It is therefore related to the reactance of the coil in the router motor armature. In order to establish the magnitude and the variation of the power factor in the router motor, a battery-operated clip-on power meter was employed to directly measure the power consumption in the router motor under no-load, and at various speeds of spindle rotation. At the same time, independent measurements of voltage and current were taken at those running conditions. Power factor for each motor condition was thus evaluated by dividing the values of power readings by those obtained from the product of the voltage and current readings. It was found that invariably the power factor in all conditions were very close to unity, suggesting that the router motor reactance was small. It was therefore safe to assume that the power used by the router motor could be obtained by multiplying the rms value of the supply voltage by the current drawn under each running condition.

The clip-on power meter was capable of measuring and digitally displaying the rms values of voltage, current, and power readings of an electrical load. It was also capable of producing a d.c. signal, as an output, corresponding to the rms value of the current drawn by the router motor. This signal was used to record the on-load currents during the experiments. The calculation of the power consumption of the router in each experiment was therefore based on this current



reading (changeable depending on the cutting load), and the voltage reading (fixed for each speed setting of the router). The measured no-load characteristics of the router motor are given in Table 4.1.

Cutting Speed (rpm)	Voltage (v)	Current (A)	Volts × Amp. (v.A)	Power (W)
8000	48.60	0.67	32.56	32.00
9000	53.82	0.69	37.14	36.00
10000	60.07	0.71	42.65	41.00
11000	64.47	0.72	46.42	44.00
12000	72.55	0.75	54.41	53.00
13000	78.82	0.76	59.90	57.00
14000	83.25	0.76	63.27	62.00
15000	89.99	0.77	69.29	69.00
16000	95.58	0.77	73.60	70.00
17000	104.07	0.80	83.26	82.00
18000	109.64	0.80	87.71	86.00
19000	117.21	0.81	94.94	92.00
20000	125.50	0.82	102.91	100.00
21000	133.07	0.84	111.78	109.00
22000	139.12	0.85	118.25	115.00
23000	150.91	0.88	132.80	130.00
24000	159.01	0.90	143.11	141.00

**Table 4.1**      *Measured no-load characteristics of the router motor*



Amongst the cutting variables under which the tests were performed are:

- i. rotational cutting speed of the router spindle
- ii. linear feed speed of the router assembly
- iii. tool rake angle
- iv. depth of cut
- v. hide types from which samples were taken

And, amongst the output results of the experiments are:

- i. cutting force in the feed direction
- ii. cutting force in the normal direction
- iii. power consumption in each cut
- iv. quality of the surface finish in each cut

In Section 4.7 it was mentioned that the corresponding voltage supply for a given no-load rotational speed of the router remained constant, and that when cutting, the speed dropped by an amount directly related to the cutting load. Although a reflection of this cutting load was measured in the form of the power used in each cutting as has been described earlier, the initial settings of the rotational speeds for the tests were in accordance with the characteristic of the motor as if running idly. That is to say, each test was performed with an initial known no-load speed. This therefore ensured that the voltage supplied to the router motor remained known and fixed during the entire period of an actual cutting test. Consequently, nine initial cutting speeds of 8000, 10000, 12000, 14000, 16000, 18000, 20000, 22000, and 24000 rpm were chosen prior to cutting. The on-board optical tachometer probe traced the true speed at any given time during the tests and its output d.c. signal was then fed to a personal computer for digitisation and storage. The feed speed of the router assembly was adjusted prior to the cutting through the stepper motor drive board. The maximum available feed speed that is given in Section 4.7 shows the capability of the stepper motor. For leather cutting however, the maximum feed speed that would allow safe implementation of the experiments, bearing in mind the method of adhesive



clamping used, was determined not to exceed  $0.1 \text{ ms}^{-1}$ . For this reason, and for the reason of practicality in the number of experiments performed, four different experimental feed speeds of 0.03, 0.05, 0.07, and  $0.09 \text{ ms}^{-1}$  were chosen. The tool rake angle was changed as required prior to the tests by changing the cutting tool with the correct tip geometry. As mentioned earlier in Section 4.4 four tools with rake angles of  $-17^\circ$ ,  $0^\circ$ ,  $19^\circ$ , and  $35^\circ$  were used. The depth of cut was adjusted, again prior to the start of the tests, by accurately adjusting the dial guage of the precision vertical bed on which the router was mounted. The different depths of cut tested for experiments were 0.2, 0.4, 0.6, and 0.8 mm. And lastly, leather samples were chosen from the two hide types that have been introduced earlier, namely hide type-1 and hide type-2.

The two cutting forces in the feed and normal directions were obtained from the two corresponding displacement transducers' d.c. signals. These were fed to the computer for digitisation, calibration, and storage. The cutting power was obtained, as described earlier, by using the d.c. signal from the clip-on power meter. This signal was also fed to the computer for further processing and storage. The assessment of the surface finish quality of the machined surfaces were done by subjectively examining the test pieces by way of tactile sensing inspection and observation.

A total of four d.c. signals (i.e. those relating to cutting speed, feed and normal dynamometer displacements for cutting forces, and router current for power calculation) were fed to the computer. An electronic interface unit containing four inverting operational amplifiers were constructed to amplify the signals prior to inputting them to the analogue to digital (A/D) convertor card available in the computer. The 8 bit resolution A/D card took input signals in the range between +5 and -5 volts. The gain and the offset of the signals were thus so designed to fall in this voltage range for maximum utilisation of all the available 8 bits in the A/D card.

A computer data acquisition program was developed to sample, read, and store the digital signals from the input ports of the computer. This program collected 100 readings from each one of the four ports, one after the other, and stored the results in four corresponding arrays. The data in each array was further processed by the relevant calibration factors so that the values in their final form could be stored in the data files. Further processing was performed to extract the maximum values read from each port. These maximum values then became the basis of the analysis of the results in the milling experimentations. In the case of



the cutting speed signal, the values started to decrease once a test began, and continued to decrease before settling around a fixed value. This fixed value was taken to be the true speed of the cutting in that test.

Experiments were conducted by clamping the leather samples that had been carefully cut from various regions of the test hides of two different types similar to those used in physical properties experiments described in Chapter Three. The method of clamping was by using double-sided adhesive tapes similar to that explained for the initial tests in Chapter Two. The samples were clearly marked so that their exact location from the hides could be easily identified.

#### **4.9 Conclusions**

This chapter is concerned with the theoretical description and the experimental design of the rig that was constructed and employed to investigate milling of leather as a high speed machining system proposed for the automation of leather skiving.

The area of milling has been well researched in the past but no published work on its application to leather as a workpiece is available. To this end, attempts were made to experimentally apply the existing relevant theory in the general milling area to this new application while improving where and when it was necessary to do so. The important theories that were deemed to be of direct interest to this work are presented at the early stage of the chapter where critical parameters involved in milling operation are introduced and discussed. Amongst these are the geometric design of the cutting tool, and in particular the importance of its rake and clearance angles, the significance of the radial and tangential components of the resultant cutting force together with their relationship with the more easily measured components in the feed and normal directions, and the usefulness of the evaluation of power consumption in cutting.

Having established the fundamental functions of the set-up and its necessary elements that are required to perform the desired experiments, the general description of a dedicated rig is given in the body of the chapter.

Initial attention is given to a more detailed study of the cutting tool with a special reference to its critical angles with the rake angle recognised to be the most critical. Tools with rake angles of  $-17^\circ$ ,  $0^\circ$ ,  $19^\circ$ , and  $35^\circ$  together with a fixed clearance angle of  $3^\circ$  were made for the tests. A quasi-static dynamometer that is



capable of measuring cutting forces in both feed and normal directions with the aid of two orthogonally positioned displacement transducers was designed and constructed. The main characteristics of the dynamometer include the use of air lubricated bearings for virtually frictionless travel of its displacement sensitive platform. The dynamometer is however capable of measuring feed and normal cutting forces simultaneously, but is aimed to target the maximum values achieved. Equations of motions relating to the dynamic behaviour of the dynamometer are also given. The cutting head assembly employs a high speed router that is capable of rotational speeds of up to 24000 rpm, driven along a linear path by a stepper motor through an assembly of a lead screw and supporting rail and wheel bearings. The depth of cut is achieved by moving the router in its vertical axis by a precision bed assembly. An optical tachometer was employed to monitor and record the actual speed of the router under cutting conditions.

A description of the operation of the rig is given in the final section of this chapter where the combined rig is further discussed. A method for measuring the power used in the cutting tests is presented which involves the electrical characteristics of the router motor armature. On the basis of this method, the power is obtained by subtracting the product of current and voltage of the motor under load condition from that obtained when the motor is running idly. The current is therefore required to be measured at each test; the value of the supply voltage is kept fixed at the start of each test. The analogue signals of the two displacement transducers together with those of the current and the tachometer were fed through amplifier circuits, and then to the analogue-to-digital converter of a personal computer. A data acquisition computer program was written to collect the results of each test and store them in relevant data files.



## **CHAPTER FIVE**

### **MACHINING SYSTEM EXPERIMENTAL RESULTS**

#### **5.1 Introduction**

In this chapter the complete results of the experiments concerning the high speed machining as a method for leather skiving are presented. The detailed descriptions of the experimental rig and the methods of measurements have already been given in Chapter Four.

Quality of the surface finish in leather machining is the most important aspect of the results that is considered. It is this factor that primarily determines the method's suitability for skiving automation. The examination of surface finish quality is performed by way of tactile sensing and visual observation. The results show that the quality of the machined surface is heavily dependent on the physical characteristics of the material. For example, it is observed that the poor original quality of a test sample is largely responsible for its poor machined surface quality. This is particularly true in the case of leather type-1. Due to this dominating effect of the materials characteristic the effects of other machine-related parameters on surface quality becomes much less noticeable. The nature of this material dependency of the surface quality results is more fully described later in this chapter.

Leather samples were cut from different regions of hide type-1 and type-2. Upon recording of the exact locations of the samples for future reference the samples were randomly mixed so as to minimise the effects of other unwanted variables in the experiments. To perform the experiments, however, a system of changing variables one at a time was employed. This method ensured that all variable possibilities are tested. Each individual test was replicated three times and the mean values were used to analyse the results.



The results of the experiment are divided into several sections. These include the examination of the repeatability of the tests, the results concerning the effects of different machine parameters on cutting forces and power consumption, results concerning depth of cut, and the analysis of tool wear. Each section of the results are separately presented. Then the role of the materials properties in the experiments and the results concerning quality of the surface finish are discussed.

## **5.2 The repeatability analysis**

The experiments were conducted in highly practical situations whereby effects of various physical variables such as feed speed, cutting speed, and depth of cut on leather samples were investigated. The results of a given test under the same conditions should ideally be identical. However, in practical tests like these, the effects of unwanted factors cannot be fully avoided. For example, the router motor may behave slightly differently when it is started from cold rather than when it has been running for a while. This may affect the power intake of its armature. There are also other factors that may slightly affect the results such as room temperature, operator's consistency in his accuracy of conducting tests, etc. Nevertheless, the most significantly undesired factor in the case of leather machining is the non-repeatability of the workpiece itself. Although three replications for each test were done on the same test sample and very close to one another, the fact that leather is a natural material and hence is not uniformly manufactured, cannot be ignored. This phenomenon was present in all the tests and is regarded as the most influencing factor in the occasional scatter observed in the results of the replication of the same test.

In order to examine its extent, experiments were conducted so that the results repeatability can be observed. It was explained earlier that the rotational cutting speed of the router drops to a certain steady value under load conditions from its no-load initial settings. This occurs due to lack of torque available at the router spindle, and the extend at which the speed drops depends upon the cutting load it is trying to overcome. In the course of the main body of the experiments observation were made to examine whether under identical test conditions the initial speeds fall to the same values. The results show that for initial speeds between 8000 and 16000 rpm the settled values are very much close to one another, and at most speeds above 16000 rpm a wider band is produced. However, at the worst case the width of the widest band does not exceed 2000 rpm. For the purpose of these experiments this is acceptable since general



guidelines and trends in the results are of importance. Fig. 5.1 (a) shows the results of a typical test conducted on leather type-1, and with feed speed of  $0.03 \text{ ms}^{-1}$ ,  $0^\circ$  tool rake angle, and 0.4 mm depth of cut. The same cutting conditions were applied to the tests to measure the power consumption of the router motor spindle. Again, at higher cutting speeds the band of the replicated results generally tend to widen, in this case at speeds above 14000 rpm. This is shown in fig. 5.1 (b).

Evaluation of the repeatability in the cutting force results also show encouraging results. The tests conducted under the same cutting conditions as above to measure the feed cutting forces (ie. those measured in the feed direction) show smaller bands at lower cutting speeds and slightly wider bands at higher cutting speeds. The results concerning normal cutting forces (ie. those measured at right angle to the feed direction) behave in much the same way except for initial cutting speeds of 14000 and particularly 20000 rpm where wider bands are noted. These results are presented in figs. 5.1 (c) and 5.1 (d) respectively.



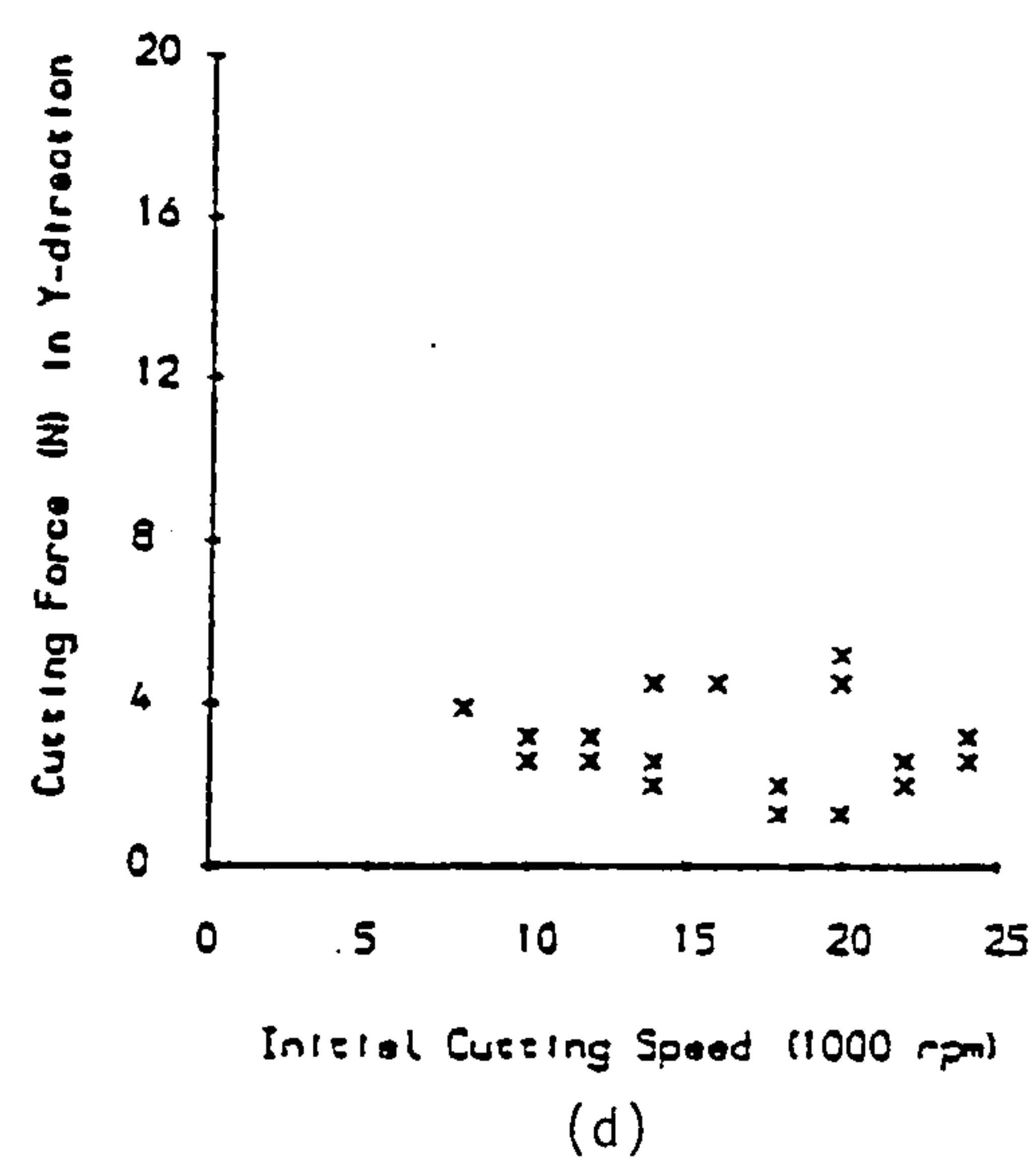
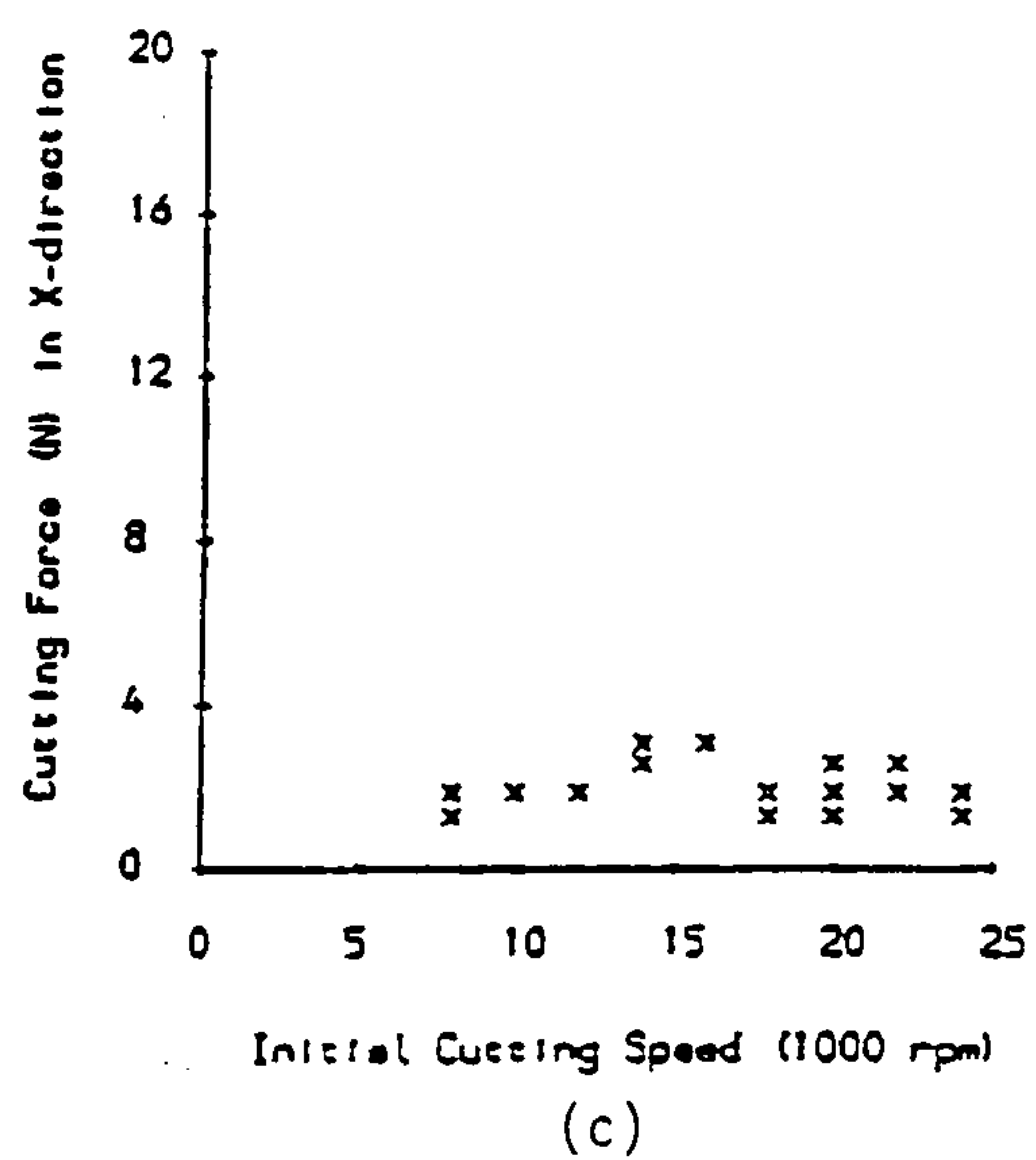
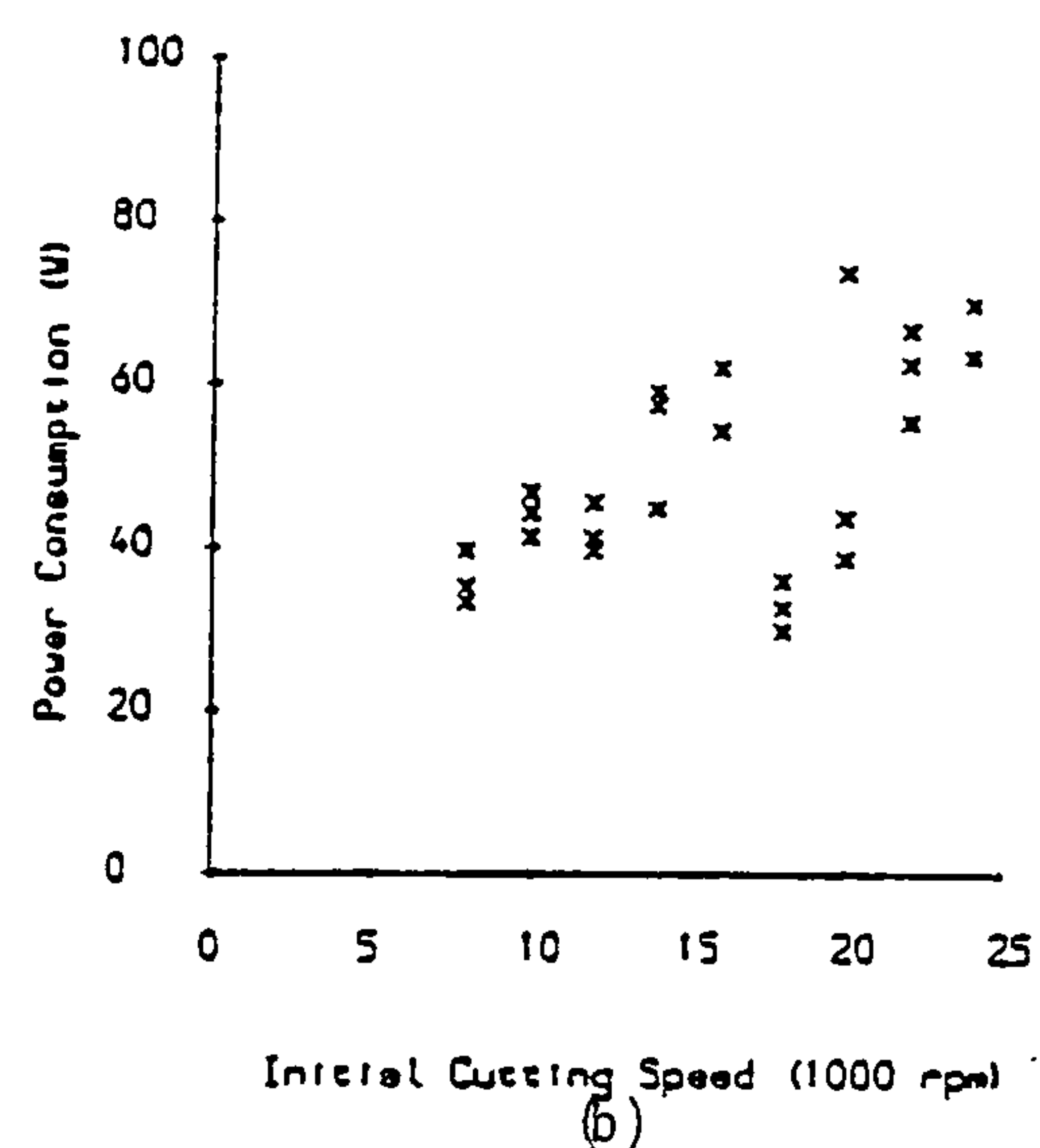
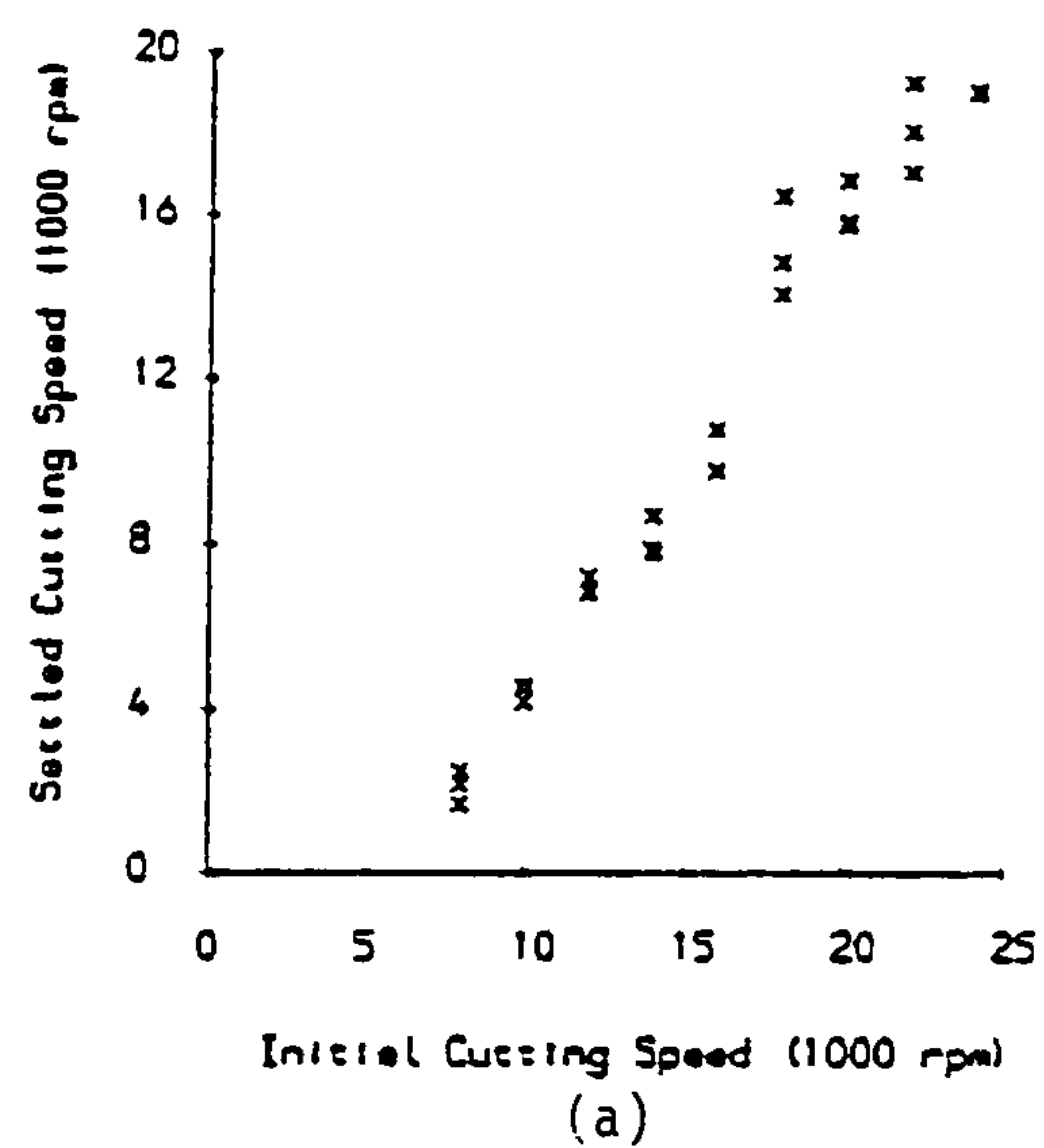


Figure 5.1 Results of repeatability analysis for leather type-1:  $0.03 \text{ ms}^{-1}$  feed speed,  $0^\circ$  cutting tool rake angle, and  $0.4 \text{ mm}$  depth of cut.



In general it is noted that for cutting speeds lower than around 14000 rpm the bands tend to be smaller than for those above 14000 rpm. This is largely attributed to the fact that when the router is running at higher speeds it transfers a certain amount of inherent vibration onto the dynamometer rig. The resulting upsets in the behaviour of the system is thought to be the main cause of the scatter described above.

In a different representation, the repeatability of the results are examined against the changes of feed speed. Tests with initial cutting speed of 24000 rpm,  $0^\circ$  rake angle, and with 0.4 mm depth of cut were conducted on leather type-1. This time the initial cutting speed, power consumption, feed cutting force, and normal cutting force are examined against changes of feed speed. The results of replication for the settled cutting speed show remarkable repeatability for the entire range of the feed speed in tests. In the case of power consumption, the replicate bands tend to widen with the increase of feed speed. Fig. 5.2 (a) and 5.2 (b) show the results.

The widening of the replicate bands with the increase of feed speeds is also noted when the feed cutting speeds are examined. Fig. 5.2 (c) and (d) show the results concerning feed and normal cutting forces. In a similar analogy to the case of higher cutting speeds, when high feed speeds are used the dynamics of the rig experiences higher degrees of undesirable vibrations that can act to upset the controlled settings which are employed to monitor the results. It is thought that these upsets help widen the replicate bands. Nevertheless, the repeatability of the results are in an acceptable range since, as mentioned before, it is the trends in the results that are sought in this work.

It can therefore be concluded that, although replication of tests in leather machining does not always yield to identical results, the bands that they produce are acceptable in the analysis of this work.



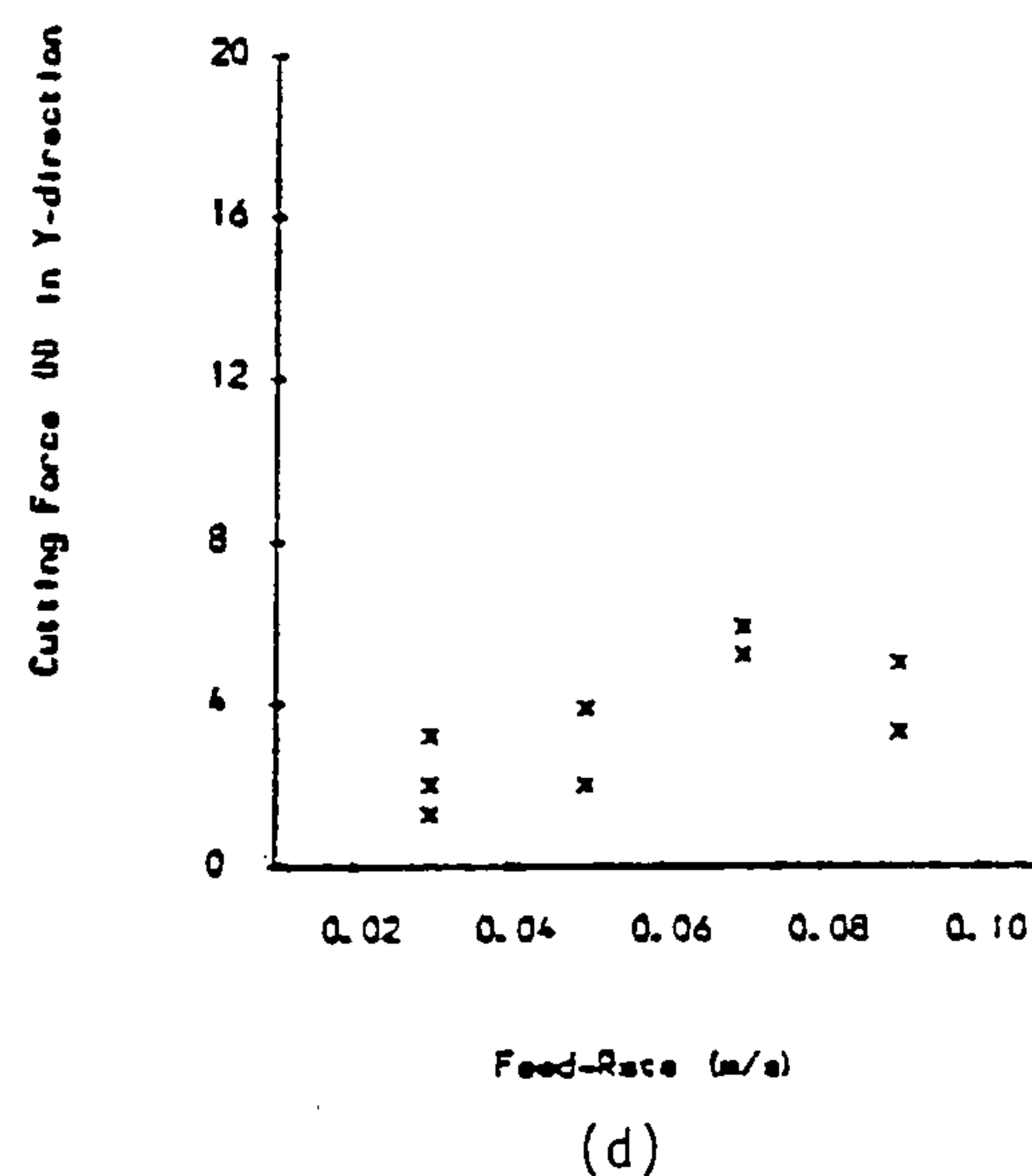
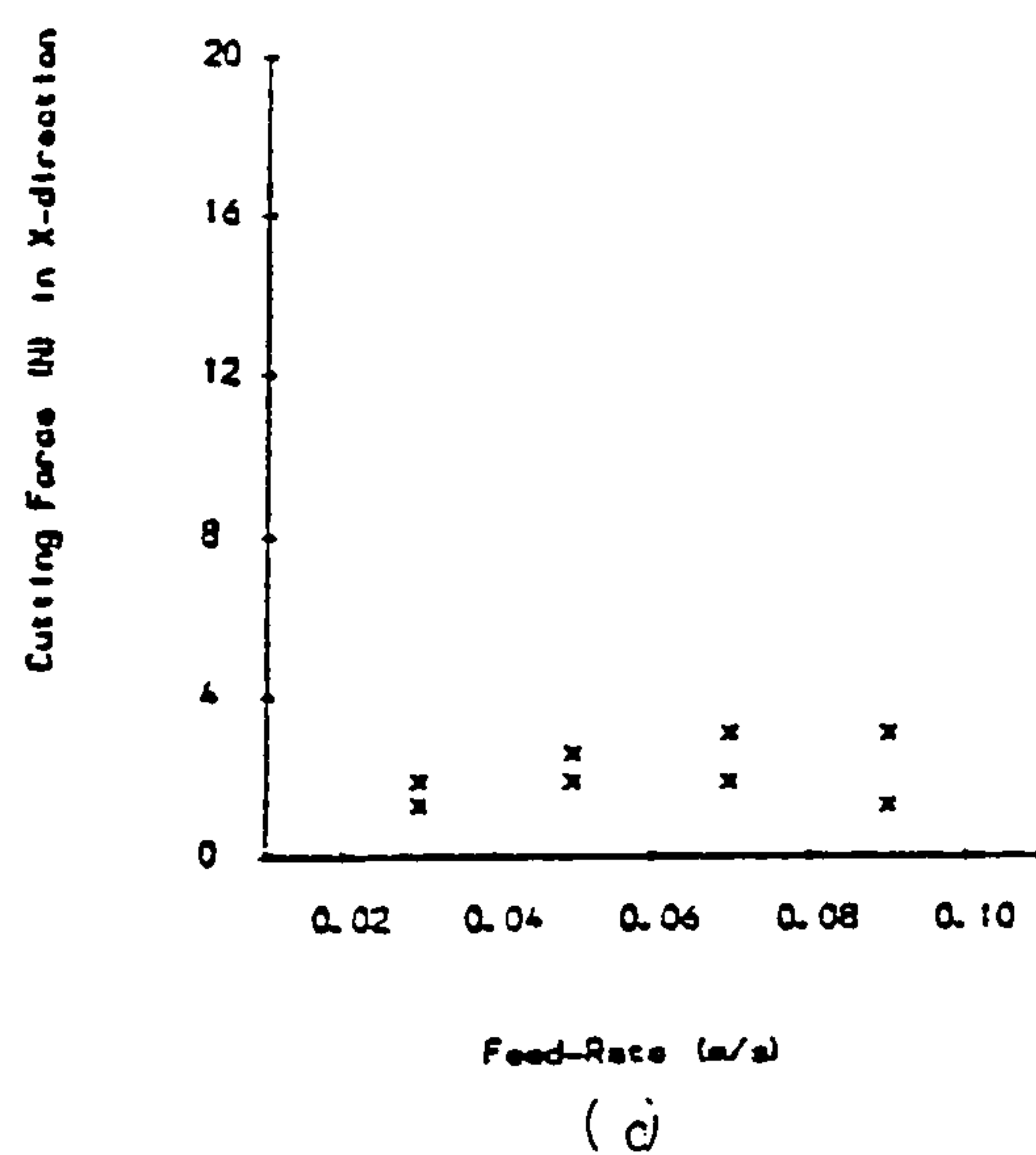
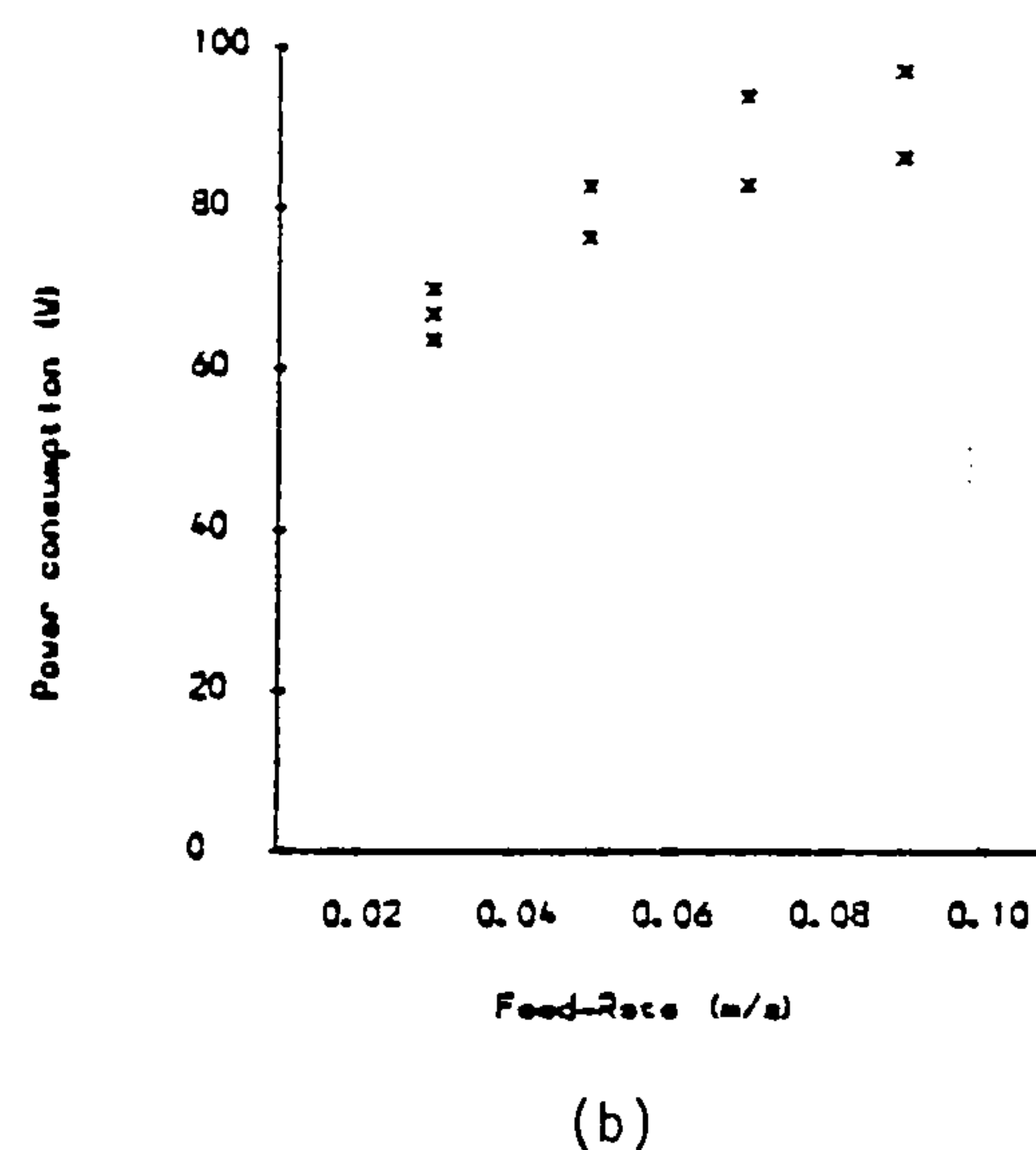
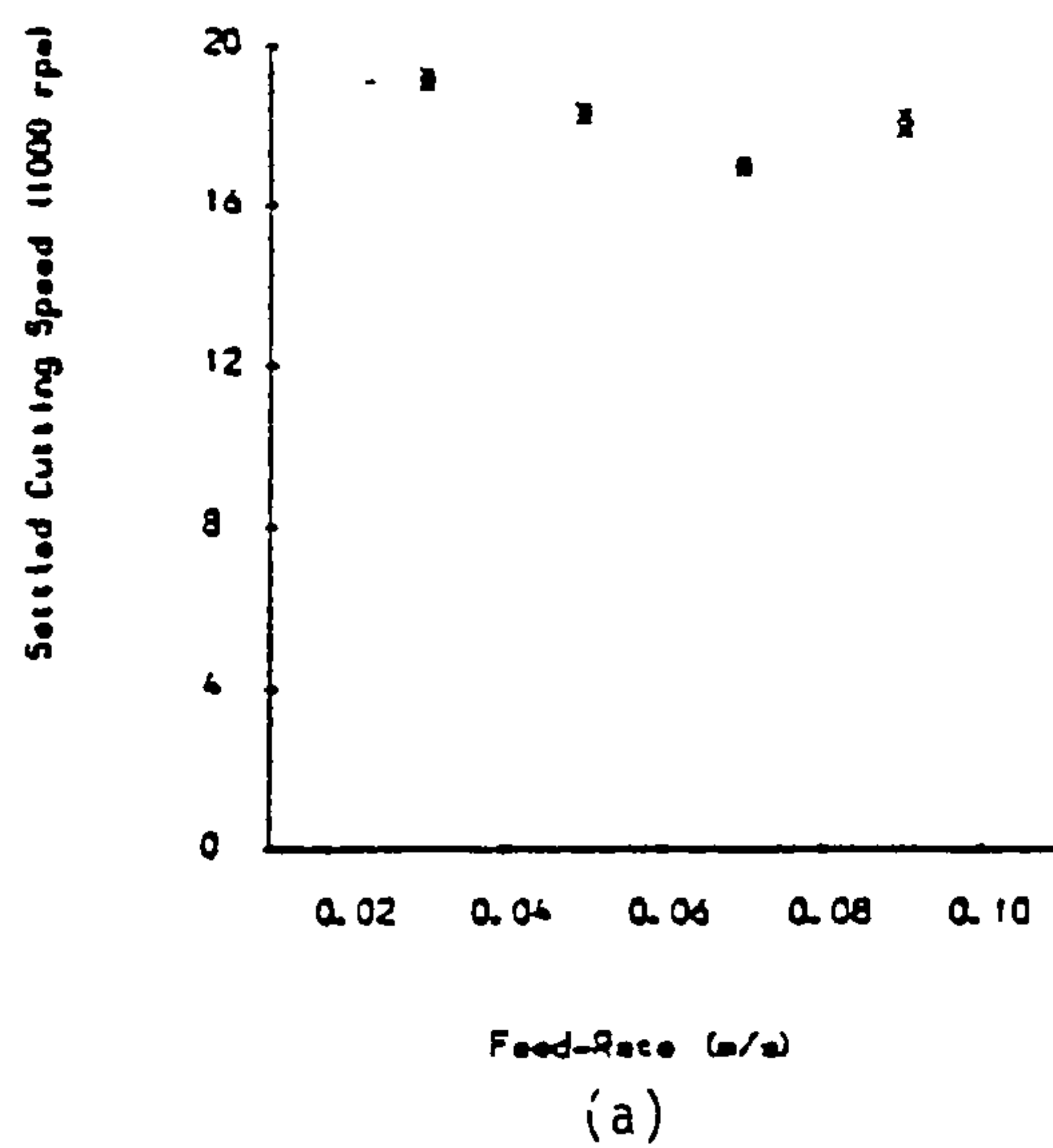


Figure 5.2 Results of repeatability analysis for leather type-1; 24000 rpm initial cutting speed,  $0^\circ$  cutting tool rake angle, and 0.4 mm depth of cut.



### 5.3 Machine parameter results

In this section the main body of the results concerning the evaluation of important machine parameters including feed and normal cutting forces as well as power consumption in the system are presented and discussed. All the tests in this section were conducted with 0.4 mm depth of cut. A total of 105 different test conditions for leather type-1 and 48 different test conditions for leather type-2 were successfully experimented with each condition repeated three times.

The cutting force results give a useful guideline for the designer of an automated skiving system based on leather machining. They give the average forces that leather is likely to require for its surface machining, and in theory, gives an indication of any workpiece clamping force required. Furthermore, estimation of cutting force provides a good measure of how efficiently cutting is taking place. Apart from determining the resistive loads due to the effects of variables that are controlled in these tests such as feed and cutting speeds, depth of cut, etc. its sudden rise can reflect events such as tool breakages or excessive tool wear.

Examination of the cutting force results immediately suggest that in all cases the value of normal cutting force is consistently higher than that of feed cutting force. This phenomenon is true regardless of leather type, tool rake angle, or feed and cutting speeds, though the ratio of normal to feed cutting force varies as the test conditions change. Table 5.1 shows the overall mean cutting force values obtained in the experiments.

	$F_x$ (N) [S.D.]	$F_y$ (N) [S.D.]	$F_x / F_y$
Leather type-1	4.04 [2.02]	7.07 [2.79]	0.57
Leather type-2	3.05 [1.72]	5.70 [2.44]	0.53

*Table 5.1 Overall mean values for cutting forces.*



The results of Table 5.1 show that leather type-1 requires more applied force to overcome its resistance to machining than leather type-2. The magnitude of the resultant cutting force for leather type-1 is 8.14 N, and the magnitude of the resultant cutting force in the case of leather type-2 is 6.46 N. Also, in both leather types the average normal cutting force is just under twice that of feed cutting force. This result is consistent throughout the experiments. The significance of the comparison of feed and normal forces is that it estimates the amount of rubbing that takes place. Small ratios of  $\frac{F_x}{F_y}$  indicate that more rubbing takes place and vice versa. The mean values of 0.57 and 0.53 indicate that though rubbing is present in the cutting tests its contribution is not very large.

The investigation of the cutting forces show that it produces less fluctuations in the feed directions than in normal direction. In the case of leather type-1 the range of the cutting forces in the feed direction is bound between approximately 2 and 11 N while the same range in the normal direction is between approximately 2 and 15 N. This phenomenon is also seen in the tests on leather type-2. The cutting force range in the feed direction in tests on this leather type is approximately between 1.5 and 7 N while the same range in the normal direction is approximately 1.5 and 12 N. The results show that the effect of increasing cutting speed generally tends to slightly decrease cutting forces especially in the range between 4000 and 10000 rpm. The cutting force values fluctuate beyond this speed range and on average show no further significant change with respect to the increase of the cutting speed.

The effects of the feed speed in the machining tests show that the cutting forces also increase with its increase. Significant increase in the cutting force is observed when the feed speed was increased from 0.03 to 0.05 and further to 0.07 ms<sup>-1</sup>. Unlike the predictions further increase in the cutting force at 0.09 ms<sup>-1</sup> was not very clearly observed in the tests. The explanation for this is related to the physical characteristics of the rig. The combination of high linear speed of the moving router (ie. the feed speed) in the experimental rig at 0.09 ms<sup>-1</sup>, and the standard length of leather samples in tests (150 mm), proved to cause the majority of tests not to acquire enough time for the dynamometer to register the potential maximum force reached. That is to say, due to the dimensional restrains of the rig the maximum force values were not reached during cutting at 0.09 ms<sup>-1</sup> feed speed. The results concerning this cutting speed are nevertheless presented in this section.



Tool rake angle plays an important part in determining the cutting forces in the experiments. The results clearly show that  $0^\circ$  rake angle gives the lowest cutting force measurement. This result is consistently observed throughout. The values of cutting force increases when  $19^\circ$  rake angle is used. And on average, the highest cutting force readings are obtained when  $35^\circ$  rake angles are employed, particularly on type-1 leathers. It is worth mentioning at this stage that leathers of type-1 in the tests have higher apparent density, and thus they are more fibrous than leathers of type-2. This phenomenon becomes particularly important when their fibre networks become directly engaged with the rake face of the cutting tool. Therefore the effect of tool rake angle is more clearly observed when more fibrous samples are machined. Examination of the rake angle yields significant conclusions from the experiments. It shows that when machining fibrous materials such as leather, lower tool rake angles give lower resulting cutting forces. This is however true in positive rake angles only. The results show that when a negative rake angle of  $-17^\circ$  is used the cutting force readings are not as low as those with the case of zero rake angle. However, it is seen from the tests that the average cutting force resulted from using negative rake angle does not reach as high a value as in the case with  $35^\circ$ . The majority of the experiments show that tools with  $-17^\circ$  rake angle give cutting force results higher than  $0^\circ$  and lower than  $19^\circ$  rake angles. The results of the tests are graphically produced in the following figures. In the case of leather type-1, the values of both feed and normal cutting forces are plotted against the variation of cutting speed for each rake angle tested. Each figure is related to a fixed feed speed. The figures are presented in the increasing feed speed order.

The results of the feed cutting forces in leather type-1 are graphically shown in figs. 5.3 (a), (b), (c), and (d) for 0.03, 0.05, 0.07, and 0.09  $\text{ms}^{-1}$  feed speeds respectively. Similarly, the corresponding results of the normal cutting forces are presented in figs. 5.4 (a), (b), (c), and (d). Then, the results concerning leather type-2 are presented. Figs. 5.5 (a) and (b) show the variations of different tool rake angles for a fixed feed speed against increase in cutting speed, while figs. 5.6 (a) and (b) show variations of different feed speeds for a fixed tool rake angle.



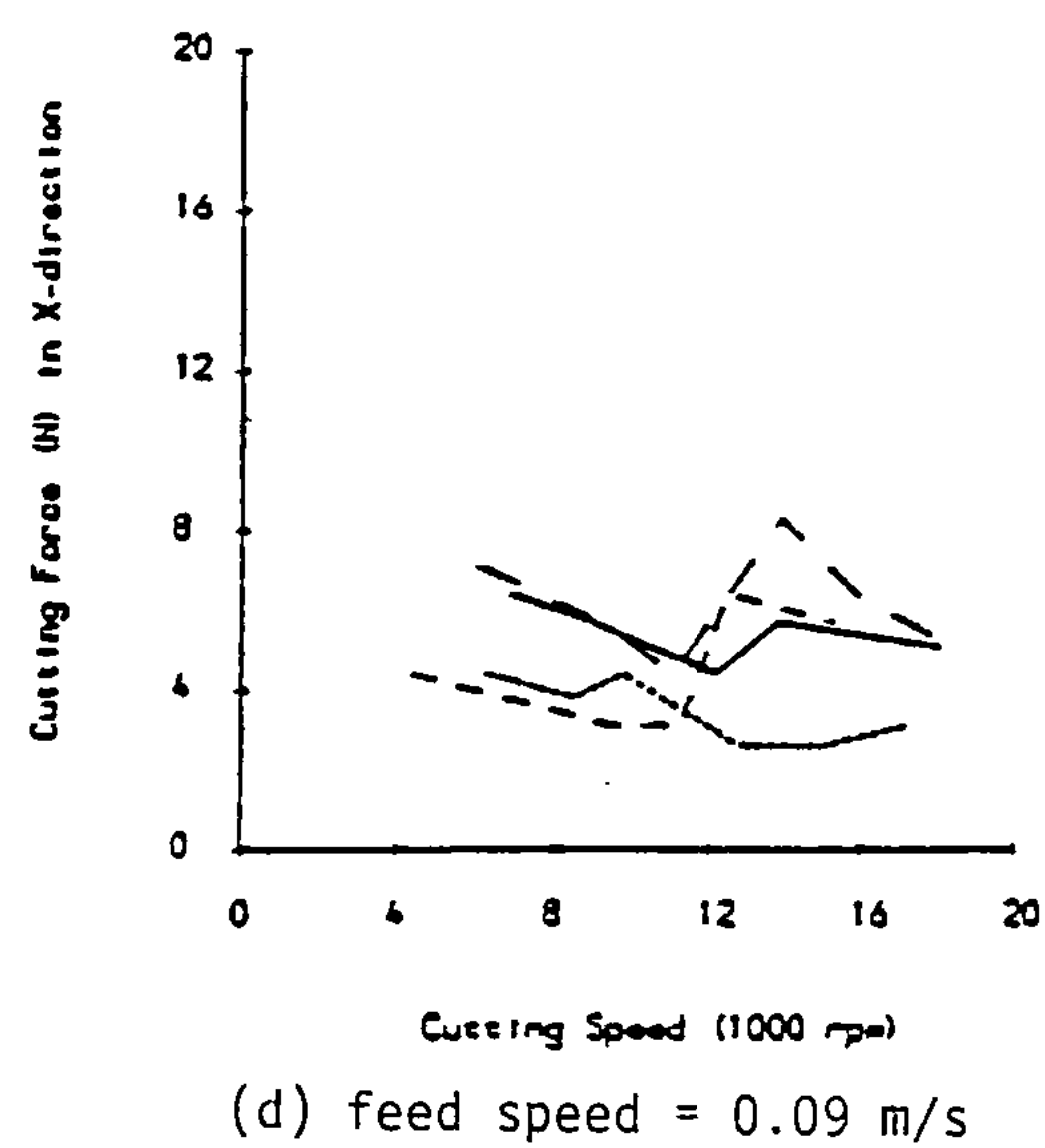
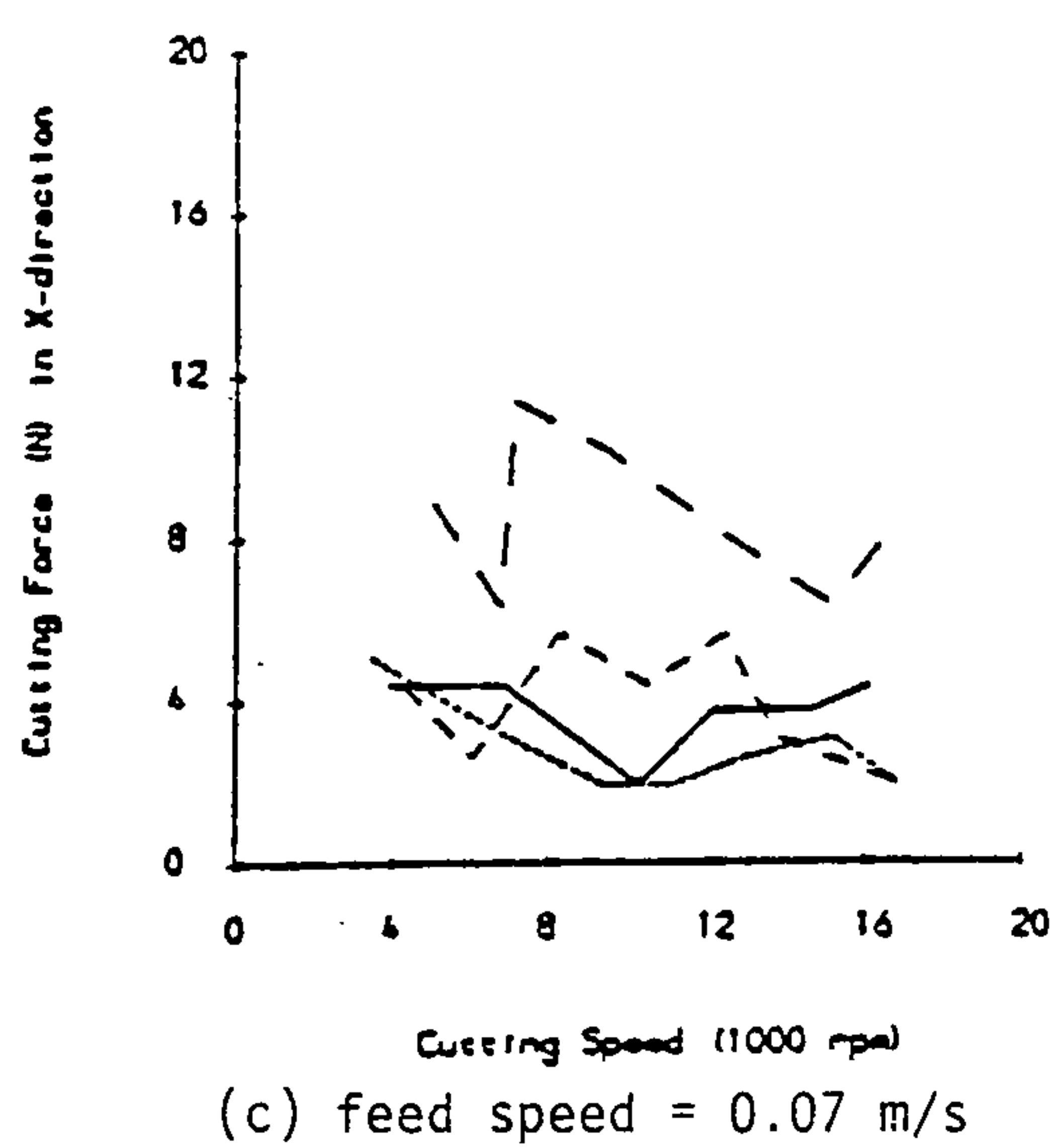
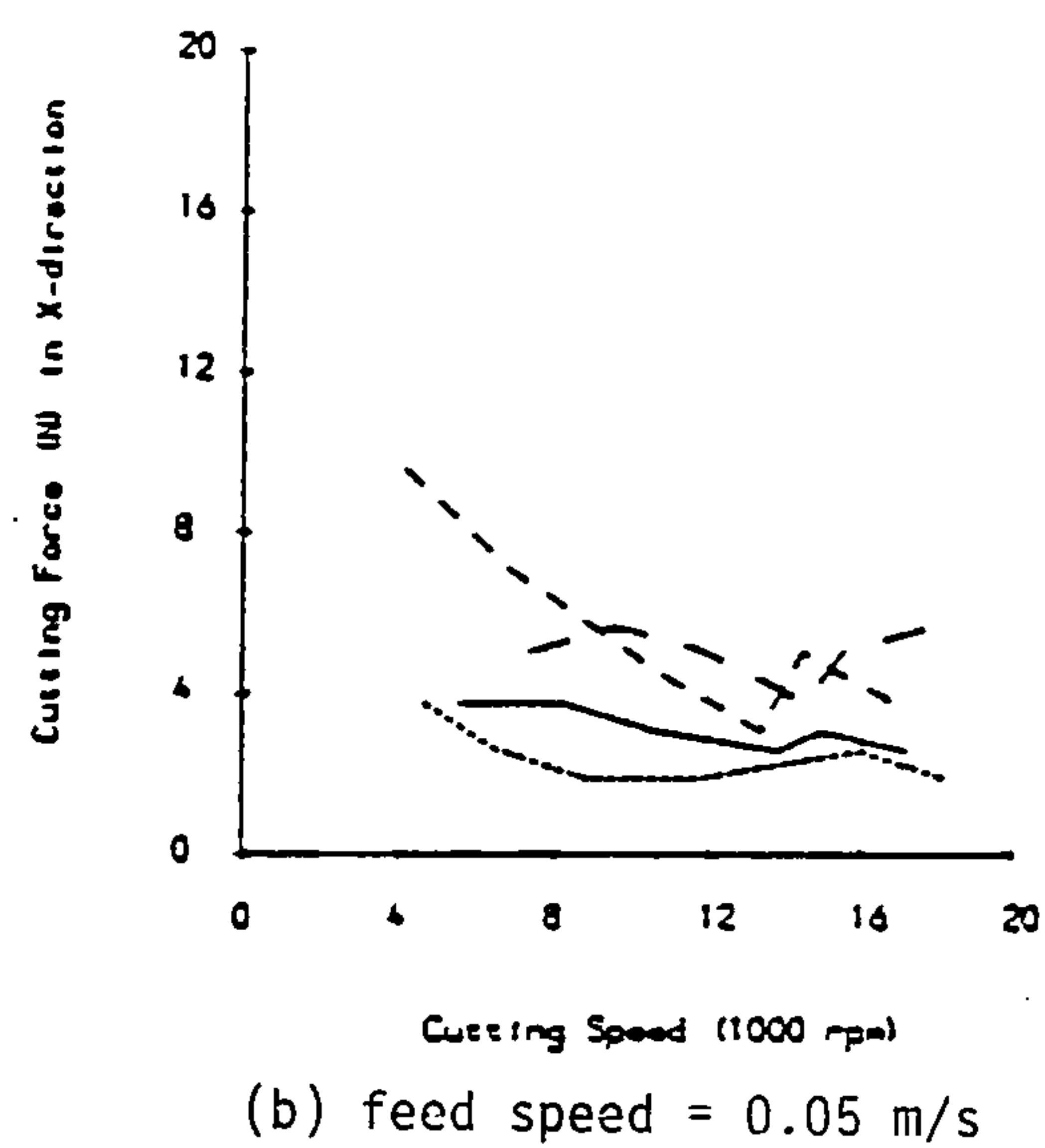
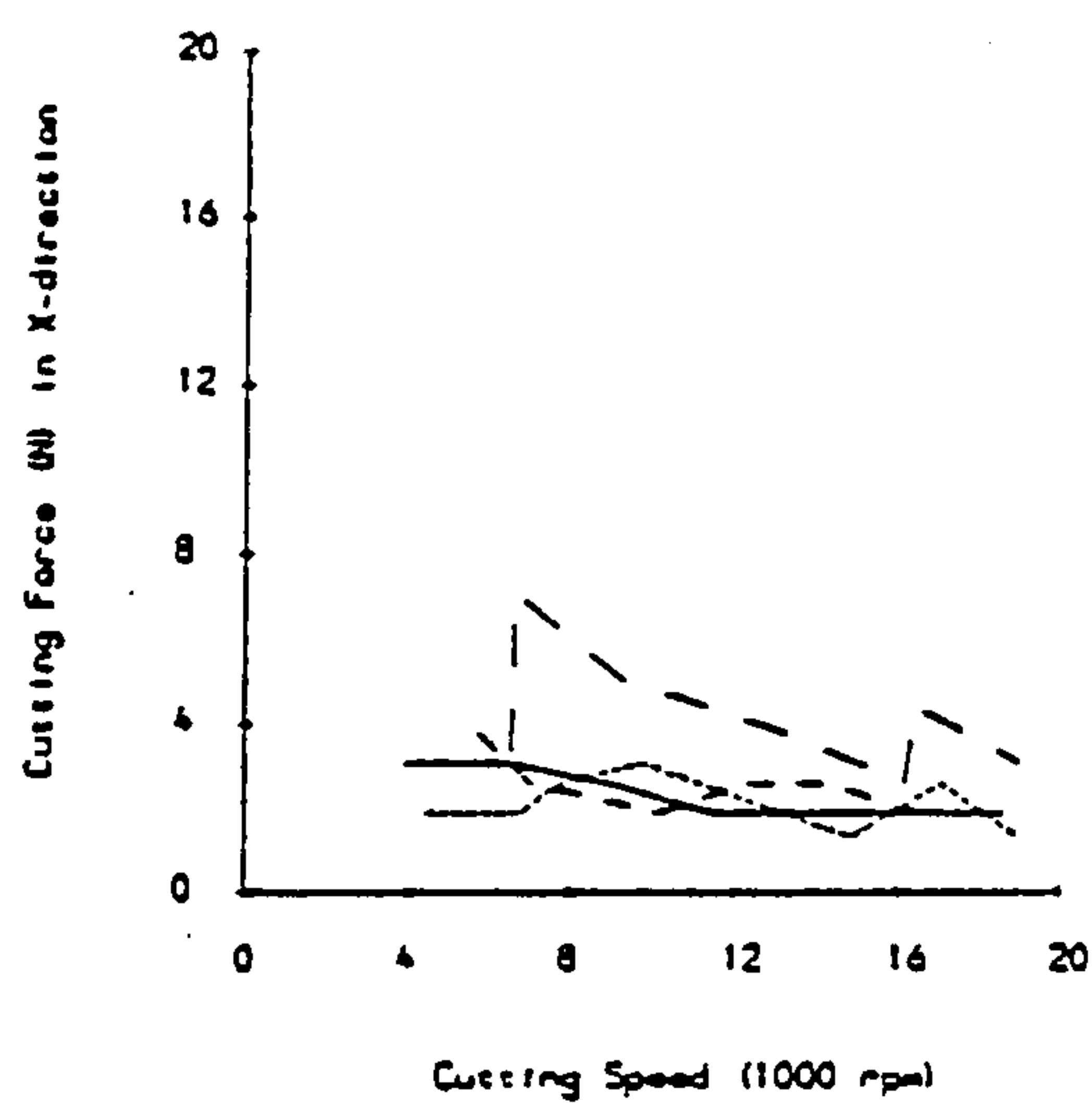
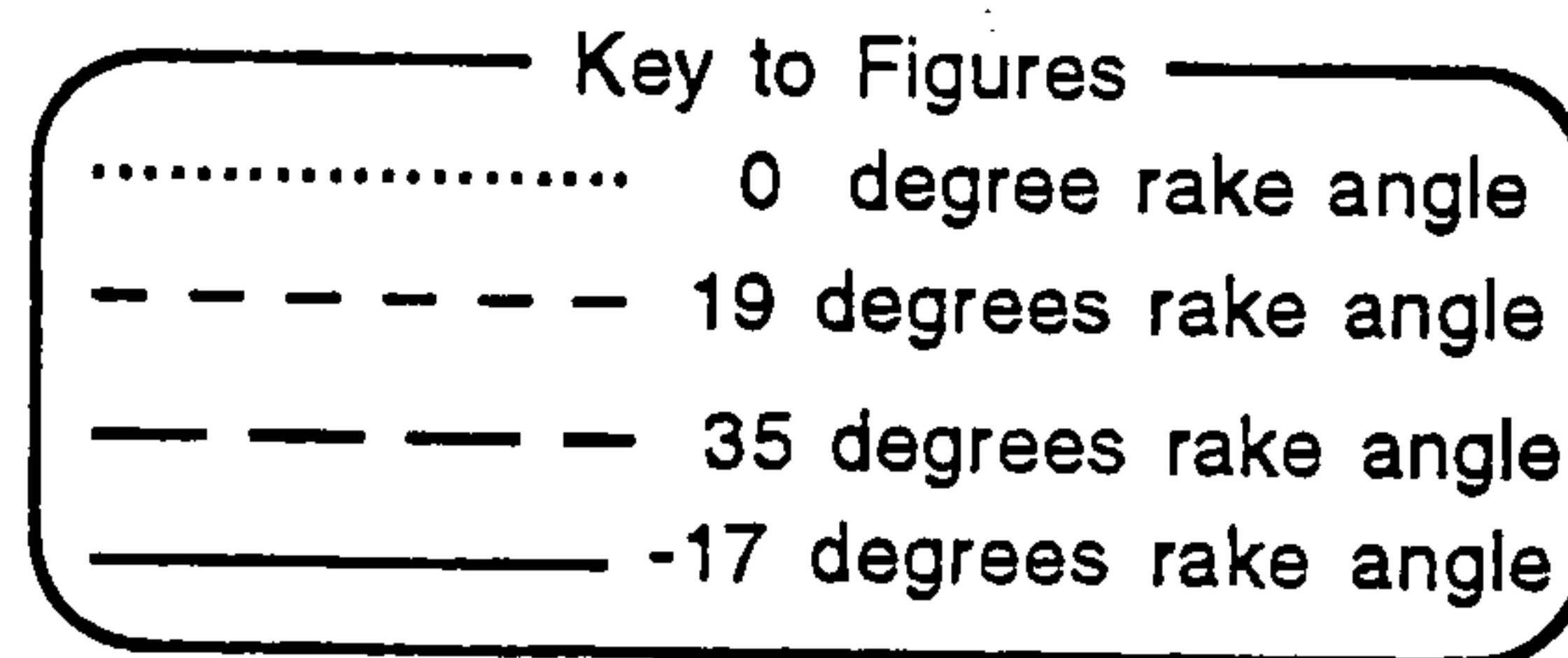


**Figure 5.3** *Graphs of variations of feed cutting force in leather type-1 against cutting speed for different tool rake angles, and with 0.4 mm depth of cut.*



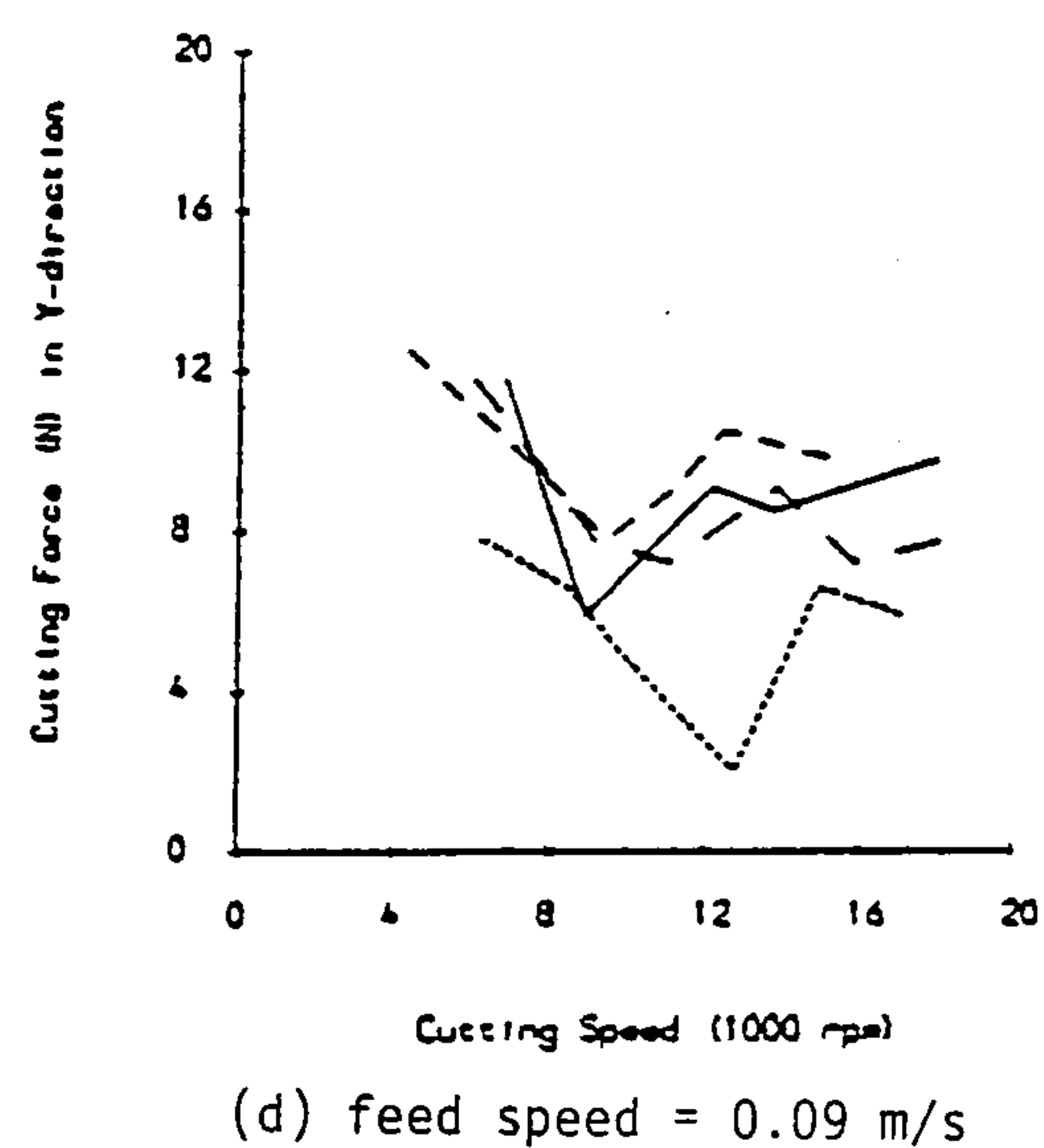
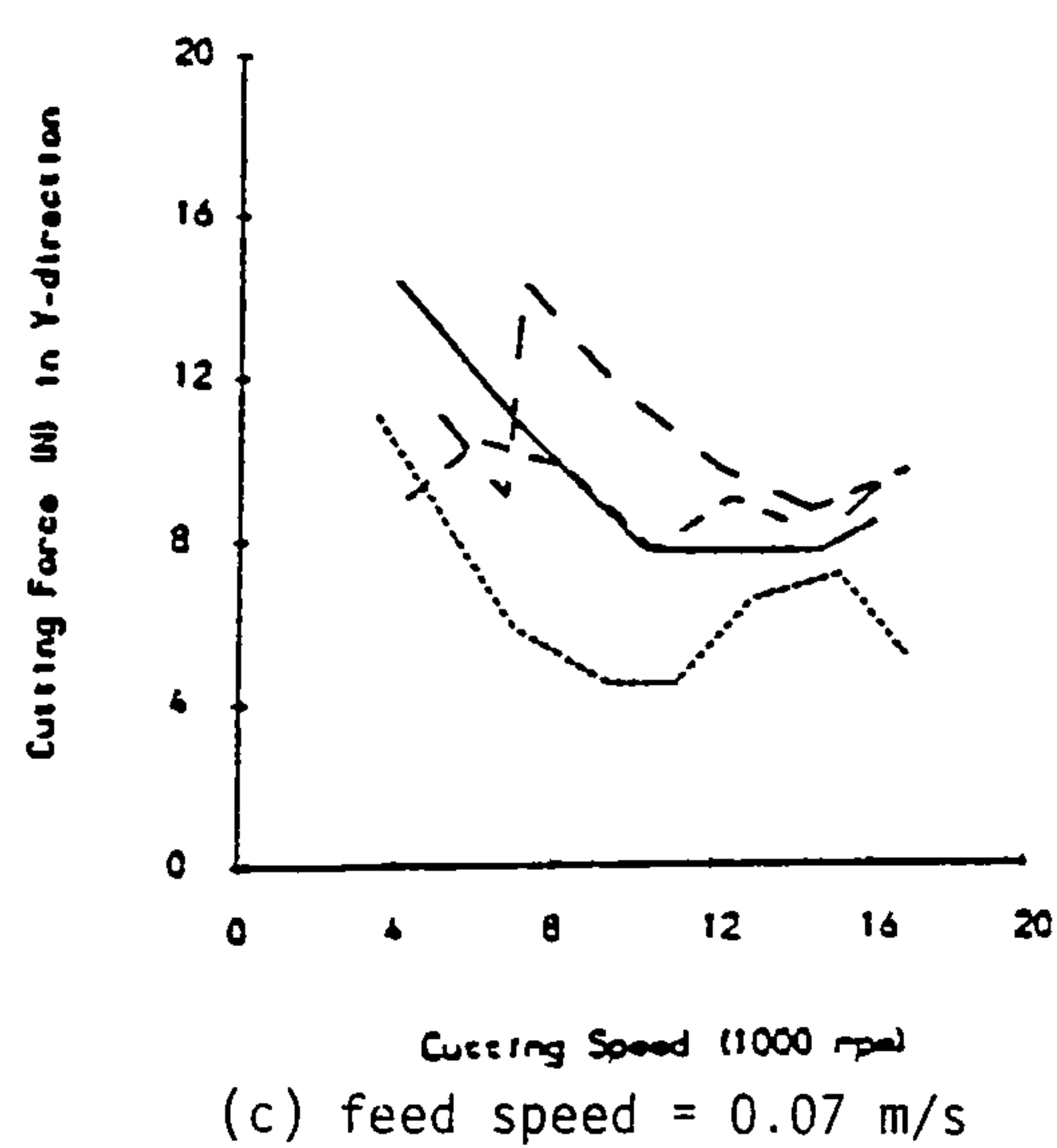
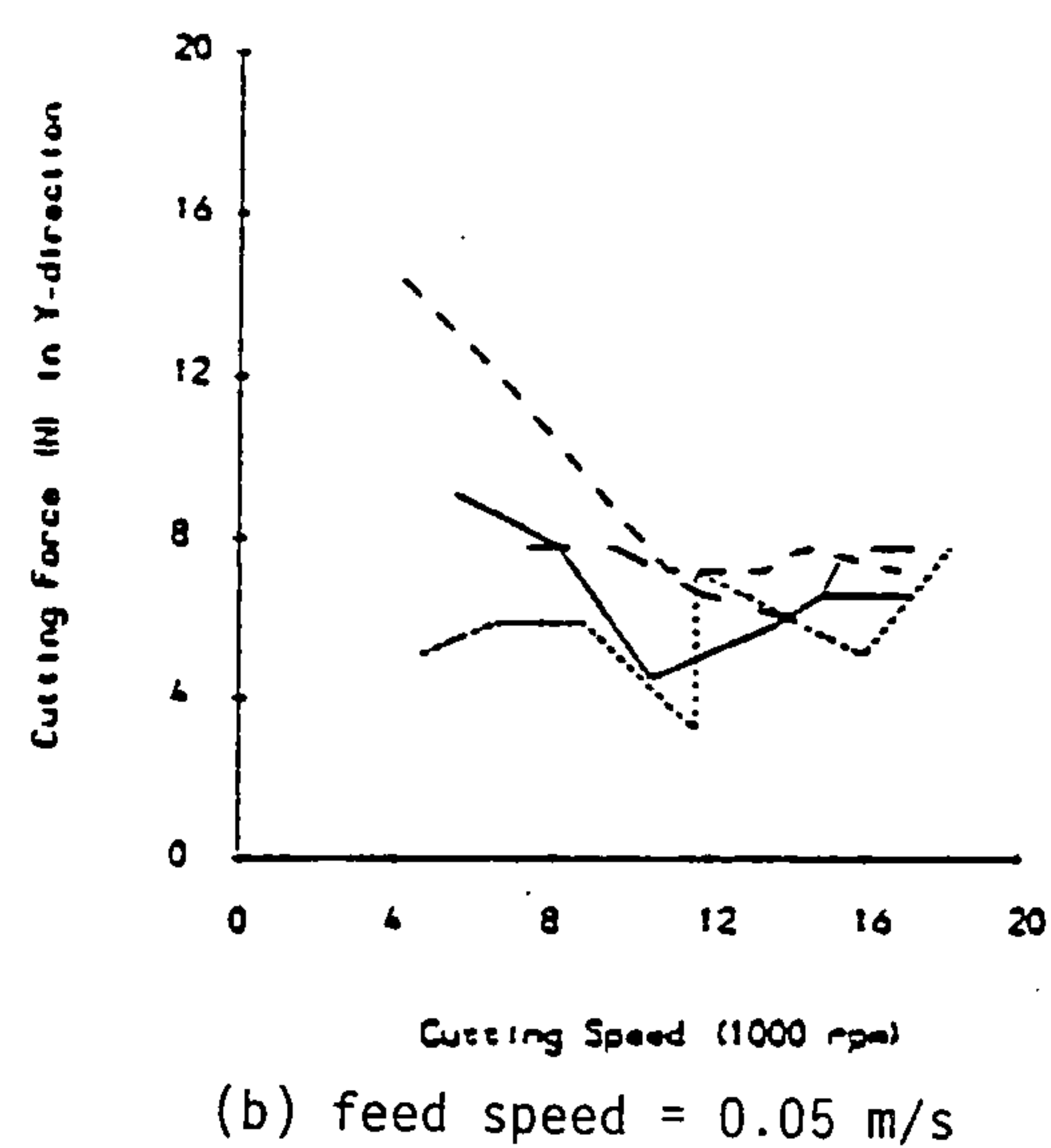
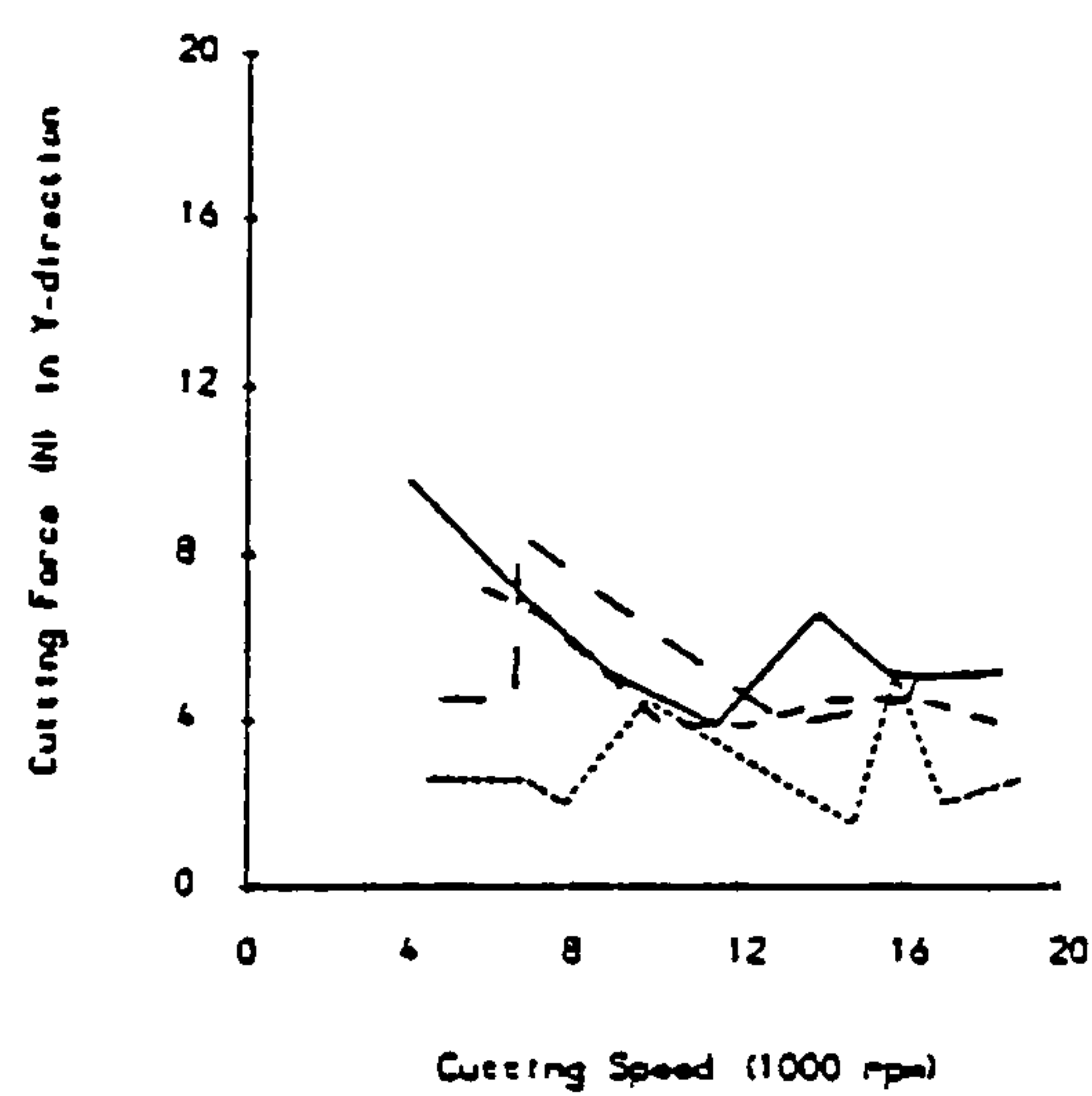
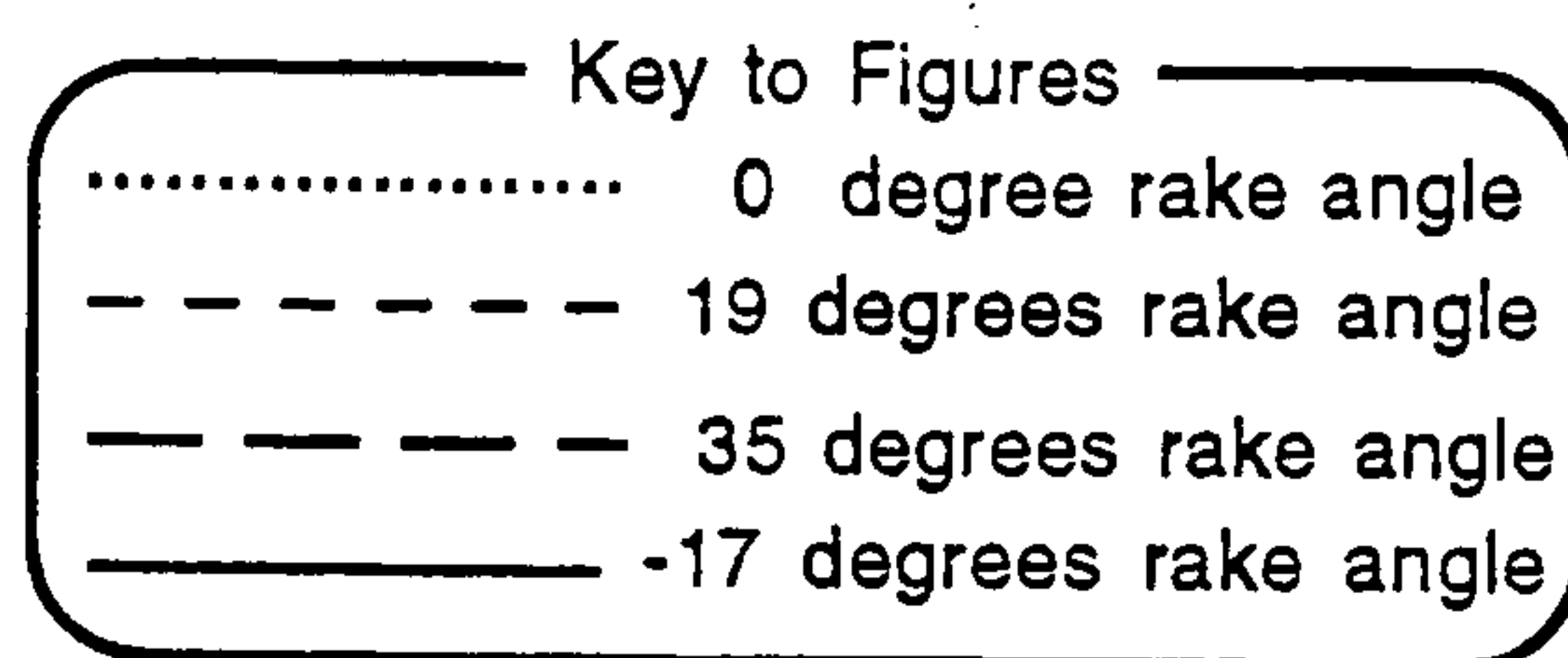
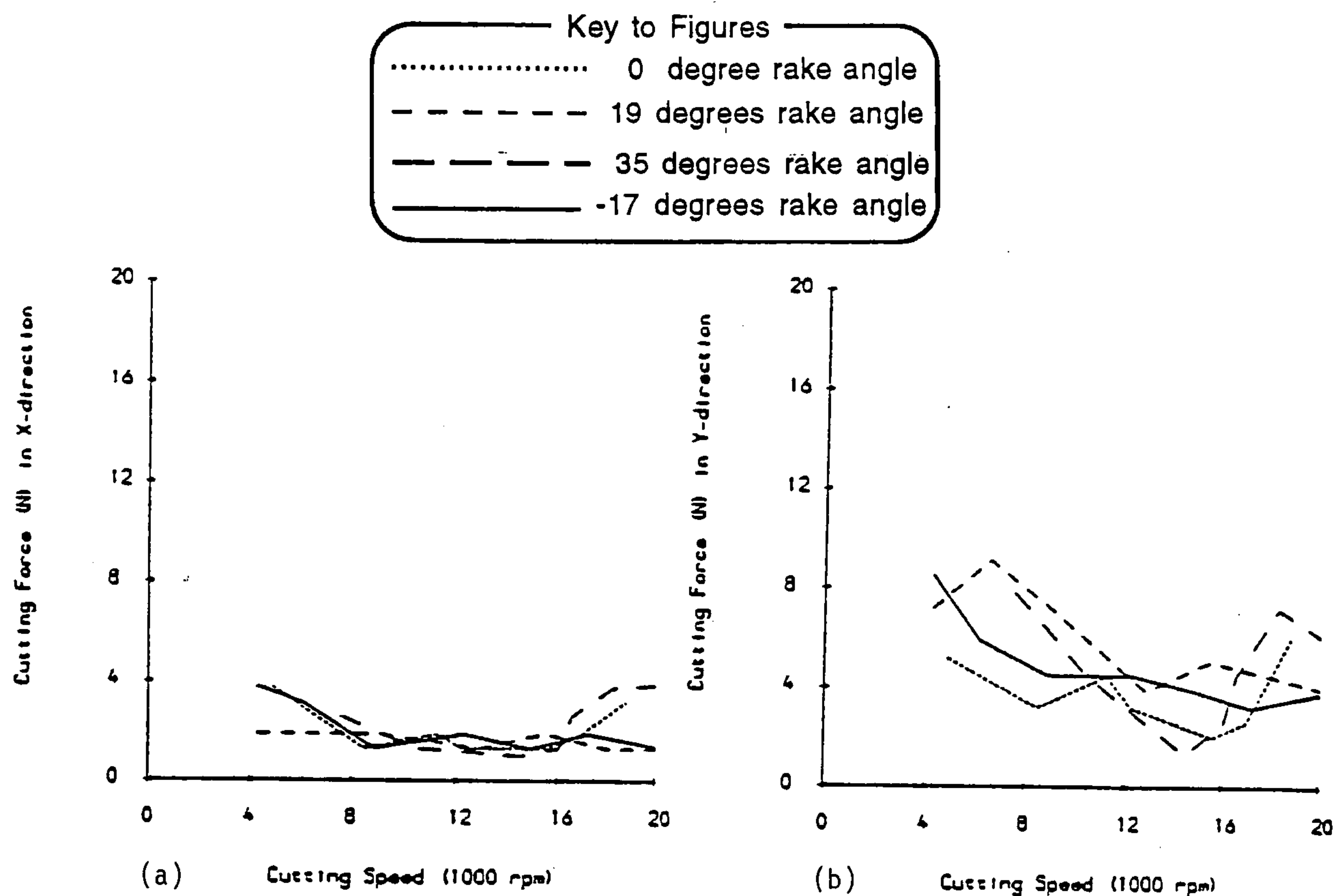
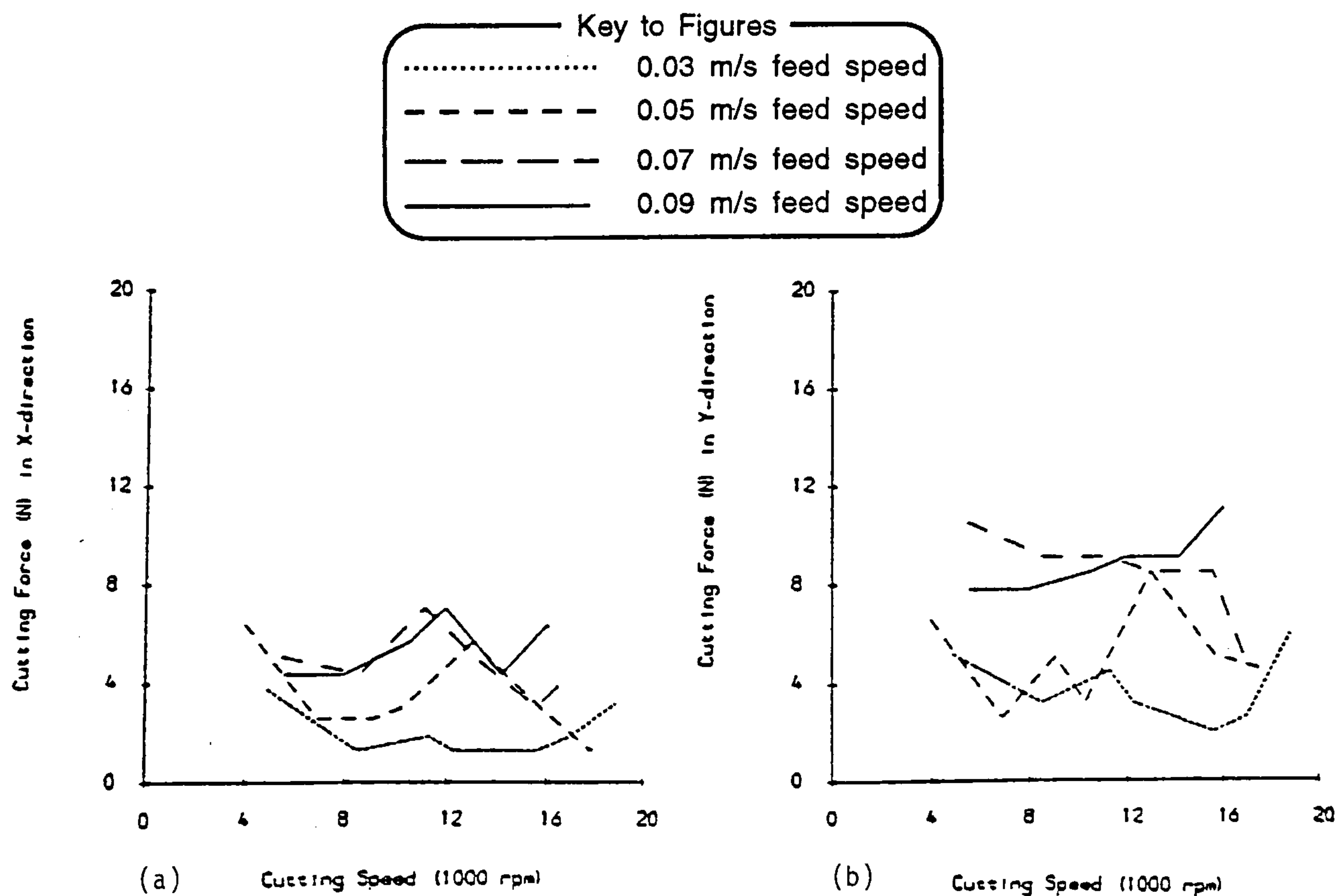


Figure 5.4 Graphs of variations of normal cutting force in leather type-1 against cutting speed for different tool take angles, and with 0.4 mm depth of cut.





**Figure 5.5** *Graphs of variations of cutting forces in leather type-2 against cutting speed for different tool rake angles,  $0.03 \text{ ms}^{-1}$  feed speed, and  $0.4 \text{ mm}$  depth of cut.*



**Figure 5.6** *Graphs of variations of cutting forces in leather type-2 against cutting speed for different feed speeds, with  $0^\circ$  tool rake angle, and  $0.4 \text{ mm}$  depth of cut.*



Another cutting condition parameter that was measured was the amount of power consumption by the router motor during each test condition. The usefulness of the power reading in machining is that it provides a way for the prediction of the efficiency of each cutting condition. Nevertheless, the evaluation of power consumption as carried out in these experiments cannot be interpreted in such a way that direct conclusions from its results are made. This is an indirect measure of efficiency and is heavily dependent on the electrical characteristics of the router motor and its power supply uniformity. The power consumption readings are therefore used to confirm some of the interpretations of the results discussed previously. They are also used to observe any abnormality in the test conditions. That is because any excessive work done during each cutting test that may have disrupted the validity of the experiments is reflected on the power used in that test. This, in a way, may be regarded as an alternative approach to the cutting force analysis. The power consumption readings in these experiments confirm the above argument.

The indications from the results are that leather cutting at higher feed speeds consume larger amount of power than at lower feed speeds. The tests show that the power consumption on experiments with leather type-1 at  $0.03 \text{ ms}^{-1}$  feed speed falls in a range between approximately 25 to 90 W whereas a similar range for  $0.05 \text{ ms}^{-1}$  is approximately between 45 and 135 W. Certainly the lower boundaries for the power readings increase with the increase of the feed speed. This behaviour is clearly observed in the tests with leather type-2. The average power reading is around 50 W at  $0.03 \text{ ms}^{-1}$  feed speed and gradually increases to around 130 W at  $0.09 \text{ ms}^{-1}$  feed speed.

The effects of tool rake angle on the power consumption are also of interest in a way that correct rake angle should result in lesser power consumption than others. Despite of the presence of the scatter the results, the tests show that in the majority of cases  $0^\circ$  and  $35^\circ$  rake angles tend to yield low power consumptions. It is also noticed that  $-17^\circ$  and  $19^\circ$  rake angles consistently use higher powers than others. These conclusions are true for both leather types. It thus further confirms the correctness of the zero rake angle in leather milling.

There are also indications that the power consumption generally decreases as the cutting speed increases up to around 10000 rpm. similar behaviour was noted earlier with regards to the cutting force. With further increase of the cutting speed, this behaviour also changes as it did ,again, in the case of the cutting force. This is seen as a confirmation of the strength of the argument that was used to



interpret the results earlier in this section. The graphical presentation of the power consumption results of milling tests on leather type-1 are given in figs. 5.7 (a), (b), (c), and (d), while those concerning leather type-2 are given in figs. 5.8 (a) and (b).

The tests that were described in this chapter were intended to help towards the design of an automated skiving machine based on face milling technology. The objectives are therefore to arrive at a set of optimal machine parameters. In terms of cutting speed, the objective is to determine the lowest speed that can be employed so that minimum cutting force or power consumptions are resulted. This speed has been shown to be around 12000 rpm. This speed is of course related to the geometry of the cutting tool used. For cutter diameter of 10 mm this gives a periphery speed of approximately  $6.3 \text{ ms}^{-1}$ . Also, the cutting tool that has produced the most optimal results is that which has a rake angle of  $0^\circ$ . So far as the feed speed is concerned, it was shown that lower feed speeds result in lower cutting force and power consumption. However, it is important to provide acceptable leather skiving with the maximum speed of operation, hence feed speed in this case. The results show that it is possible to achieve speeds of operations as high as  $0.09 \text{ ms}^{-1}$ , but with increasing amount of cutting force and power consumption. The conclusions that are reached here do not yet take account of the surface quality results. It is important to note that, as mentioned at the beginning of this chapter, the results concerning surface quality in the tests have the overriding influence in the selection of machine parameters. Section 5.6 presents the details of the results and shows its high level of dependency on the properties of material.



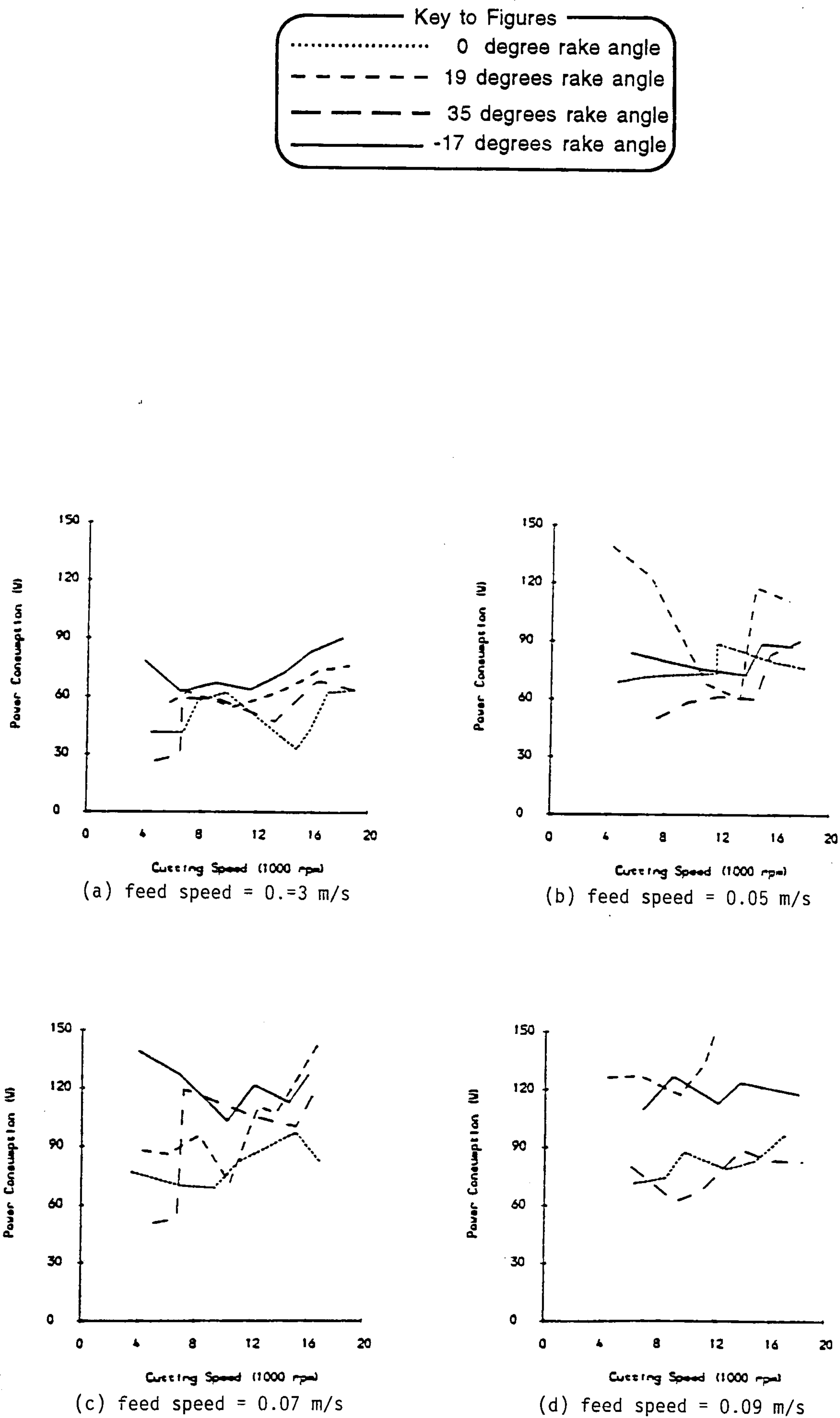


**Figure 5.7** *Graphs of variations of power consumption in leather type-1 against cutting speed for different tool rake angles, and with 0.4 mm depth of cut.*



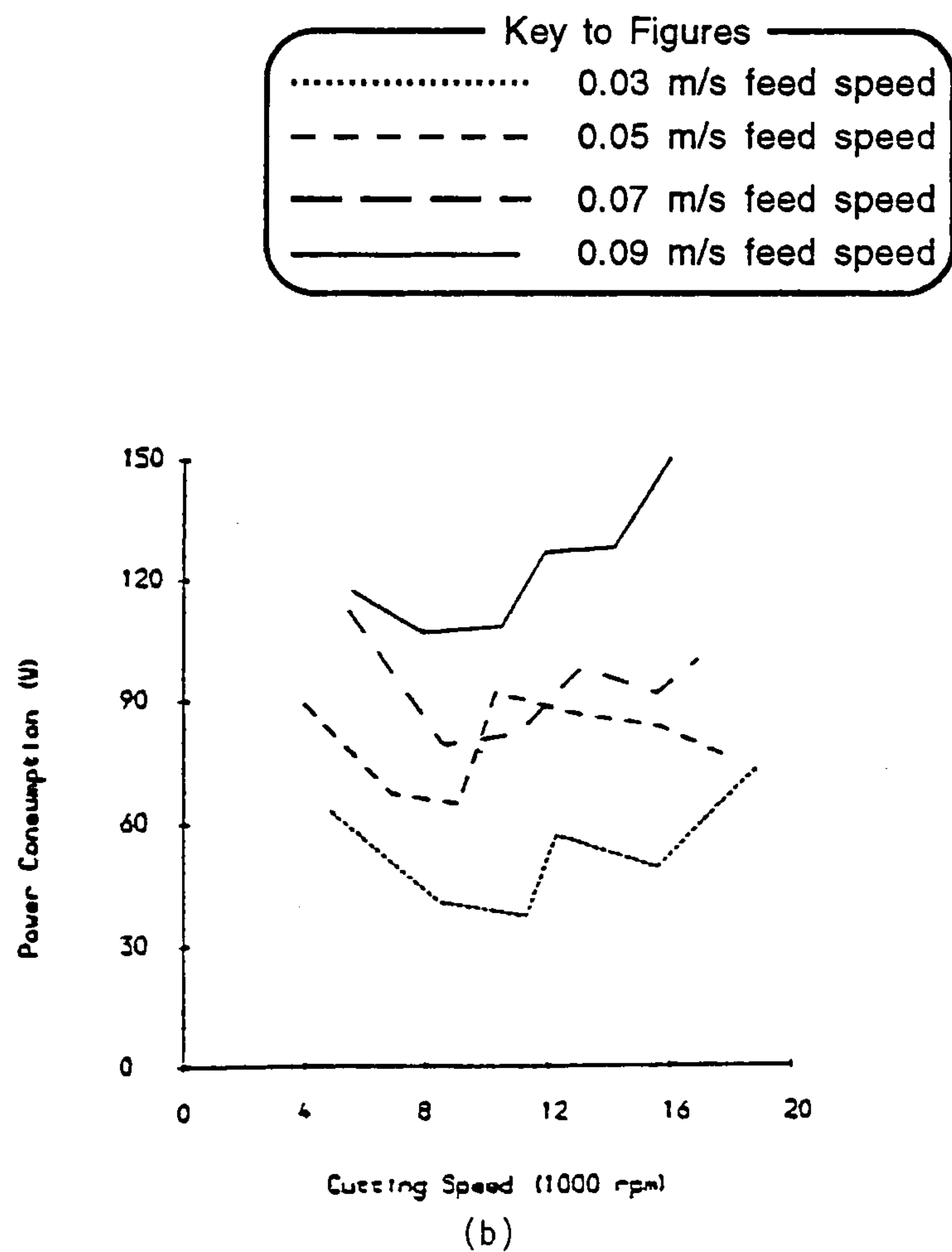
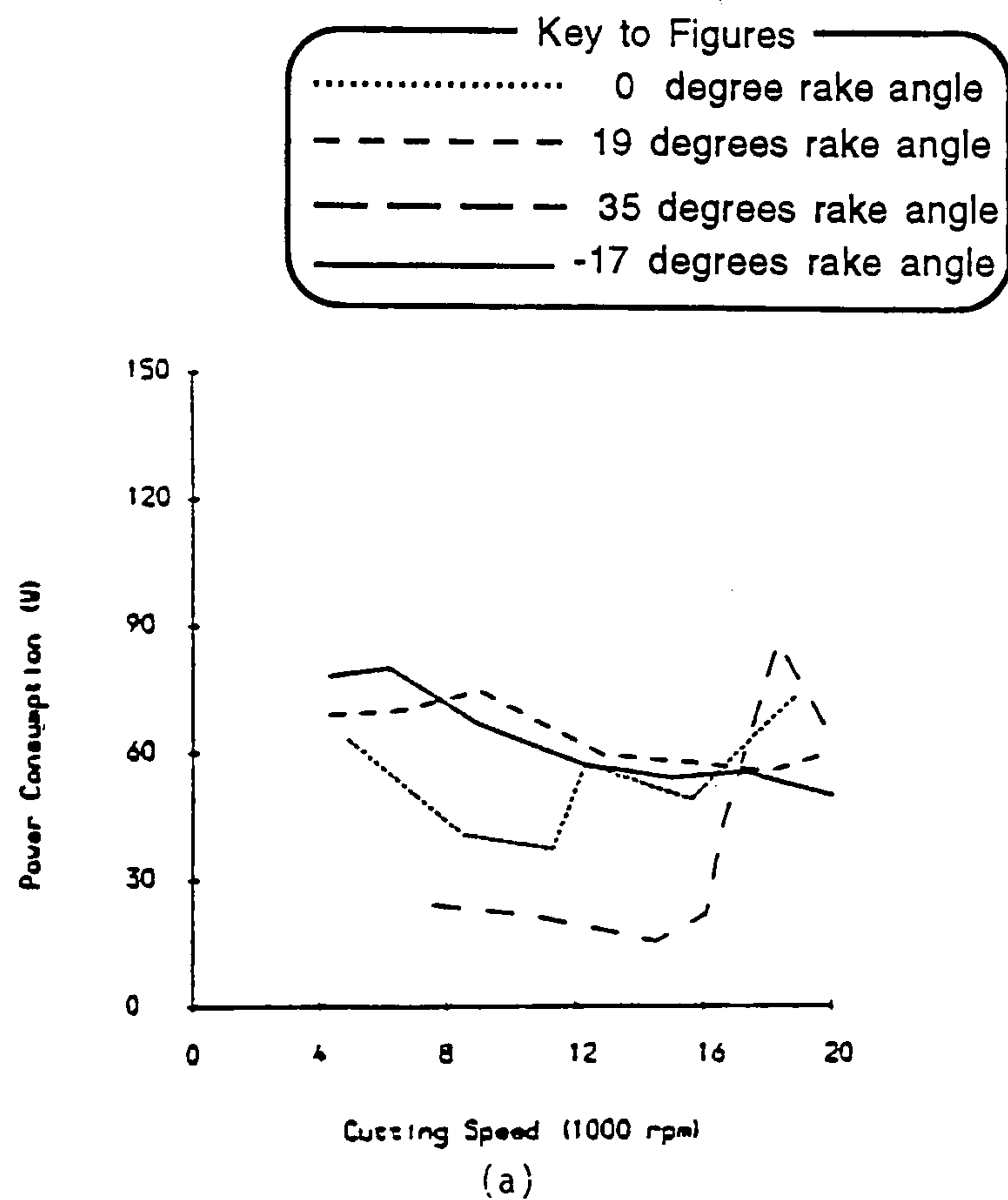


**Figure 5.8** Graphs of variations of power consumption in leather type-2 against cutting speed for (a) different tool take angles and  $0.03 \text{ ms}^{-1}$  feed speed, and (b) different feed speeds and  $0^\circ$  tool rake angle. In all cases with 0.4 mm depth of cut.



#### **5.4 Effects of depth of cut**

In this section effects of the variation of depth of cut is investigated. Dedicated tests on leather type-1 were carried out to observe how different depths of cut, ranging from 0.02 to 0.08 mm, affect the cutting force and power consumption. The results very clearly show that for deeper cuts more cutting force is required. This is true for both feed and normal cutting forces. The results further indicate that deeper cuts require more power than shallower cuts.

When the force and power results of different depths of cut are analysed under different cutting speeds it is observed that for all speeds the pattern of variations are very similar. This is also true when force and power results are examined under varying feed speed. It is therefore concluded that the effect of depth of cut in leather milling is clearly seen in the cutting force and power consumption. Also, In section 5.2 it was shown that the actual cutting speed of the router drops from its initial value when under cutting load condition. The tests to show this effect were carried out with 0.4 mm depth of cut. However, when different depths of cut were tested, it was further observed that this drop increases with the increase of the depth of cut. This shows that, under cutting condition, an increase in cutting speed also involves an increase in the available torque at the head of the cutting spindle. This, therefore, further confirms the subsequent increases in cutting forces and power consumption.

Figs. 5.9 (a), (b), (c), and (d) show the plotted results of varying depths of cut, for a fixed feed speed of  $0.03 \text{ ms}^{-1}$ , as the cutting speed changes, while figs. 5.10 (a), (b), (c), and (d) show the same variations, but this time the cutting speed is fixed at 24000 rpm, and the feed speed changes.



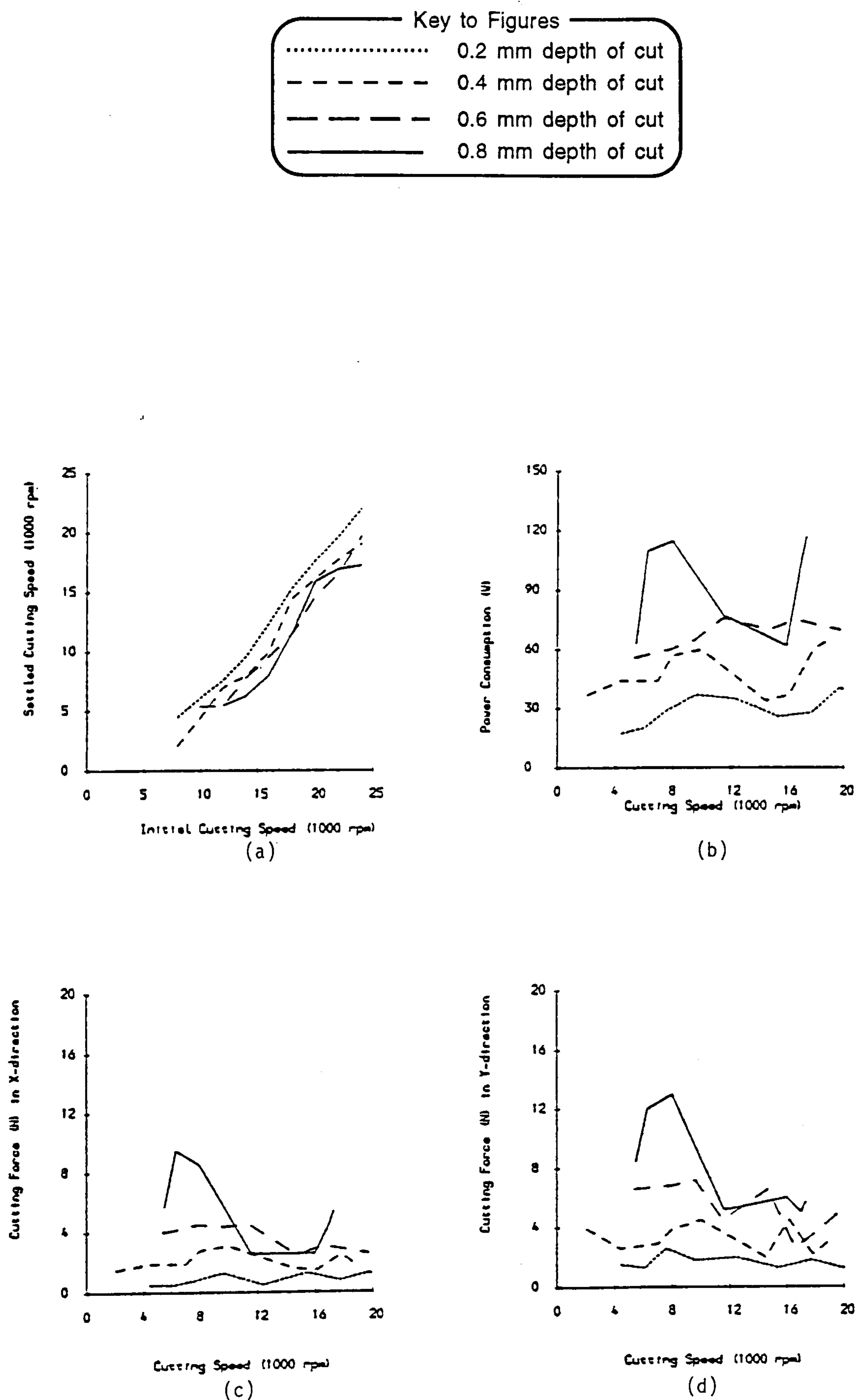


**Figure 5.9** *Graphs of variations of the cutting results in leather type-1 against cutting speed for different depths of cut, with fixed feed speed of  $0.03 \text{ ms}^{-1}$ , and  $0^\circ$  tool rake angle.*



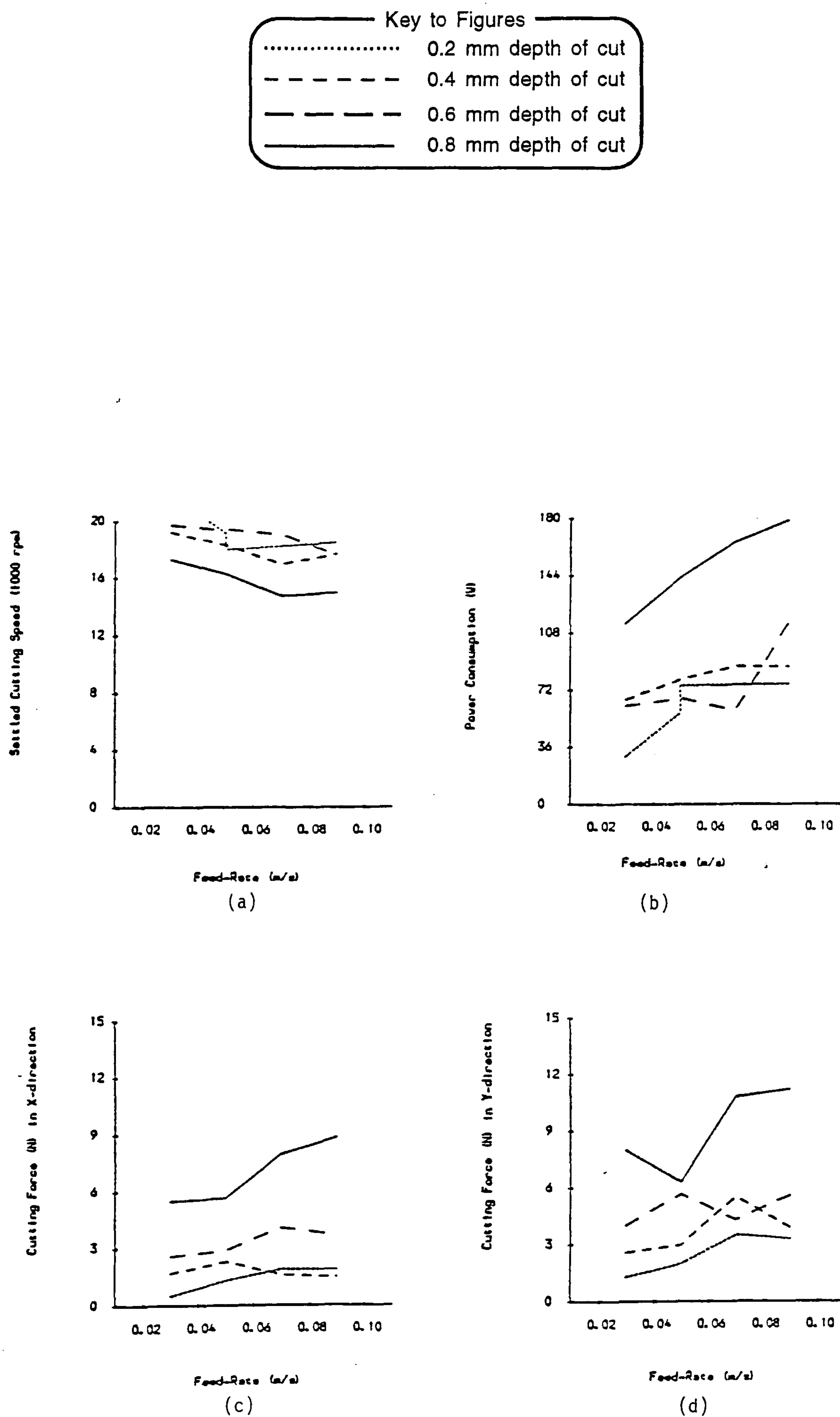


**Figure 5.10** *Graphs of variations of the cutting results in leather type-1 against feed speed for different depths of cut, with initial cutting speed of 24000 rpm, and 0° tool rake angle.*



## 5.5 Tool wear considerations

It is very important to employ cutting tools that are capable of sustaining an acceptable degree of sharpness during an acceptable operational lifetime. This is because an automated skiving machine must be able to continue its operation with as little downtime as possible during a production period. Frequent machine stoppages to sharpen/change tools cannot be satisfactory especially with the view that operations of other machine cells are likely to be dependent on the production rate of the skiving cell. The cumulative number of hours that the tool has been used before wear is a measure of its suitability.

To detect tool wear or breakage a number of indirect methods including examination of cutting force or power consumption are used. Unusual increase in force or input power measurements, or sudden increase in their values could be the result of tool cutting edge wear or breakage [41]. Moreover, the ratio of feed to normal cutting force is another way of predicting tool wear for a low ratio indicates high rubbing between the tool and the leather sample. Rubbing is the direct result of tool wear. Temperature measurement of the tool cutting surface at its interface with leather sample is another indirect method of predicting wear. This temperature will frequently increase as the tool wears. Indirect methods are mostly employed on-line and measurements are obtained during the actual cutting process. Using the cutting force and input power method, no excessive tool wear or breakage was detected during the investigation of leather milling.

There are however a number of direct tool wear measurement methods that can be employed [42]. Determination of contact resistance using electrical techniques, or measurement of the distance from the tool post to the workpiece are examples of such a method. This method, however, does not apply on non-conducting materials. Tool geometry measurement is another method. However, photographic evidence of the state of tool edge after each cutting cycle is one of the simplest methods for direct tool wear inspection. A high enough magnification factor would be required to allow visual inspection of the photographs by the naked eye. Ideally a magnification factor of 50 is required. This method entails comparing photographs of the cutting surface of the tool when new, and after a cutting cycle.

Photographic method was employed as a direct tool wear inspection in this investigation. To this end, the total cumulative usage of a tool during the complete period of this investigation was assumed to be its cutting cycle. This amounted to approximately 20 m length of leather skiving. Though this may not be a high



enough operational cycle it does provide useful information regarding the suitability of the cutting tools that were used.

In the experiments tungsten carbide tools were used throughout. In order to monitor their wear during the tests magnified photographs of a selected cutting edge of one of the tools were taken both before and after the entire tests. The tools had not been used before the experiments. A magnification factor of 100 was used. The comparison of the cutting edge profile of the tool show that some wear has taken place. This is expected since it indicates that the tool has been used. However, during the experiments there was no indication of any tool deterioration, especially towards the end of the experiments. On the other hand, using a factor of 100 gives a very high magnification of the object. It is therefore thought that the amount of wear that has actually happened is not very high. However, much longer cutting tests are needed to determine how well these tools retain their sharpness in a factory cutting cycle situations. Figs. 5.11 and 5.12 show the photographs of the cutting edge of the tool with zero rake angle before and after the tests.



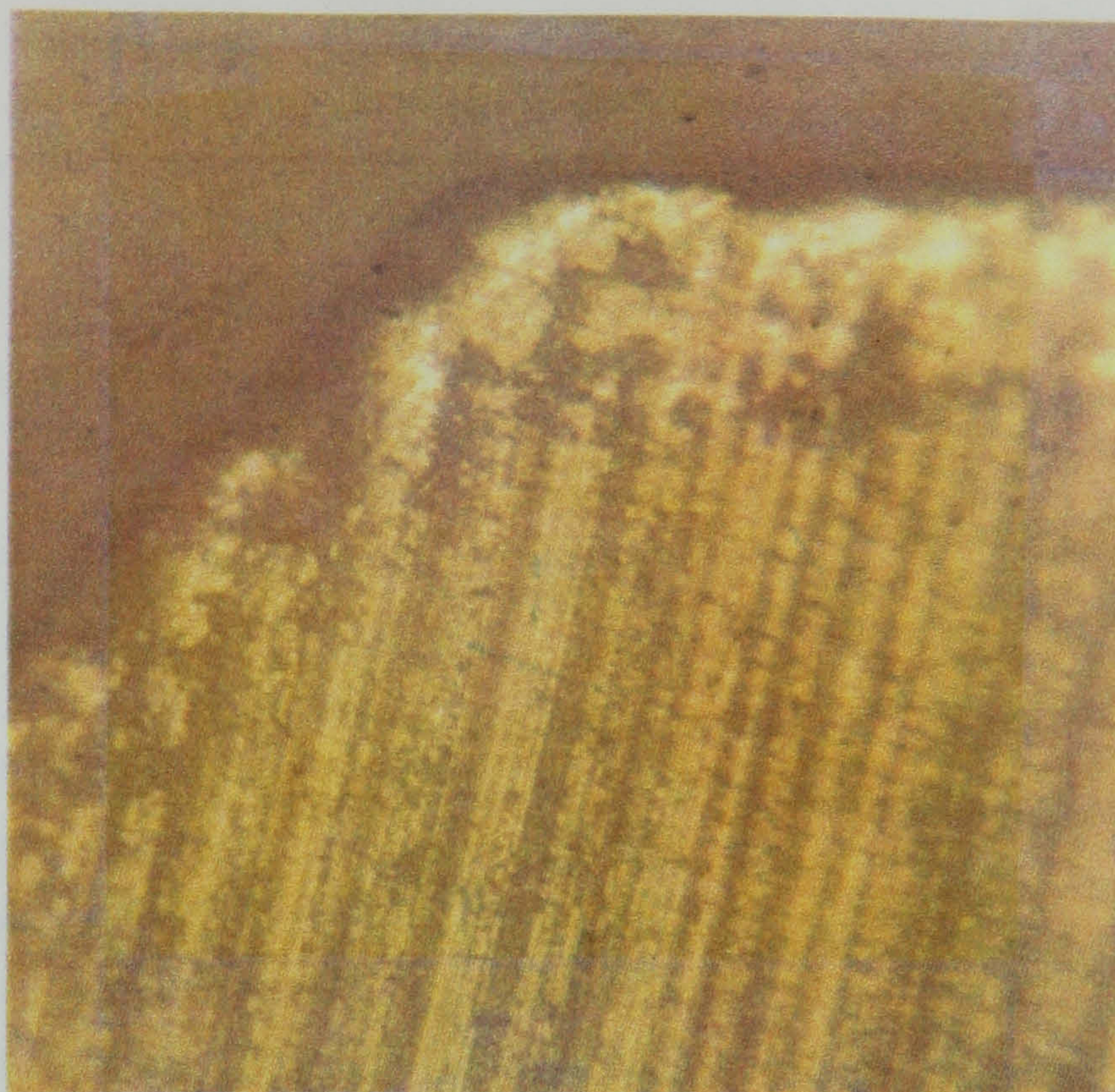


*Figure 5.11* Photograph of a cutting edge of the tool with  $0^\circ$  rake angle taken *before the experiments*. Magnification factor = 100.

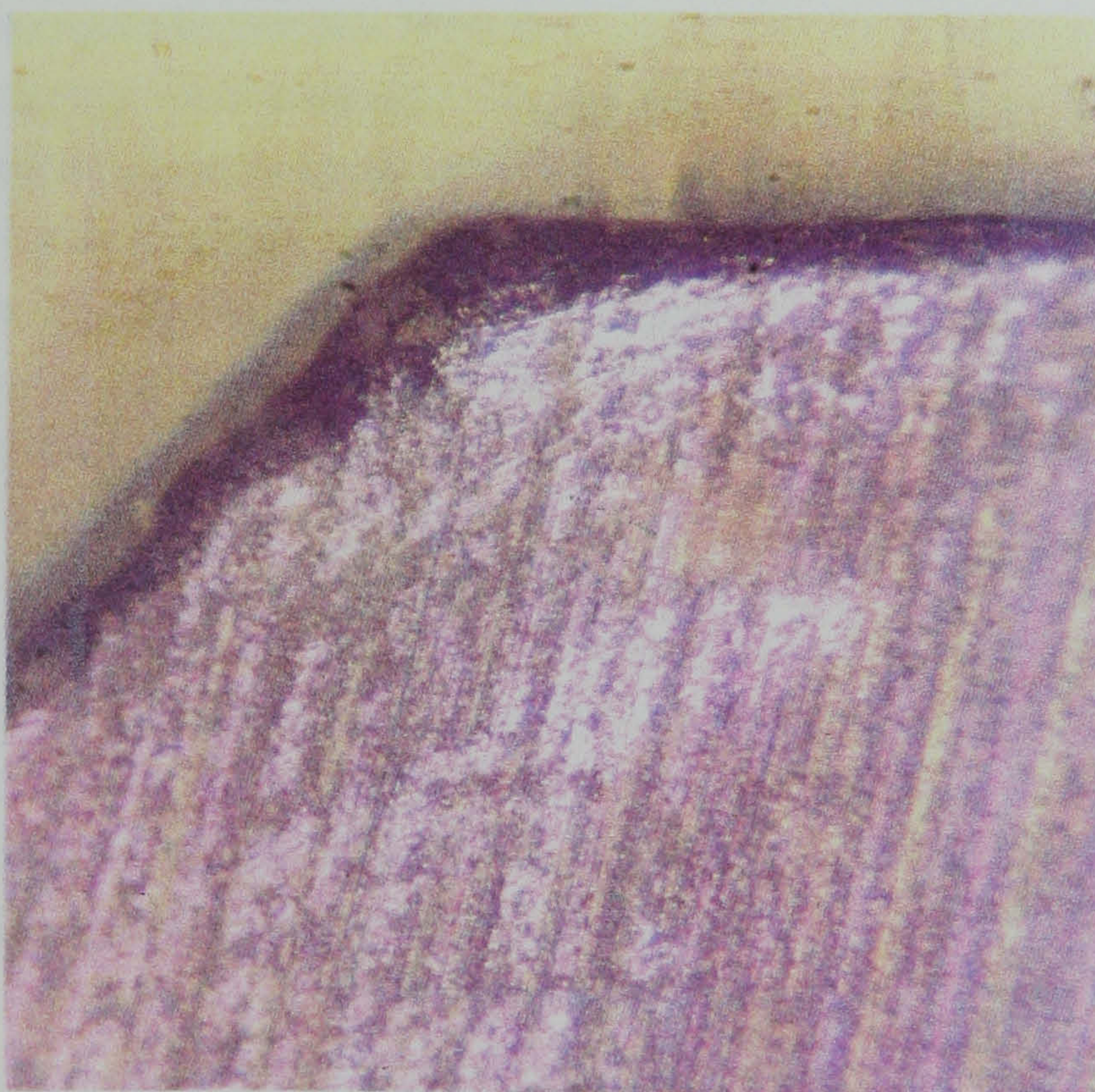


*Figure 5.12* Photograph of the same cutting edge as in fig. 5.11 taken *after the experiments*. Magnification factor = 100.



## **5.6 Surface finish quality and the role of materials properties**

During the course of the preliminary investigations in Chapter Two it was concluded that leather skiving by way of face milling produces good surface finishes when samples near backbone region of the hides are used. It was also concluded that when samples are cut from hides' belly regions poorer surface quality results. This phenomenon is clearly confirmed in the work of this chapter.

In Section 5.1 it was mentioned that the surface quality results in leather machining investigation heavily depend on the physical characteristics of the sample material, especially in the case of leather type-1. Prior to the start of the experiments, the samples, that had been cut from the entire regions of the original hides, were randomly mixed. As a result, each cutting experiment was performed on a randomly selected sample. The results show that the quality of the surface finish of the samples is very much indicative of where in the original hide the samples had been cut. In Chapter Three it was established that the physical properties varies not only from hide to hide, but also from different regions of the same hide. It was also established that in most hides the belly region is characteristically known for its floppiness. As a result, the fibre network in belly region is not as homogeneous and orderly as that near backbone. These fibres have been subjected to great degree of stretch and exhibit large amount of fluffiness. Consequently, samples taken from this region do not seem to produce good surface quality when machined. In this case a poor surface finish is that which still contains a certain degree of fluffiness on its surface. In comparison, a good surface finish is completely free from the presence of any uncut fibres. Often, poor surface finishes also exhibit poor edges along the line of cut. This, again, is related with the presence of a high degree of neighbouring bundled of usually long fibres.

In the machining tests the fibres in the belly area tend to resist the cutting action of the cutting tool and as a result a high degree of rubbing takes place. Examination of the normal cutting forces appears to confirm this argument. It is generally seen that high normal cutting forces are resulted in machining tests if the test sample is taken from the belly region. It has been explained earlier that the presence of rubbing during face milling is mainly reflected in the normal cutting force.

Referring to the investigation that was carried out in Chapter Three, it is noted that hide regions close to the belly area have typically smaller tensile strength values than those near backbone. On the other hand, in these regions the values of



percentage elongation that is reached before rupture during tensile strength tests are typically higher than backbone areas. Though weaker in strength, the fibres in the belly regions can therefore sustain a higher degree of stretch under an applied load. It is thought that this ability to stretch causes the fibres to 'give' under the action of the cutter. Therefore, it can be said that high tensile strength and low percentage elongation produce better surface finishes.

Other properties that have been described in Chapter Three do not seem to have any significant influence on the machining results. In general, for the two hide types, tearing and resistance to compression properties are very close to one another. In the case of burst load and indentation index values, the hide type-1 generally exhibits higher values than type-2. However, the laboratory experience gained during the experimentation did not suggest any significant effect of these properties on leather machining. Also, it has been established that hide type-2 is approximately 7 times more flexible than hide type-1. Again, during the investigation of leather machining no significant relationship between flexibility and machining of leather were observed. The reason for this is that in determining the flexibility of leather samples, values of flexural rigidity of the whole body of the samples in their entirety were measured. This included the grain layer in the samples. However, in machining of leather only the fibre network layer is subjected to cutting, and hence, no reference is made to the grain layer in the description of the workpiece.

The results of leather properties in relation to its machining properties are very significant. They suggest that in order to obtain good surface finishes most leather components can be skived as long as they possess high tensile strength and low percentage elongation.

The examination of the surface finish of the machined samples also confirm that up-cut milling results in a better machined edge than down-cut milling. The machining tests that were performed in the investigation of this chapter produced full cut milling. That is to say, at a given instant all sections of the cutting tool were involved with the cutting process. As a result, the generated machined surfaces were in the form of a groove whose widths were of the same size as the diameter of the cutter. The combination of the rotational and linear traverse of the cutter produces up-milling along one edge of the groove and down-milling along the other. It is the comparison of the quality of the edges that confirms up-milling is more suited to leather face milling. This is a general result, however, and is one which applies to leather in general.

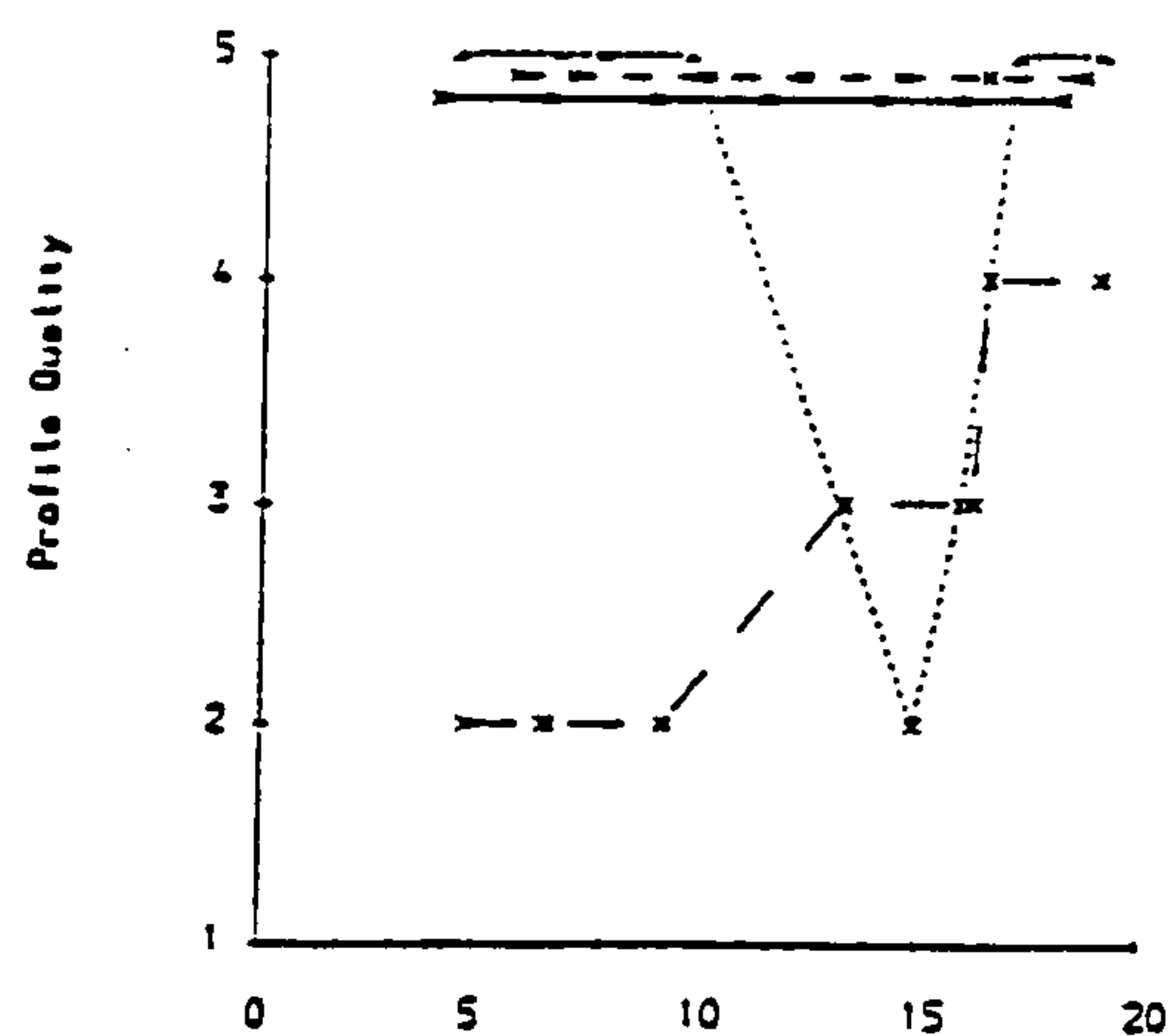
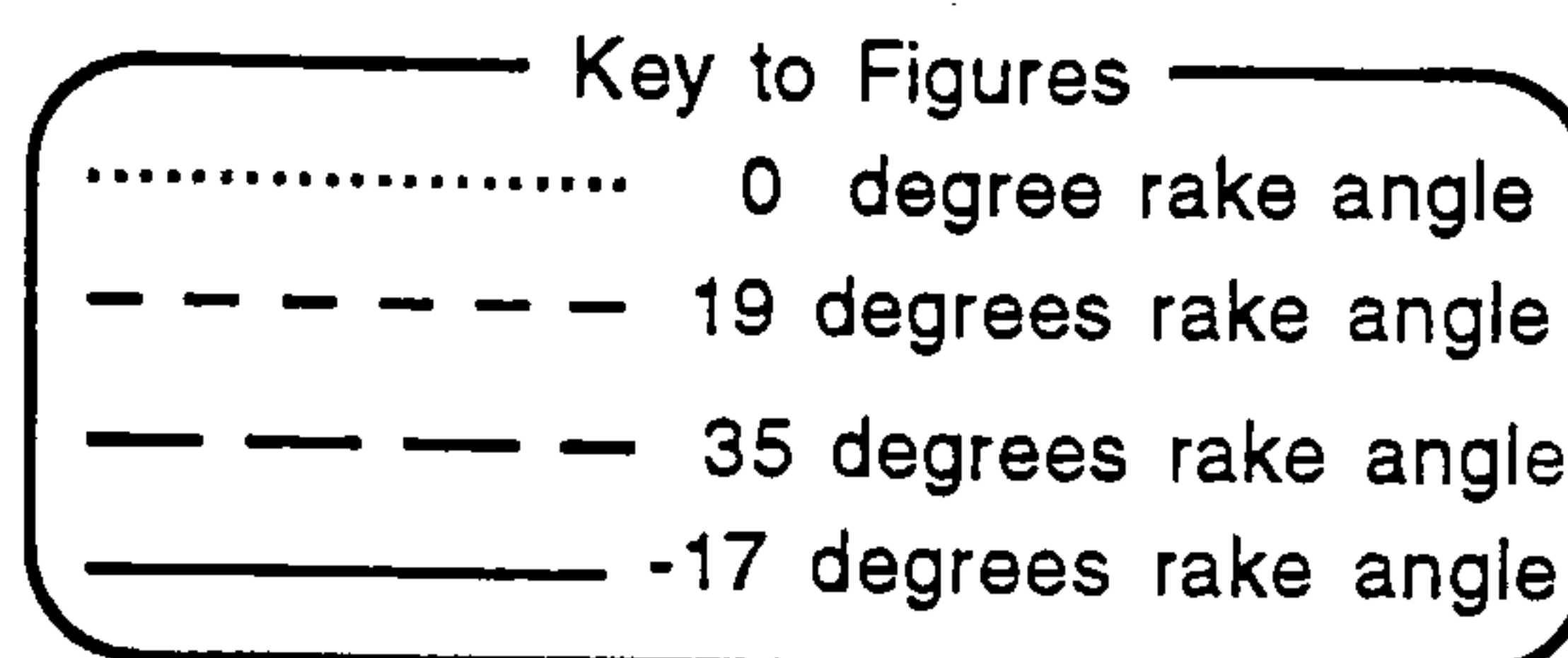


The effects of tool rake angle on the surface finish results are also considered. From the evidence available, all the rake angles that were tested produced good surface finish provided the samples did not originate from the fluffy regions near the belly area of the hide. However, it is evidently noticed that the tool with the negative rake angle still produced good surface finish even though the tested samples came from hide's belly region. This is a significant result since, as discussed earlier, this tool is noted to produce relatively high cutting forces. It is also noted that the tool with  $-17^\circ$  rake angle generally consumes more power than other angles. It can therefore be said that though it does more work in removing the material the tool with negative rake angle produces relatively better surface finishes.

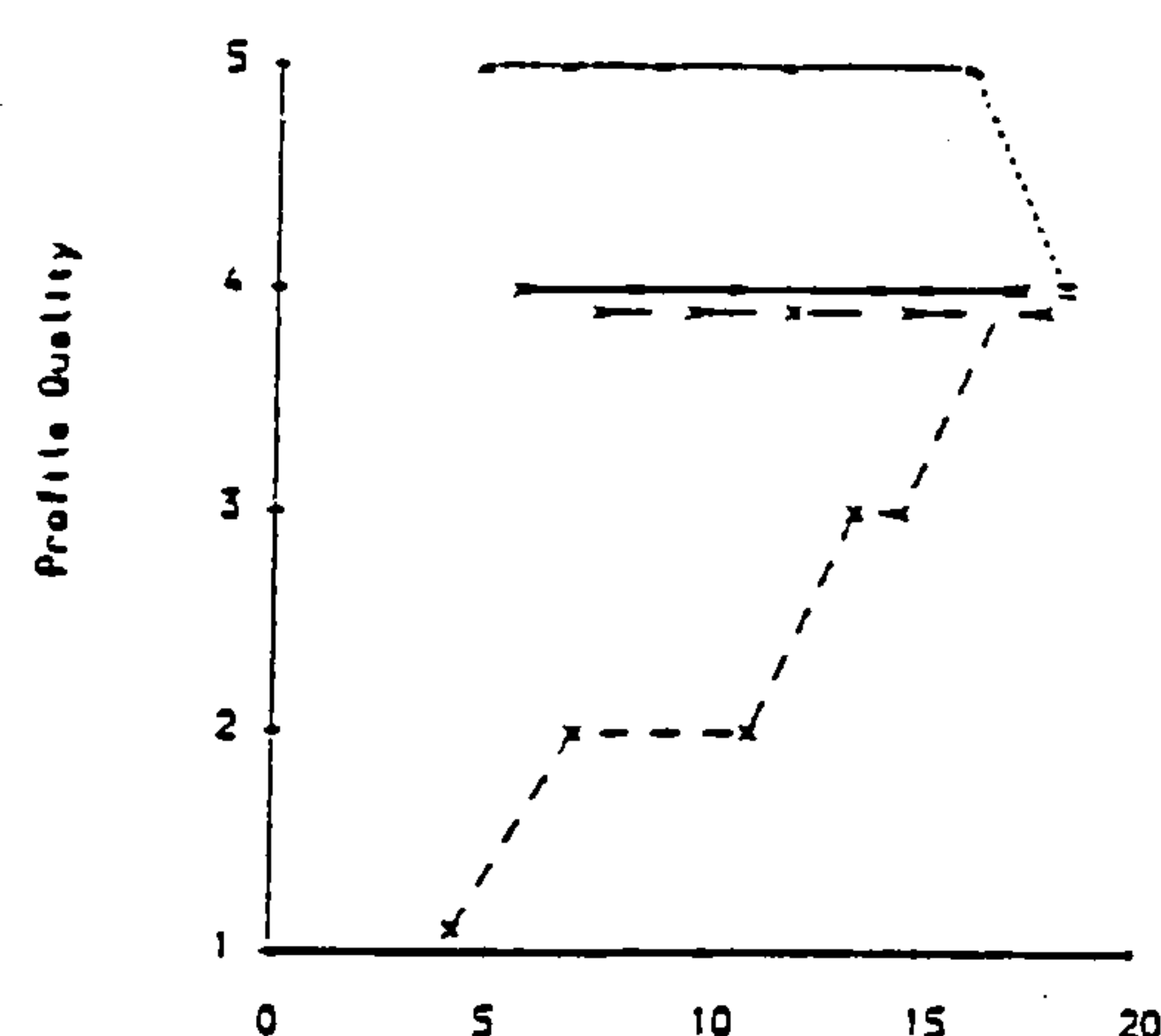
The effects of cutting speed on surface finish have already been discussed in Chapter Two. The increase of cutting speed tends to increase the surface finish quality. Due to direct material dependability of the surface finish quality this cannot be clearly seen from the results of this chapter. Nevertheless, it can be said that the tests show no sign of surface finish quality deterioration when the feed speed is increased. In fact, the majority of the tests that were conducted at  $0.09 \text{ ms}^{-1}$  feed speed produced good results.

The surface finish quality results are subjectively quantified. An arbitrary scale was used with each result being given a whole number between 1 to 5. Numbers 1, 2, 3, 4, and 5 represent extremely poor, poor, acceptable, good, and very good quality results. The effects of various rake angles on the quality of surface finish against cutting speed are graphically presented in the following figures. Each figure is for a fixed feed speed, and they are presented in the order of increasing feed speed. Furthermore, in exactly similar presentation fashion as the quality graphs, another set of figures are produced to show the location of each sample from its original hide. These are provided as references to the interpretation of the quality graphs. Figs. 5.13 (a), (b), (c), and (d) are the quality results graphs while figs. 5.14 (a), (b), (c), and (d) show the location of each samples within its original hide. Fig. 5.15 shows the photograph of a typical test sample where the quality of the machined surfaces is very good, and fig 5.16 shows a test sample with poor machined surface quality.

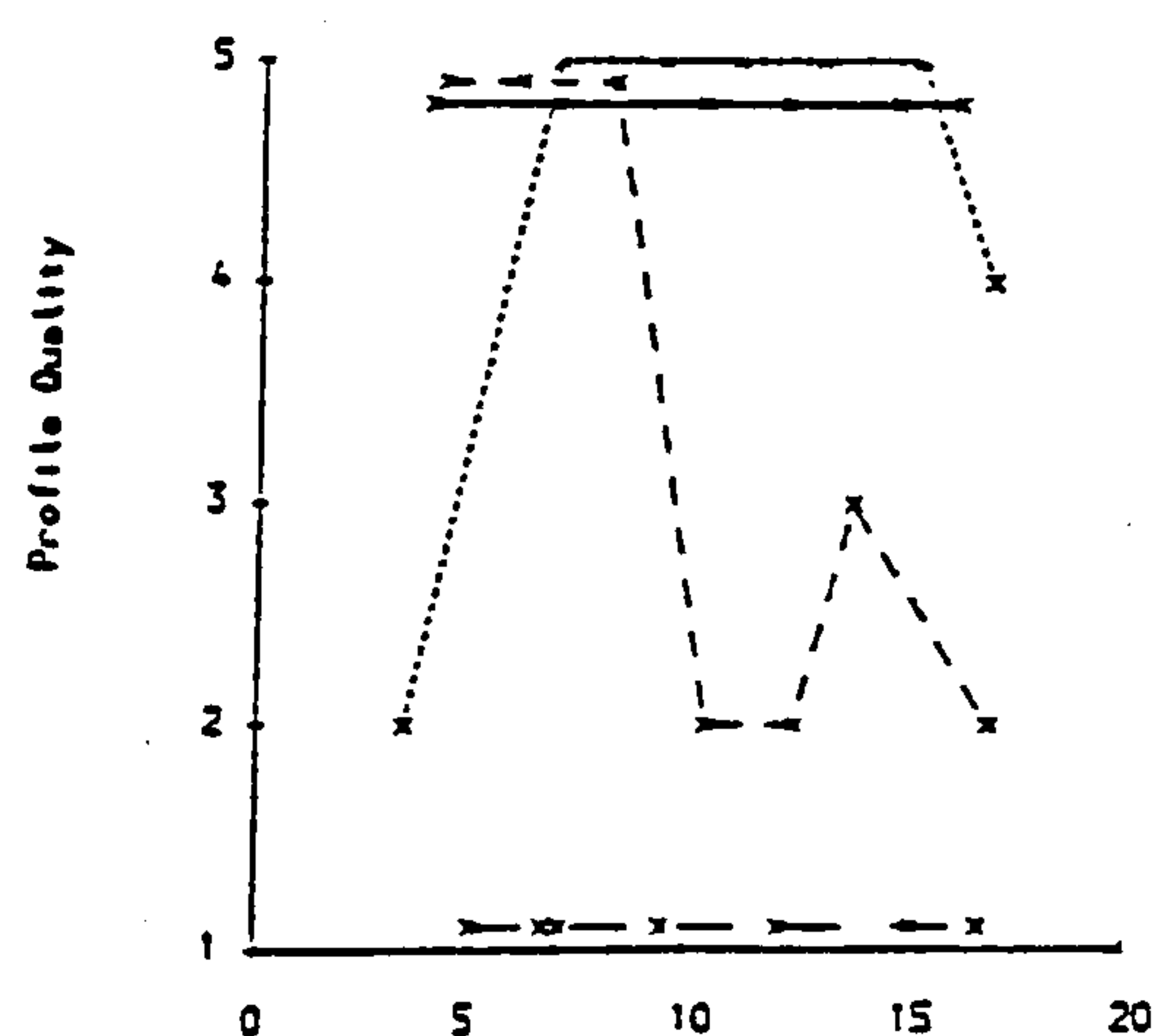




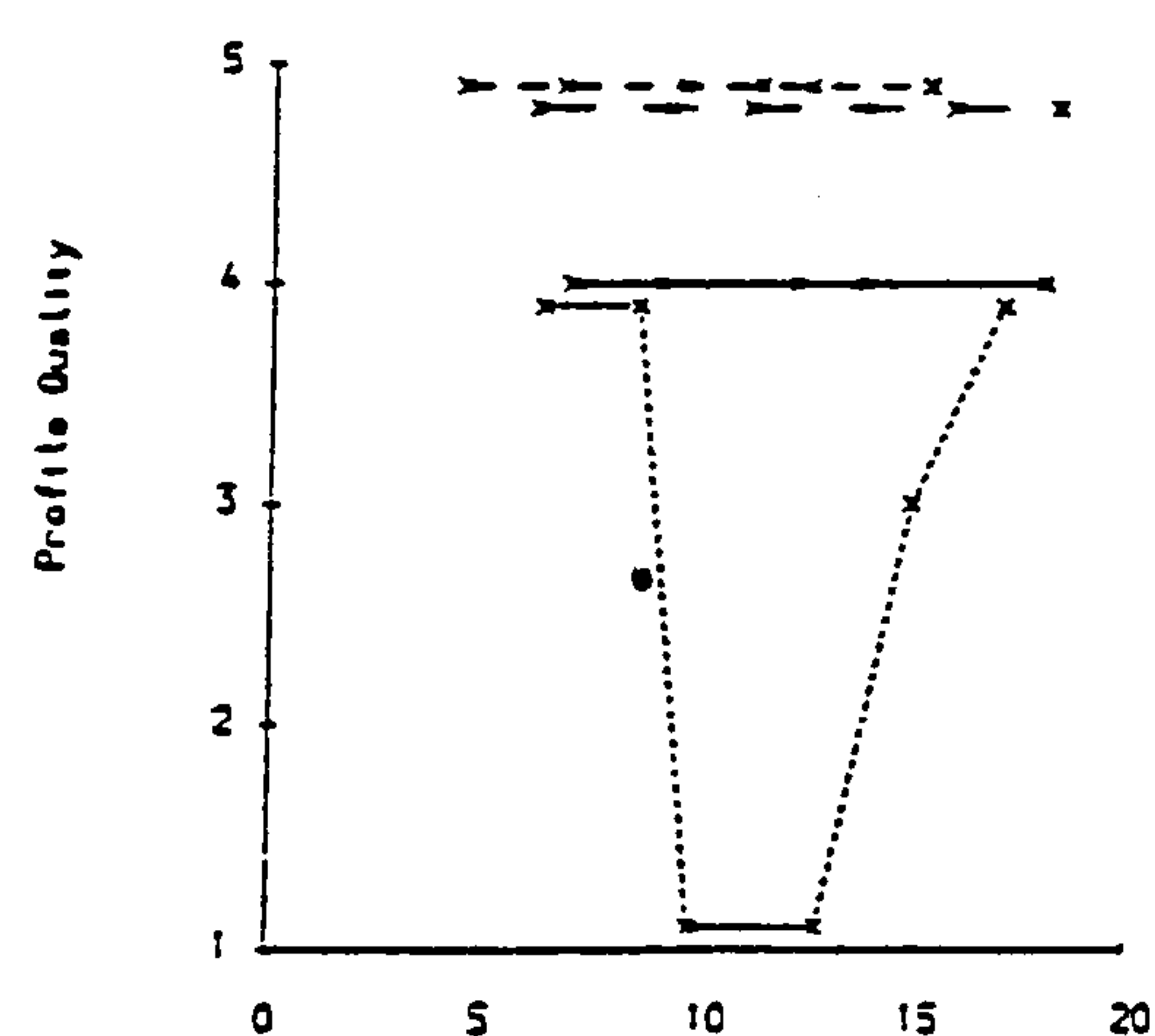
(a) feed speed = 0.03 m/s



(b) feed speed = 0.05 m/s



(c) feed speed = 0.07 m/s



(d) feed speed = 0.09 m/s

**Figure 5.13** A subjective comparison of the surface finish quality of leather type-1 samples shown graphically for different tool rake angles against cutting speed, with 0.4 mm depth of cut.



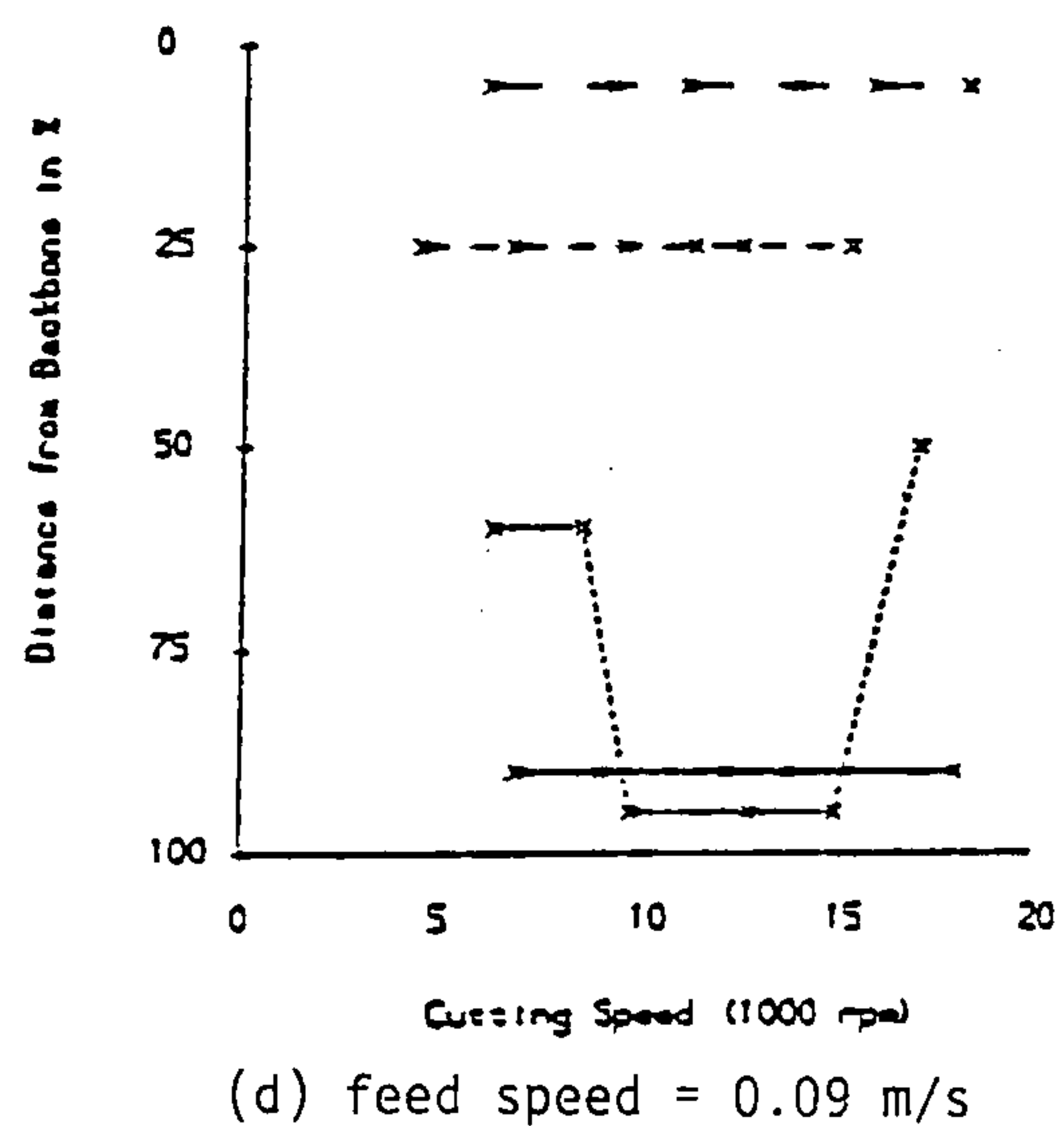
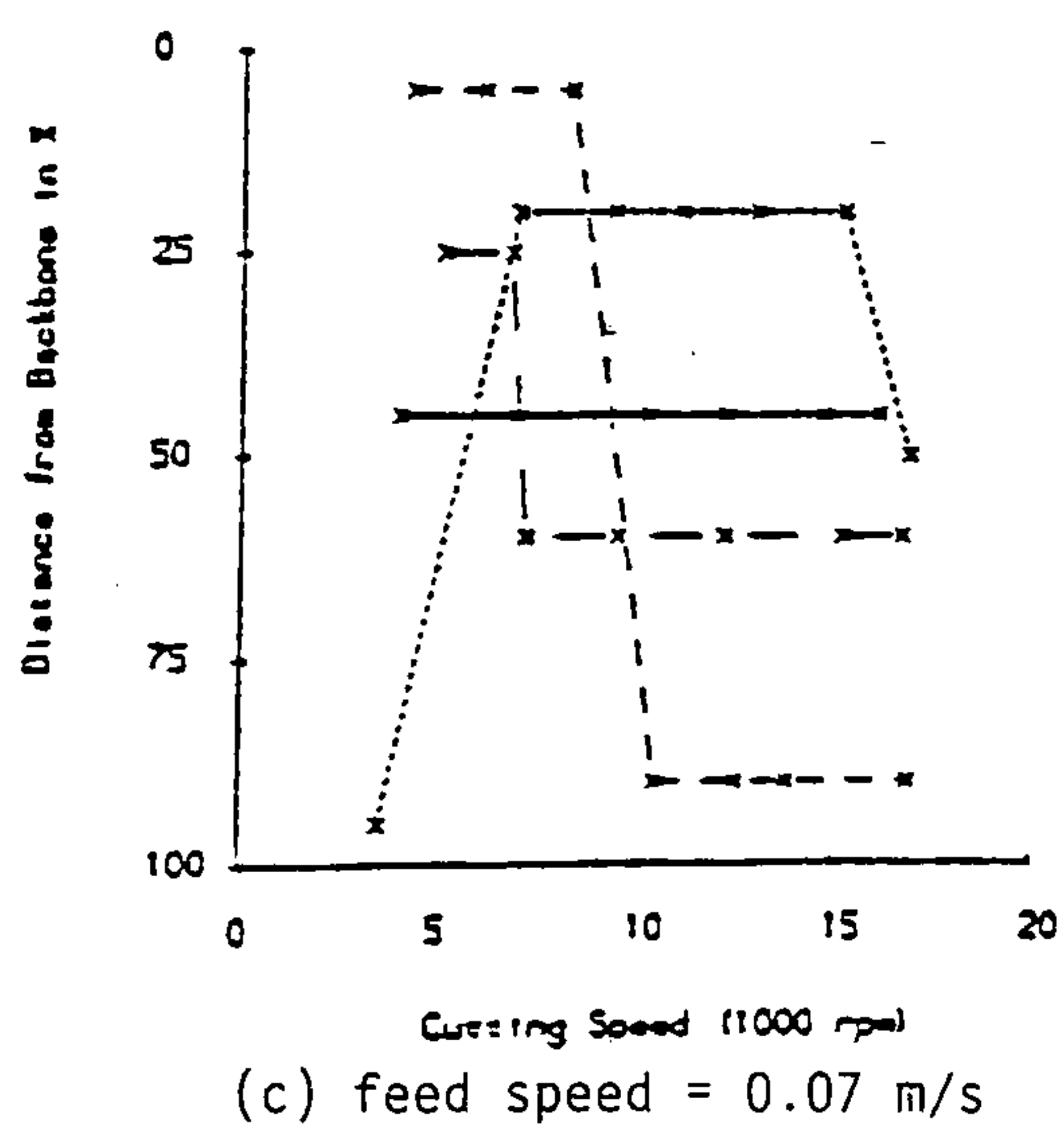
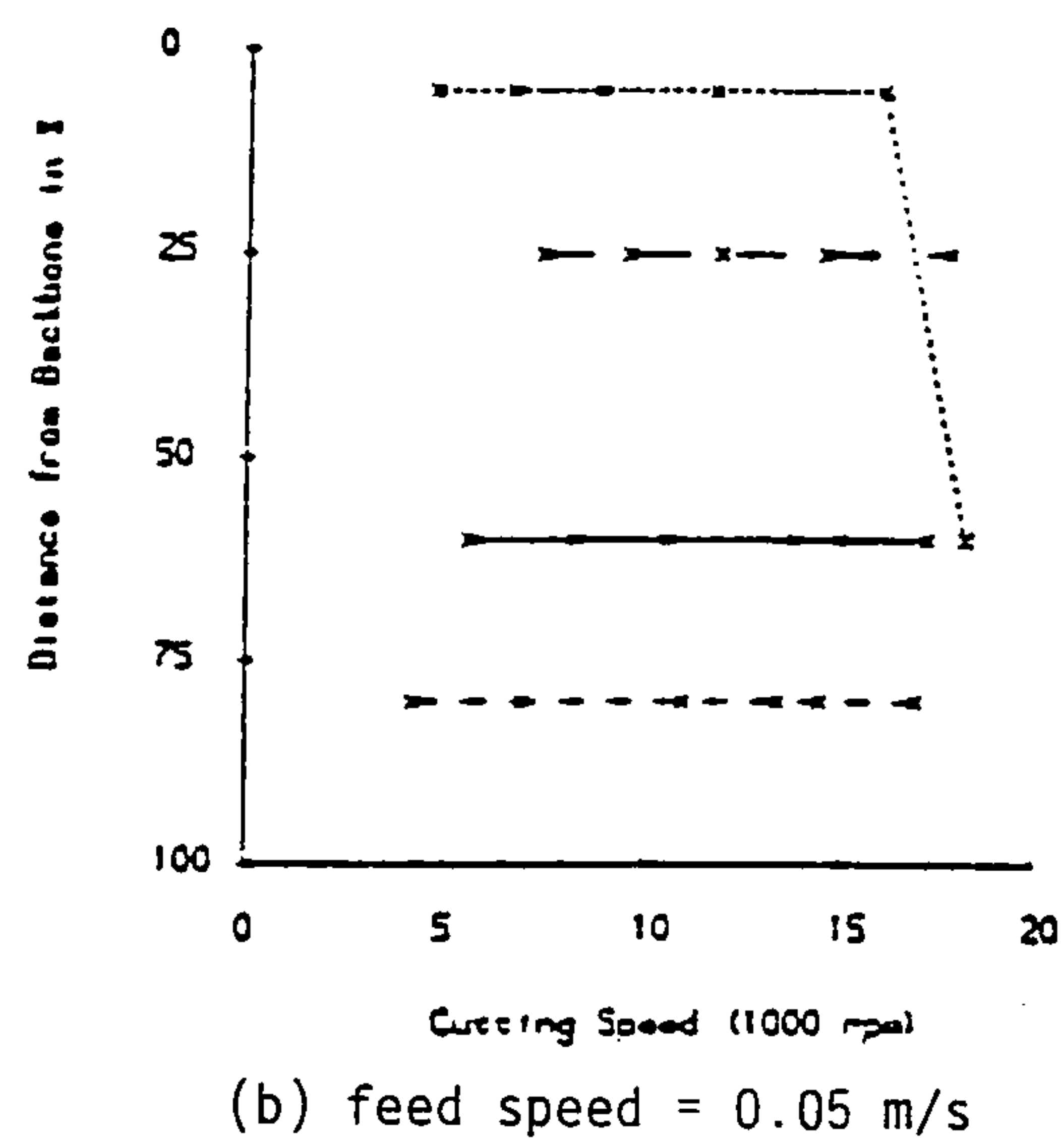
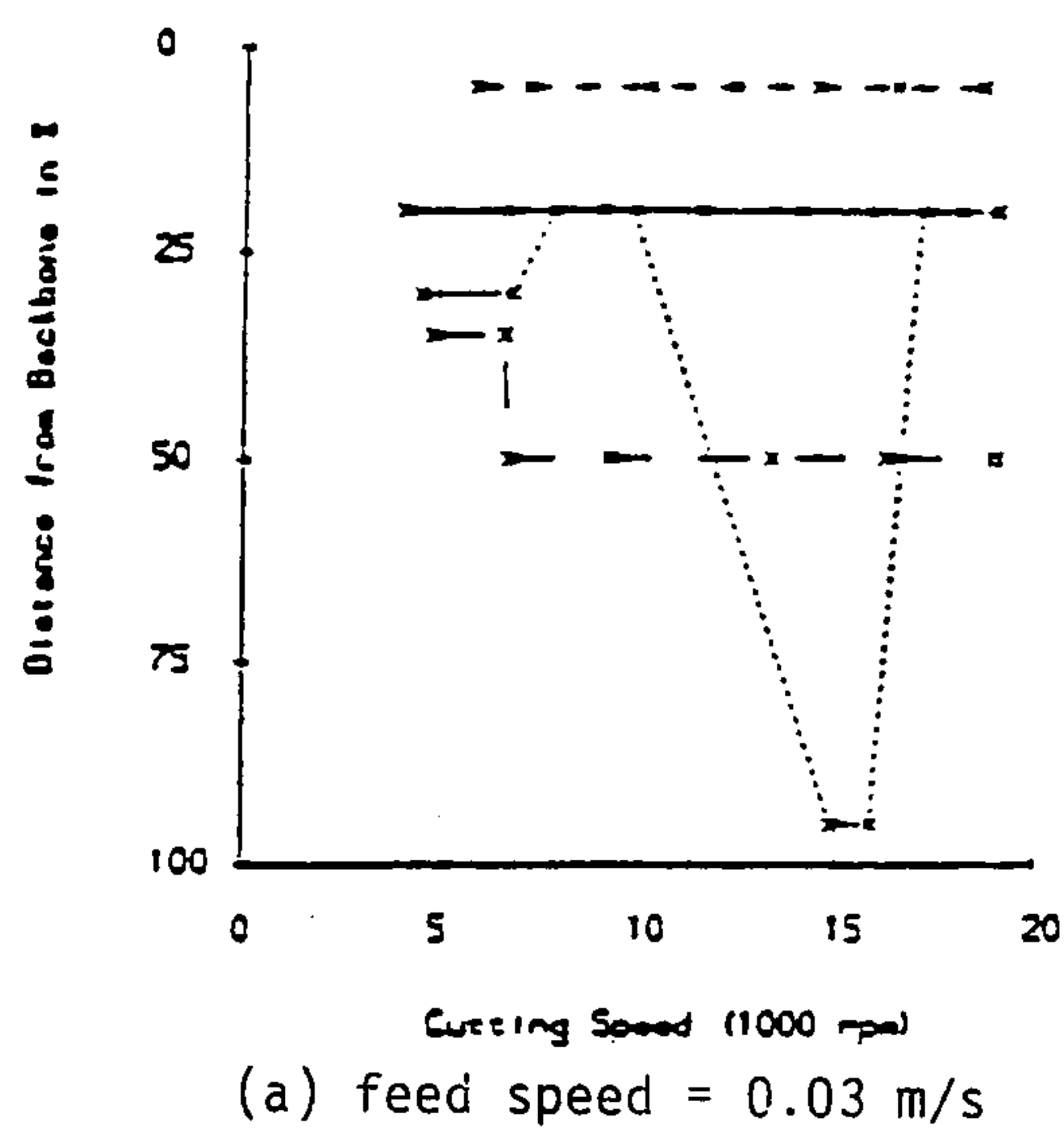
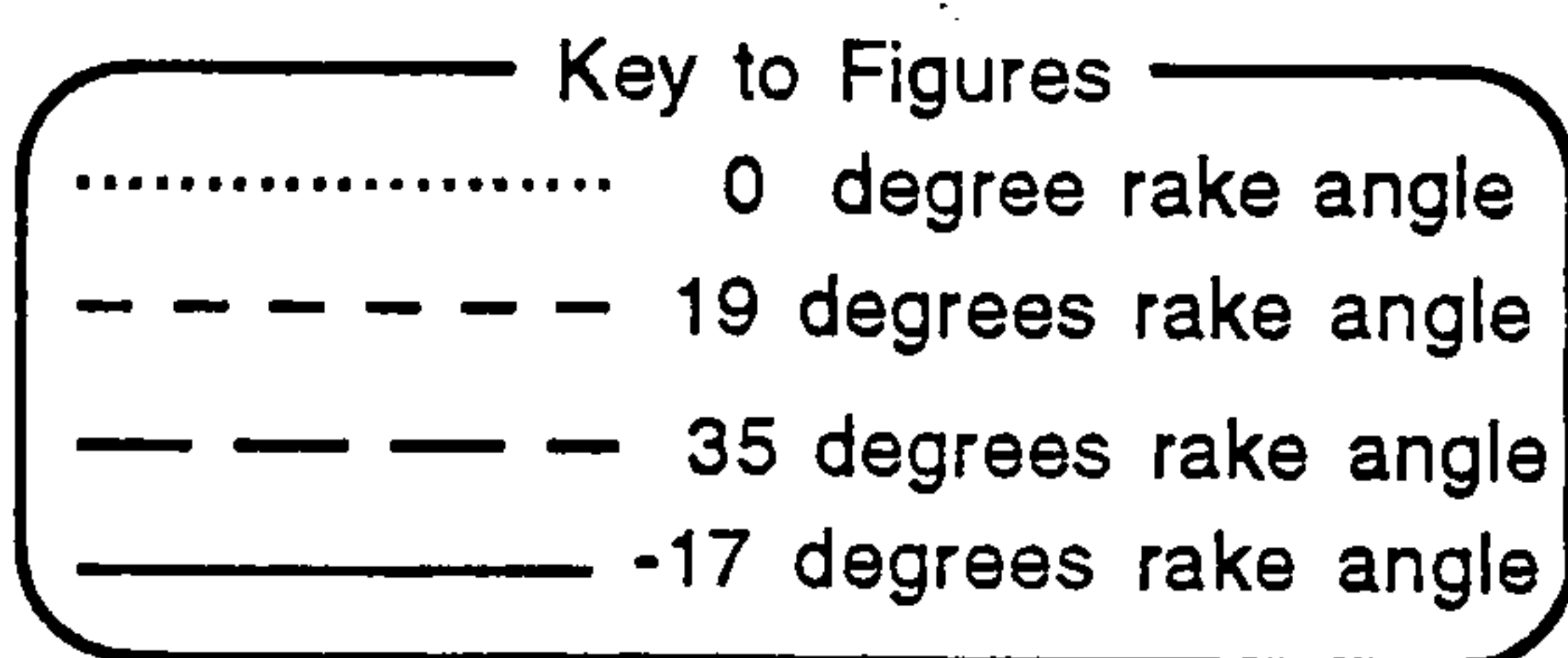


**Figure 5.14** *Presentation of the leather sample positions in their original hides, shown graphically in the same way as the surface finish results in fig. 5.13.*





Figure 5.15 Photograph of a typical test sample with very good machined surface quality.



Figure 5.16 Photograph of a typical test sample with poor machined surface quality.



## 5.7 Conclusions

This chapter presents and discusses the results of the experiments that were carried out during the course of the investigation in the face milling operation as a method for automatic leather skiving. Leathers of type-1 and type-2, variable in their physical properties, were tested. Each test condition was replicated three times and was carried out on a randomly selected test piece. The mean values of the results were then quoted.

Having established that the most important result in this investigation is the quality of the machined surface finish of leather, its dependency on physical properties of leather is highlighted. The results show that the effect of material's original quality on the surface finish is dominating, and masks the effects of other machine-related factors such as feed and cutting speeds or the cutting tool rake angle. It is noticed that, when samples that have been originated from an area close to the belly region in a hide are machined, poor surface finishes are often resulted. A high degree of fluffiness of the nonhomogeneous bundles of fibres in this hide region tend to resist the action of the cutter, and as a consequence, an increased amount of rubbing takes place. The degree of stretchability of the fibres in this region is also noted.

It is further concluded that up-cutting generally produces better surface finishes, especially at the edges. The tests of the tool with negative rake angle gave encouraging results in the quality of the surface finish. This tool however, was noted to be associated with the presence of higher cutting forces and power consumptions than most of the other tools. The tool with zero rake angle generally proved to produce the smallest cutting forces and power consumptions.

It was further concluded that the quality of surface finish improves with the increase in the cutting speed, though speeds of around 12000 rpm show signs of optimality in terms of the resulting cutting force and power consumption. That is to say, larger cutting speeds tend to produce higher cutting forces and power inputs. It is also established that the increase in the feed speed is associated with the increase of cutting forces and power consumptions. No sign of deterioration in the quality of surface finish was observed when the feed speed was increased to its maximum value in the tests at  $0.09 \text{ ms}^{-1}$ .

In general leather type-1 requires more cutting force than leather type-2, with the resultant cutting forces of 8.14 N and 6.46 N respectively. However, the ratio of the feed to normal cutting forces in both cases varies between 0.5 and 0.6.



This suggests that no excessive rubbing between the cutter and the workpiece was present. Tests also show that a deeper cut requires more cutting force and power input.

Comparison of the magnified photographs of a cutting edge of a selected cutting tool taken both before and after the entire tests revealed that, although a certain amount of wear has taken place, no tool breakage or significant deterioration has taken place. This was a promising result. Nevertheless, more comprehensive tests will have to take place to examine the lifetime suitability of tungsten carbide tools in a factory-like situation.

The tests were performed on leather; a workpiece that, as a natural material, exhibits a high degree of variation in terms of physical characteristics. This phenomenon is the most significant factor that upsets the repeatability of the tests. However, the repeatability analysis shows that the bands of the results produced in the experiments generally give clear trends, and therefore are acceptable for the purpose of this investigation.



## **CHAPTER SIX**

### **DYNAMIC MATRIX CUTTING SYSTEM**

#### **6.1 Introduction**

Use of the principle of localised material removal of leather workpieces with the aid of feed rollers and a rotating band knife was the second method that was considered in the preliminary study of skiving automation in Chapter Two. In this technique, termed *matrix skiving*, the leather component is fed through a driving roller and a pressure bar and is passed over a high speed rotating band knife. Localised cutting then takes place when at any point along the width of the component, that is momentarily passing above the band knife, the component is depressed against the sharp edge of the knife. The attractiveness of such a material removal method in an automated discrete part manufacturing environment is its concept of continuous flow operation. Moreover, the availability of an existing technology in leather splitting facilitates rapid implementation of the method.

In the preliminary investigation of matrix skiving, a system of linear array of matrices in the form of pins was described such that each pin is independently activated by its own solenoid mechanism. In this way, exact synchronisation between the independent actuation of the pins and the speed of the travel of the leather component results in producing the desired shape of the cutting profile on the component. Initial experimental results suggest that the critical parameters involved in matrix skiving are the resolution of the pins and the edge to edge distance (spacing) between the neighbouring pins. Measurement of the amplitudes of the waveform produced as the result of pin impressions along the cutting profile in test samples help the quantification of the quality results. These results show that high pin resolution and low pin spacing produce better quality of cut.

A practical method for the realisation of the above system is a linear assembly of spring loaded pins housed in a steel bar, as was explained in Section



2.4.3. Such a bar is used to replace the pressure bar mounted on a leather splitting machine such that instead of uniform splitting across the width of the leather component, localised cutting, or skiving, takes place. In this way the important parameters influencing the surface quality results are pin diameter and pin spacing. In this chapter further experimental investigation are conducted so that the effects of various pin diameters and spacings on leather materials of different physical properties are established. Furthermore, in order to design an automated matrix skiving machine the vertical forces exerted by the pins on the leather components during cutting are also measured.

The sections that follow begin with a discussion of the requirements from an experimental system before describing the elements of the rig in detail. The design of the pin matrix assembly, the method of actuation, and the force measurement system are amongst those described. Later, the operation of the combined rig together with its computer data acquisition system are explained. The method and the results of the experiments are finally presented.

## **6.2 General requirements from the experimental system**

The static matrix tests performed in the preliminary investigation of the automated matrix skiving determined that better surface results are produced by increasing the matrix resolution and decreasing the matrix spacing. These tests were carried out with the aid of fixed toothed substrates on which test samples had been attached. The results, though give reasonable guidelines towards designing the matrix parameters, cannot be regarded as the basis for any practical implementation where matrix pins are used. The experimental system that is described here, therefore, employs the actual assembly of pins, housed in a suitable bar, so that more practical results are obtained. It is therefore necessary to design and manufacture various suitable bars and pins assembly so that a combination of matrix resolution and spacing are tested.

One of the industrial requirements that has been specified in Chapter One for designing of an automated skiving system is the ability of achieving comparable speeds of the production, or better, with the existing mechanised techniques. It is therefore amongst the aim of this work to achieve skiving in the fastest production rate possible. To this end, the influence of the speed of travel of the leather component through the experimental rig is required to be examined.



In designing an automated matrix skiving machine where use of a linear array of pins is made it is also important to have a prior knowledge of the magnitude of the forces that are required to depress the pins against the leather component so that correct amount of material removal takes place. The magnitude of the force may vary depending upon the desired depth of cut, the geometric shape and configuration of the pins, the speed of the workpiece, and its physical properties such as its rigidity. The rig must therefore provide facilities to record the exerted forces involved on the leather. A suitable load cell is employed for this purpose. Use of a personal computer is made to record and store the values of the force measurements monitored by the load cell in the rig.

It was mentioned earlier that the essential components of a leather splitting machine is used to perform the experiments. This is because acceptable surface finishes by using a band knife is achieved. The action of the knife is such that the unwanted material is sliced away from the leather component leaving a smooth skived surface. The concern for obtaining a good quality of cut in a matrix skiving would be to achieve continuous path of the skived profile with a minimum degree of waviness along its edges as described in section 2.4.2 (ii). It is therefore sufficient to require from the experimental rig to be able to produce a single straight line of cut resulting from the contribution of several adjacent pin matrix.

Finally, to test the effect of the physical properties of leather on the results leathers of varying physical properties are to be tested.

### **6.3 Pin matrix Assembly**

The concept of pin matrix assembly has already been explained in Section 2.4.3 (iii). It consisted of a pressure bar of hard steel material incorporating an equidistant linear array of small and identical spring-loaded pins of hardened silver steel material. The bar replaced that which is normally used in a splitting machine. The sketch of the design of a typical bar is shown in fig. 6.1.



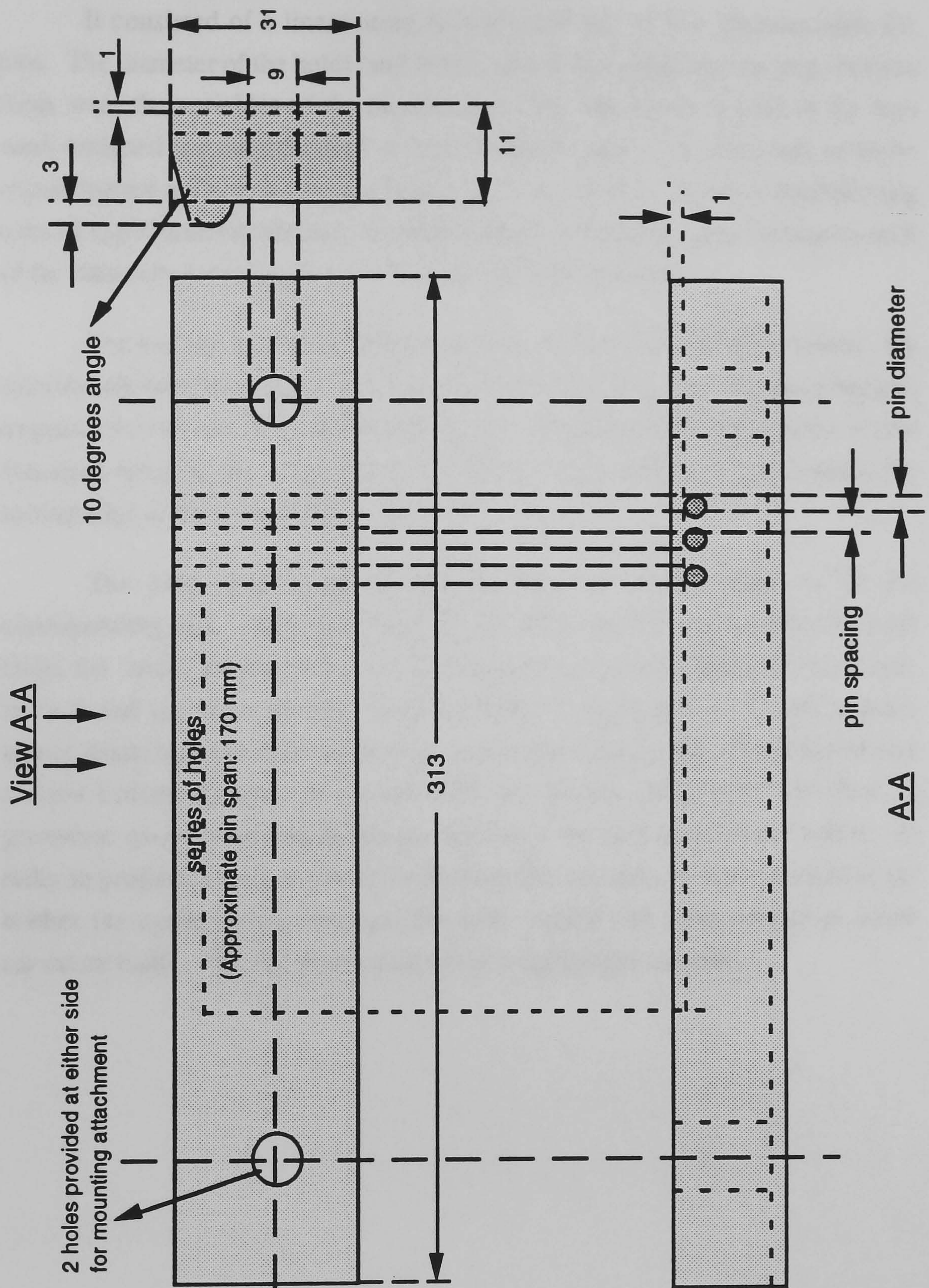


Figure 6.1 Design of a pressure bar to house matrix pins (all dimensions in mm, sketch not to scale).



It consisted of a linear array of holes that are used to accommodate the pins. The diameter of the holes (and hence the pin diameters) and the gap between them were the variables of the experiments. For this reason a total of six bars were designed and manufactured so that pin diameters of 3, 4, and 5 mm could be experimented each with pin spacings of 1, 2, and 3 mm. Given a total skiving span of approximately 170 mm, it is therefore clear that the number of pins in each of the bars vary according to the hole sizes and their spacings.

The bar was positioned directly above the feed roller of the machine. By suitably adjusting the height of the bar above the feed roller the workpiece became trapped between the feed roller and the bar. Correct height adjustment would therefore result in the workpiece being traversed by the feed roller towards the cutting edge of the rotating band knife.

The pins were designed and individually manufactured to fit the corresponding bars. The main components of the design of a pin included its main body, the 'neck' section to house a load-return compressive spring at the centre, and a thread and nut at the top. The main body of the pin is of a cylindrical shape whose diameter was equal to that of its corresponding hole. The base of this section became directly in contact with the leather component and thus its geometric shape would influence the profile of the skived groove it makes. In order to produce a smooth transition between the cut and the uncut section of the leather (as against a step change) the base surface has been shaped as a low curvature dome. Fig. 6.2 shows a sketch of a typical pin assembly.



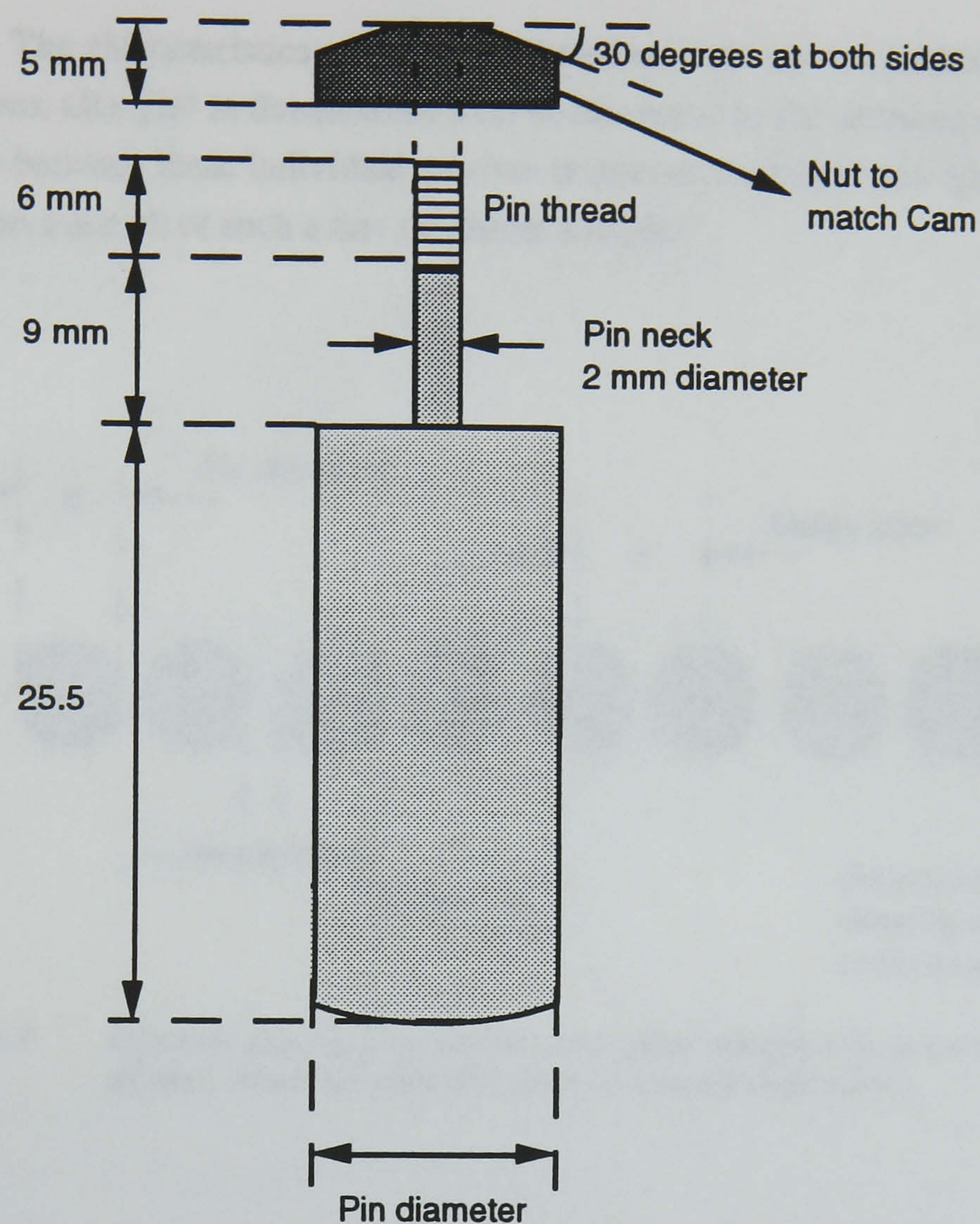


**Figure 6.2** *Schematic diagram of a matrix pin and the associating nut (Drawing not to scale).*

#### **6.4 Method of actuation**

It was mentioned earlier in this chapter that it is only sufficient from the rig to produce a straight line of skiving in order to be able to extract the necessary information from the results. This straight line of cutting is to be produced while the leather component is being traversed by the feed roller through the band knife. When at any instant during the component's motion several adjacent pins are caused to be depressed momentarily, and simultaneously, a skived line is resulted on the leather sample which is parallel to the axis of the roller. The resulting skived line is in fact a collection of all the impressions of the depressed pins on the



leather. The characteristics of the line is therefore such that it consists of a series of grooves, all equal in dimensions, with widths equal to the diameter of the pins. The gap between these individual grooves is determined by the pin spacing. Fig. 6.3 shows a sketch of such a line on leather samples.

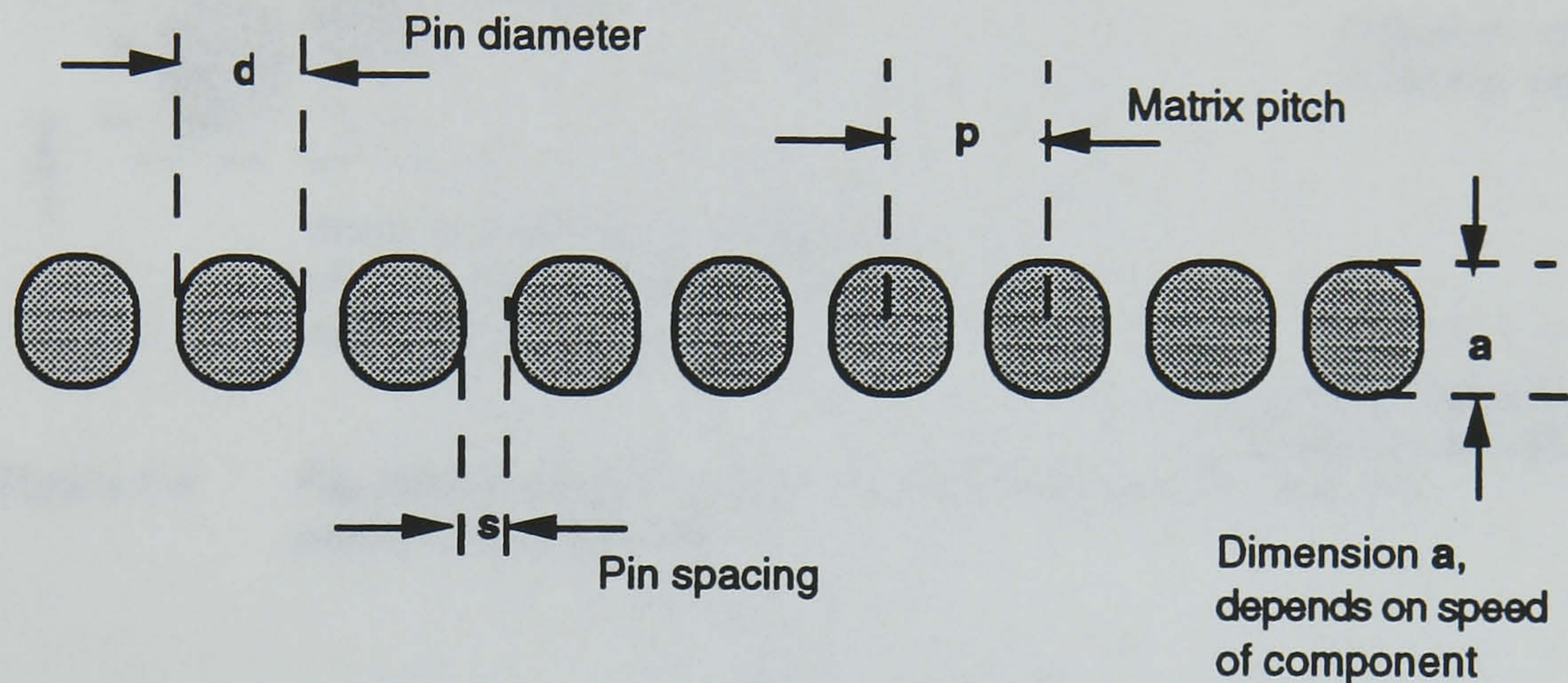


**Figure 6.3** *Discrete skiving impressions on leather samples by a linear array of pins, when all pins are simultaneously depressed.*

If now the pins are depressed one after the other and sequentially so that at any one time only one pin is fully depressed, then the resulting straight line will be at an angle to the direction of the axis of the band knife. This is because the leather component will have moved further along its path by the time a new pin is depressed. Obviously the angle at which the line makes with the roller depends upon the rotational speed of the roller as well as the rate in which the pins are sequentially depressed. Fig. 6.4 shows the sketch of such a line.



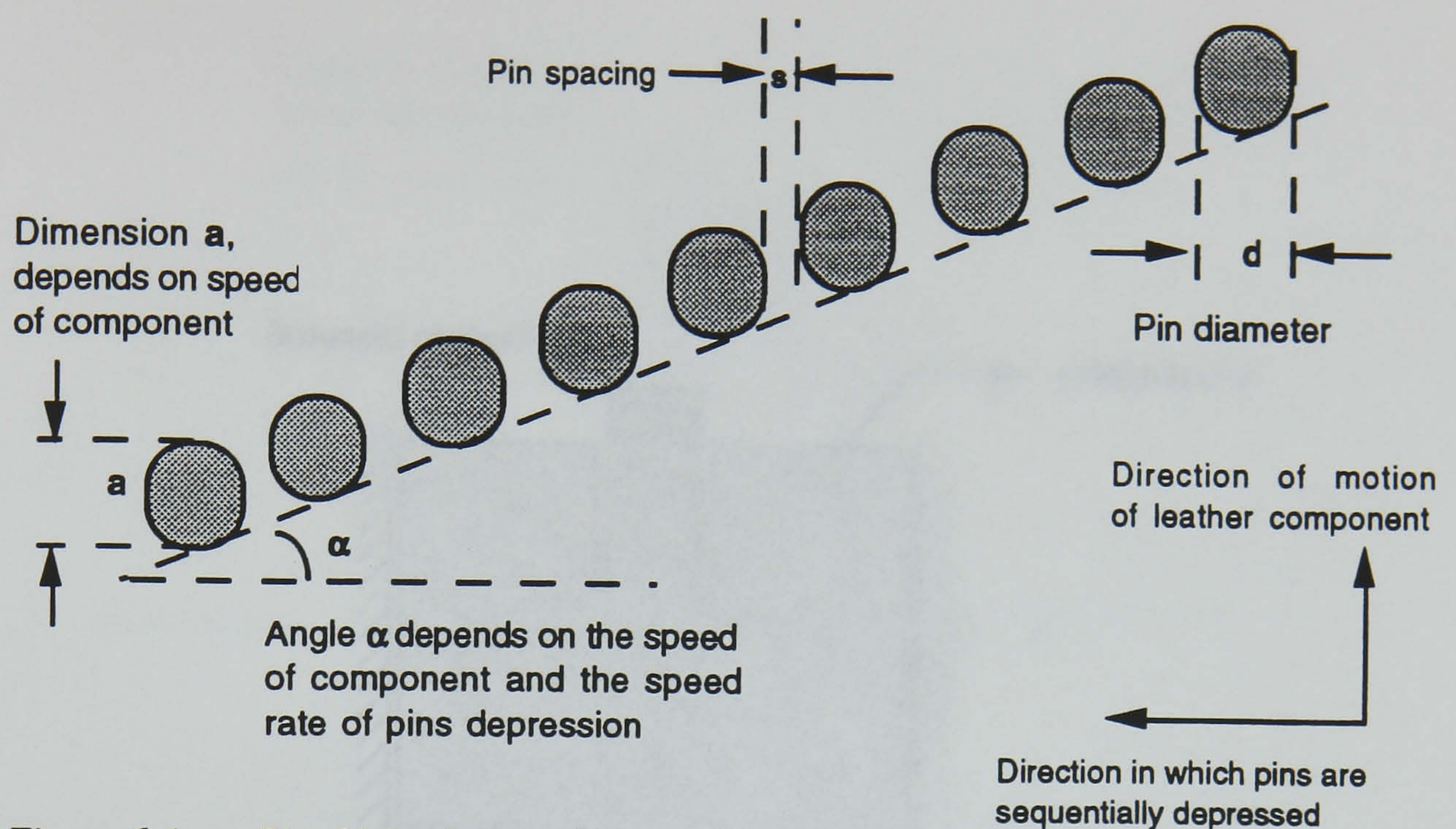


**Figure 6.4** *Pin skiving impressions on a leather sample when pins are sequentially depressed.*

Though in this way lines of different directions were produced, the interpretation of the results were unaffected. The pin actuation mechanism that was designed for the experiments produced a similar line of individual pin impressions on the leather samples. It consisted of a d.c. motor that accelerated an assembly of a solenoid, a plunger, a load cell, and a cam as shown in the sketch of fig. 6.5. The moving assembly traversed along a lead screw which was fixed directly above the line of matrix pins and in parallel to it. The solenoid's core was attached to the system's plunger while its main body was fixed. When the solenoid was energised its core transferred a certain amount of force to the plunger, and it in turn caused the matrix pins to be depressed through the designed cam. The geometry of the cam was of an inverted conical shape such that its  $30^\circ$  profile matched that of the pin nuts. Fig. 6.6 clearly shows the angles of contact between the cam and the pins. Assuming a situation where the solenoid is energised, as the plunger moves laterally along the matrix line the cam meets a pin nut, and as it moves, the matching surfaces of the two components slide against each other so that the transferred force to the pin causes the pin to be depressed vertically downwards through its guide hole of its housing pressure bar.



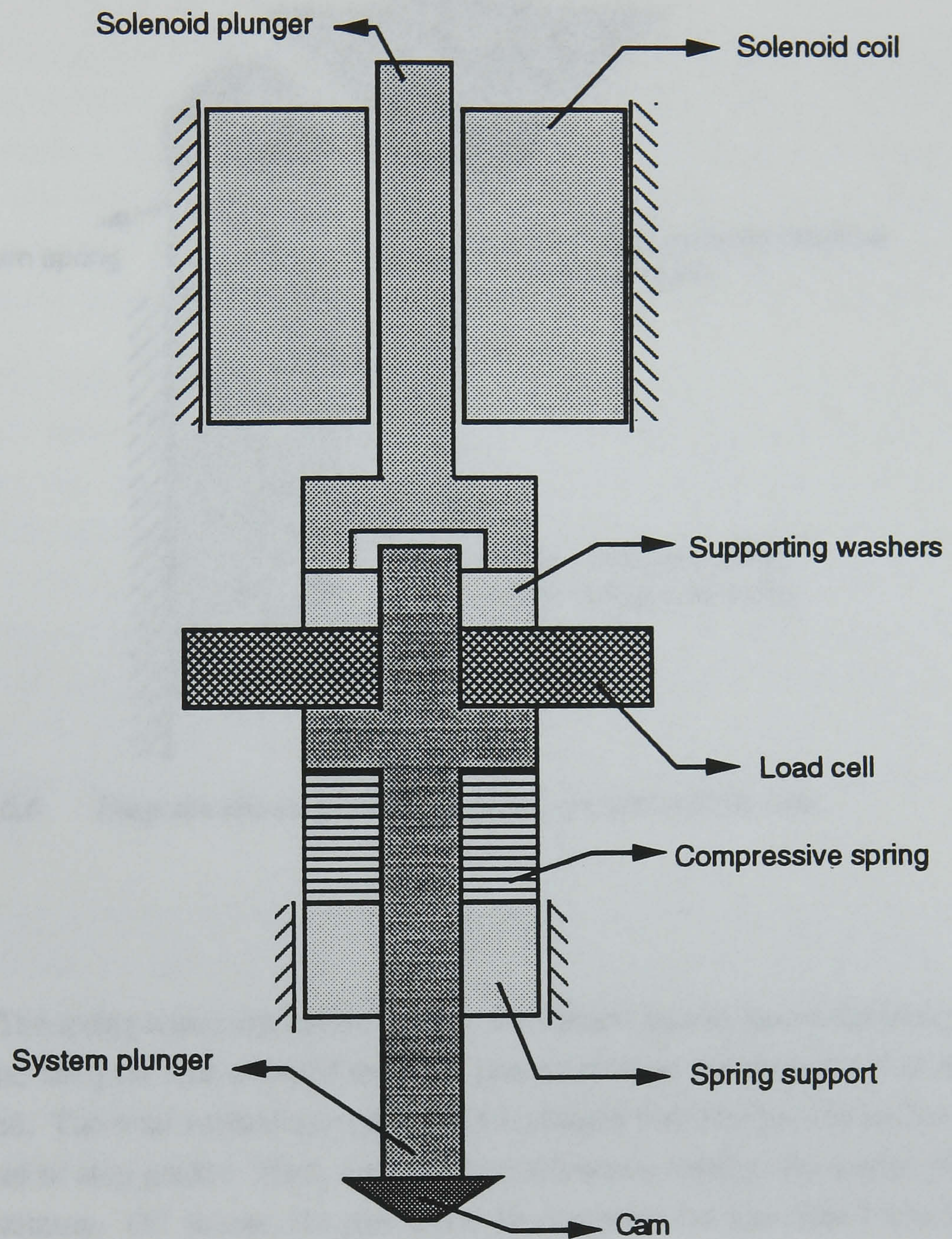


**Figure 6.5** A schematic diagram showing the complete plunger actuation assembly.



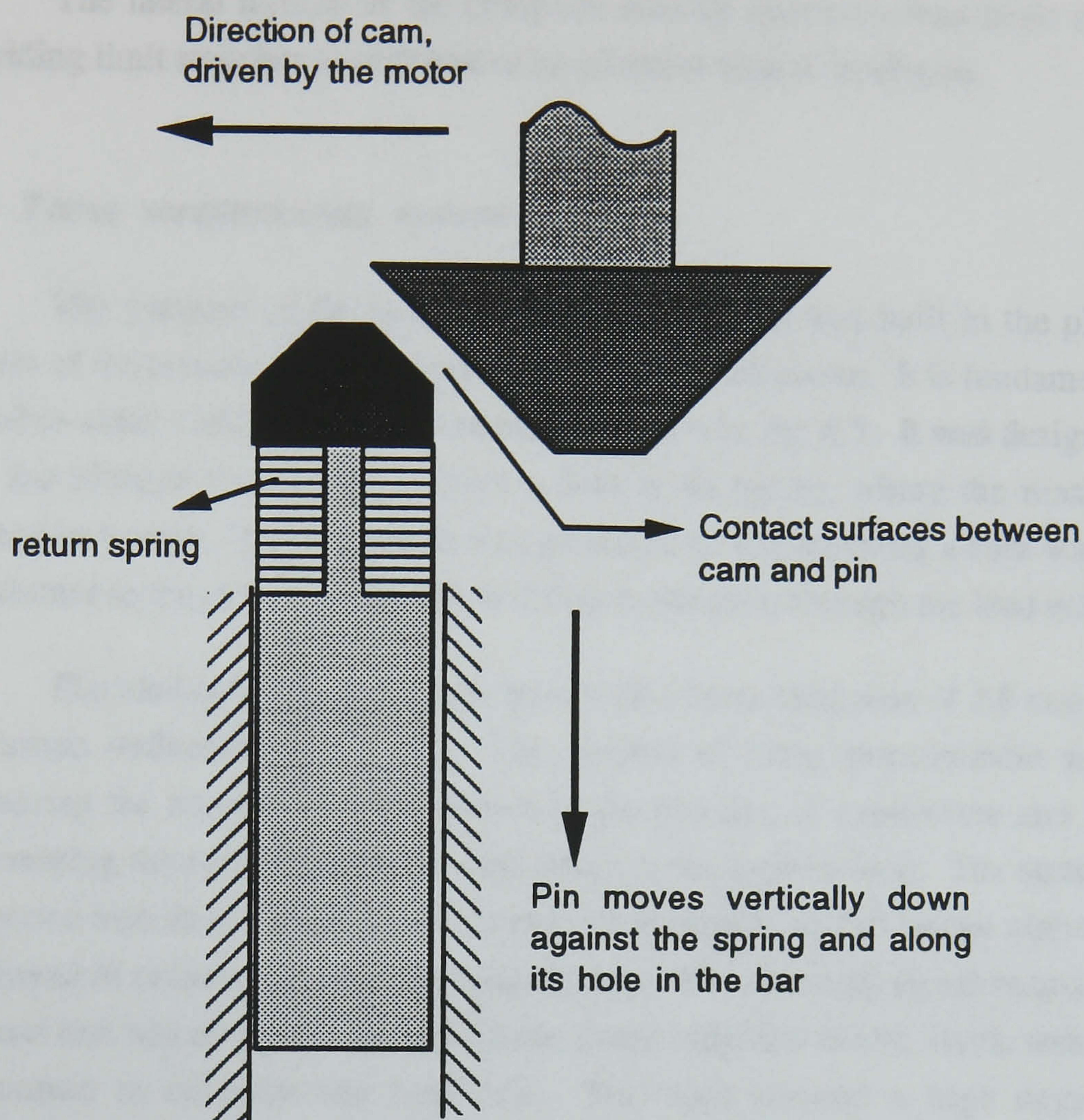


*Figure 6.6 Diagram showing contact surfaces of a pin and the cam.*

The spring return mechanism built in the plunger system forced the plunger to release the pins and returned upwards just as soon as the solenoid was de-energised. The total vertical movement of the plunger was designed to be 2 mm by the aid of stop guides. Thus, the pins were allowed a vertical depression of 2 mm maximum. Of course, the pins could be depressed for less than 2 mm by adjusting the gap between the pressure bar and the knife.

The purpose of the load cell in the system was to provide the vertical force reading that was exerted by the plunger, through the pins, onto the leather component. The results were then indicative of the amount of force required to produce acceptable matrix skiving on the samples. The load cell and the method of force measurement are described in Section 6.5.



The lateral motion of the complete moving assembly was made safe by providing limit switches at each end of its effective span of operation.

### **6.5 Force measurement system**

The purpose of the load cell that was designed and built in the plunger system of the actuation mechanism has been explained above. It is fundamentally a double-sided cantilever beam structure as shown in fig. 6.7. It was designed so that the plunger could pass through a hole at its centre, where the maximum deflection occurs. The force that was produced by the solenoid's core was thus transferred to the system's plunger, and then to the pins, through the load cell.

The load cell was made from steel with a beam thickness of 1.5 mm and a maximum deflection of 0.2 mm. The method of force measurement was by measuring the amount of compression in the bending of cantilevers and hence determining the resulting proportional strain to the applied load. The strain was converted into an electrical signal using a strain gauge. A full bridge circuit was employed in conjunction with the strain gauge. The electrical signal output from the load cell was amplified through an electronic amplifier board. Static tests were performed to calibrate the load cell. The tests showed a high degree of repeatability between 0 and 10 Kg loads in both load increasing and decreasing directions.

Use of a personal computer was made to collect the data from the load cell. The amplified d.c. signal from the load cell, conditioned to fall in the range of -5 and +5 volts for maximum utilisation of all the 8 bits available, was fed into the analogue-to-digital (A/D) converter board in the computer. After digitisation, a computer program for data acquisition collected the data and stored them in the relevant data files.



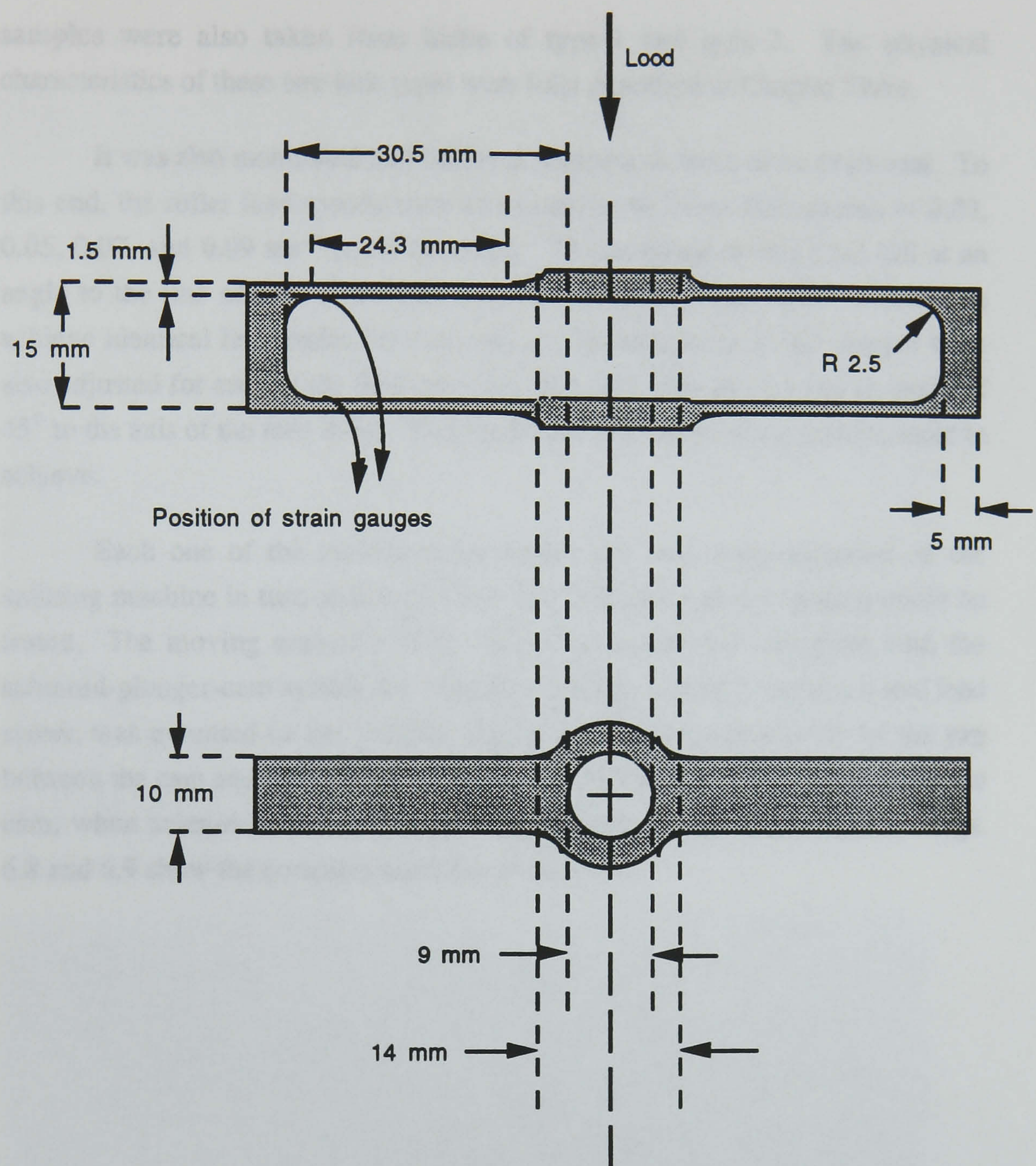


Figure 6.7 Design of the load cell used in matrix skiving tests (not to scale).

## 6.6 Operation of the combined rig

It was mentioned earlier that the requirements from the experimental set up were to produce skived lines using varying pin matrix characteristics, and on leather samples of varying physical properties. The pin diameters of 3, 4, and 5 mm along with the pin spacings of 1, 2, and 3 mm were used. The leather



samples were also taken from hides of type-1 and type-2. The physical characteristics of these two hide types were fully described in Chapter Three.

It was also mentioned that different feed speeds were to be examined. To this end, the roller feed speeds were so adjusted that linear feed speeds of 0.03, 0.05, 0.07, and 0.09 ms<sup>-1</sup> could be tested. The resulting skived lines fall at an angle to the line of axis of the roller as was previously described. In order to achieve identical line angles for each test, the lateral speeds of the plunger were also adjusted for each of the feed speeds so that all skived lines make an angle of 45° to the axis of the feed roller. This made the comparison of the results easier to achieve.

Each one of the manufactured matrix pin bars were mounted on the splitting machine in turn so that different pin diameter and pin spacing could be tested. The moving assembly of the actuation mechanism complete with the solenoid-plunger-cam system for vertical actuation, mounted on its nut and lead screw, was mounted on the splitting machine. The fine adjustments of the gap between the cam and the pins were made so that for all tests the 2 mm reach of the cam, when solenoid was energised, could produce similar depth of cuts. Figs. 6.8 and 6.9 show the complete assembly in position.



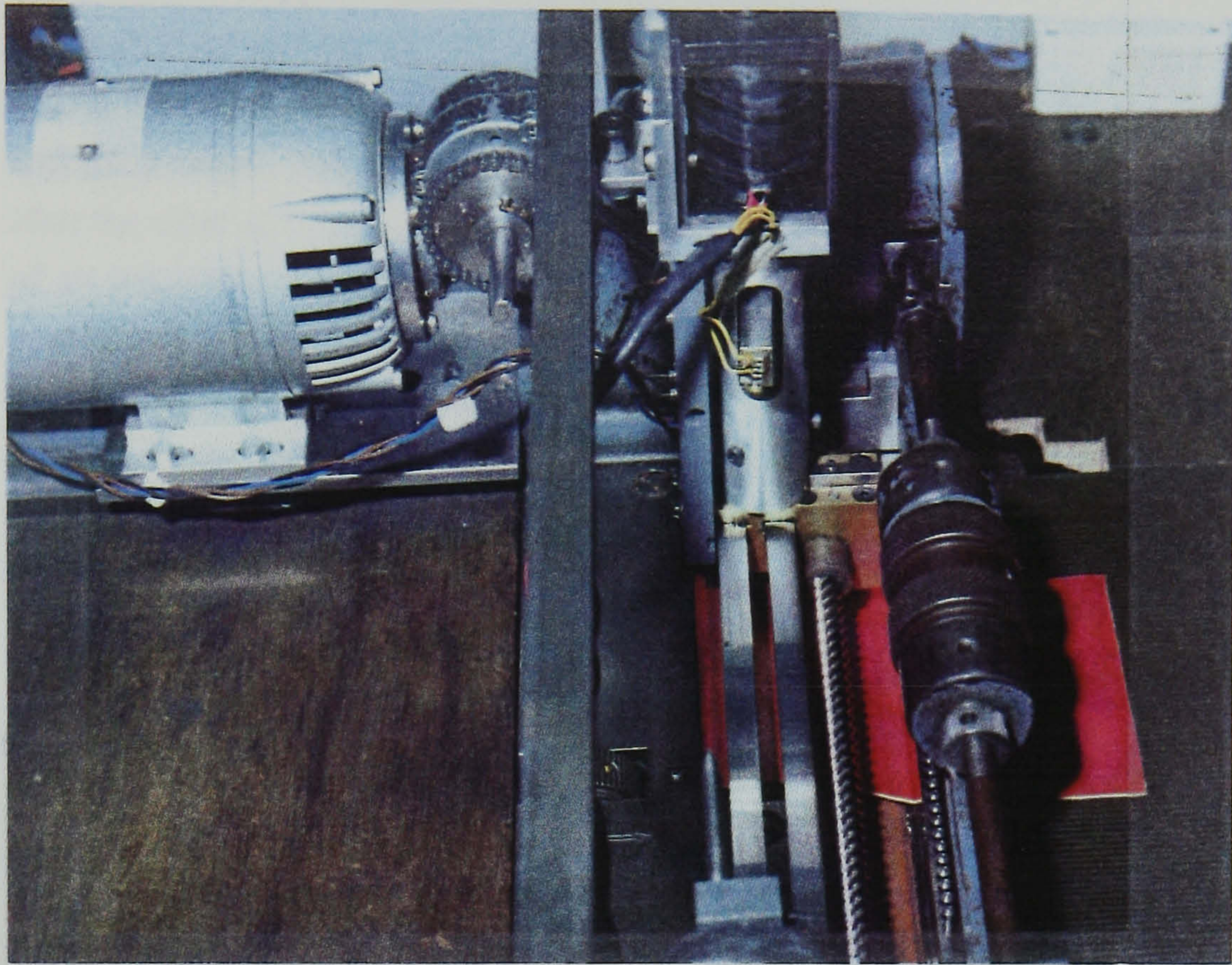


*Figure 6.8* A close-up view of the matrix skiving rig in operation.

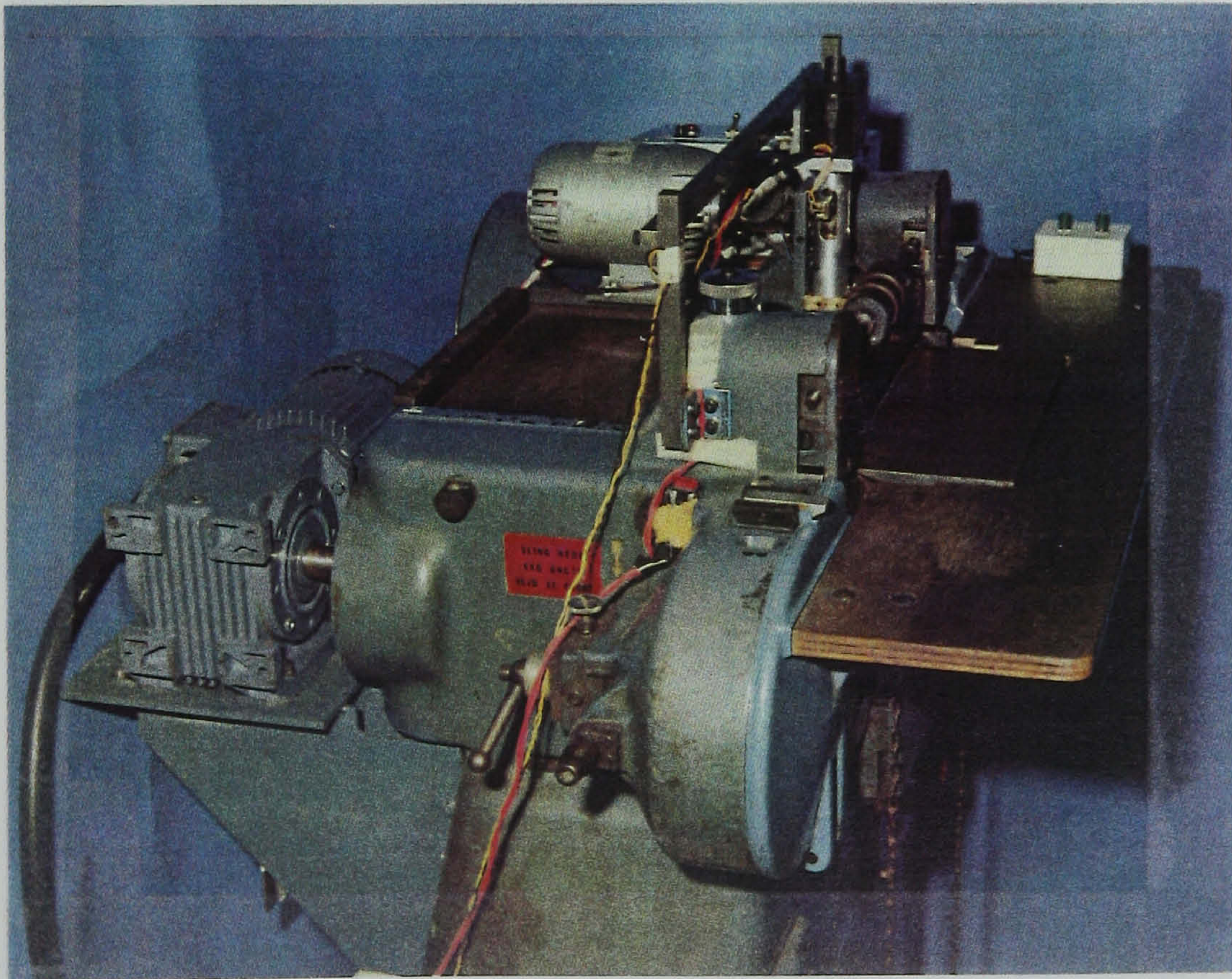


*Figure 6.9* A view showing the complete matrix skiving rig.



Leather samples were manually fed through the feed roller and the pressure bar. While a trapped sample was being passed over the band knife, the solenoid was energised and the d.c. motor was switched on so that the plunger mechanism begins its travel across the pins. Given the correct linear speeds of the samples and the plunger, the cam pushed the pins down against the leather samples, one after the other as it traversed across the entire span of the pin array. The dynamics of an individual pin in the array would therefore be such that it began to slide down its hole in the pressure bar against the action of its return spring. The downward motion of the pin continued until the bottom end of the cam reached the top end of the pin. After that, and as the cam carried on with its linear motion across, an upward motion of the pin began, that is caused by the action of its spring. At this stage the cam may have already started to push down a neighbouring pin depending on the pin diameter and the spacings of that particular matrix pin assembly. The combined impressions on the leather samples of each individual pins in an ideal case resembles a continuous straight line, and in a worst case would appear like a discrete series of pin impressions, similar to the sketch of fig. 6.4.

In the experiments that were carried out the following variables were thus tested:

- i. pin diameter
- ii. pin spacing
- iii. feed speed of leather samples
- iv. physical properties of leather samples

The results of the experiments were of two forms:

- i. performance of the matrix skiving in terms of surface finish
- ii. skiving force

The method for deducing the performance results of matrix skiving in these experiments resembles that of static tests described in Section 2.4.3 (ii). Fundamentally, two distinct areas for the representation of the results exist. One is



the case where the discrete and separate skived impressions of the pins on leather are analysed, while the other is the case with overlapping skived pin impressions on leather. Direct measurements are used for quantification of the results. In the first case, the percentage of the skived area from the pins pitch is obtained. As shown in the lower half of fig. 6.10, the ratio of  $\left[ \frac{P-x}{P} \right] \times 100$  indicates, as a percentage, a measure of closeness of the discrete skived impressions of the pins on leather. The performance quality therefore tends to increase with higher percentage values, and decrease with lower percentage values. In the second case however, the waviness of the profile of the skived line is a measure of skiving quality. As shown in the upper half of fig. 6.10 smaller amplitude of the skived line profile are indicative of increased quality performance while larger amplitudes show decreased quality performance. The amplitudes are measured in mm.

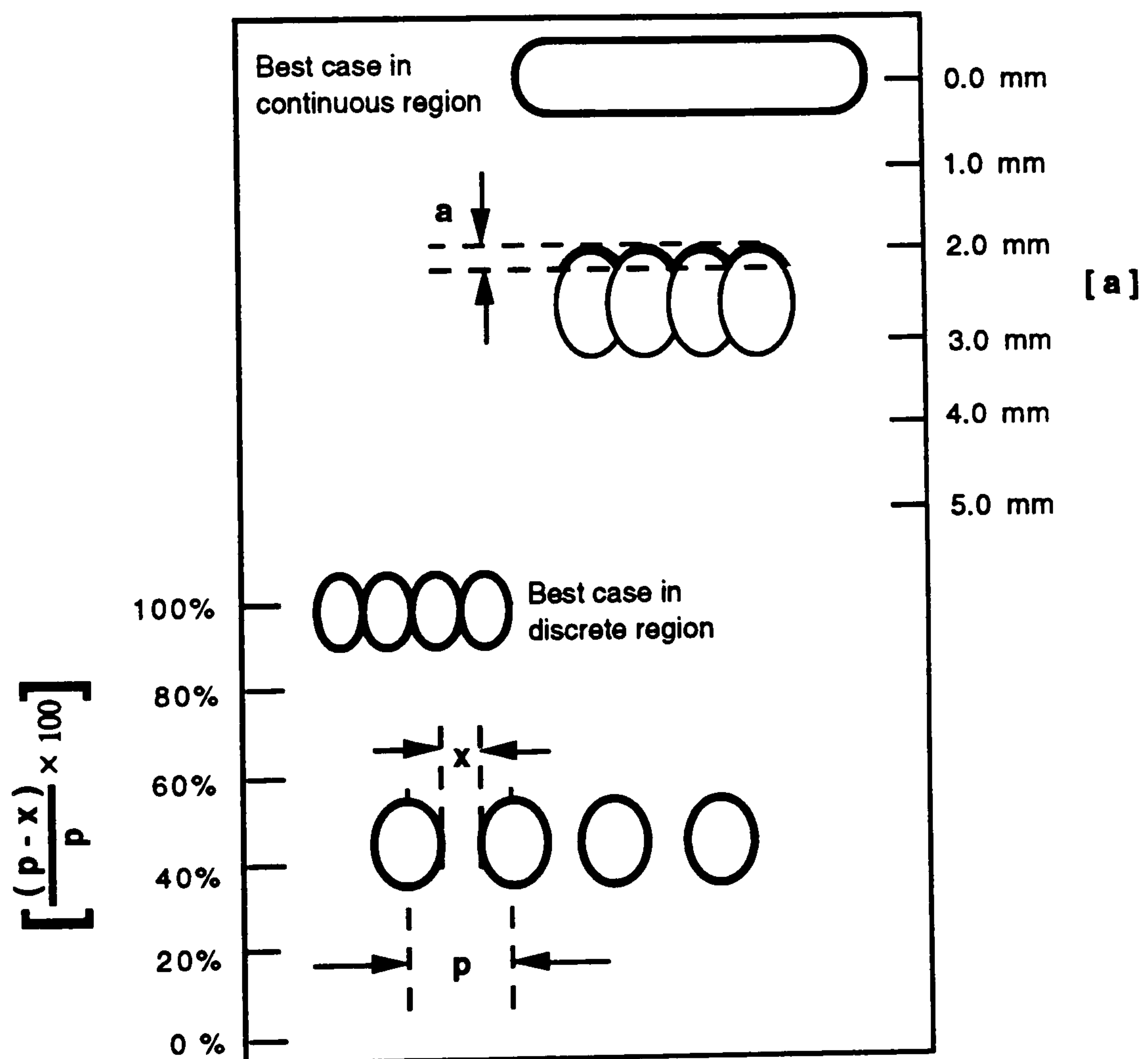


Figure 6.10 Diagram showing method of measurement of matrix skiving surface quality results.



Evaluation of the skiving force measurement is the other objective of the experiments. These values are automatically measured and recorded by the on-board strain-gauged load cell and the data acquisition system of the rig's personal computer. Skiving force is measured and recorded in N. In analysing the results only the maximum force reached during each test was taken into account. This is to establish the order of magnitude of the forces required in matrix skiving systems.

## **6.7 Experimental results**

The matrix skiving experiments were conducted using leather samples cut from all areas of the hide types 1 and 2. In order to minimise the influence of the unwanted factors on the tests the samples from each hide type were separately mixed so that each test is conducted on a sample drawn at random. The experiments were conducted with only one variable change at a time. Each test was replicated three times.

On presentation of the results of the experiments care has been taken to highlight the direct points of the objectives. For this reason the data has been analysed so that obvious effects of each variable in the experiments could be shown. Therefore, all the measured results for each leather type concerning each variable on its own have been separately collected and analysed. That is to say, for each leather type the mean value of all the available results concerning only one variable is calculated without due respect to any other variable. Using the mean values, graphs of skiving quality performance and skiving force are thus produced to show how they are affected by the three variables, namely pin spacing, pin diameter, and feed speed. Each point on the graphs represent the mean of 36 individual results in the case of pin spacing and diameter, and 27 individual results in the case of feed speed. For each point, therefore, bands of 90% confidence intervals are calculated [43][44].

In general, the skiving quality decreases as the pin spacing increases. This phenomenon is shared for both leather type cases. Larger pin edge to edge spacings produce more inferior quality of the matrix skiving. In the majority of cases, the results produced during the tests fall in the region of discrete skiving impressions. Leather type-1, nevertheless, is capable of achieving much better results than leather type-2. In fact, when 3 mm pin spacing is tested on leather type-2 the skived portion along the span of the pitch of two adjacent pins is only around 55% of the pitch. This value reaches to nearly 80% in the case of 1 mm



spacing. On the other hand, similar percentage value for leather type-1 is around 90% in the worst case, ie. when 3 mm pin spacing is used, and rises beyond the much acceptable level of 100%. As described earlier, any values above 100% on matrix quality results fall in a region of continuously skived line, rather than skived patches, and the quantification of the results are done using the amplitude measurement of the waveform that is produced along the profile of the skived pattern. The amplitude of the waveform resulted in the tests on leather type-1 with 1 mm pin spacing is approximately 4.5 mm. A graphical presentation of the results together with the bands of confidence intervals are shown in fig. 6.11.

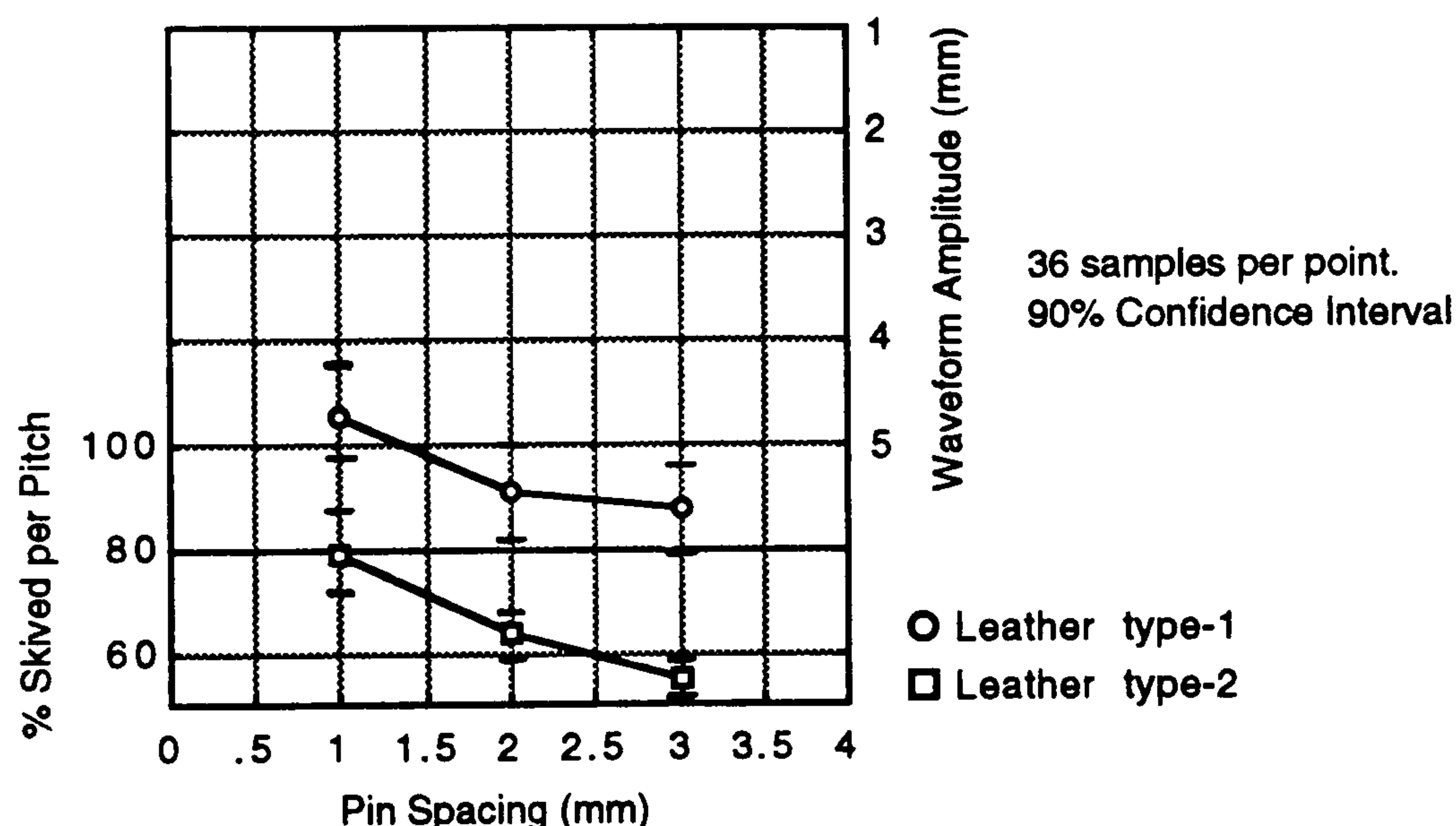
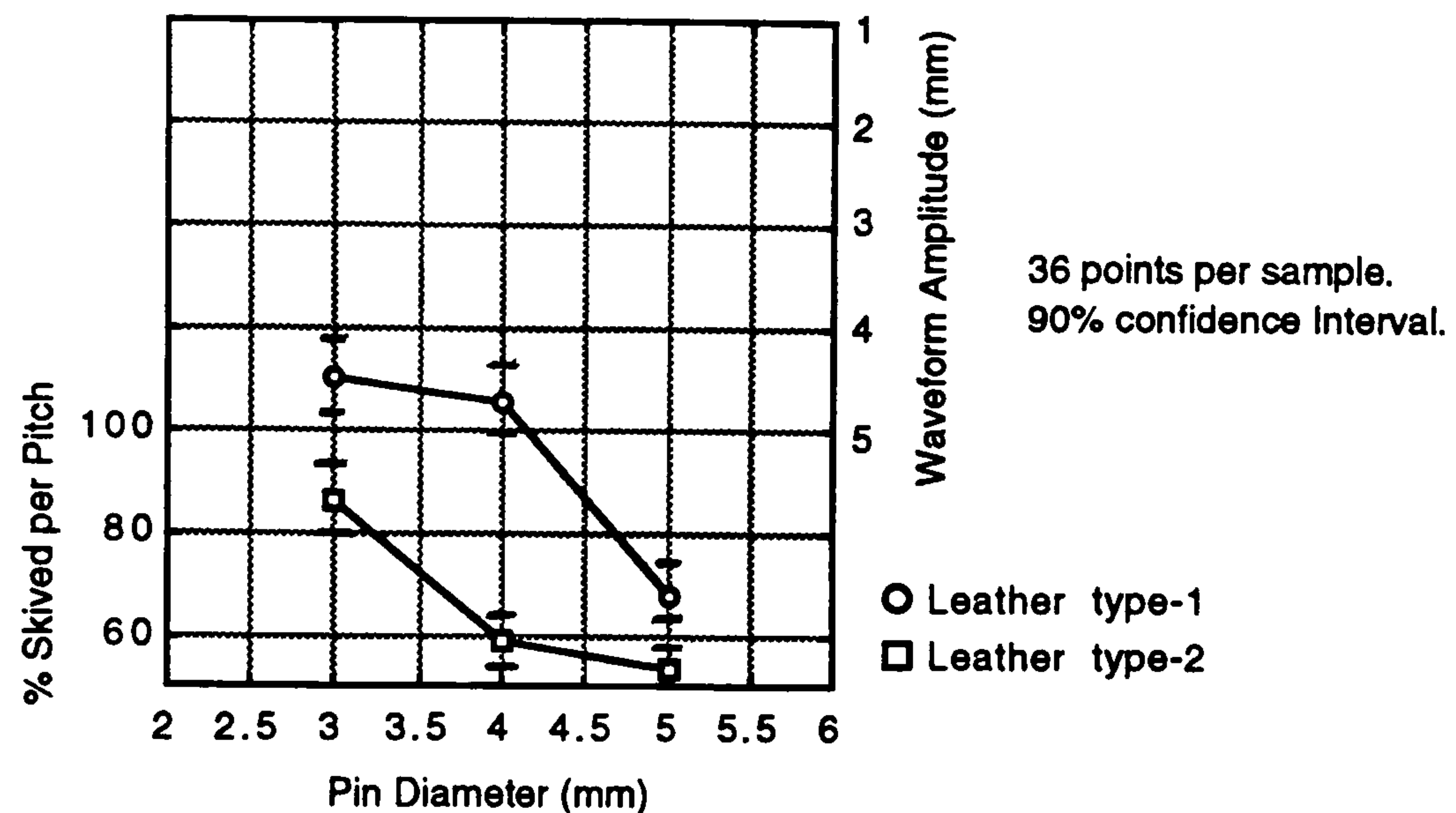


Figure 6.11 Graphs of skiving quality variation against pin spacing.

The results concerning pin diameter show similar patterns of behaviour for both leather types. For both leather types the 3 mm diameter pin matrix gives the best results while the 5 mm pin matrix gives the worst. However, the results concerning leather type-1 indicate that this leather material yields to better matrix skiving performance. In fact, for the 3 and 4 mm pin diameters the experiments resulted in a continuous line of skived pattern giving approximately 4 and 4.5 mm profile amplitude respectively, while all the tests on leather type-2 produced discrete skived patches ranging from 85% to 55% of skived length from the pitch. The results therefore suggest that thinner, more flexible leather materials show a



high degree of sensitivity to the pin diameters. These results are graphically depicted in fig. 6.12.



*Figure 6.12 Graphs of skiving quality variation against pin diameter.*

Matrix skiving quality performance however does not vary greatly with respect to the changes of leather sample feed speed. The performance results show that, for although leather type-1 again produces a much better skiving quality, it is not sensitive to the speed at which the leather samples are traversed through the skiving machine. Graph of fig. 6.13 shows this insensitivity. This, therefore, means that higher feed speeds can be employed in a matrix skiving machine with a reasonable assurance that the quality results are not affected. It is a very important result and suggests that matrix skiving is indeed capable of achieving fast speeds of operation; a desired ability which ranks amongst the primary objectives of this exercise, as explained in Chapter One.



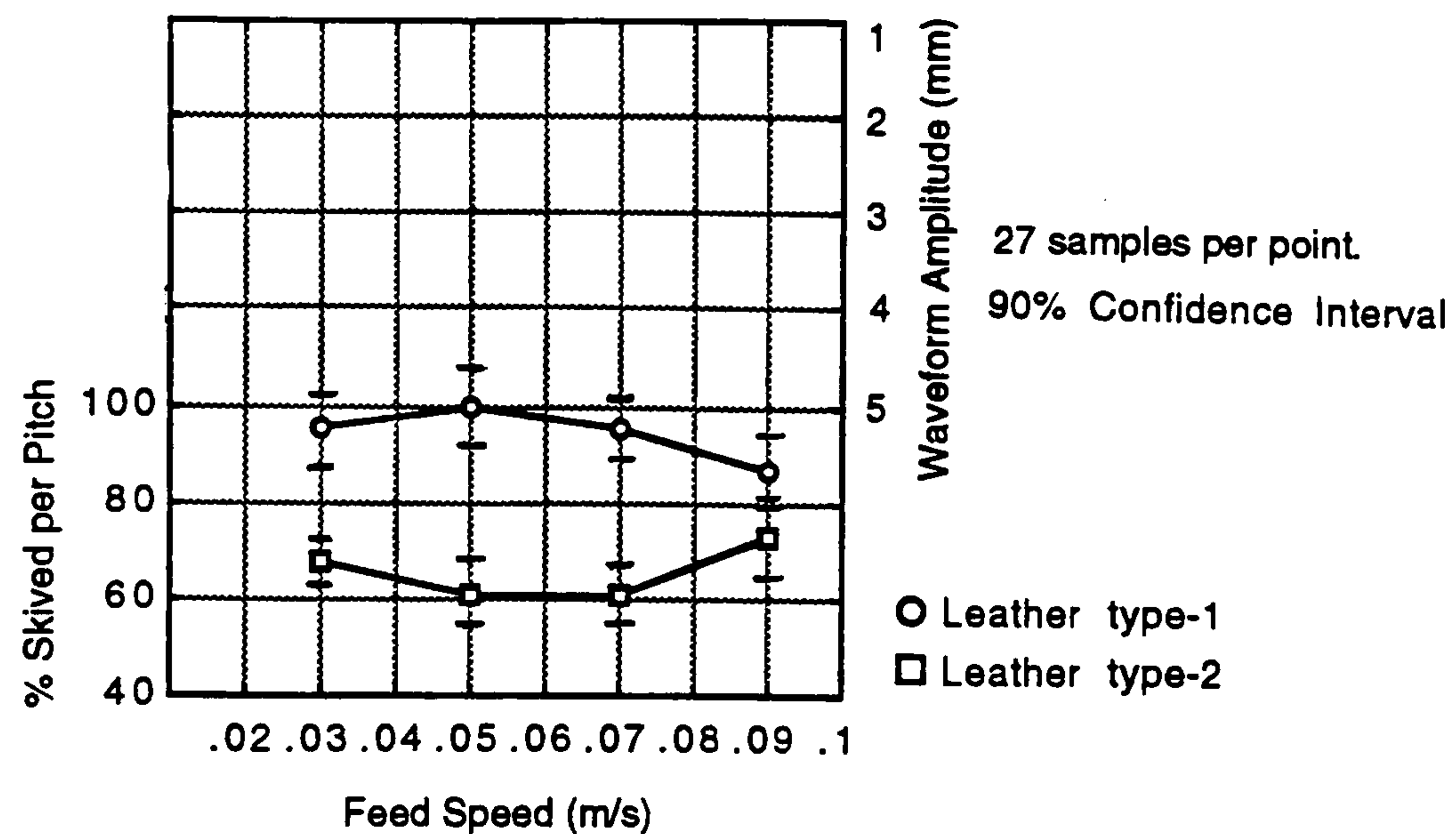


Figure 6.13 Graphs of skiving quality variation against feed speed.

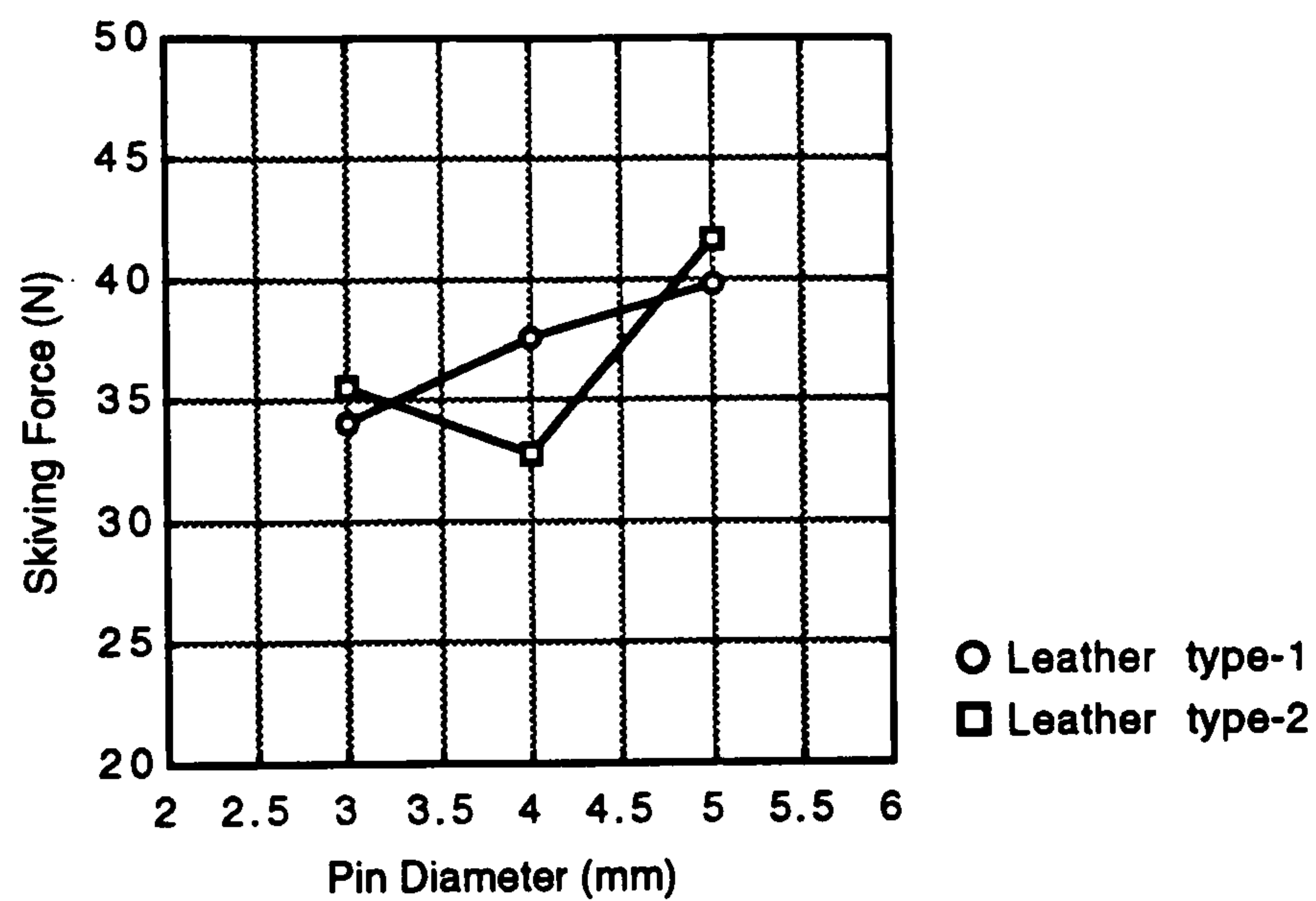
Skiving forces have also been measured during the experiments. These are the vertical forces that were exerted directly on the leather surface by the pins. Unlike the behaviour of the quality results, skiving forces tend to increase with the increase of both pin spacing and diameter. On average, the amount of force required to sufficiently depress a pin to achieve skiving lies in a range between 30 to 45 N. Also, in similar test situations the force magnitudes for both leather types more closely follow each other than their resulting performance quality. This is particularly noticeable when their changes are noted with the variations of feed speed.

Fig. 6.14 shows the variation of skiving force as the pin diameter changes while fig. 6.15 shows the same variation against pin spacing. In both cases the band in which the force magnitudes lie are very similar with extreme values of 32.7 N and 41.6 N. However, when the skiving force variation against changes in feed speed is considered, as depicted in fig. 6.16, two significant conclusions are drawn. Firstly, the force magnitudes band is smaller than with the case of pin diameter and spacing. In this case, the values are restricted between 34.8 N and 37.8 N. This suggests that the skiving force does not vary greatly with the speed in which leather is passed through the skiving machine. And secondly, the two leather types with different physical properties require similar amount of skiving force. These conclusions are very important to the designer of the automated



skiving machine since he has to design pin actuators such that they can be capable of successful operations when different leather types and feed speeds are used.

The results in this section show that any actuator, in the form of solenoid or otherwise, can successfully skive most leather types and at most feed speeds of up to  $0.09 \text{ ms}^{-1}$  so long as it can produce a force of at least 42 N.



*Figure 6.14* Graphs of skiving force variation against pin diameter.



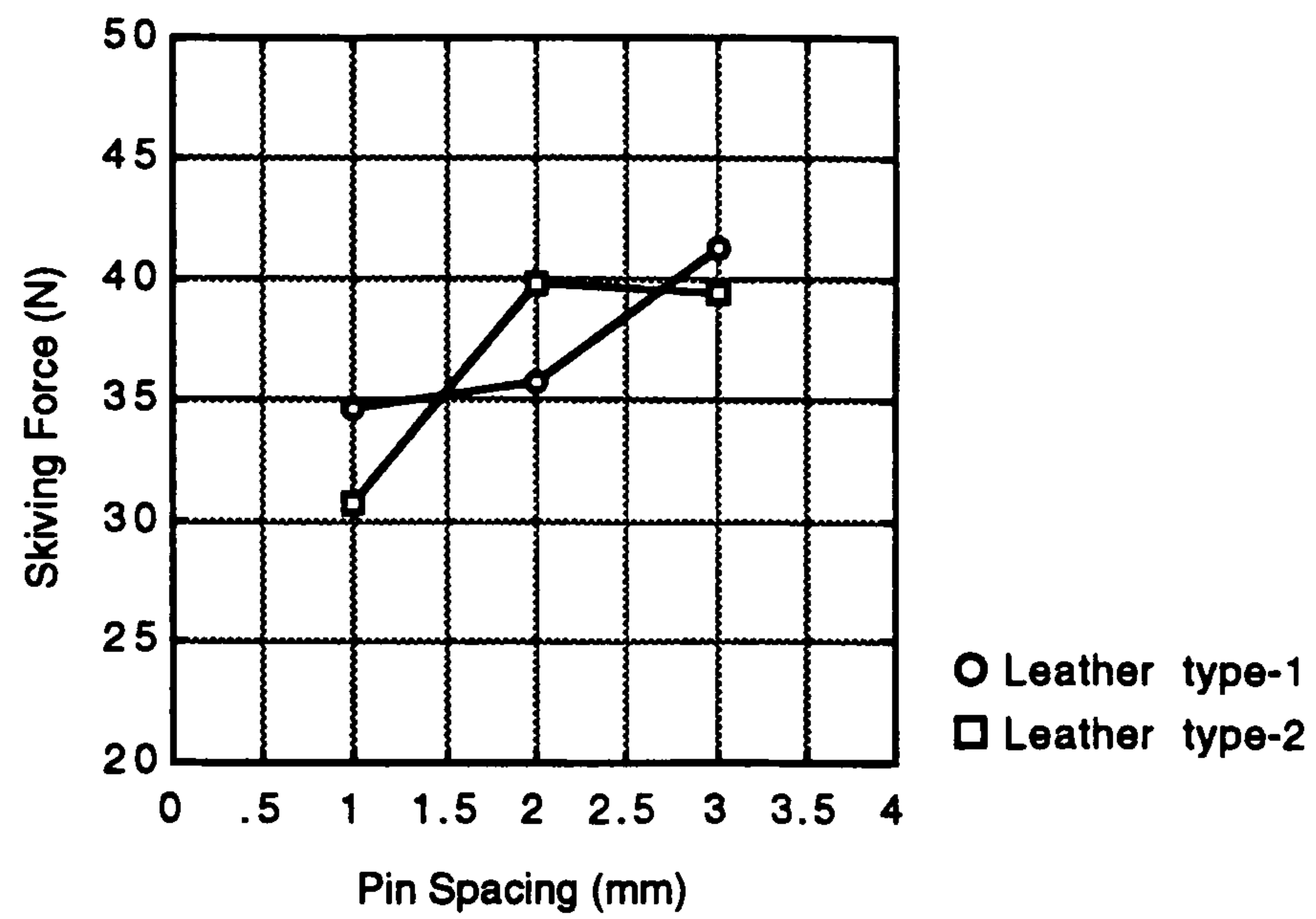


Figure 6.15 Graphs of skiving force variation against pin spacing.

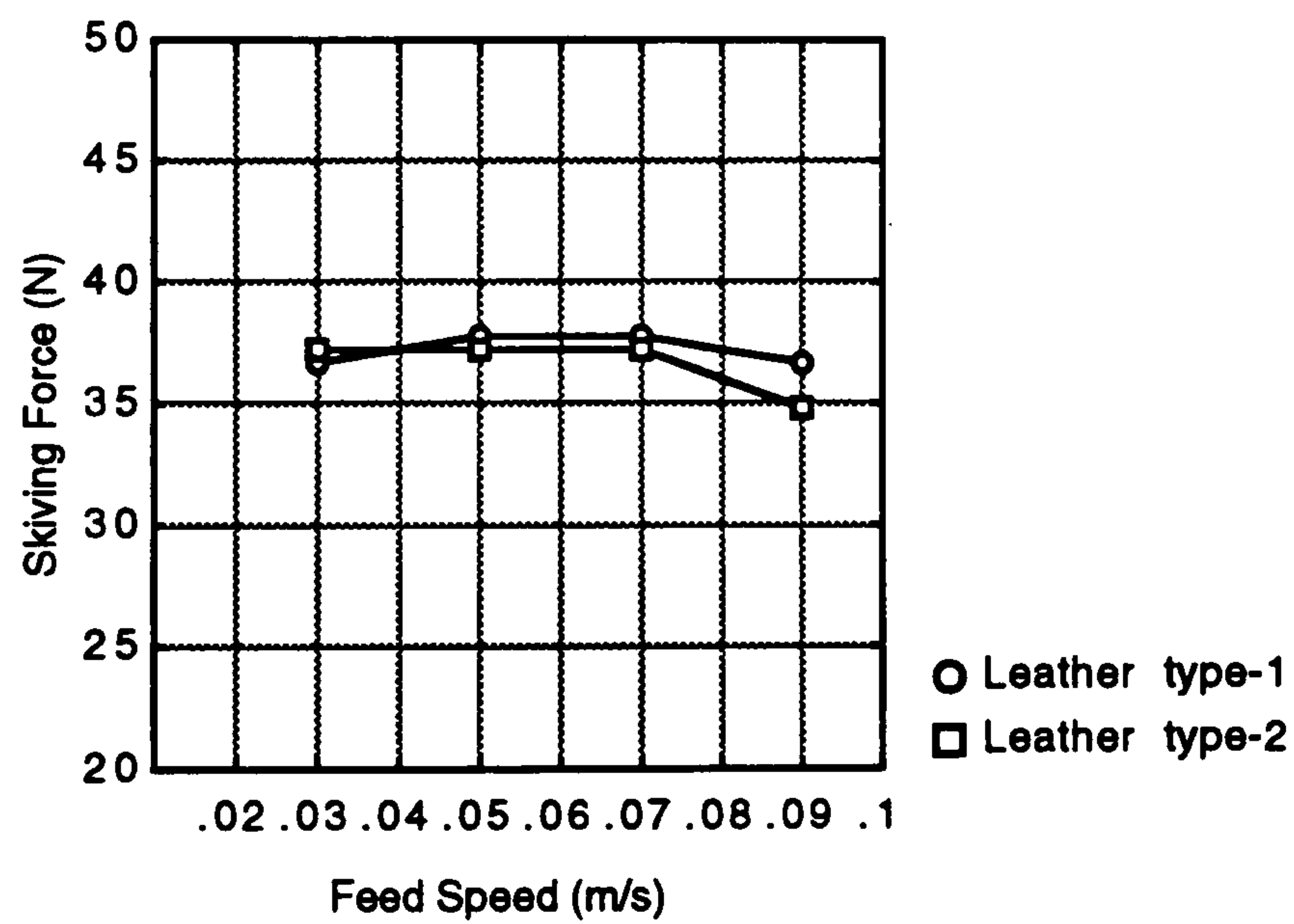


Figure 6.16 Graphs of skiving force variation against feed speed.



## 6.8 The role of properties of materials in matrix skiving

The results produced in Section 6.7 refer to the effects of various machine parameters on the performance quality and the resulting force in matrix skiving. In this section it is intended to produce more detailed correlation of the results with the properties of different leather types. To this end, the conclusions that are reached in Chapter Three are used. In that Chapter, the physical properties of two distinct leather types, primarily with respect to rigidity (which is inversely related to flexibility), are critically analysed. The summary of the results of this analysis is given firstly in Table 3.5, and then graphically in fig. 3.30, both in Section 3.12. These results are then correlated with those obtained in this chapter.

The performance quality results of matrix skiving show that invariably hide type-1 yields to better skiving quality. Also, since matrix skiving is achieved by way of local deflections of leather, then its flexibility is thought to play an important role in its behaviour under this cutting method. Leather materials of type-1 have higher flexural rigidity and are thicker than those of type-2. The mean flexural rigidity of the former is approximately 7 higher than the latter. It thus means that generally leathers of higher flexural rigidity perform better in matrix skiving. These conclusions are true for all the pin diameters and spacings tested in the experiments. However, at higher feed speeds the quality performance results of these leather materials tend to converge to a much closer values. Tests at  $0.09 \text{ ms}^{-1}$  show this phenomenon. It therefore suggests that at elevated feed speeds the performance of the two leather types in general are quite similar regardless of their thickness or their rigidity.

Examination of the comparison of other physical properties of the two leather types does not reveal significant variations between them. This is particularly true in the cases of their resistances to compression and tearing loads. In both cases the mean values are very close to each other. However, significant variations exist between the mean values of the tensile strength and the burst loads for the two hide types. Nevertheless, no correlation between these properties and matrix skiving quality results were detected during experimental investigation. Leathers of type-1 and type-2 also vary significantly in terms of their hardness. Indentation index values for these leathers show that leather type-2 is about 2.5 times as hard as leather type-1. In Chapter Three it was concluded that lower hardness is in general associated with higher material fluffiness. It follows that, since hide type-1 is generally fluffier and produce better matrix skiving results than



hide type-2, then harder leather components result in poorer skiving quality results.

Insofar as skiving forces in matrix skiving systems are concerned, it would be appropriate to conclude that, since the results are very close to each other for both leather types, then the variations in their physical properties are not of significant importance.

## **6.9 Conclusions**

This chapter brings together a comprehensive account of the work carried out to determine some important machine parameters in dynamic matrix skiving for the purpose of its system automation in the manufacture of shoe uppers.

Dynamic matrix skiving is a system comprising a linear array of independently actuated pins in conjunction with an assembly of high speed rotating band knife, and a feed roller. In such a system the roller feeds the component into the machine and passes it over the rotating knife at a pre-determined speed. The pins are positioned over the knife and are aligned in the direction of the knife. When the correct pins are pressed over the leather at the right time and with the correct amount of time duration and force, then sections of leather are engaged with the knife, and a desired cut pattern is produced on the component. Matrix skiving has then been taken place. This is a continuous system of operation since the workpiece does not stop its travel during the entire duration of the process.

In the practical study of the system an existing leather splitting machine was employed whose feed roller and band knife proved to perform successfully for test purposes. It was established in this chapter that pin diameter, pin spacing, and the speed at which the leather component is passed through the system are the important parameters that affect the quality of the results. For this reason, matrix pin assemblies were manufactured to cater for pin diameters of 3, 4, and 5 mm, and pin spacings of 1, 2, and 3 mm. Provisions for achieving linear speeds of 0.03, 0.05, 0.07, and 0.09 ms<sup>-1</sup> were provided for the feed roller. Use of a d.c. solenoid was made to apply sufficient force through a cam on the pins so that they could in turn press the leather component against the band knife. The solenoid assembly was allowed controlled travel along the pin array so that when energised a straight line of matrix skiving can take place. Furthermore, because it is



important to determine the correct magnitude of the force that is required to press the pins against the leather, a load cell was designed and mounted in cascade along the solenoid plunger so that applied forces during each test could be measured. While the quality results were directly measured from the test samples, use of a personal computer and a data acquisition system were made to collect and store the measured force values.

Experiments were conducted on the leathers type-1 and type-2. The results indicate that for both leather types, lower pin diameters and pin spacings produce better skiving quality results, while variation of feed speed does not significantly affect the results. The mean skiving force values fall in a range bound by 32.8 and 41.6 N.

Finally, correlations were made to interpret the results with physical properties of leather. Referring to the conclusions of the work in Chapter Three, leather flexural rigidity and hardness were noted to affect the matrix skiving results more significantly than any other. Whereas more rigid leather components produce better surface quality in matrix skiving, harder components result in poorer surface quality.



## **CHAPTER SEVEN**

### **INTEGRATION CONSIDERATIONS FOR AUTOMATION**

#### **7.1 Introduction**

It was shown in the previous chapters that two inherently different principles exist that can be considered for the automation of leather skiving process in shoe manufacturing industry. The first involves the application of high speed milling operation on leather components, while the second relies on the action of a band knife and a linear array of independently actuated pins to achieve skiving. However, the work that has been so far presented concentrated on the fundamentals of cutting with the aim of flexible automation in mind. For each principle, important machine parameters were identified and their operational ranges were examined. Investigations were also conducted to determine the dependency of the results such as quality of surface finish and speed of operation on the materials properties.

In recognition of the aims of this work, which are fully described in Chapter One, this chapter will be concerned with the examination of systems automation of the two cutting principles that were considered. In the introduction of these principles, in Chapter Two, possible methods for their automation were briefly described. In this chapter, however, automation methods are more rigorously considered. In doing so, integration of the machines based on each of the cutting principles with other elements such as parts recognition and transportation systems is examined.

Initially, general aspects of the automation system are discussed. Then, methods for component recognition and transportation are presented. Later, important design elements are outlined for the automation of skiving process based on the two cutting principles that were described in previous chapters.



## 7.2 General systems considerations

Automation of the skiving process must be compatible with the automation of other processes in the manufacture of shoe uppers. In Chapter One it was mentioned that research is continuing to automate other shoe upper manufacturing processes in parallel with the skiving process. Examples of these include automation of 'stitching' process at Hull University [45], and automation of 'stitchmarking' process at Durham University [4]. Furthermore, in other areas of shoe manufacturing automation work has progressed such as automation of 'last cementing' process at Lancaster University [46]. With these processes being automated one after the other, *islands of automation* in a typical shoe manufacturing factory may be envisaged in the intermediate term. The vision for the long term is however one of implementation of a *Computer Integrated Manufacture* (CIM) environment for the shoe industry. This requires the complete 'compatibility' and 'standardisation' of each of the automated processes so that the flow of work-in-progress is achieved uninterrupted by the human operators. Process compatibility is achieved at the machine hardware level. Physical components incorporating in the machines are so designed that strategic characteristics of the automated cells such as method of parts recognition before the operation, transportation within the cell, and speeds of operations, are comparable. Process standardisation is concerned with the inter-communication of the machine cells and is primarily achieved at the software level. It is the process compatibility of the skiving cell that is of main concern in this chapter.

Throughout the work on the fundamental aspects of cutting mechanisms in both machining and matrix skiving methods that were described in the previous chapters, emphasis were placed on achieving a *flexible automation* objective. The automated skiving cell must be capable of accepting any shoe part of any size and model, 'thrown' on a conveyor belt at any orientation, achieve skiving within the specified accuracy, and in a speed that is comparable with the speeds of operations of the cells before and after the skiving cell. The main features of such a cell comprise a parts recognition system, the skiving machine, a series of conveyer belts to transport the shoe components, and computer software to control and operate the combined system. When all these elements are made to interact together successfully, then, system integration within the cell has taken place.

Some elements of an envisaged integrated skiving cell have already been developed during the course of the investigation of the automation of other



processes. When these elements were developed, they were intended to be used in conjunction with any other process that would be automated at a later stage. A system of component recognition is one such element. Another, is the research into parts transportation. Although the extent of development of the former has been much more than the latter, both areas can be usefully exploited in designing a skiving cell. More detailed description of these elements are given in the following sections.

### **7.3 Component recognition system**

Much thought have been given in choosing the correct recognition transducer in the automatic manufacture of shoe upper projects. Commercially available recognition systems are designed for general applications. Consequently, they were thought to be unable to provide the optimal solutions for the specific applications in shoe upper manufacturing. A purpose-built system was therefore required. The system that needed to be developed could be relatively simple to cater for the recognition of the two-dimensional shoe components. Also, each shoe component can be assigned to a particular class of components in terms of size, model, etc. This makes the system deterministic. Albeit, there are several problematic areas of object recognition when dealing with shoe components. Firstly, at any given time there may be up to 50 different design varieties in a typical shoe manufacturing factory. Considering that there could be up to 18 half sizes, and up to 20 individual components per pair, then the total number of individual component variations could reach a figure of 18000 [4]. Furthermore, there are usually very similar components where the area difference between them does not exceed 2%. There are also mirror imaged components. These pose certain complexity in the recognition exercise of shoe components. Therefore, a system was required that was capable of overcoming these problems, as well as meeting the specifications for speed, accuracy, reliability, cost, and other matters concerning environmental susceptibility.

An optical recognition system, based on machine vision, was developed by BUSM at City University to provide for the general needs of any future process automation in shoe manufacturing [47]. This system was further refined and optimised in the course of the stitchmarking automation project [4]. It uses a solid-state linescan imaging transducer to view and scan straight lines of the passing shoe component as it passes over a high frequency fluorescent tube. The tube provides illumination, from underneath the passing component, so that the edges



of the component can be determined. The sensing transducer, or the camera, is focused on the component and the image is obtained by dividing the view area into a matrix of discrete picture elements, called *pixels* [48]. Each pixel has a value that is proportional to the light intensity of the portion of the scene. The linescan device that is mentioned above is a 2048 pixel device, giving a digitised cell size (resolution) of 0.203 mm, and a pixel spacing of 13  $\mu\text{m}$ . This gives a total imaging width of  $(2048 \times 0.203) = 415.7$  mm. Each line scan takes 1.1 m.sec. of time.

A binary vision system is used so that the light intensity of each pixel is ultimately reduced to either two values, white or black, depending on whether or not the light intensity exceeds a given threshold level. Because shoe components are of two-dimensional shape, only one camera is needed to perform a complete image of the silhouette of the component. The vision system works in conjunction with a system of conveyor belts as shown in fig. 7.1.

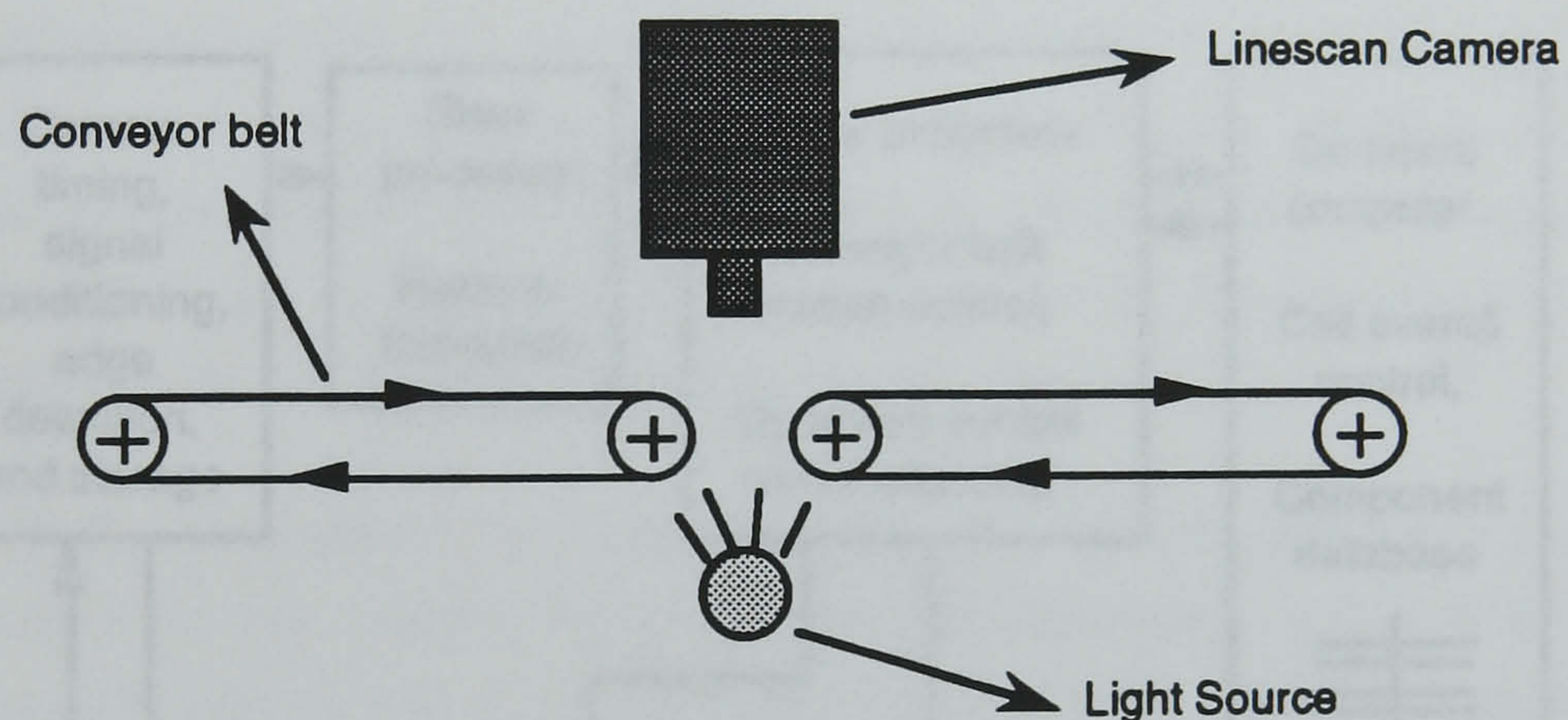


*Figure 7.1* Diagram showing the vision system and the conveyor belts.

Referring to fig. 7.1, the camera is mounted above the gap between two conveyor belts which are driven with the same velocity. The leather component is passed by the belts from over the gap so that the camera could scan the component in a form of series of lines. A light source underneath the gap provides a clear differentiation between the passing component and the surroundings. This can help the object outlines be more easily detected. The image information thus



obtained by the camera is used to describe the position, orientation, and the type of component on the conveyor belt. Data acquisition is obtained by the line scanning of the component, while shape recognition is achieved by a suitable method of feature extraction. In the system that was developed by BUSM, the component's centroid is determined and used to detect the position of the component on the conveyor belt. Also, calculations are performed to obtain the principal axis of the second moment of area of the component shape, so that its orientation could be determined. These calculations are achieved by means of a 'slave' 16-bit microprocessor while a 'master' 16-bit microprocessor is used to control the conveyor belts drive system. A personal computer with a 386 processor board provides an interface between the master processor and the particular shoe processing machine in question. It also holds a data base that keeps the details of each component shape. It is calculated that the time duration of the scan and recognition of a typical shape takes 2.9 sec. Fig. 7.2 gives a block diagram presentation of the integration of vision system with an operation station.

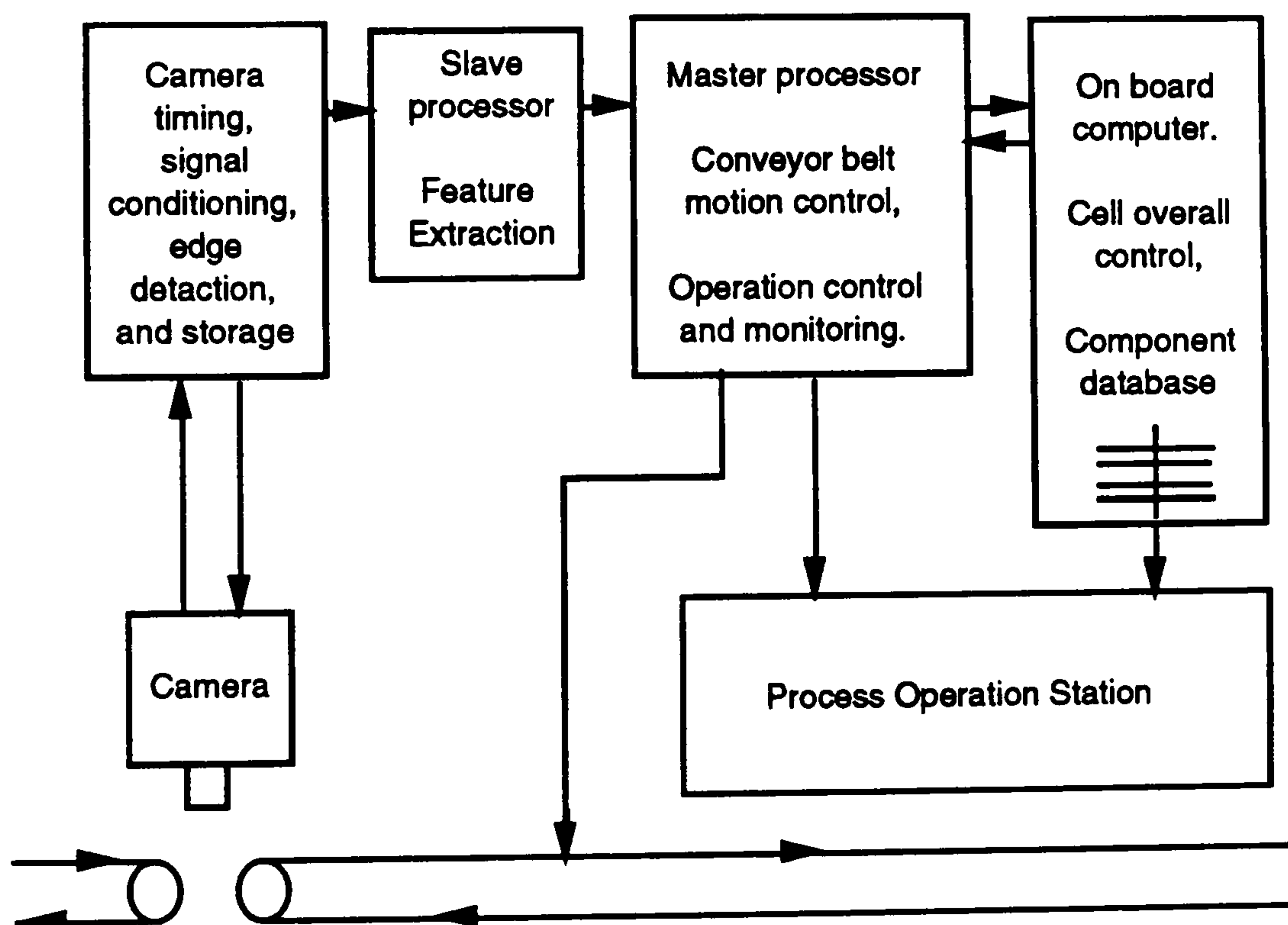


*Figure 7.2 Integration of the vision system with a process operation station.*



When a new shoe component shape is fed through the vision system, the camera extracts geometric features of the components before they are stored permanently in the computer data banks. If now a component is fed through the vision system whose features had been previously 'taught' to the computer, then its features are matched against the information held in the database. The component is subsequently recognised, and the system is now ready to send the component through the particular manufacturing operation in that cell.

#### **7.4 Component transportation system**

The concept of conveyor systems to transport parts between operation stations has been long established in the attempts to automate production lines [49][50]. Different conveyor systems can be configured to suit the requirements of the production environments in which they are designed. Muth and White produced a comprehensive survey of the research in the area of conveyor theory in which they classified the conveyor system [51]. Kwo investigated the theory of conveyors and concluded that his most important result was the observation that a conveyor is not an isolated object; it is part of a large system [49]. In that system, two or more conveyors may be allowed to interact with one another, as well as with other elements or processes. These interactions are subject of further dynamic analysis involving parameters such as speed of travel of parts, their inclination in space, mass and dimension properties of the parts, contact forces between the parts and the platform on which the parts rest, and so on [52].

In the manufacturing automation of shoe uppers, conveyor belts are thought to be the best solution for component transportation to and from the vision station and the particular shoe manufacturing station within a cell. The advantages of belts are that they provide fast means of operation, are inexpensive, and give comparatively little problem in handling flexible objects such as leather components. In a belt system, the components are placed on the belt surface and travel along the moving pathway. The belt is made into continuous loop so that half of its length can be used for delivering components, and the other half is the return run. It is supported by a frame, and at each end is connected to driver pulleys that power the belt.

The conveyor belt system that is used in conjunction with the camera vision system is of closed-looped industry-standard toothed belt system. The belts are driven by the output pulses of the same stepping motor control drive to achieve identical motions. To be compatible with the resolution of the camera, a 0.203



mm step size is used by the motor. The belts can produce a constant speed of  $0.185 \text{ ms}^{-1}$ .

Using this method of leather component transportation has not been completely trouble free. The leather components must be kept completely flat on the conveyor belts during the camera scanning process. In his research, Tout observed that thick and small leather components travelling on the conveyor belts have the greatest tendencies to move sideways during the accelerating and/or decelerating of the belt [4]. For these reasons he mounted a series of soft unskinned polyurethane coated rollers (of 23 mm diameter) on the conveyor belt so that the component is transported on the belt, trapped underneath these rollers. He concluded that the effects of these rollers were negligible, and explained that “the (undesirable) movement was caused by the backward components of the force caused when the component had to lift and drive each roller as it passed underneath”. In his later investigation, Tout found that if a leather component had been pulled on the belt in a given direction, then, unlike the first time, any further pull in that direction requires little force. This suggested that the degree of movement of a leather components on the conveyor belt is dependent upon the history of its immediate past movement. The characteristic nature of the fibrous structure of the leather component is thought to be responsible for this behaviour.

Furthermore, in a more recent investigation, the cumulative error, or “drift” properties of leather was studied in more detail [45]. This is a property of leather when handling of leather components are achieved using rollers. In this study it is suggested that drift is closely related to the compressive properties of the workpiece, such that, increase in compressibility results in increase in drift. It is further concluded that the most practicable arrangement involves the use of a ‘soft plastic’ upper roller against the fibrous side.

In a skiving cell it is required to transport the component with the fibrous side facing up. However, if upper rollers are used, it is anticipated that the component’s tendency to lose its original position on the belt is sharply reduced when the fibrous side is facing up. This is because that a much less complicated surface finish at the grain side of a component lends itself to a more predictable dynamics. Clearly more research will be required to examine the automatic handling of leather workpieces with the fibrous side facing up.



## **7.5 Integration of the high speed machining system**

The system of high speed leather machining that was described in the previous chapters relies on the leather component being clamped on a platform which is stationary. In that system, the cutting tool spindle is intended to move in a three dimensional cartesian coordinate system. The reverse could also be configured, whereby the cutting tool post is fixed and the platform assembly could describe the linear motion to generate the necessary feed. In any case, it is assumed that conveyor belts are used to transport the leather components within the skiving cell and thus, as in a conventional system, the motion of the component comes to a halt for the duration of cutting. The system is thus not a continuous process. If however, the system is to be viable in terms of compatibility with other potentially automated shoe manufacturing processes, then compensations will have to be made in its cell design so that its speed of operation, or the cell production rate, can be justified. This is measured against other factors such as design complexity, reliability, and cost. To this end, a method of continuous machining operation, whereby the component does not become to a halt, is also suggested. This will make the system continuous. In both cases the cutting head assembly can employ a modern computer-controlled 3-axis cartesian motion control system which has been well developed in the area of machine tool technology [48][53].

Efficient and effective component clamping in automatic leather machining remains an important challenge to the problem. Various techniques have been suggested to clamp/grip flexible materials such as leather automatically [54][55]. Vacuum technology however offers a more readily available solution [56]. In this section primary design considerations concerning the automation of skiving by way of leather machining are outlined. Initially, the concept of vacuum technology in relation to leather clamping is introduced. Then, practical machining station configurations are discussed. The characteristics of the skiving cell is finally proposed.

### **7.5.1 Component clamping**

It was mentioned earlier that vacuum technology can be used to clamp leather components for the purpose of machining. This technology relies on holding the workpiece by the suction power produced as a result of an induced negative pressure (vacuum) in a chamber (or cup). A vacuum pump is used to



achieve this. To produce this vacuum, it is necessary to draw air out and this should be done as economically as possible. The amount of energy required to draw the air out increases asymptotically with the increase in the level of vacuum. It is therefore costly to produce a higher vacuum than is required. For example, if an energy factor of 10 is required to produce 60% vacuum, this will increase to 100 for 90%, 1000 for 99%, and 10000 for 99.9%. Relating this information to a 50 mm diameter suction cup would have a holding power of about 176 N at 90% vacuum (energy factor of 100), whereas a 60 mm diameter cup at 60% vacuum would have the same holding power but an energy factor of only 10. This thus represents a significant reduction in energy cost. It is therefore better to increase the holding area and reduce the level of vacuum. Fig. 7.3 shows a sectional view of a vacuum cup with a circular inlet. According to this figure, the suction force  $F$ , measured in N, is obtained by the following formula [57]:

$$F = \frac{[P^-] \times A}{n} \quad (7.1)$$

where  $A$  = the area of the suction cup ( $\text{m}^2$ )

$[P^-]$  = negative pressure (-Pa)

$n$  = safety factor (= or  $> 2$ )

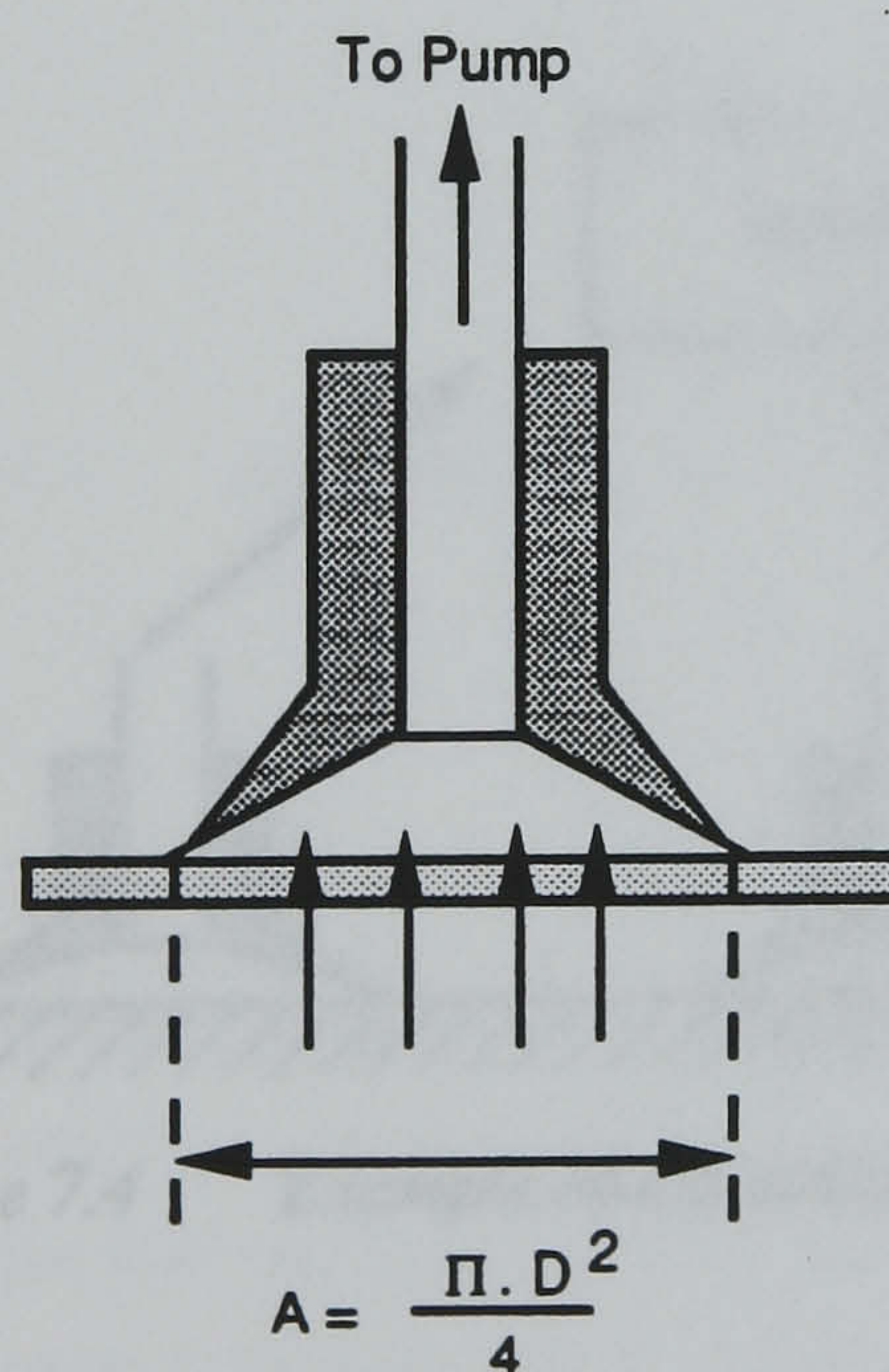
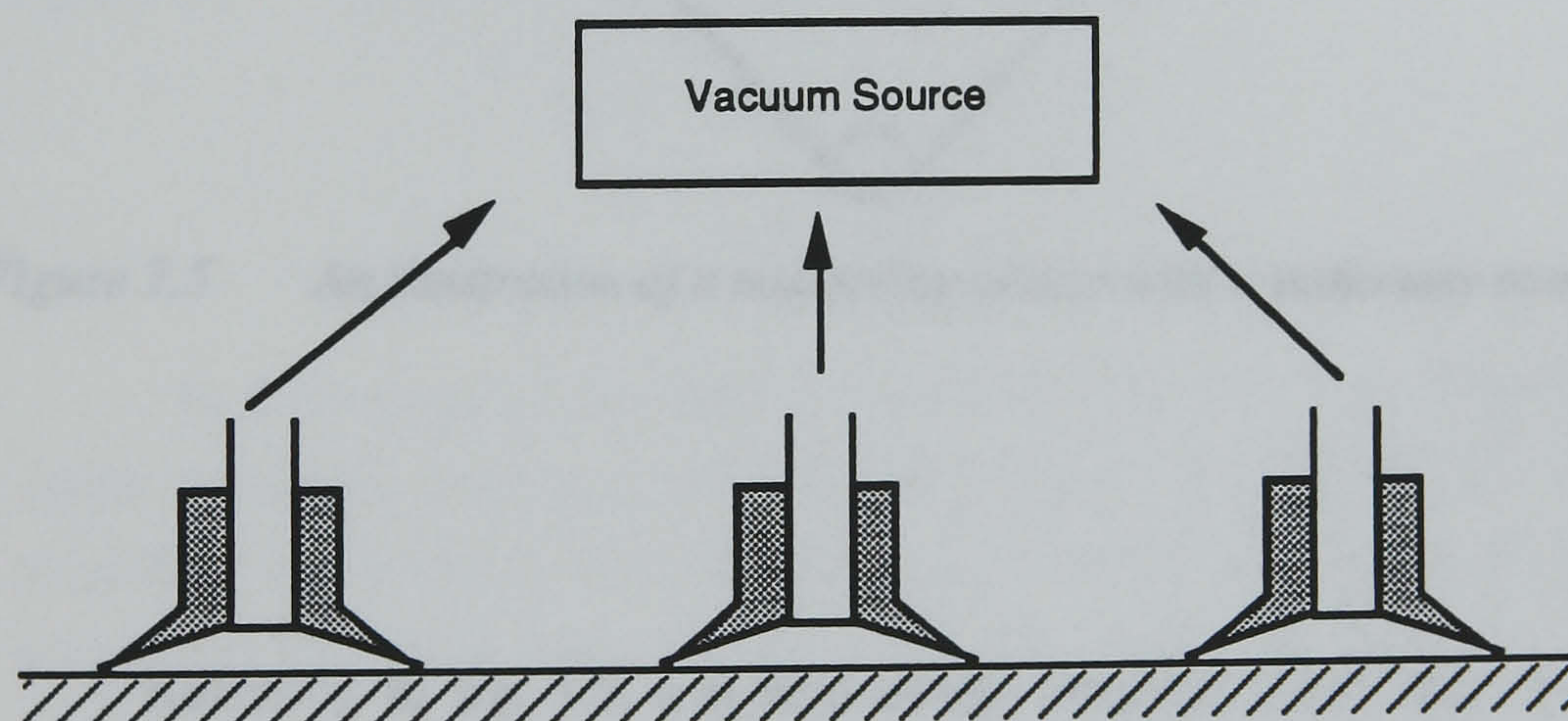


Figure 7.3 Sectional view of a vacuum cup with circular inlet.



The application of vacuum technology in clamping flexible leather components on the machining platform requires a system of distributed suction chambers. This can be realised by employing a perforated work-top on which the component is placed. This can take a form of a 2-D matrix of circular holes of a given resolution and hole diameter. The important design criteria here are the evaluation of correct hole size and matrix resolution for two reasons. Firstly, as discussed above, vacuum energy economy must be observed. Secondly, for a given component shape, only those chambers that are covered by the component contribute to the clamping force. It means therefore that the rest of the holes remain uncovered, and this may result in significant vacuum 'leak' which sharply increases the energy factor in the system. This is a major design challenge of vacuum applications in the gripping/clamping automation of random shape flexible materials, and has been subject of much research in the recent years. Various attempts have been made to design an intelligent cellular vacuum matrix such that the required holding power is achieved in conjunction with minimum amount of leak. It is clear that such a system strives to obtain an optimum trade off between the matrix resolution and cost considerations. Fig. 7.4 shows a typical distributed vacuum system.

Whilst the design of efficient vacuum clamping system remain the topic of much research today, a system is proposed for the purpose of this work which has already been used in industry. This is described in section 7.5.2.



*Figure 7.4 Example of a distributed vacuum system.*



### 7.5.2 The high speed machining station

The simplest method of configuring a machining station is to employ a machining platform which is fixed relative to the cutter, and is capable of automatic clamping/unclamping the components of various shapes and sizes. The machining is achieved when the cutting head mechanism is able to describe the skiving profile using a computer-controlled 3-axis system. An important design consideration in such a machining station in which the clamping platform is stationary, involves the method of parts transfer to and from the platform. This can be achieved by delivering the shoe component to a special skiving belt where vacuum clamping can take place. The cutting head assembly is placed directly above the vacuum belt. This configuration is illustrated in fig. 7.5.

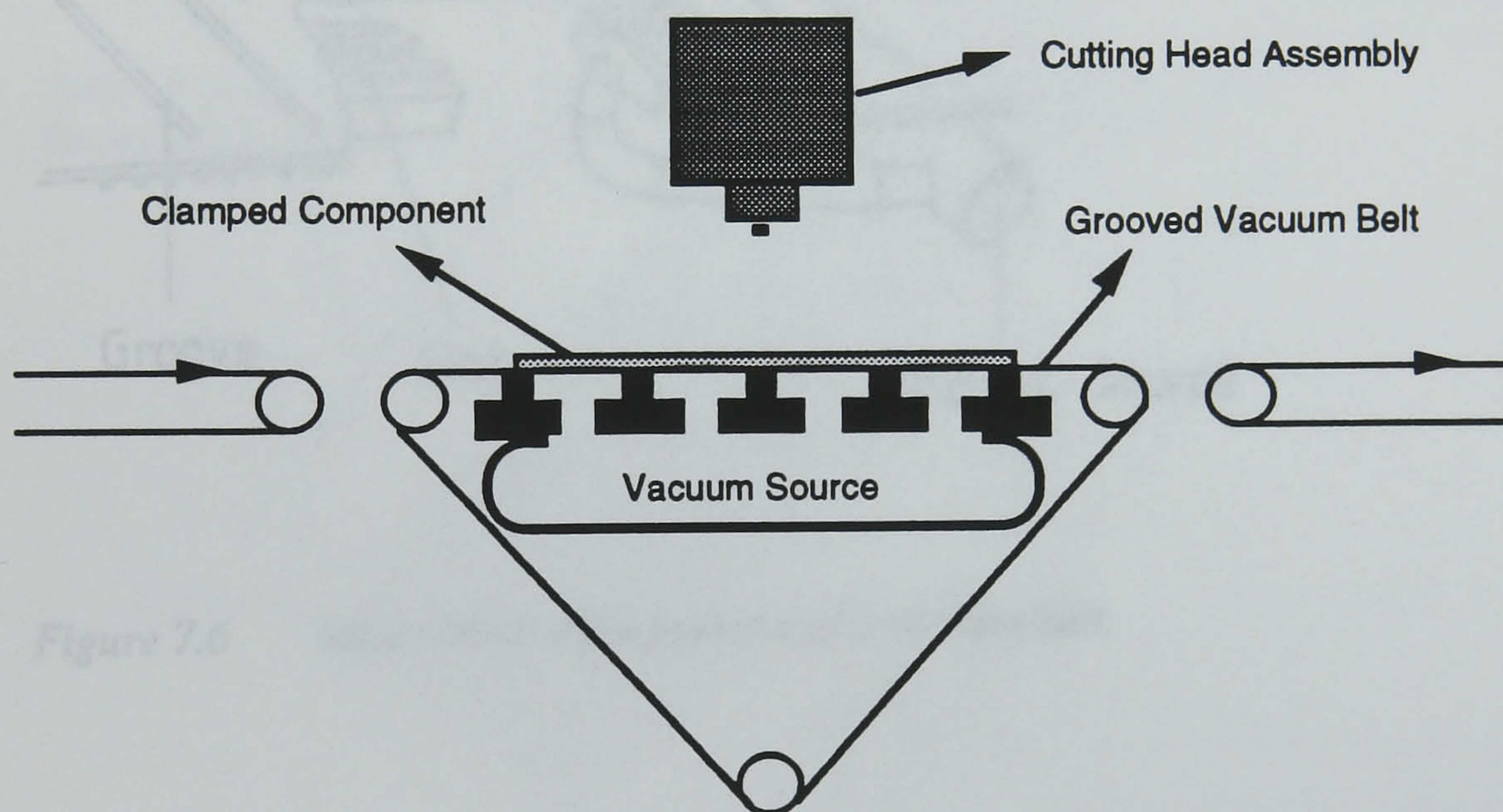


Figure 7.5 An illustration of a machining station with a stationary component.

Referring to fig. 7.5, a typical design employs a belt that clamps the component by suction created in the closely spaced shallow grooves extending nearly the full width of the belt surface. The belt's effective clamping length is placed over a vacuum table. A hole in the centre of each of the belt grooves is positioned directly over a slot running the entire length of the top of a vacuum



chamber. Specially designed guides on either side of the slot provide a vacuum seal. A vacuum pump is employed to produce the necessary suction power.

For the duration of the clamping a partial vacuum is created under the component by continuously evacuating air from the vacuum chamber by the pump. The vacuum spreads into the belt grooves through the belt holes and the slot cut along the top length of the vacuum chamber. Fig. 7.6 shows a vacuum belt revealing its incorporated vacuum system.

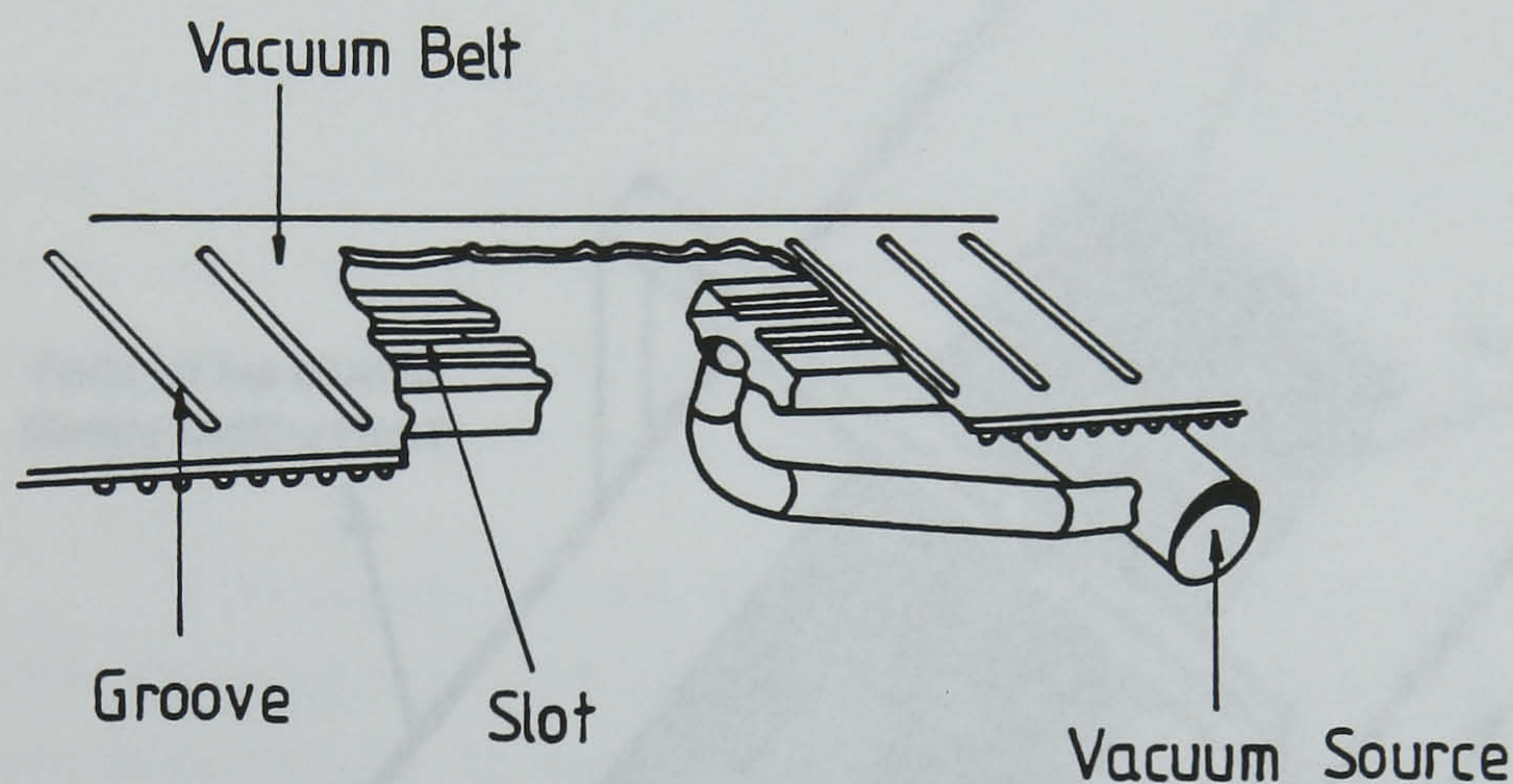


*Figure 7.6 Illustration of the features of a vacuum belt.*

In such a system the shoe component has already been identified by the vision recognition station, and thus its position, orientation, and other data regarding the skiving location and machining conditions such as cutting speed are extracted from the data base available in the associated computer.

So far it has been generally assumed that, to achieve high speed machining, it is required to bring the leather component to a halt while machining. This is however a traditional approach where, in a fixed frame of reference, either the workpiece or the cutter is stationary relative to the other. It is nonetheless



conceivable to achieve a manufacturing operation on a moving workpiece while keeping its relative motion with respect to the cutter unaltered. An example of this is the process of "flying shear", where sections such as extruded pipes are cut off as the workpieces lie on a moving conveyor system. In a machining example, the cutting head assembly can be envisaged to be attached to a computer-controlled moving gantry mechanism which is positioned above a conveyor belt carrying the leather components. This configuration is schematically illustrated in fig. 7.7.

length of machining that is now required as a component in the work

When the components enter the effective machining zone, the cutting head assembly positions itself at a pre-determined position above the conveyor belt and assumes a linear speed identical to that of the belt.

of the cutter with respect to the workpiece is zero. The speed of the workpiece treated as its reference speed. From this point onwards the cutting head moves backwards and forwards relative to the workpiece and the cutting head moves in the usual way. It is a computer-controlled system which can perform the work in the usual way. It is a computer-controlled system which can perform the work in the usual way. It is a computer-controlled system which can perform the work in the usual way.

If the system is to be used for the machining of a component, then, changing the speed of the workpiece and the speed of the cutting head drive system is necessary. In this case, the speed of the workpiece is changed by the conveyor belt drive system and the speed of the cutting head is changed by the gantry drive system.

parts using a computer-controlled system. In this case, the speed of the workpiece is changed by the conveyor belt drive system and the speed of the cutting head is changed by the gantry drive system.

industry. In this case, the speed of the workpiece is changed by the conveyor belt drive system and the speed of the cutting head is changed by the gantry drive system.

being produced by the system. In this case, the speed of the workpiece is changed by the conveyor belt drive system and the speed of the cutting head is changed by the gantry drive system.

hole in the belt material. In this case, the speed of the workpiece is changed by the conveyor belt drive system and the speed of the cutting head is changed by the gantry drive system.

the vacuum spreader is used to pick up the workpiece and travel its length, the vacuum spreader is used to pick up the workpiece and travel its length, the vacuum spreader is used to pick up the workpiece and travel its length.

zero as each belt hole passes under the vacuum spreader.

The system that is shown in fig. 7.7, the leather component is assumed to have entered the machining station, firmly clamped on a conveyor belt which is moving at a fixed speed. It is further assumed that the recognition system has just

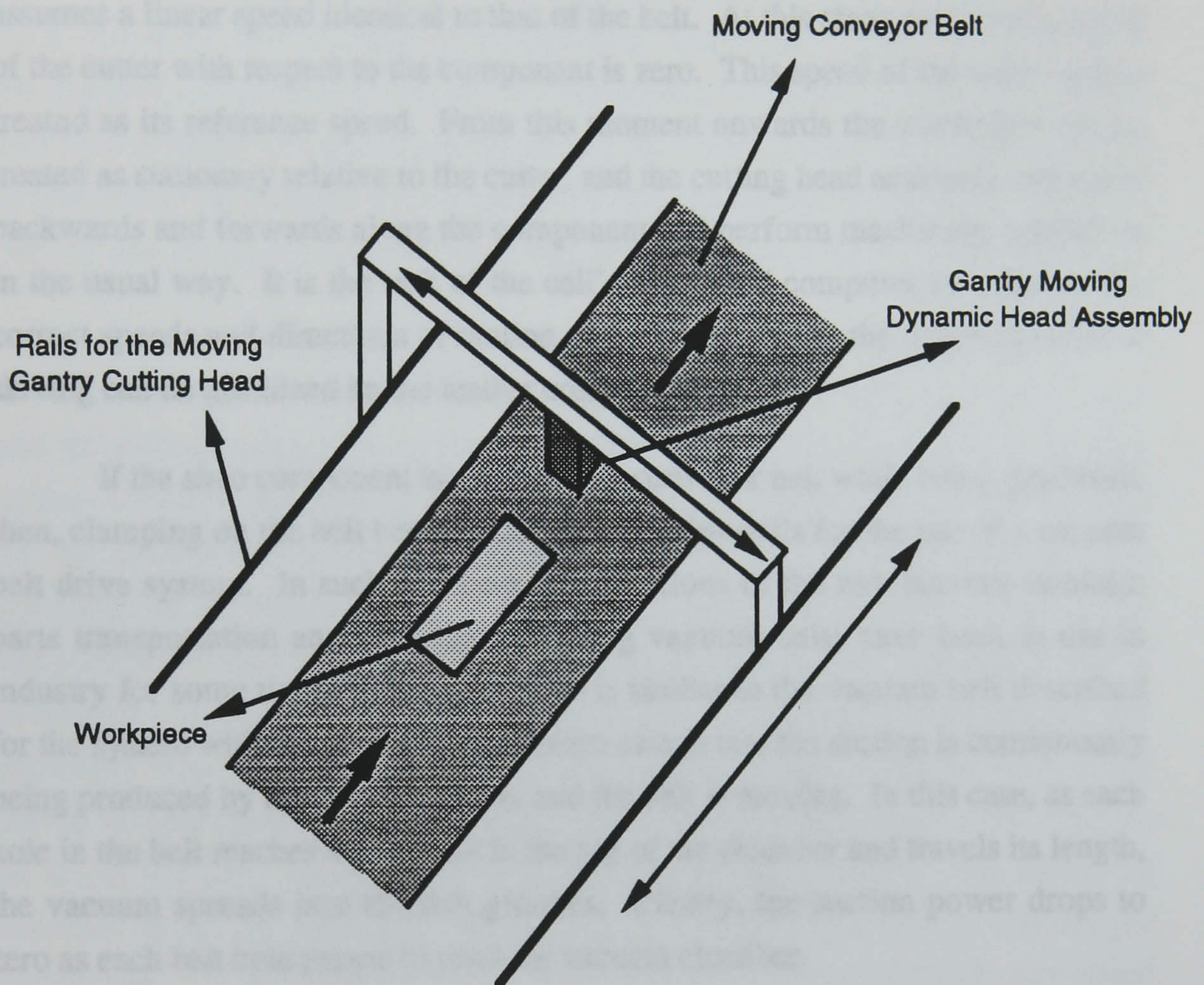


**Figure 7.7** An illustration of a moving gantry type machining station.

In a system that is shown in fig. 7.7, the leather component is assumed to have entered the machining station, firmly clamped on a conveyor belt which is moving at a fixed speed. It is further assumed that the recognition system has just



identified the component in terms of its shape, size, location, and orientation, as well as the details of the machining operation including its location and shape profile on the component, and other cutting conditions such as cutting speed. These information are stored in the associated computer. For a fixed belt speed, a maximum span of operation is allowed so that all the necessary machining on a component can take place inside this span. The length of this span will depend on the speed of the conveyor belt, the feed speed of the cutter, and the maximum length of machining that is ever required on a component in real life.

When the component enters the effective machining area, the cutting head assembly positions itself at a pre-determined position above the component, and assumes a linear speed identical to that of the belt. At this stage the relative speed of the cutter with respect to the component is zero. This speed of the cutter is thus treated as its reference speed. From this moment onwards the workpiece can be treated as stationary relative to the cutter, and the cutting head assembly can travel backwards and forwards along the component and perform machining operations in the usual way. It is the task of the cell's integrated computer to calculate the correct speeds and directions of motion of the cutter so that the desired profile of skiving can be machined on the leather component.

If the shoe component is moving on a conveyor belt while being machined, then, clamping on the belt becomes necessary. This calls for the use of a vacuum belt drive system. In such a system, the functions of the belt become twofold; parts transportation and clamping. Moving vacuum belts have been in use in industry for some time [58]. Their design is similar to the vacuum belt described for the system with the stationary workpiece except that the suction is continuously being produced by the vacuum pump, and the belt is moving. In this case, as each hole in the belt reaches the slot cut in the top of the chamber and travels its length, the vacuum spreads into the belt grooves. Clearly, the suction power drops to zero as each belt hole passes beyond the vacuum chamber.

The system that is described above provides leather component machining while the component is moving. However, the advantages of such a system depend very much on the feed speed of the cutter as well as the belt speed. The aim is to be able to complete skiving of a shoe component in the fastest time possible. Assuming a given minimum time per component (taking into account that different components may require different amount of skiving), no definite conclusions can be reached with regards to the viability of this method in terms of its production speed without further investigation.



The preceding discussion suggests that dedicated machinery can be designed and built towards the design of a leather skiving station based on high speed machining principle. The specifications and the detailed design of such a station will depend on the findings of the investigation of an automation research rig that will have to be built. This investigation will also include evaluation and optimisation of the rig so that important specifications such as production speed and accuracy can be obtained.

### **7.5.3 Overall cell operation**

In this section the case of a system of machining where cutting takes place on a stationary shoe component is discussed. In this system, therefore, the main elements of the automatic skiving cell comprise of a conveyor belt to deliver the component to the vision recognition station, the vision recognition station, another conveyor belt to transfer the component to the machining station, the machining station, and finally a conveyor belt to exit the component from the skiving cell.

To evaluate the speed of operations of the system empirical values relating to a real skiving rig must be used. Some speed values relating to the vision system and the cutting feed speed are already known. Others such as skiving profile and cutting condition generation by the computer can be estimated based on the work on the stitchmarking automation project [4]. In this system the speed of the operation of the vision system including scan and recognition is 2.9 sec. The transporting of the component from the vision station to the machining station is estimated to take about 1 sec. The time taken for the computer to generate the necessary data regarding the cutting conditions from the database, such as the correct cutting speed and depth of cut, as well as the skiving profile is estimated to be about 0.3 sec. As far as cutting is concerned, the speed of the operation depends on (a) the feed speed of the cutter, and (b) the length of cutting per component. On the assumption that the maximum feed speed of  $0.09 \text{ ms}^{-1}$  tested in this work is used, and achieving a maximum of 3 skiving lengths per component each typically 10 cm long [14], and allowing 1.5 sec. for the positioning/re-positioning of the cutting head assembly, an estimated average time duration of 4.8 sec. is taken for the skiving operation. The cumulative time that a shoe component can typically spend in a skiving cell, from the beginning of the vision recognition operation to the end of the machining operation, adds up to 9.0 sec. Table 7.1 illustrates the operation timings of this example.



Cell Operation per Component	Time (sec.)
Vision scan and recognition of component	2.9
Data generation of cutting condition and skiving profile	0.3
Transport component to machining station	1.0
Machining operation on component	4.8
<b>Total Time</b>	<b>9.0</b>

*Table 7.1 Time evaluation of a typical component visit to the machining cell.*

In present day skiving technology, a range of values for the speed of the operation by the human operators varies from 2.67 to 9.38 sec. depending on the length and complexity of skiving pattern [59]. However, a comparable skiving time achieved by an operator in terms of the complexity of the above example is 8.28 sec. This figure is very close to the estimated figure of 9.0 sec. in the automation analysis. It can therefore be concluded that, though the timing analysis in this section is partially based on certain assumptions, the objectives of the project in terms of speeds of operation can be realistically reached. Clearly, further improvements such as increasing the feed speed achieved by the cutting head assembly and decreasing the computational time for feature extraction in the shape recognition system will increase the production rate of the system.

Machine accuracy and repeatability are two important features of a machining cell. Considering the machining station in isolation, accuracy is a measure of the control system's capacity to position the cutting head assembly at a desired location, and will depend primarily on the machine control resolution. This is defined as machine's capability to divide the range of a given axis



movement into closely spaced points that can be identified by the cutting head assembly controller. If stepping motors are used to drive the cutting head assembly through its three orthogonal axes, then the size of the step angles of the motors determine this resolution. On the other hand, machine repeatability is the ability of the control system to return to a given location that was previously programmed into the controller. Mechanical errors such as gear backlash, leadscrew play, and other inaccuracies in the mechanical positioning system impact on the machine's accuracy and repeatability.

## **7.6 Integration of dynamic matrix cutting system**

The dynamic matrix skiving is fundamentally a continuous operation where the component continues to travel at its maximum possible speed while being skived. This is the main attraction of this system. Another attractive aspect of matrix skiving is that the actual process of cutting is achieved by a band knife; a cutting method that has been successfully employed in the component splitting process in the shoe manufacturing industry. Furthermore, the dynamic matrix skiving system is mechanically simpler than the high speed machining system, and hence is not subject to similar mechanical positioning errors. The combination of these aspects makes the dynamic matrix skiving method a ready candidate for the implementation of flexible automation in skiving. The work that was carried out and described earlier in this thesis had the objective of investigating some of the critical and important parameters that can affect the quality of the results such as matrix pin diameter and spacing. In this section various considerations in the design of an automated skiving cell based on dynamic matrix skiving are discussed. To this end the functional elements that exist in the cell are outlined.

An envisaged dynamic matrix skiving cell comprises of a vision recognition station to identify the shoe components, conveyor belts to transport the components within the cell, and a skiving station. The details of the conveyor belts and the vision recognition systems have already been discussed in sections 7.3 and 7.4. In the following sections a typical configuration of a skiving station as well as an overall integrated cell operation are outlined.

### **7.6.1 The dynamic matrix skiving station**

The main features of a dynamic matrix skiving station include a base structure comprising a band knife mechanism, a supporting plate for the band



knife, a feed roller , and an assembly of linear array of pins positioned above the horizontal span of the band knife. This arrangement has already been fully illustrated in Chapters Two and Six. Additionally, for a flexible automated station these pins must have individual actuations. It is therefore required to provide individual actuating source for each pin. This can be achieved using a bank of solenoids although other means of actuation can be used. The decision on the choice of the method of actuation is more relevant to the machine development stage which will be affected by such considerations as force and power requirements, size, practical and environmental suitability, and cost. However, to demonstrate the principle of the system, d.c. solenoids are used in this work. Figs. 7.8 and 7.9 are the front and side views of an especially designed and constructed structure of solenoids, levers, pin bar assembly, and matrix pins. The pins diameter and spacing are 3 mm and 2 mm respectively. This bank of solenoid-lever-pin assembly was used to demonstrate the collective actions of the individual actuation of the pins in conjunction with the band knife rig described in the previous chapters. The design of this assembly, though adequate for the purpose of the conclusion of this research, requires further modification to cater for a more acceptable skiving resolution, ideally not more than 2 mm.

The solenoids can be connected to a microprocessor control board for controlled activation. It is therefore possible to generate any skiving shape on the computer, and down-load the data into the machine by sending the correct control and actuation pulses to the solenoids.



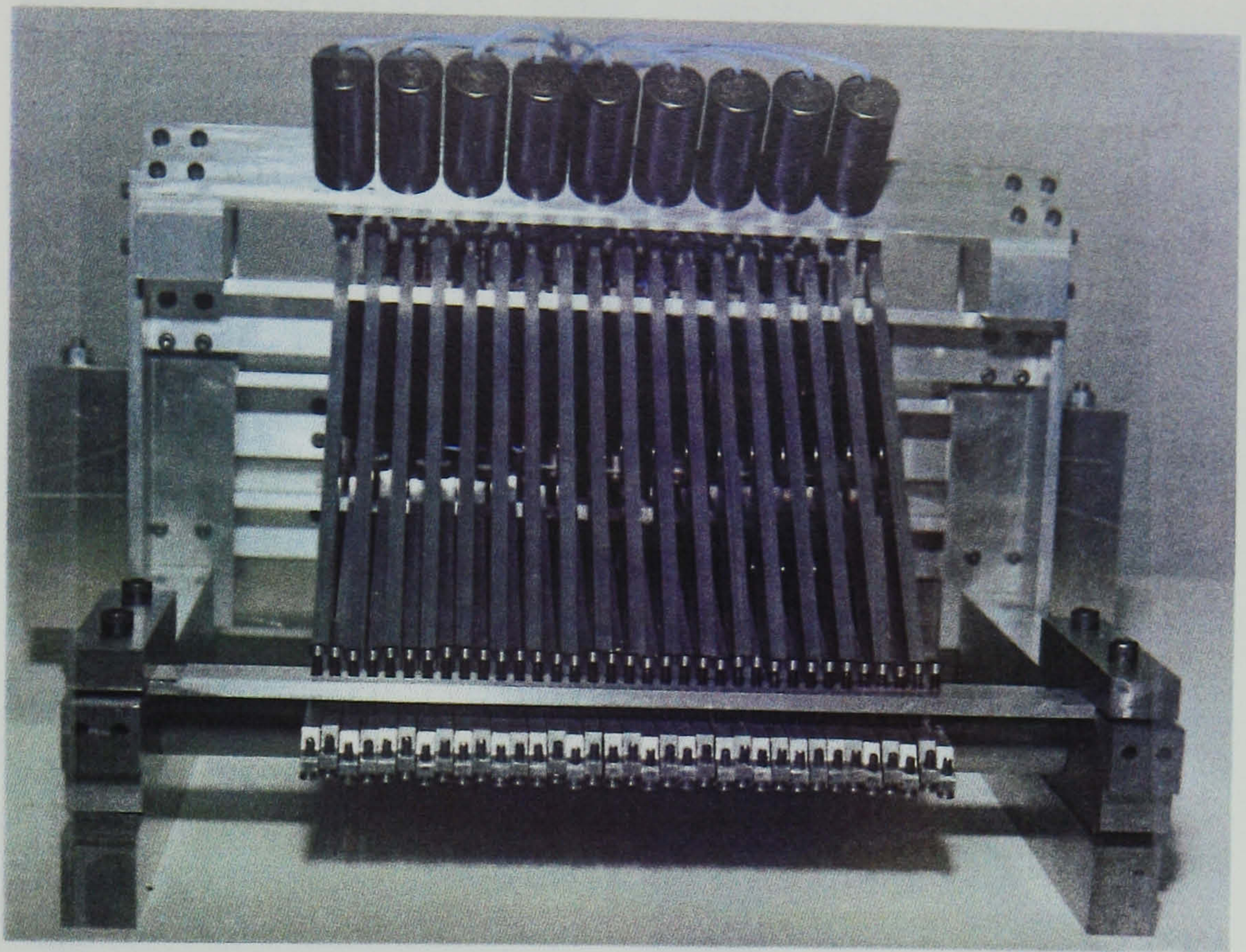


*Figure 7.8 A front view of the constructed bank of solenoid-lever-pin assembly.*

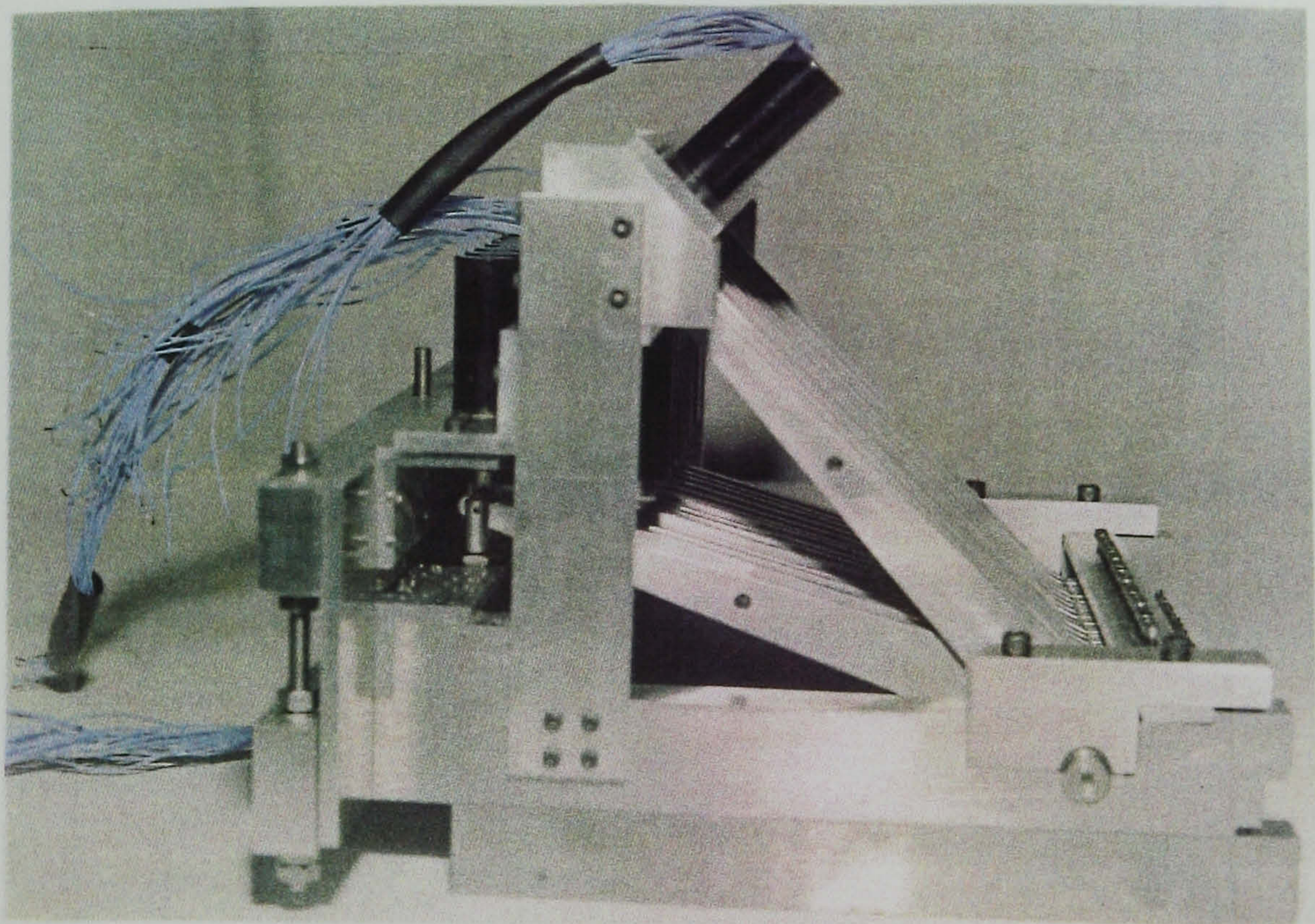


*Figure 7.9 A side view of the constructed bank of solenoid-lever-pin assembly.*



In order to transport the shoe component to the dynamic matrix skiving station a conveyor belt is used. Several arrangements can be envisaged to couple the belt with the machine, but the simplest is to directly connect the belt to the feed roller of the band knife rig. This arrangement is schematically shown in fig. 7.10. Referring to this figure, the belt is driven by the machines feed roller at one end, and is supported by another roller at the other end. After further modifications on the solenoids structure, the assembly was mounted on the band knife rig. The rig now included the essential features of a dynamic matrix skiving station comprising computer-controlled independently activated solenoids, a built-in conveyor belt transport mechanism, all mounted on a high speed band knife machine. This is shown in fig. 7.11.

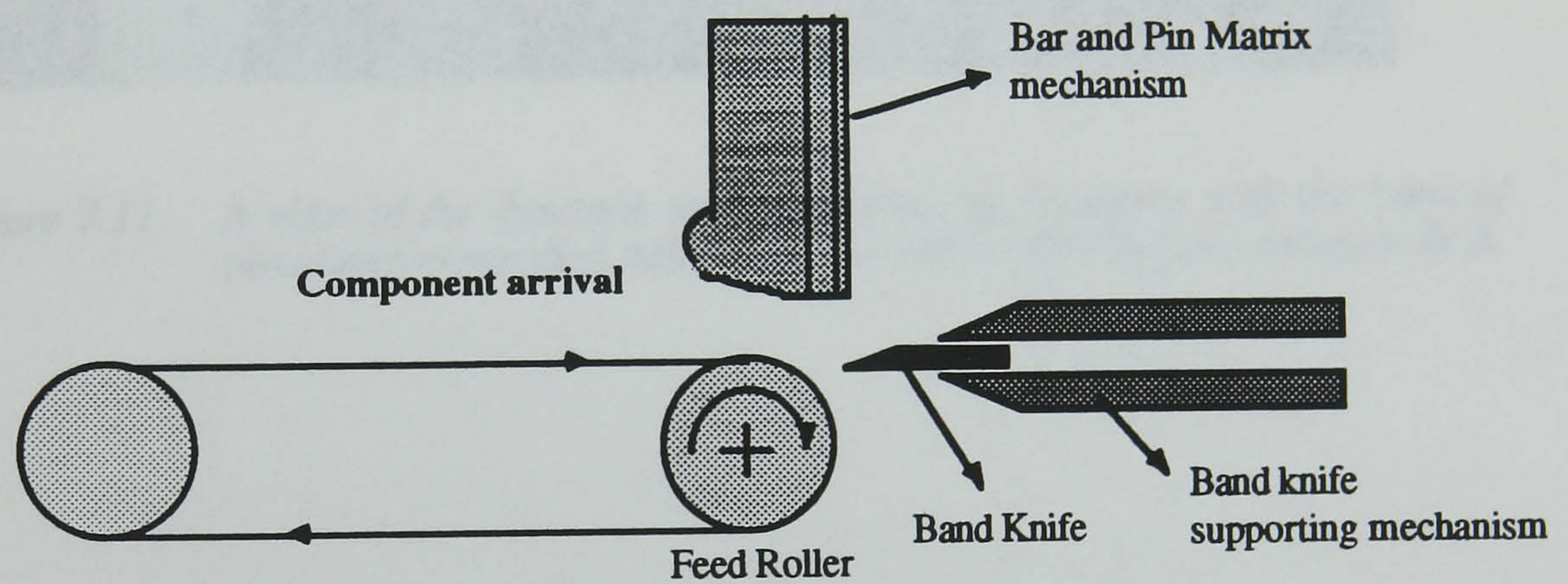


**Figure 7.10** *Integration of the feed conveyor belt with the matrix skiving station.*



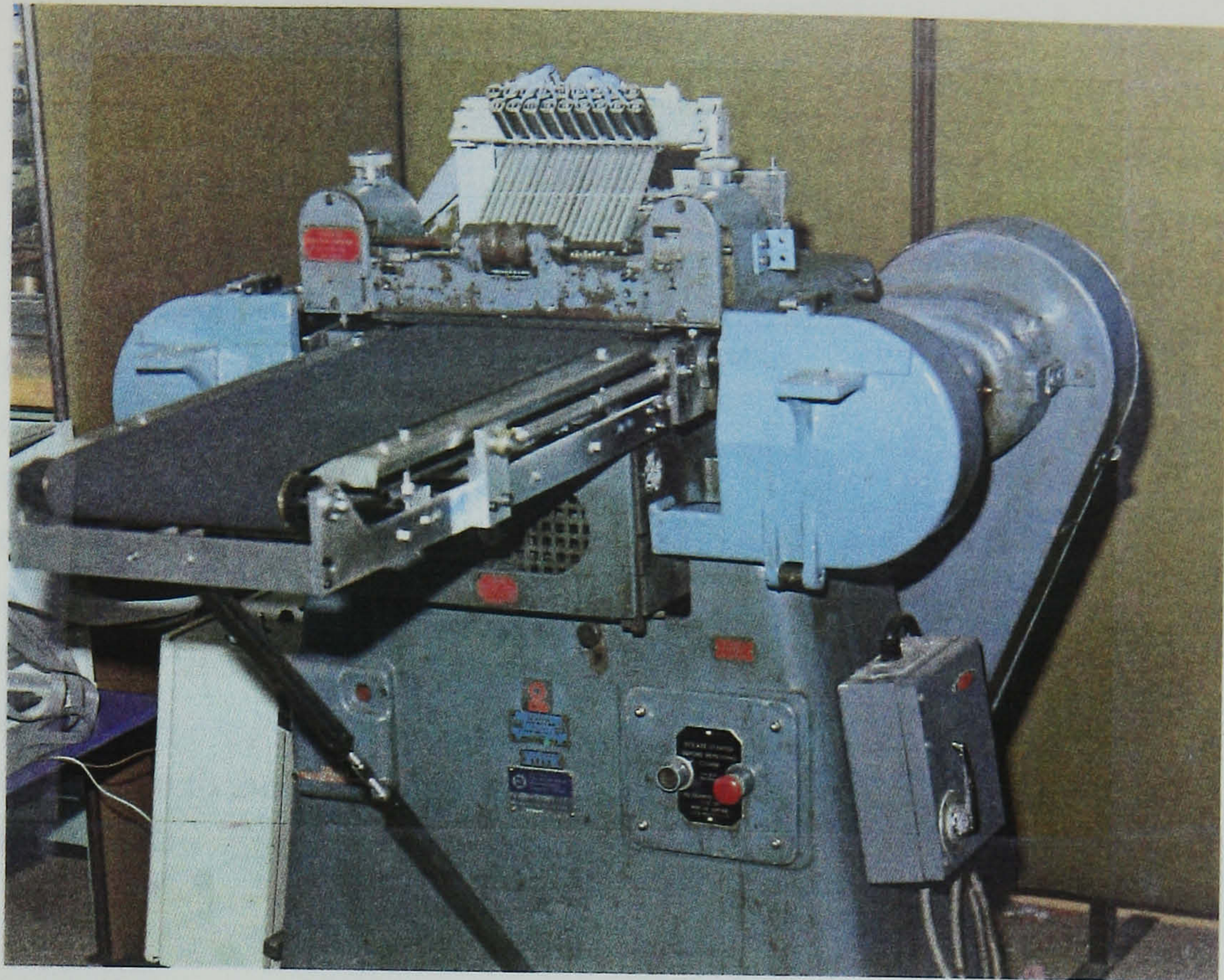


*Figure 7.11 A view of the dynamic matrix skiving rig complete with the bank of computer-controlled activated pins and a built-in feed conveyor belt.*

### **7.6.2 Overall cell operation**

An automated dynamic matrix skiving cell comprises of a conveyor belt to deliver the shoe component to the shape recognition station, the vision recognition station, the conveyor belt to transfer the component from the vision system to the skiving station, and finally the matrix skiving station. Once a component has been identified by the vision system, then its position and orientation on the belt, as well as the information regarding the skiving profile that corresponds to its shape, are determined from the computer data base. The skiving profile is then mapped into the computer processor responsible for the controlling of the solenoids, and instructive on/off pulses are sent to the solenoids to activate/de-activate the pins against the shoe component. Clearly, operation of the solenoids is accurately synchronised by the linear speed of the component carrying belt to avoid skiving profile distortion on the component.



According to the tests that were carried out in the work of Chapter Six, the skiving station that is described above is capable of at least  $0.09 \text{ ms}^{-1}$  speeds of operation. In this system the overall timing of the matrix skiving per component depends very much on the distance between the component recognition and skiving stations. This distance is determined by the maximum length of a shoe upper component. It ranges from a few centimetre for small components to 0.5 m for boot components. In the majority of the cases the maximum length does not exceed 0.25 m. Nevertheless, assuming a maximum distance of 0.5 m between the two stations and a component travel of  $0.09 \text{ ms}^{-1}$ , an estimate of total time per component visit to the cell can be obtained. From section 7.3, it takes 2.9 sec. to scan and recognise a component shape by the vision system. It also takes a further 0.3 sec. to generate data relating to the skiving profile. Based on the speed and distance assumptions above, a total of 5.6 sec. for a typical component to be transported to the matrix skiving rig, and be skived. The total component per cell time will thus amount to 8.8 sec. These values are shown in Table 7.2.

Cell Operation per Component	Time (sec.)
Vision scan and recognition of component	2.9
Data generation of skiving profile	0.3
Transport component to skiving station, matrix skiving	5.6
<b>Total Time</b>	<b>8.8</b>

*Table 7.2 Time evaluation of a component visit to the matrix skiving cell.*

The rig that was described in section 7.5 gives a 5 mm skiving resolution, while the resolution obtained by the vision recognition system is 0.203 mm. The



present rig is incapable of fully translating the shape of the skiving profile as held by the computer onto the component. Its resolution therefore must be significantly improved. Furthermore, due to the complexity of the nature of matrix skiving mechanism, the accuracy determination can only be achieved by way of experimental trial and error methods.

## **7.7 Conclusions**

In this chapter the basic configurations of a flexible automation cell based on the two cutting principles are outlined. At the beginning of the chapter it was pointed out that the design of an automation cell must conform to the global shape of the relevant CIM environment. In shoe manufacturing several process areas are strong candidates for automation. Work has already begun on a number of them including the process of skiving. As a consequence, it is aimed to create independent automation cells for a particular operation in the short to medium term, and an integrated environment in the long term. It is therefore vitally important to progress towards systems that are compatible. For example, it is intended that processes that are automated are continuous. That is to say, the workpieces continue travelling by the conveyor belts while being subjected to an operation, or at least the stoppage times are relatively small. Another example is that the same method of component recognition system be used before any operation so as not to duplicate work.

A system of linescan vision recognition that had been developed prior to the start of this project is proposed. This includes a camera to detect the edges of a two dimensional shape, a microprocessor to calculate shape features so that the component can be identified, and another microprocessor to control the component carrying conveyor belt as well as to communicate with the main computer to extract relevant operational data from its database.

A problem associated with the use of conveyor belts was discussed. This entailed moving of the leather component relative to the belt during belt acceleration/deceleration times. The conclusions of different studies on this subject reveal that both the history of the fibres' immediate past movement as well as their compressive properties are likely factors affecting the undesirable movements.

In designing a flexible automation cell for the machining principle, a method of vacuum clamping was proposed. The clamping takes place while the



component is either stationary on a conveyor belt, or the belt is moving. In the former case, a three-axis computer-controlled cutting head assembly machines the clamped component, and in the latter case, a similar head assembly is connected to a gantry structure that can synchronise its motion with the moving component before machining it. In both cases a design for a vacuum belt was proposed. It was estimated that for a typical component shape the total time of the component visit to the cell can be around 9.0 sec.

In the case of dynamic matrix skiving it was mentioned that this system is of a continuous nature, and can be readily integrated with other essential elements such as the conveyor belt, and hence with the vision recognition system. A bank of computer-controlled independently-activated solenoid-lever-pins, mounted on a band knife machine, can produce the desired skiving profile on the component. Accurate feed speed synchronisation with the action of the solenoids is necessary to avoid skiving profile distortion. An estimated time duration of 8.8 sec. for total operation time, based on a 0.5 m component length, was evaluated.



## **CHAPTER EIGHT**

### **CONCLUSIONS**

#### **8.1 Machining methods for automation**

It has been successfully demonstrated in this work that automation of the machining of flexible fibrous materials can be achieved by way of two different cutting principles. The first involves the application of high speed milling technology, while the second relies on the action of a band knife to remove the waste material from the workpiece. It has been further shown that while the second method can be directly implemented to achieve a continuous manufacturing system, further development work is required to implement the high speed milling method so that a comparable system may result, primarily in terms of operation speed. Leather as the workpiece in the manufacture of shoe uppers has been used throughout the work.

The experiments that were carried out in both systems were aimed to produce a set of optimum cutting condition so that satisfactory surface finish could result with a maximum speed of operation. These included determining correct values for the rotational cutting speed (given a fixed cutter diameter) and the cutting tool rake angle in the case of high speed machining, and matrix pin diameter and spacing in the case of dynamic matrix skiving.

In both machining methods similar leather types were employed as the workpiece. Furthermore, an identical production speed range, with a maximum speed of  $0.09 \text{ ms}^{-1}$ , was used in both systems. The effects of material physical properties were also examined. In the case of high speed machining system, samples taken from the fluffy regions of the original hide resulted in poorer surface finish. This was thought to be related the stretchability of the fibres in these regions. In the case of the dynamic matrix skiving system, it was found that more flexible samples tend to produce poorer quality of surface finish.



## 8.2 Summary

Work began by identifying two alternative methods for leather machining, namely the high speed milling operation and the dynamic matrix skiving operation. In both cases it was necessary to identify, and subsequently optimise, the associated cutting parameters. Experimental work were separately performed for each method, though useful information from one method were used in aid of the other whenever applicable.

In the case of milling system, it was found at the early stage of the work that high rotational speeds are required to achieve a successful milling operation on leather material. For this reason a high speed router was employed. It was also found that the shape of the cutting tool played an important role in achieving a satisfactory quality of surface finish. After testing of a number of different shaped tools, an inverted dovetail shape cutting tool proved to produce very good surface finishes. Cooling by an air jet was used to eliminate the effects of material burning as a result of heat generated due to the friction between the cutting tool and the workpiece. It was the aim of the project to identify, within the experimental limits, the maximum speed of operation achievable. For this reason the linear feed speed of the cutter was taken as an experimental cutting parameter. Another parameter was the rotational speed of the cutter. This, for a fixed cutter diameter, is related to the peripheral speed of the cutter. The preliminary experiments in leather milling showed that the quality of the surface finish of the tested results improves with the increase of the cutting speed and the decrease of the feed speed.

In the case of dynamic matrix skiving, use of a leather splitting machine was made to achieve material removal. The rig involved a rotating band knife, a feed roller, and a pressure bar that was positioned above the knife. Several configurations were examined to achieve matrix skiving, but a linear array of independently-actuated pins was chosen. The preliminary experiments were conducted by means of static matrices using template matrix dies. The results showed that the skiving quality decreases when the matrix resolution decreases. It was therefore decided to carry out further tests using especially constructed pin-bar assemblies so that various pin diameters and spacings could be tested in a dynamic test condition.

The preliminary tests for both of the methods mentioned above showed that the machining results were heavily dependent on the physical properties of leather. For this reason, comprehensive tests were carried out to examine the



effects of some physical properties thought relevant to the work. Based on observation and tactile inspection of different leather samples two properties can be easily detected; the material thickness and its relative flexibility. Other properties that were considered for further investigation were tensile strength, hardness, compression, the leather tearing load, and another measurable load called the burst load. The burst load test involved pushing a small ball through the surface of a clamped leather sample until the material breaks. This load was taken as the material's burst load. The physical properties experiments were conducted on two different leather samples, originated from namely hide type-1 and type-2. The results showed that hide type-1 is approximately twice as thick as hide type-2, while the latter is approximately twice as hard as the former. It was also shown that there is little difference between the two hide types in terms of material resistance to compression and tearing. Furthermore, it was also shown that samples taken from hide type-2 exhibit higher amount of tensile strength than those taken from hide type-1. The mean difference was measured to be around 16%. In terms of the burst load, the hide type-1 was shown to have an approximately 26% higher burst load than hide type-2. However, the greatest difference between the two hide types was seen to be associated with the material flexibility. Measured in terms of flexural rigidity, it was found that hide type-2 is approximately 7 times more flexible than hide type-1. The results of the physical properties tests were later used so that machining parameters could be correlated to materials properties. This can help designing machines that can produce acceptable surface finishes when leather samples of different physical properties are used.

Having conducted the preliminary tests for both of the machining methods, and having evaluated some of the important physical properties tests, further, more comprehensive and more systematic experimentations were conducted for both systems. For the high speed machining method a description of the theoretical background to the work was first presented. Based on the work carried out for metal machining, it was established that the measurement of the feed and normal cutting forces in a machining system leads to useful information regarding the effectiveness of the cutting condition. It was mentioned that these forces are related to the tangential and radial forces that are exerted on the cutter. The radial force is regarded as the rubbing force while the tangential force is related to the torque on the cutter. The ratio of the radial to tangential force is of significance since it determines the amount of rubbing present in the system. It is generally aimed to produce cutting conditions that result in lower cutting forces. Another important factor affecting the cutting condition is the effects of the cutting tool rake



angle. This angle determines the angle of approach of the cutting face of the tool towards the workpiece. Efficiency of the system can further be considered by the measurement of the power consumption in the system. It was therefore decided to perform experiments on leather types 1 and 2 using various tool rake angle and depths of cut. Both positive and negative rake angles were used. The cutting speed and feed speeds were also other cutting parameters. To conduct the tests, a quasi-static dynamometer was constructed to measure feed and normal cutting forces and the power consumption during cutting. Air lubricated bearings were made to allow frictionless movement of the dynamometer. Displacement transducers were used to correlate the dynamometer's displacement to the applied forces in two orthogonal directions, and measurement of the spindle motor current were related to the power reading of the motor. It was also noticed that the actual rotational speed of the cutter drops from an initial no-load value to a 'settled' value under load. To monitor the correct cutter speed, therefore, an optical transducer was used to measure this speed during the cutting condition. A high speed router was used to achieve spindle speed of up to 24000 rpm. The router was allowed controlled motorised travel so that accurate feed could be achieved.

The results of the machining experiments show that the effect of the material's original quality on the surface finish is dominating, and masks the effects of other machined-based parameters. It was particularly noticed that the degree of the materials fluffiness severely decreases the quality of surface finish. The degree of stretchability of the fibres in leather was shown to be related to this phenomenon. Also, up-cutting was found to give better quality results. The tests with negative tool rake angle produced encouraging quality results albeit giving higher cutting forces and power consumptions. It was further concluded that the quality of the surface finish improves with the increase in cutting speed, though speeds around 12000 rpm showed signs of optimality in terms of cutting force and power consumption. In general, leather from hide type-1 required more cutting force than that of type-2, with the resultant cutting forces of 8.14 N and 6.46 N. However, the increase in the feed speed also increased the cutting forces and the power consumption, but did not affect the quality of surface finish especially at the maximum speed of  $0.09 \text{ ms}^{-1}$ . Photographic evidence of the cutting edge of the cutting tool both before and after the experiments does not show excessive tool wear. However, determination of tool life requires much more exhaustive tests to be carried out.

The experimentation for the dynamic matrix skiving method involved the testing of several linear arrays of pins with different pin diameter and spacing. An



existing leather splitting machine was employed whose feed roller and band knife proved to perform successfully for test purposes. In conjunction with this machine matrix pins were manufactured to cater for pin diameters of 3, 4, and 5 mm, and pin spacings of 1, 2, and 3 mm. The bars, each housing an array of a fixed pin diameter and spacing, were mounted on the machine for each experiment. A travelling, solenoid-operated plunger was used to push the pins down as it travelled over the pins. A d.c. motor was used to produce the linear travel. Linear speeds of up to  $0.09 \text{ ms}^{-1}$  were used. Furthermore, because it was important to determine the correct magnitude of the force that was required to force the pins against the leather, a load cell was designed and mounted in cascade along the solenoid plunger so that the applied forces during each test could be measured. The tests were conducted on leather samples taken from hide types 1 and 2.

The results of the dynamic matrix skiving experiments showed that for both leather types lower pin diameters and pin spacings produce better skiving quality results, while variations of feed speed does not significantly affect the results. The mean skiving force values fell in a range bound by 32.8 and 41.6 N. When these results were correlated with the physical properties of leather it was subsequently concluded that variation of leather flexural rigidity and hardness affect the matrix skiving results more significantly than any other. Whereas more rigid leather components produced better surface quality in matrix skiving, harder components resulted in poorer surface quality.

Having established the fundamental factors related to the two system of leather machining, some of the important considerations for the automation of the skiving process were highlighted. It was mentioned that the aim of the project was to provide design information for an independent automation cell for the skiving process so that it is compatible with other shoe manufacturing automation projects. To this end, suggestions were made to use an already developed linescan camera, as a means of parts recognition system, in conjunction with a system of computer-controlled conveyor belts to transport the components. In the case of the high speed milling system, the use of vacuum belts was suggested to clamp the components while cutting takes place. Two methods were suggested to achieve this. The first method required the leather component to be clamped while stationary, and the second method suggested that the component rests on a moving vacuum conveyor belt at all times during machining. In the former case the cutting head assembly consists of a 3-axis motion control spindle system, and in the latter case a similar spindle system could be envisaged to be attached to a moving gantry



mechanism. This would then make the system continuous. An estimated production time of 9.0 seconds was evaluated for the stationary cutting system.

In the case of the dynamic matrix skiving system, it was mentioned that the system is of a continuous nature, and can be readily integrated with other essential elements such as conveyor belts and the recognition system. A bank of computer-controlled independently-activated solenoid-lever-pin assembly, mounted on a band knife machine, can produce the desired skiving profile on the component. Accurate feed speed synchronisation with the action of the solenoids becomes necessary to avoid skiving profile distortion. An estimated time duration of 8.8 seconds was evaluated for the complete operation time.

### **8.3 Future directions**

The work that was presented in this thesis was primarily involved with the investigation of the fundamental principles involved in machining of leather, as a flexible fibrous material, for automation applications. A high speed machining method and a dynamic matrix skiving method were employed. In this project, the important design considerations were to test the capabilities of the two machining methods in terms of (a) achieving acceptable surface finishes on different leather materials, and (b) determining the maximum speeds of operation. To this end, it was shown that most common leather materials can be machined using both methods. It was further shown that an operation speed of at least  $0.09 \text{ ms}^{-1}$  can be achieved in both methods.

Nevertheless, the results of this investigation were affected by the limitations of the experimental system. One important aspect of the experiments that is a candidate for further investigation is the speeds of operation tested. This is true for both machining system. However, work can be done to increase the maximum speed tested (ie.  $0.09 \text{ ms}^{-1}$ ) even higher. This of course will require experimental rigs that are capable of coping with higher speeds.

In the case of high speed machining system, there can be occasions when the cutter can result in erratic pull of the workpiece and may lead to its subsequent destruction. This is related to the flexible nature of the workpiece, and occurs when a sudden disturbance in the system such as increase of the cutter torque is resulted. To avoid these situations, strong clamping of the workpiece is required. A method of dealing with the clamping problem is to increase the rigidity of the workpiece for the duration of cut. One way of achieving this is by temporarily



freezing the material [60]. Thorough investigation will be required to study the lasting effects of this process on the workpiece. So far as clamping of flexible materials is concerned, further work will be required to develop an efficient and effective method so that random shaped components can be clamped automatically. Though the tungsten carbide cutting tools performed satisfactorily in the experiments, it is expected that much harder tool materials will be required to cope with a factory situation. Diamond tools are more expensive but can retain their sharpness for a much longer production cycle.

In the dynamic matrix skiving system, it was found during the investigation that use of substrate can improve the quality of the skived component. This was noted when soft substrates were positioned under the workpiece in such a way that the composite component was fed through the cutting mechanism. Improvements were noticed by observing decreased amplitudes of the resulting waveform on the skived samples. Another problem associated with the dynamic matrix skiving mechanism is to avoid undesirable rotation of the workpiece as it is engaged with the matrix pins. This situation occurs as a result of the moments produced on the surface of the component by different engaged pins at various locations. A clamping system will have to be developed to guide the component through the cutting mechanism such that no component rotation may occur.

The integration work that will have to be carried out towards the designing of an automated cell involves a number of strategic and important points that needs to be considered. These include ensuring that the automated skiving cell is compatible with other automated process cells in terms of component flow continuity and production rate. Furthermore, various cells will ideally need to communicate with one another to exchange data and command information. This calls for standardisation of communication at the software level.



## REFERENCES

1. Zirkle D; "Men robots and machines"; American Shoemaking; 3 March 1986.
2. Cole J N; "Survey of preparation-for-closing operations"; Internal report; Ref: AJS/SD; British United Shoe Machinery Ltd.; 24 November 1978.
3. Snape R; "Upper skiving"; Internal report; Ref: JRP/JNC/SMC; British United Shoe Machinery Ltd.; 19 May 1978.
4. Tout N R; "Investigation of the processes required for the automation of stitchmarking in shoe manufacture"; PhD Thesis; University of Durham; 1989.
5. Browne J W; "The theory of machine tools: Book 1"; Cassell and Company Ltd.; 1965.
6. Roberts A D, Lapidge; "Manufacturing processes"; McGraw Hill Inc.; 1977.
7. Kalpakjian S; "Manufacturing engineering and technology"; Addison-Wesley Publishing Company; 1989..
8. Sabberwal A J P; "Chip section and cutting force during the milling operation"; Annals of the CIRP; Vol. 10; 1961.
9. Chapman W A J; "Workshop technology: Part 2"; 4<sup>th</sup> edition; Edward Arnold (Publishers) Ltd.; 1972.
10. Martellotti M E; "An analysis of the milling process"; Transactions of the A.S.M.E.; Volume 63; 1941.
11. Tlusty J; "Dynamics of high speed milling"; Journal of Engineering for Industry; Volume 108; May 1986.
12. Devor R E, Kline W A, Zdeblick W J; "A mechanistic model for the force system in end milling with application to machining airframe structures"; Eighth North American Manufacturing Research Conference Proceedings; 1980.



13. Kobayashi A; "Machining of plastics"; Robert E Krieger Publishing Company; 1981.
14. Pope J R; "Matrix skiving"; Internal report; ref. JRP/RS/SMC; British United Shoe Machinery Ltd.;1976.
15. Snape R; "Upper preparation Survey"; Internal report; ref. JRP/RS/SMC; British United Shoe Machinery Ltd.;1977.
16. Reed R; "Science for students of leather technology"; Pergamon Press Ltd.; 1966.
17. Stromberg M, Swerdlow M J; "Pores in collagen leather"; Journal of American Leather Chemist's Association; Volume 52; 1955.
18. British Standards 3935; "Guide to classification and marking of cattle hides and calf skin"; 1991.
19. Hodus H J, Stubbings R; "A laboratory method for measuring effects of process variables on leather quality; (1): Selection of samples for laboratory experiments"; Journal of American Leather Chemist's Association; Volume 52; 1957.
20. Mandel J M, Mann C W; "A statistical solution of a problem arising in the sampling of leather"; Journal of Research of the National Bureau of Standards; Volume 46; 1951.
21. Randall E B, Carter T J, Kilduff T J, Mann C W, Kanagy J R; "The variation of the physical and chemical properties of split and unsplit chrome-tanned leathers"; Journal of American Leather Chemist's Association; Volume 47; 1952.
22. Kanagy J R, Randall E B, Carter T J, Kinmouth R A, Mann C W.; Journal of American Leather Chemist's Association; Volume 47; 1952.
23. Wilson J A; "Modern practice in leather manufacture: The properties of leather" Reinhold Publishing Corporation; 1941.
24. Wilson J A; "Effect of splitting on the tensile strength of leather"; Industrial and Engineering Chemistry; Volume 18; 1926.



25. Wilson J A; "Variation of strength and stretch over the area of calf leather"; Industrial and Engineering Chemistry; Volume 17; 1925.
26. Butlin J G; "The plasticity and related properties of upper leather"; BBSI Journal; July 1962.
27. British Standards 3144; "Method of sampling and physical testing of leather"; 1966.
28. British Standards 3356; "Determination of bending length and flexural rigidity of fabrics"; 1990.
29. Peirce F T; "The handle of cloth as a measurable quantity"; A confidential document; 1931; BTTG, Manchester.
30. The Shoe and Allied Trade Research Association; "The lastometer"; Satra Instrument Instructions STD. 104/M: Test method PM.24; 1968.
31. Lissaman A J; Martin S J; "Principles of Engineering Production"; 1982; Hodder and Stoughton Publishers.
32. Kronenberg M; "Machining Science and Applications; Theory and Practice for Operation and Development of Machining Processes"; 1966; Pergamon Press Inc.
33. Gygax P E; "Experimental Full Cut Milling Dynamics"; Annals of the CIRP; Vol. 29; January 1980.
34. Tlustý J, MacNeil P; "Dynamics of Cutting Forces in End Milling"; Annals of the CIRP; Vol. 24; January 1975.
35. Koenigsberger F, Sabberwall A J; "An Investigation into the Cutting Force Pulsation During Milling Operation"; International Journal of Machine Tool Design and Research"; Vol. 1; 1961.
36. Gygax P E; "Dynamics of Single Tooth Milling"; Annals of the CIRP; January 1979.
37. Barney G C; "Intelligent Instrumentation"; 1985; Prentice Hall International (UK) Ltd.
38. Morrison J L M, Crossland B; "An Introduction to the Mechanics of Machines"; Second Edition; 1970; Longman Group Ltd.



39. Hannah J, Stephens R C; "Mechanics of Machines; Advanced Theory and Examples"; Second Edition; 1972; Edward Arnold (Publishers) Ltd.
40. Hughes E; "Electrical Technology"; Fifth Edition; 1979; Longman Group Ltd.
41. Victor H; "Computer Aided Measurement of Cutting Forces Applied to the Wear of an End Mill Cutter"; Wear; Vol. 62; 1980
42. Cook N H; "Tool Wear Sensors"; Wear; Vol. 62; 1980.
43. Bajpai A C, Mustoe L R, Walker D; "Advanced Engineering Mathematics"; 1977; John Wiley & Sons Ltd.
44. Murdoch J, Barnes J A; "Statistical Tables for science, engineering, management and business studies."; Second Edition; 1970; The Macmillan Press Ltd.
45. Smith D L; "The Manipulation of leather workpieces for the assembly of shoes"; PhD Thesis; University of Hull; 1991.
46. Howard M A; "The design and development of various aspects of a robotic flexible manufacturing system for shoe production; MPhil Thesis; University of Lancaster; 1989.
47. Koulopolos C; "Automated vision for identification of silhouette shapes with an application to industrial automation"; PhD Thesis; City University; 1982.
48. Groover M P; "Automation, production systems, and computer integrated manufacturing"; 1987; Prentice-Hall Inc.
49. Kwo T T; "A theory of conveyors"; Management Service; Vol. 5; Part 1; 1958.
50. Muth E J; "Analysis of closed-loop conveyor system"; AIIE Transactions; Vol. 4; Part 2; 1972.
51. Muth E J, White J A; "Conveyor theory: A survey"; AIIE Transactions; Vol. 11, Part 4; 1979.
52. Yeo S H, Tadmory M J, Foster K, Hodgson D C; "Dynamics of an object discharging off a belt conveyor"; Proceedings of the IMechE; Vol. 204; 1990.
53. Nastali W F; "Machine control: Smarter than ever"; Manufacturing Engineering; January 1986.



54. Taylor P M, *et al*; "Electrostatic grippers for fabric handling"; Proceedings of the IEEE Conference on Robotics and Automation; Philadelphia; April 1988.
55. Nicholson P R, Sarhadi M; "Flexible porous material handling in a CIM environment"; 10<sup>th</sup> International Conference on Production Research; Nottingham; 1988.
56. "Vacuum techniques in Automation"; OEM Design; July 1986.
57. "The design of a vacuum plant"; The Vacuum Design Manual; Piab Ltd., UK.
58. "Vacuum Traction"; Design Manuals; Simon Container Machinery Ltd., Stockport Cheshire.
59. Snape R. "Upper Skiving"; Internal Report; Ref. JRP/JNC/SMC; British United Shoe Machinery Ltd; May 1977.
60. Guse R; "Freeze/thaw technique part of automated handling study"; Knitting International; July 1988.